

Winter 2007

# Probing regioselectivity in the Diels -Alder cycloadditions between \*[60]fullerene and aryl substituted acenes

James Eric Rainbolt

*University of New Hampshire, Durham*

Follow this and additional works at: <https://scholars.unh.edu/dissertation>

---

## Recommended Citation

Rainbolt, James Eric, "Probing regioselectivity in the Diels -Alder cycloadditions between \*[60]fullerene and aryl substituted acenes" (2007). *Doctoral Dissertations*. 414.  
<https://scholars.unh.edu/dissertation/414>

This Dissertation is brought to you for free and open access by the Student Scholarship at University of New Hampshire Scholars' Repository. It has been accepted for inclusion in Doctoral Dissertations by an authorized administrator of University of New Hampshire Scholars' Repository. For more information, please contact [nicole.hentz@unh.edu](mailto:nicole.hentz@unh.edu).

PROBING REGIOSELECTIVITY IN THE DIELS-ALDER CYCLOADDITIONS  
BETWEEN [60]FULLERENE AND ARYL SUBSTITUTED ACENES

BY

JAMES ERIC RAINBOLT

B.S., James Madison University, 2002

DISSERTATION

Submitted to the University of New Hampshire  
in Partial Fulfillment of  
the Requirements for the Degree of

Doctor of Philosophy

in

Chemistry

December, 2007

UMI Number: 3290107

### INFORMATION TO USERS

The quality of this reproduction is dependent upon the quality of the copy submitted. Broken or indistinct print, colored or poor quality illustrations and photographs, print bleed-through, substandard margins, and improper alignment can adversely affect reproduction.

In the unlikely event that the author did not send a complete manuscript and there are missing pages, these will be noted. Also, if unauthorized copyright material had to be removed, a note will indicate the deletion.

**UMI<sup>®</sup>**

---

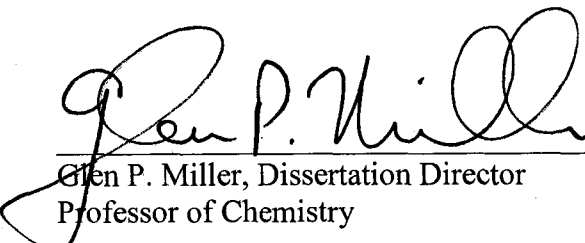
UMI Microform 3290107


Copyright 2008 by ProQuest Information and Learning Company.

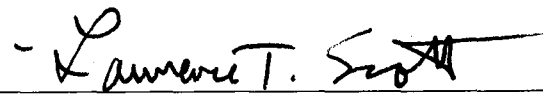
All rights reserved. This microform edition is protected against unauthorized copying under Title 17, United States Code.

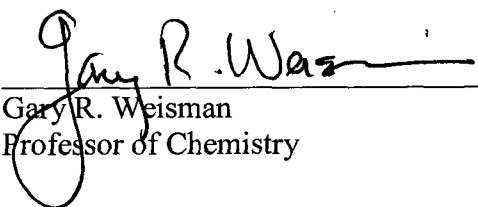
ProQuest Information and Learning Company  
300 North Zeeb Road  
P.O. Box 1346  
Ann Arbor, MI 48106-1346

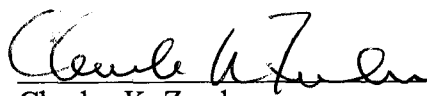
This dissertation has been examined and approved.

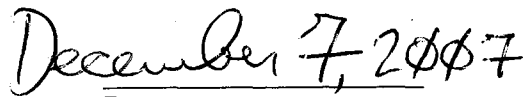
  
Glen P. Miller, Dissertation Director  
Professor of Chemistry

  
Roy P. Planalp  
Associate Professor of Chemistry

  
Lawrence T. Scott  
Professor of Chemistry, Boston College

  
Gary R. Weisman  
Professor of Chemistry

  
Charles K. Zercher  
Professor of Chemistry

  
Date

## ACKNOWLEDGMENTS

I could not have completed my dissertation without the support of many people, all of whom deserve acknowledgment. I am forever grateful for my lovely wife, Jill. So many days did I come home frustrated only to forget my troubles upon seeing her beautiful smile. She is the best friend I have ever had. I am thankful for our daughter Eve, whose vim for knowledge and cookies inspires me. I owe my development as a person to my parents, Dee and Eric Rainbolt, and could not successfully thank them for their dedication with words. They embody all that I strive to be for my daughter. I thank Dr. Glen Miller for his guidance and support during my graduate research. Glen taught me the meaning of work, finish, publish. My thanks goes to Cindi Rohwer and Peggy Torch for always helping me in my times of need. The department is very fortunate to have them. I thank Bob Constantine for helping me learn my way around the Chemistry library. Of all the things I found there, Bob was the most valuable. I thank the members of the University Instrumentation Center for all there work in maintaining the NMR instruments, especially Kathy Gallagher who was critical in helping me with NMR. My acknowledgments could not be complete without thanking Dr. Mikaël Jazdyk, who made invaluable contributions to both my research and well being. He is one of the best chemists and persons I have had the pleasure of knowing. I thank the researchers, past and present, of the Miller research group, including Drew Athans, Jon Briggs, Joe Dunn, Wenling Jia, Irvinder Kaur, Jeremy Kintigh, Ryan Kopreski, Jung-Fu Liu, and Chandrani Pramanik. Their guidance and suggestions have been invaluable. The following research is an extension of the accomplishments of those before me and, with any fortune, will enjoy the same fate as a point of vantage for others to follow.

## TABLE OF CONTENTS

ACKNOWLEDGMENTS.....	iii
LIST OF TABLES.....	viii
LIST OF FIGURES.....	ix
LIST OF SCHEMES.....	xi
LIST OF NUMBERED STRUCTURES.....	xiv
ABSTRACT.....	xxiv
 CHAPTER 1: INTRODUCTION.....	 1
1.1    Carbon.....	1
1.2    [60]Fullerene.....	3
1.2.1    Discovery of [60]Fullerene.....	3
1.2.2    Synthesis of [60]Fullerene.....	4
1.2.3    Physical Properties of [60]Fullerene.....	5
1.2.4    Diels-Alder Chemistry of [60]Fullerene.....	9
1.3    Acenes.....	14
1.3.1    Properties of Acenes.....	14
1.3.2    Synthesis of Acenes.....	16
1.3.2.1    Tetracene Syntheses.....	17
1.3.2.2    Pentacene Syntheses.....	19
1.3.3    Substituted Acenes.....	24
1.3.4    Diels-Alder Chemistry of Acenes.....	28

1.3.4.1	Diels-Alder Reactivity of Acenes with [60]Fullerene.....	30
1.3.4.2	Diels-Alder Reactivity of Phenyl Substituted Acenes with [60]Fullerene.....	34
CHAPTER 2: 4,7-DIPHENYLISOBENZOFURAN: A USEFUL INTERMEDIATE FOR THE CONSTRUCTION OF PHENYL-SUBSTITUTED ACENES.....		
2.1	Introduction.....	36
2.2	Synthesis of 4,7-Diphenyl-1-hydroxyphthalan ((±)-4).....	37
2.3	In Situ Formation and Reactivity of 4,7-diphenylisobenzofuran ( <b>5</b> ): Construction of Three and Four-ring Acene Derivatives.....	38
2.3.1	Reactivity of 4,7-Diphenylisobenzofuran with Maleic Anhydride.....	39
2.3.2	Reactivity of 4,7-Diphenylisobenzofuran with 1,4-Naphthoquinone.....	41
2.3.3	Unusual Diastereoselectivity in the Reaction Between 4,7-Diphenylisobenzofuran ( <b>5</b> ) and <i>p</i> -Benzoquinone.....	42
2.3.3.1	Structural Analysis of <b>16c</b> .....	45
2.3.3.2	Structural Analysis of <b>16b</b> .....	46
2.3.3.3	Analysis of Borohydride Reduction Products of <b>16b</b> .....	47
2.3.4	Construction of a New Pentacene from <b>16b</b> .....	52
2.4	A Re-examination of the Reaction Between 1,3-Diphenylisobenzofuran ( <b>23</b> ) and <i>p</i> -Benzoquinone.....	53
CHAPTER 3: A STUDY OF THE DIELS-ALDER CYCLOADDITIONS BETWEEN 1,4-DIARYLTETRACENES AND [60]FULLERENE.....		
3.1	Introduction.....	57

3.2	Diels-Alder Reactions Between 1,4-Diphenyltetracene, <b>15</b> , and [60]Fullerene.....	60
3.3	Diels-Alder Reactions Between <b>15</b> and Other Dienophiles Under Kinetically Controlled Reaction Conditions.....	65
3.3.1	Synthesis and Characterization of Diels-Alder Adducts <b>28-32</b> .....	66
3.3.2	Irreversible/Reversible Nature of Experiments 3-8.....	71
3.3.3	Summary of Results for Reactions of <b>15</b> Run Under Kinetically Controlled Conditions.....	72
3.4	Diels-Alder Cycloaddition Between Tetracene and Maleic Anhydride....	73
3.5	Synthesis and Diels-Alder Reactivity of 1,4-Diaryltetracenes <b>41-45</b> .....	74
3.5.1	Synthesis of 1,4-Diaryltetracenes <b>41-45</b> .....	74
3.5.2	Diels-Alder Reactivity of 1,4-Diaryltetracenes <b>41-45</b> Under Kinetically Controlled Reaction Conditions.....	76
3.6	Thermodynamically Controlled Diels-Alder Reactions of <b>15</b> And <b>41-45</b> .....	82
3.7	Ab Initio Calculations of Acenes and Acene Adducts.....	86
3.7.1	Ab Initio Calculations of <b>15</b> and <b>45</b> .....	86
3.7.2	Ab Initio Calculations of the Ground State Energies of Ethylene Adducts of <b>15</b> , <b>41</b> and <b>42</b> .....	87
3.7.3	A Computational Examination of Compound <b>27a</b> .....	88
3.8	<sup>1</sup> H NMR Evidence for Aryl CH–Fullerene $\pi$ Interactions.....	90
3.9	Survey of the Cambridge Crystallographic Database.....	94
3.10	Diels-Alder Reactivity of 1,4,8,11-Tetraphenylpentacene, <b>22</b> .....	96
3.10.1	Introduction.....	96
3.10.2	Diels-Alder Reactivity of <b>22</b> with [60]Fullerene, <sup>1</sup> O <sub>2</sub> , Maleic Anhydride, and DDQ.....	97



CHAPTER 4: CONCLUSIONS.....	101
CHAPTER 5: EXPERIMENTAL SECTION.....	103
5.1    General Methods.....	103
5.2    Solvents.....	104
5.3    Reagents.....	105
5.4    Syntheses.....	107
REFERENCES.....	133
APPENDIX: NMR SPECTRA.....	143

## LIST OF TABLES

<u>Number</u>	<u>Page</u>
1	Rate constants associated with the addition of maleic anhydride to acenes.....29
2	Diels-Alder reactions between <b>5</b> and maleic anhydride.....39
3	Diels-Alder reactions between <b>5</b> and 1,4-naphthoquinone.....41
4	Diels-Alder reactions Between <b>5</b> and <i>p</i> -benzoquinone.....45
5	Expected <sup>1</sup> H NMR spectra for compounds <b>17a-c</b> and <b>18a-b</b> .....49
6	Survey of reactions between <b>23</b> and <i>p</i> -benzoquinone under various conditions...55
7	Diels-Alder reactions between <b>15</b> and [60]fullerene.....61
8	Reactions between <b>15</b> and various dienophiles run under kinetic and thermodynamic conditions.....66
9	Diels-Alder cycloaddition reactions between 1,4-diaryltetracenes <b>41-45</b> and [60]fullerene run under kinetic conditions.....77
10	Diels-Alder cycloaddition reactions between 1,4-diaryltetracenes <b>41-45</b> and singlet oxygen.....80
11	Diels-Alder cycloaddition reactions between 1,4-diaryltetracenes <b>41-45</b> and [60]fullerene run under thermodynamic conditions.....84
12	Relative energies of ethylene adducts of <b>15</b> , <b>41</b> and <b>42</b> calculated at various levels of theory.....88
13	Energetic and geometric properties of <b>27a'</b> and <b>27a''</b> as found by AM1.....89
14	<sup>1</sup> H NMR chemical shifts ( $\delta_o$ ) for <i>syn-ortho</i> and <i>anti-ortho</i> protons on [60]fullerene-acene compounds.....92
15	Diels-Alder cycloaddition between <b>22</b> and [60]fullerene run under kinetic conditions.....98
16	Diels-Alder reactions between <b>22</b> and singlet oxygen, maleic anhydride, and DDQ run under kinetic conditions.....99

## LIST OF FIGURES

<u>Number</u>	<u>Page</u>
1	The structure of diamond.....2
2	The structure of graphite.....2
3	The cage structure of [60]fullerene.....4
4	The carbon skeleton of corannulene and [60]fullerene.....6
5	Bond lengths and pyramidalization in benzene and [60]fullerene.....7
6	Pyramidalization angles of select PAHs and [60]fullerene.....8
7	The eight chemically distinct sites for addition to functionalized [60]fullerene.....10
8	Nakamura and co-workers <i>ortho</i> -quinodimethane benzolog adducts of [60]fullerene.....12
9	The structures of the known acenes.....14
10	MMFF optimized geometry of the endo,exo <i>syn</i> dual cycloaddition product arising from the reaction between 2 equivalents of 1,3-diphenylisobenzofuran and <i>p</i> -benzoquinone.....43
11	The six possible diastereomers that can form in the dual cycloaddition of <b>5</b> to <i>p</i> -benzoquinone.....44
12	Isolated dual cycloaddition product exo,exo <i>anti</i> <b>16b</b> and theoretical dual cycloaddition product exo,exo <i>syn</i> <b>16a</b> .....46
13	The three possible products arising from borohydride reduction of the hypothetical exo,exo <i>syn</i> <b>16a</b> and the two products formed during the borohydride reduction of exo,exo <i>anti</i> <b>16b</b> .....47
14	The central aliphatic diagnostic region for hypothetical structures <b>17a-c</b> and isolated molecules <b>18a-b</b> .....48
15	Diols <b>18a</b> and <b>18b</b> shown in boat conformations as predicted by molecular models and MMFF.....49
16	Variable Temperature NMR spectra of the type H <sub>I</sub> protons of <b>18b</b> .....51

17	Diels-Alder reactive sites of <b>15</b> and <b>22</b> .....	58
18	The 5,12 and 6,11 cycloaddition adducts of <b>15</b> are distinguished by NOE spectroscopy.....	63
19	<sup>1</sup> H NMR spectrum and NOE spectra for a mixture of <b>27a</b> and <b>27b</b> .....	64
20	NOESY2D spectrum of type H <sub>I</sub> and H <sub>II</sub> protons of <b>31a-31b'</b> .....	69
21	NOESY2D spectrum of type H <sub>I</sub> and aromatic protons of <b>31a-31b'</b> .....	70
22	Hammett plots of [60]fullerene cycloaddition products <b>46-50</b> formed under kinetically controlled reaction conditions.....	78
23	Hammett plots of <sup>1</sup> O <sub>2</sub> cycloaddition products <b>51-55</b> formed kinetically controlled reaction conditions.....	81
24	Hammett plots of [60]fullerene cycloaddition products <b>46-50</b> formed under thermodynamically controlled reaction conditions.....	85
25	HOMOs of tetracene, <b>15'</b> , <b>15''</b> and <b>45</b> found at the B3LYP/6-31G(d) level of theory.....	87
26	Ethylene adducts of <b>15</b> , <b>41</b> and <b>42</b> .....	88
27	Conformation isomers <b>27a'</b> and <b>27a''</b> as found by AM1.....	89
28	MM2 structures for compounds <b>56</b> and <b>57</b> .....	90
29	Two views of a [60]fullerene-acene substructure of compounds <b>56</b> , <b>57</b> , <b>58</b> and <b>59</b> .....	91
30	MM2 structures for compounds <b>58</b> and <b>59</b> .....	92
31	Structure and number of hits for Cambridge Crystallographic Database search of short aryl CH/[60]fullerene contact distances.....	94
32	Example compounds from Cambridge Crystallographic Database search of short aryl CH/[60]fullerene contact distances.....	95

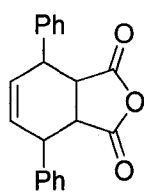
## LIST OF SCHEMES

<u>Number</u>	<u>Page</u>
1	Scott and co-workers' rational synthesis of [60]fullerene.....5
2	Diels-Alder cycloadditions of [60]fullerene.....9
3	Murata and co-workers synthesis of an open-cage [60]fullerene.....11
4	Rubin and co-workers' carbocyclic protection/deprotection of [60]fullerene.....12
5	Formation of bis[60]fullerene adduct of bis o-quinodimethane.....13
6	Taki and co-workers' trapping of an unusual acenaphthylene diene with [60]fullerene.....13
7	The photodimerization and photooxidation of anthracene.....16
8	Syntheses of tetracene: Clar; Hart and Lou; Thummel, Carvey and Nutakulalso.....17
9	Syntheses of tetracene: Rickborn and co-workers; Gribble and co-workers.....18
10	Syntheses of tetracene: Bowles and Anthony.....19
11	Clar's original synthesis of pentacene.....20
12	Hart and Luo's synthesis of pentacene.....20
13	Rickborn, Netka and Crump's synthesis of pentacene.....21
14	Yamashita and co-workers' synthesis of pentacene.....22
15	Known syntheses of 6,13-pentacenequinone.....23
16	Known syntheses of pentacene from 6,13-pentacenequinone.....23
17	Takahashi and co-worker's synthesis of alkyl-substituted tetracene and pentacene.....24
18	Some of the known 6,13-disubstituted pentacenes derived from 6,13-pentacenequinone.....25
19	Anthony and co-workers' syntheses of 6,15-bis(tri-tert-butylsilylethynyl)

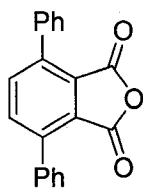
	hexacene and 7,16-bis(tris(trimethylsilyl)silylethynyl)heptacene.....	26
20	Miao and co-worker's synthetic approach to phenyl-substituted acenes.....	27
21	Pascal and co-worker's benzannelated hexaphenyl pentacene with an end-to-end twist of 144°.....	27
22	Generic Diels-Alder reaction between anthracene and ethylene.....	28
23	Diels-Alder adducts of maleic anhydride and anthracene and pentacene.....	29
24	[60]Fullerene cycloaddition to anthracene.....	30
25	[60]Fullerene cycloaddition across tetracene.....	32
26	[60]Fullerene cycloaddition across pentacene.....	32
27	Komatsu and co-workers' synthesis of bis[60]fullerene-pentacene adduct.....	33
28	Diels-Alder cycloaddition between 5,7,12,14-tetraphenylpentacene and [60]fullerene.....	34
29	Diels-Alder cycloaddition between 6,13-diphenylpentacene and [60]fullerene.....	35
30	Synthesis of (±)- <b>4</b> from 1,4-diphenylbutadiene and maleic anhydride.....	37
31	Acid catalyzed formation of transient <b>5</b> from lactol (±)- <b>4</b> .....	39
32	Synthesis of tetraphenylanthracene <b>11</b> from lactol (±)- <b>4</b> .....	40
33	Synthesis of diphenyltetracene <b>15</b> from lactol (±)- <b>4</b> .....	42
34	Formation of <b>16b</b> and <b>16c</b> from (±)- <b>4</b> .....	45
35	Synthesis of 1,4,8,11-tetraphenylpentacene, <b>22</b> .....	53
36	The addition of 1,3-diphenylisobenzofuran to <i>p</i> -benzoquinone under various conditions.....	54
37	Diels-Alder cycloaddition between <b>15</b> and [60]fullerene.....	61
38	Diels-Alder cycloaddition between <b>15</b> and various dienophiles.....	65
39	Diels-Alder cycloaddition between tetracene and maleic anhydride run under kinetic conditions.....	73

40	Synthesis of dibromomethyl terphenyl derivatives <b>34-38</b> (performed by Dr. Jazdzyk).....	74
41	Synthesis of 1,4-diaryltetracene derivatives <b>41</b> and <b>42</b> .....	75
42	Synthesis of 1,4-diaryltetracene derivatives <b>43-45</b> (performed by Dr. Jazdzyk).....	76
43	Diels-Alder reactions between 1,4-diaryltetracenes <b>41-45</b> and [60]fullerene run under kinetic conditions.....	77
44	Diels-Alder reactions between 1,4-diaryltetracenes <b>41-45</b> and singlet oxygen.....	80
45	Diels-Alder reactions between 1,4-diaryltetracenes <b>41-45</b> and [60]fullerene run under thermodynamic conditions.....	83
46	Diels-Alder cycloaddition between [60]fullerene and pentacene and 6,13-diphenylpentacene.....	96
47	Diels-Alder cycloaddition between <b>22</b> and [60]fullerene.....	98
48	Diels-Alder cycloaddition between <b>22</b> and singlet oxygen, maleic anhydride, and DDQ.....	99

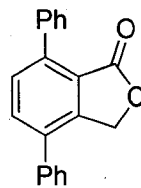
# LIST OF NUMBERED STRUCTURES



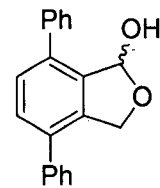
**1**



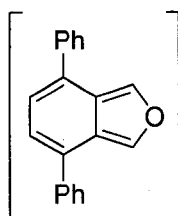
**2**



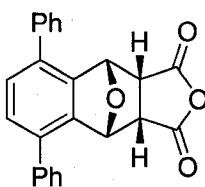
**3**



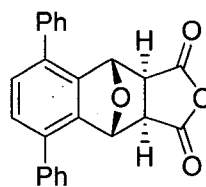
**(±)-4**



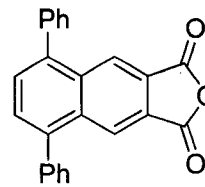
**5**



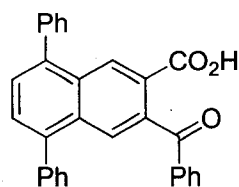
**6a**



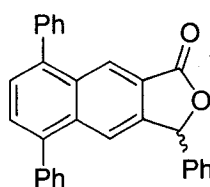
**6b**



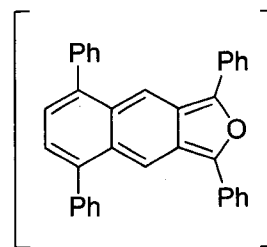
**7**



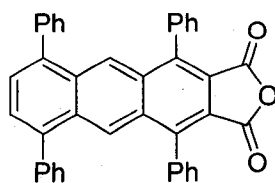
**8**



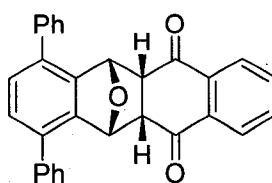
**(±)-9**



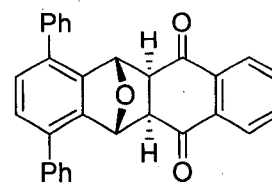
**10**



**11**

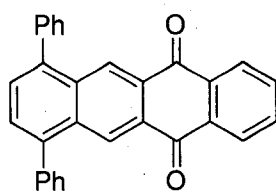


**12a**

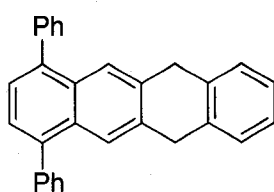


**12b**

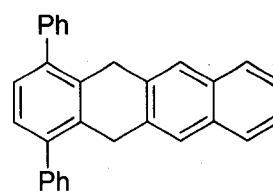




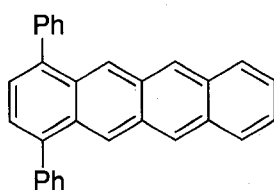
**13**



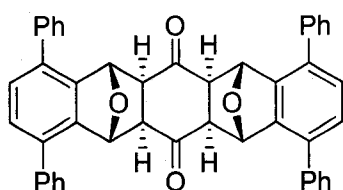
**14a**



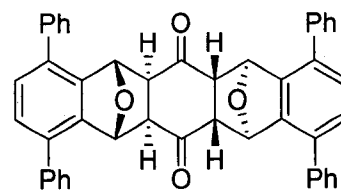
**14b**



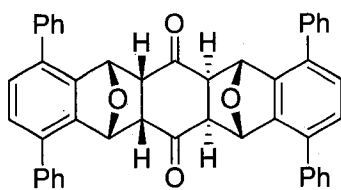
**15**



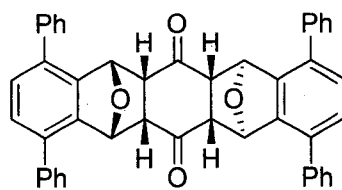
**16a**



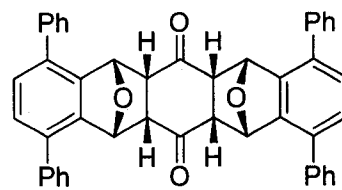
**16b**



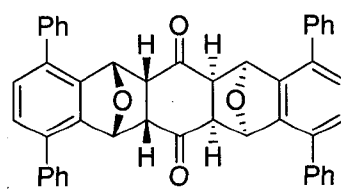
**16c**



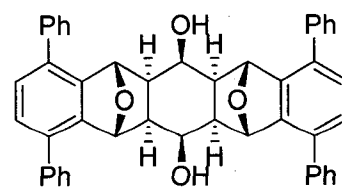
**16d**



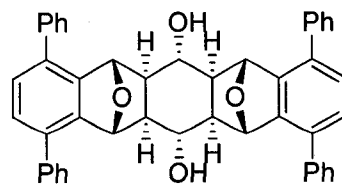
**16e**



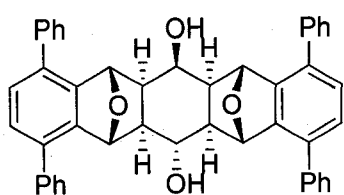
**16f**



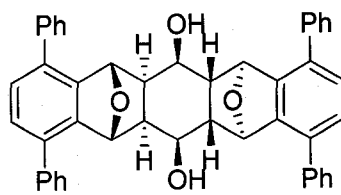
**17a**



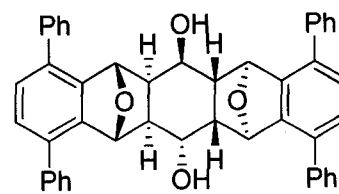
**17b**



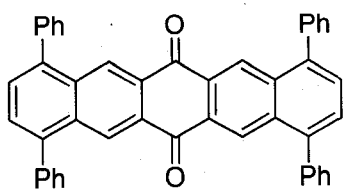
**17c**



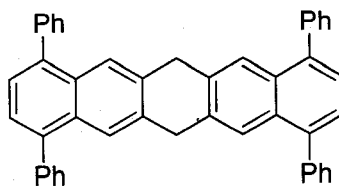
**18a**



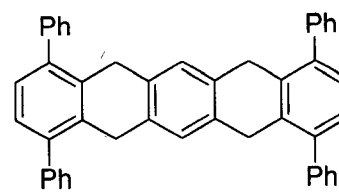
**18b**



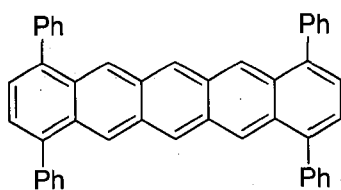
**19**



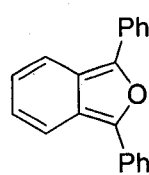
**20**



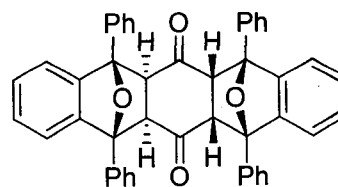
**21**



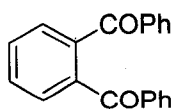
**22**



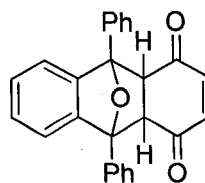
**23**



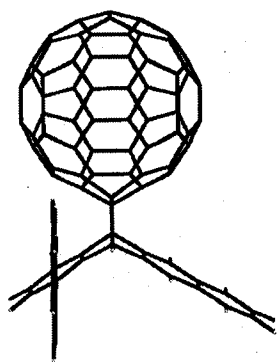
**24**



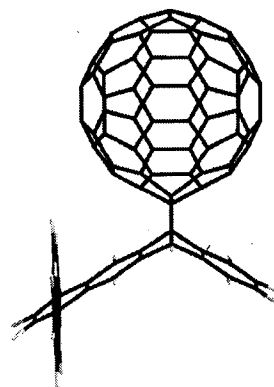
**25**



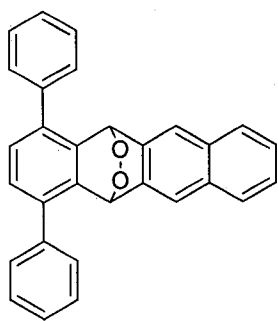
**26**



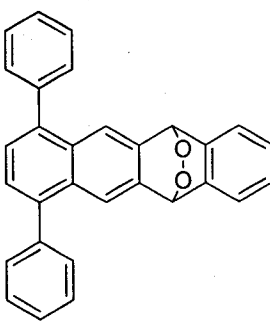
**27a**



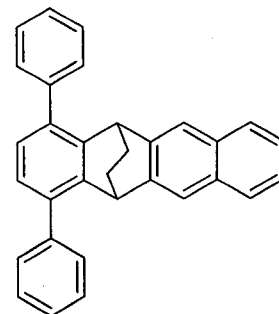
**27b**



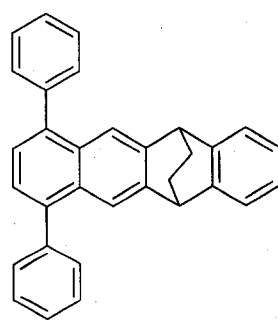
**28a**



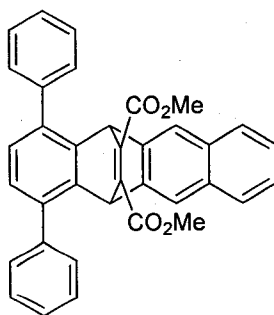
**28b**



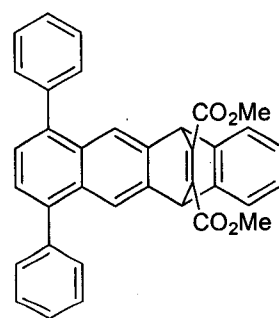
**29a**



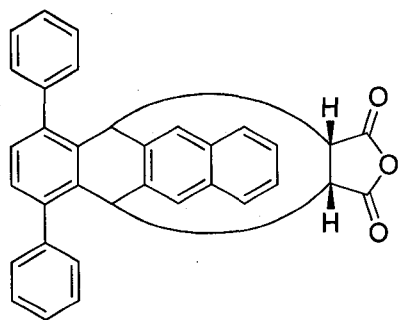
**29b**



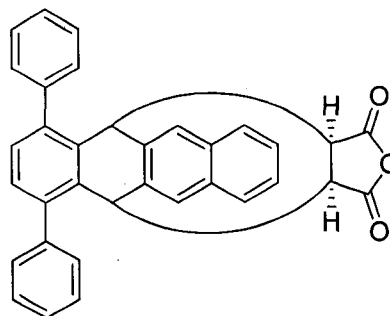
**30a**



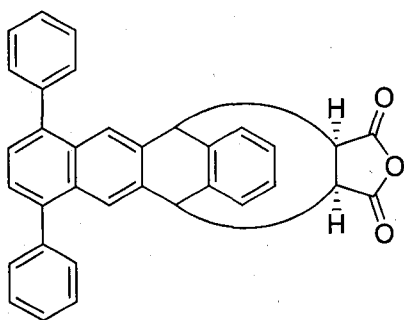
**30b**



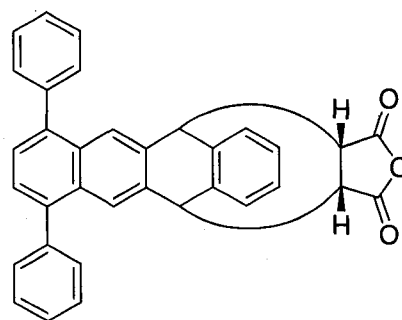
**31a**  
endo



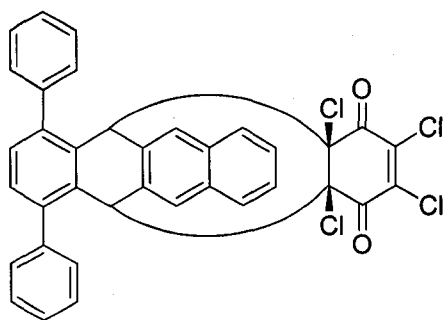
**31a'**  
exo



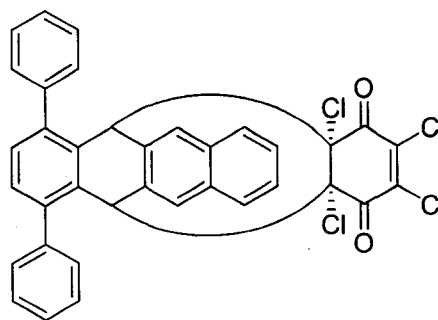
**31b**  
endo



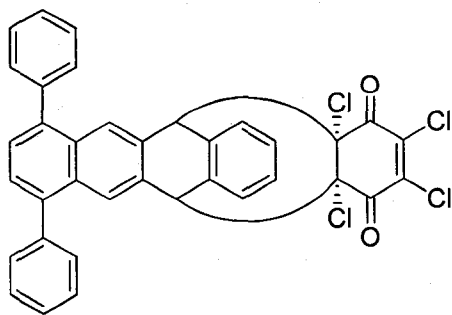
**31b'**  
exo



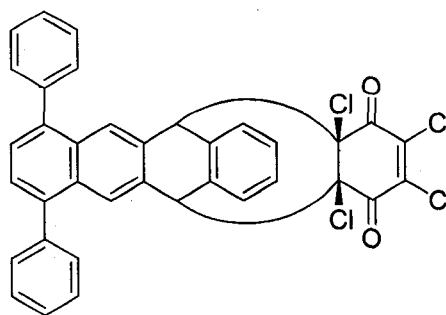
**32a**  
endo



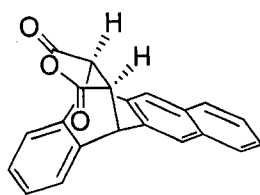
**32a'**  
exo



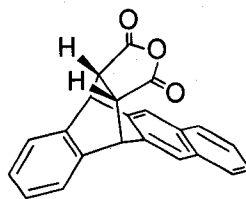
**32b** endo



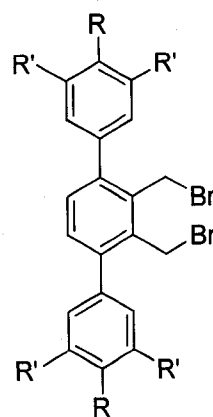
**32b'** exo



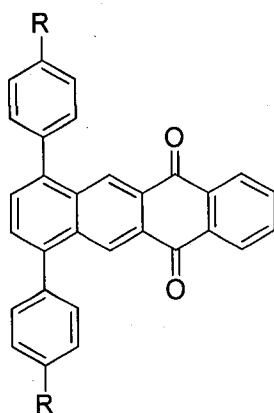
**33a**  
exo



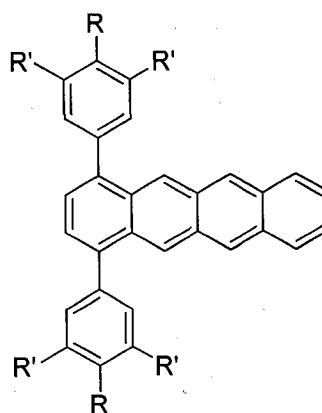
**33b**  
endo



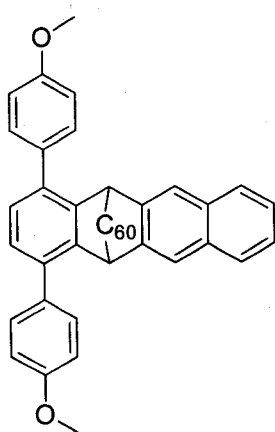
<u>R</u>	<u>R'</u>	
MeO	H	<b>34</b>
tBu	H	<b>35</b>
CN	H	<b>36</b>
CF <sub>3</sub>	H	<b>37</b>
H	CF <sub>3</sub>	<b>38</b>



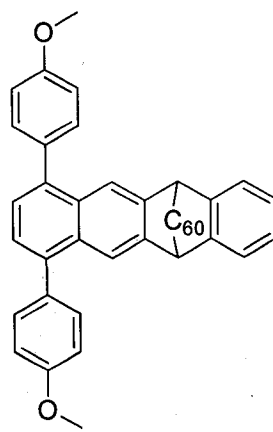
<u>R</u>	
MeO	<b>39</b>
CF <sub>3</sub>	<b>40</b>



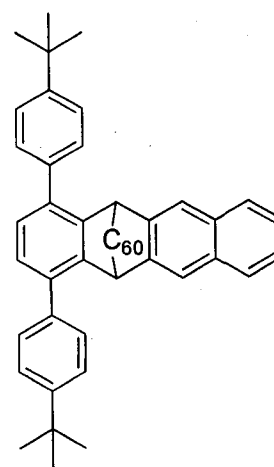
<u>R</u>	<u>R'</u>	
MeO	H	<b>41</b>
CF <sub>3</sub>	H	<b>42</b>
tBu	H	<b>43</b>
CN	H	<b>44</b>
H	CF <sub>3</sub>	<b>45</b>



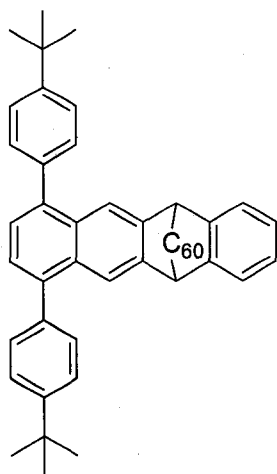
**46a**



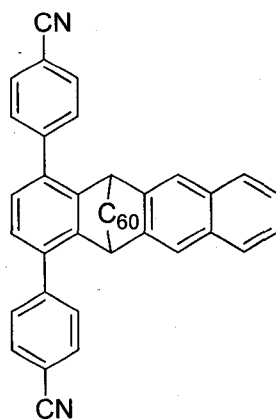
**46b**



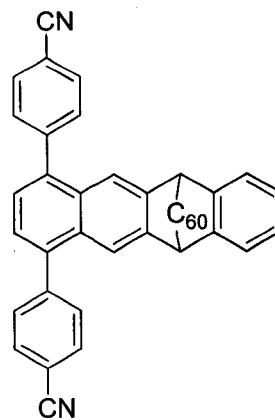
**47a**



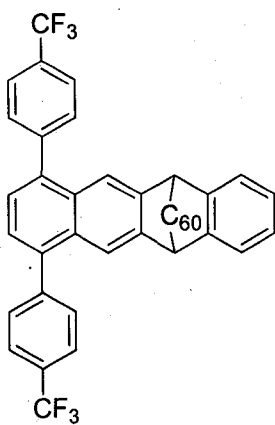
**47b**



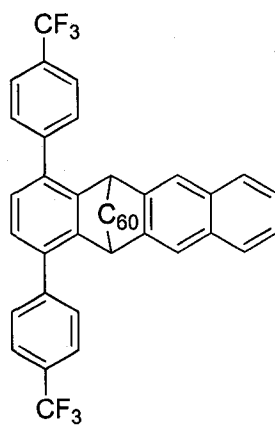
**48a**



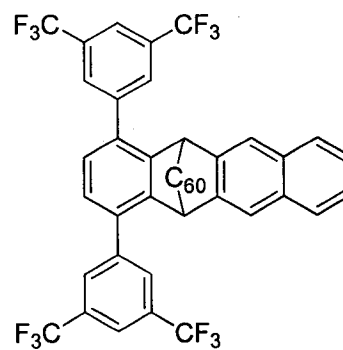
**48b**



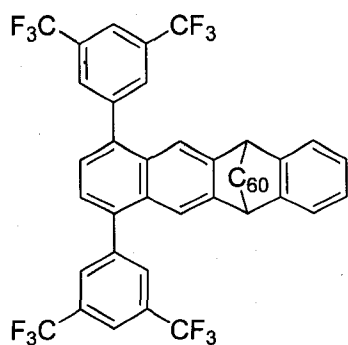
**49b**



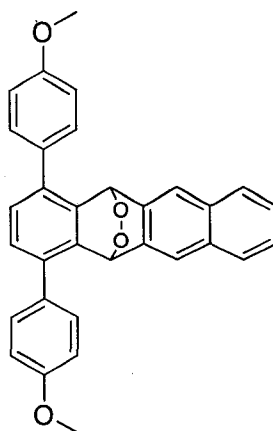
**49a**



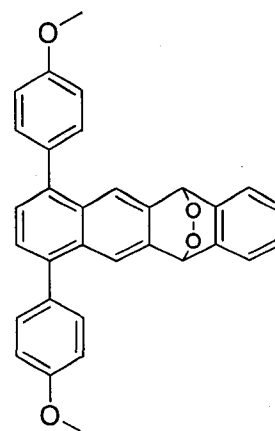
**50a**



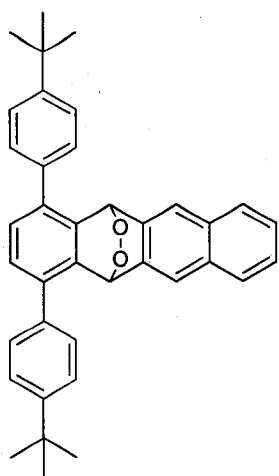
**50b**



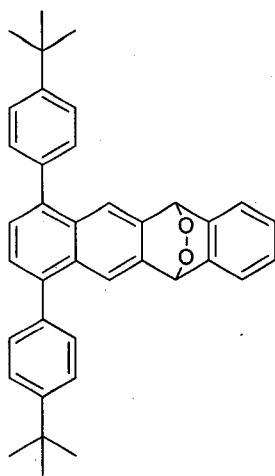
**51a**



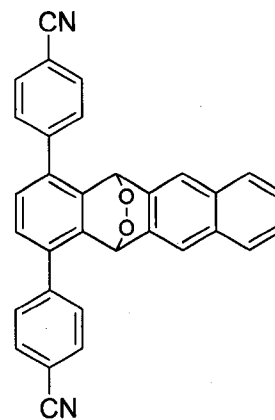
**51b**



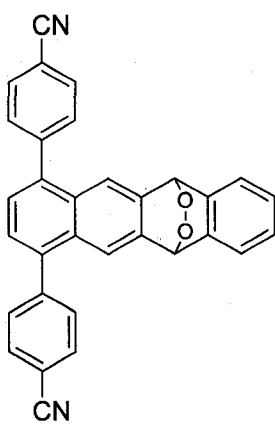
**52a**



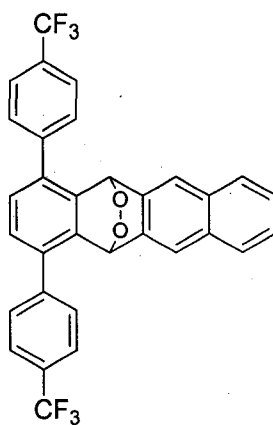
**52b**



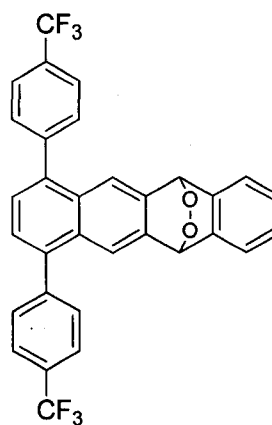
**53a**



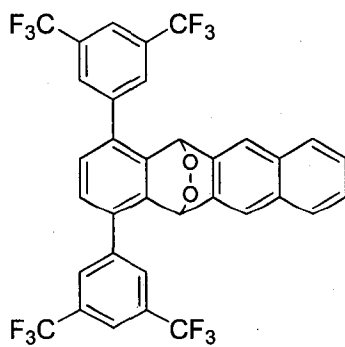
**53b**



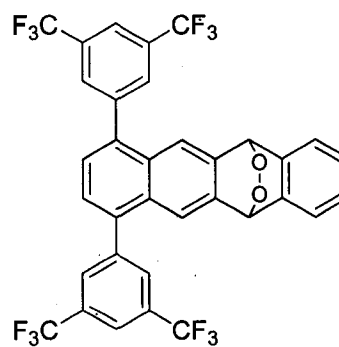
**54a**



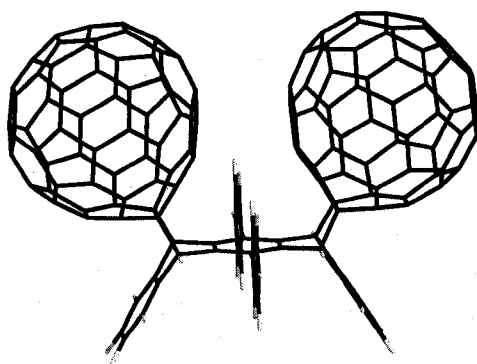
**54b**



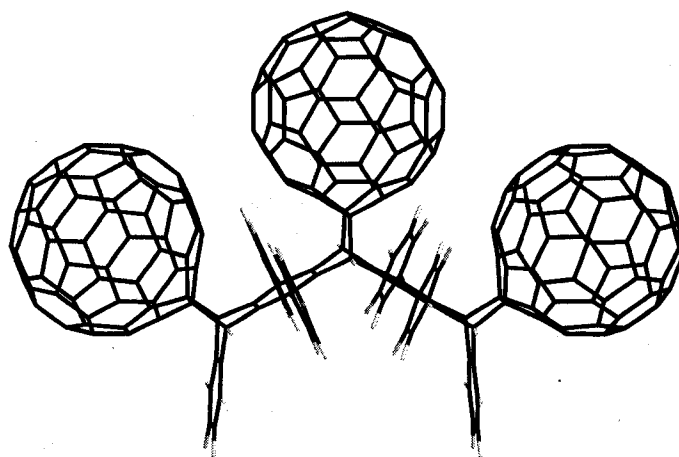
**55a**



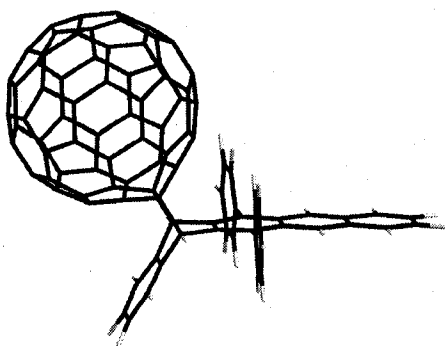
**55b**



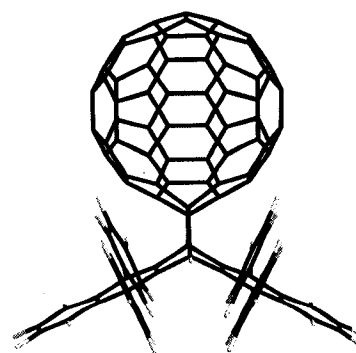
56



57

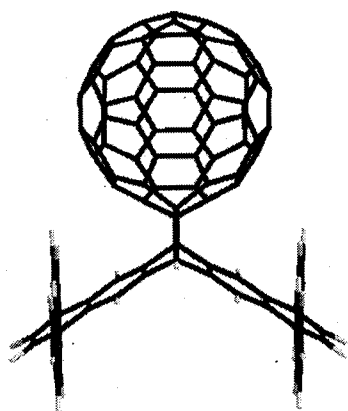


58

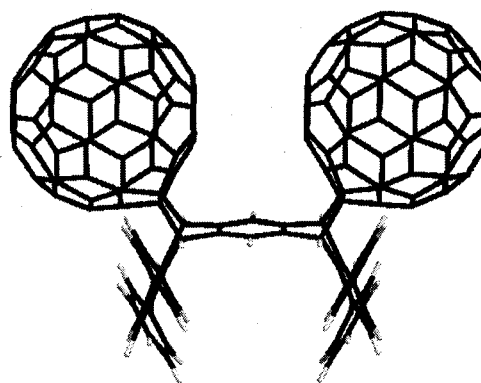


59

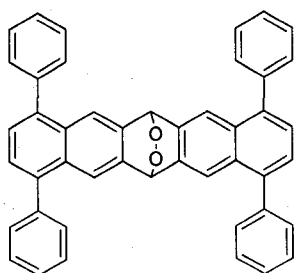




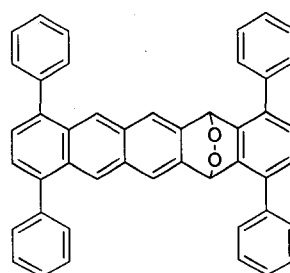
60



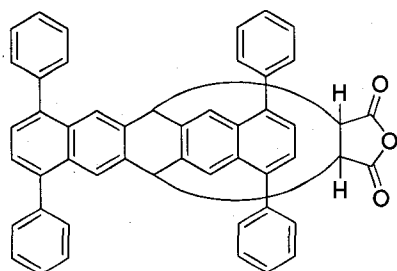
61



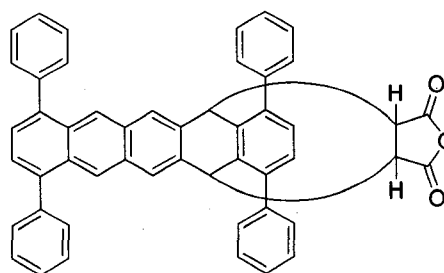
62a



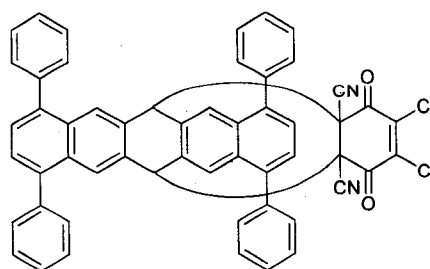
62b



63a



63b



64a

## ABSTRACT

### PROBING REGIOSELECTIVITY IN THE DIELS-ALDER CYCLOADDITIONS BETWEEN [60]FULLERENE AND ARYL SUBSTITUTED ACENES

By

James Eric Rainbolt

University of New Hampshire, December 2007

The formation and reactivity of previously unknown 4,7-diphenylisobenzofuran, **5**, is reported. The Diels-Alder reaction between **5** and *p*-benzoquinone in boiling glacial acetic acid yields an unprecedented *exo,exo anti* dual cycloaddition product, **16b**, in excellent yield and with 100% diastereoselectivity. Differences between the reactivity of **5** and the more common 1,3-diphenylisobenzofuran are highlighted. Reactive **5** is utilized to form the anthracene **11**, tetracene **15**, and pentacene **22**. The latter two compounds are reacted with [60]fullerene to explore the potential role of CH/ $\pi$  interactions in the cycloaddition of [60]fullerene across phenyl substituted acenes. [60]Fullerene shows an unusual propensity for cycloaddition across the 5,12 position of **15** and the 5,14 and 7,12 positions of **22**. This reactivity is compared and contrasted to the reactivity of other dienophiles including dimethyl acetylenedicarboxylate, ethylene, singlet oxygen, maleic anhydride, tetrachloroquinone, and 2,3-dichloro-5,6-dicyanobenzoquinone. NOESY (nuclear Overhauser effect spectroscopy) methods are especially useful for the

discrimination of 5,12 and 6,11 cycloaddition regioisomers of **15** and **41-45**, as well as select Diels-Alder cycloaddition regioisomers of **22**. The Diels-Alder reactivities of [60]fullerene across various aryl substituted derivatives of **15**, compounds **41-45**, are also studied. It is observed that electron donating substituents enhance regioselective [60]fullerene addition across the 5,12 position while electron withdrawing groups reduce 5,12 regioselectivity. Direct evidence for aryl CH–fullerene  $\pi$  interactions comes from a careful examination of  $^1\text{H}$  NMR chemical shifts for the *ortho* phenyl protons in fullerene-acene adducts. A careful review of the Cambridge Crystallographic Database reveals numerous instances of aryl CH/fullerene contacts within 3 Å. The combined results suggest that aryl CH–fullerene  $\pi$  interactions play a significant role in fullerene-acene chemistries. The tantalizing possibility that this interaction involves  $\pi^*$  orbitals on [60]fullerene and  $\sigma$  orbitals on the aryl CH donors, an *inverse electron demand* CH/ $\pi$  interaction, is suggested, but more study is required.

## CHAPTER 1

### INTRODUCTION

#### 1.1 Carbon

Carbon is unique among the elements for its capacity to form an enormous number and diverse array of molecules.<sup>1</sup> This feature led Mother Nature to choose carbon as the framework upon which living systems are built. Consequently, while only the 15<sup>th</sup> most abundant element in the earth's crust, carbon is the 2<sup>nd</sup> most abundant element (23% by mass) in the human body, behind oxygen.<sup>1</sup> The ubiquity of carbon in plants and animals led to the organic branch of chemistry, a division dedicated solely to the study of carbon-containing molecules. Science bestows no other element such particular study. For all of its history, carbon, derived from the Latin *carbo* for charcoal, was known as just two forms: diamond and graphite. Both of these allotropes form deep below the surface of the earth where decayed plant and animal matter are exposed to extreme heat and pressure. Interestingly, diamond and graphite possess vastly different properties, a reflection of the differences in their respective structures.

Diamond is composed of  $sp^3$ -hybridized carbon atoms arranged in a tetrahedral geometry (Figure 1). Each atom is bound via  $\sigma$  bonds to four other atoms. Mined for centuries for its beauty and utility, diamond is a translucent and extraordinarily hard material owing to its tetrahedral lattice. The localized bonding network makes it a good electrical insulator. The name diamond derives from the Greek *adamas* for invincible.

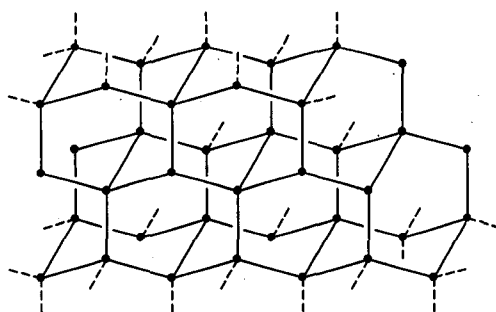


**Figure 1.** The structure of diamond.

The more common allotrope of carbon, graphite, differs sharply from diamond. Graphite is made up of stacked sheets of  $sp^2$ -hybridized carbon atoms (Figure 2). Each carbon is bound to only three other atoms to create sheets of fused hexagonal rings. Each graphene sheet is conjugated through a  $\pi$ -orbital network. The stabilizing  $\pi$ - $\pi$  interaction between these networks causes the sheets to stack 3.35 Å apart.<sup>2</sup> This loose association results in a material which easily sheers along its planar sheets. Hence graphite, in contrast to diamond, is soft and often employed as a lubricant. Graphite is grey to black in appearance, and its  $\pi$  network makes it an excellent electrical conductor. The name graphite comes from the Greek *graphein*, to write or draw.

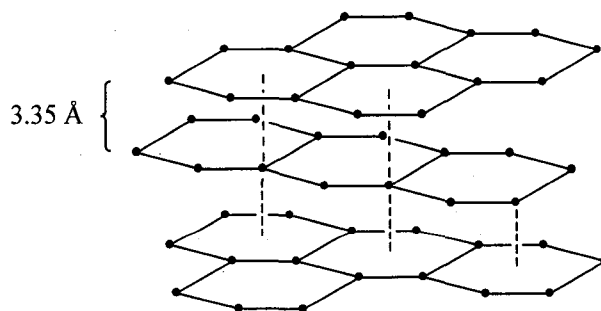


**Figure 2.** The structure of graphite.

Although diamond is much stronger and harder than graphite, the latter is more thermodynamically stable. The heat of formation ( $\Delta H_f^\circ$ ) for diamond is 1.9 kJ/mol (0.45 kcal/mol) greater than that for graphite. However, diamond does not readily transform into graphite, due to high kinetic barriers. The formation of diamond from graphite or amorphous carbon is also slow and proceeds only at extreme pressure and temperature. Until recently these two vastly different allotropes of carbon were the only known. The discovery of [60]fullerene, the first truly all carbon allotrope, would bring about renewed interest in the study of carbon.

## 1.2 [60]Fullerene

### 1.2.1 Discovery of [60]Fullerene

[60]Fullerene was first observed spectroscopically, albeit unknowingly, in 1984 by Rohlffing, Cox, and Kaldor. They exposed graphite to pulsed laser vaporization to generate neutral carbon clusters  $C_n$  for  $n$  ranging from 2 to approximately 200.<sup>3</sup> For those signals corresponding to  $40 < n < 120$ , only even clusters were observed, with a local intensity maximum at  $n = 60$ . They theorized that the even-only distribution was a consequence of clusters composed of polymeric carbyne<sup>4</sup> clusters ( $-C\equiv C-$ ). One year later a group of physicists and chemists from England and the United States, repeating the work of Rohlffing, *et al.*, found graphite vaporization conditions in which the carbon cluster  $C_{n=60}$  formed selectively, along with a minor amount of  $C_{n=70}$ .<sup>5</sup> The researchers theorized that the  $C_{60}$  cluster corresponded to a closed-cage structure (Figure 3). The  $C_{70}$  cluster was also thought to have an analogous cage structure. The researchers, somewhat

tongue-in-cheek,<sup>6</sup> coined the  $C_{60}$  cluster 'Buckminsterfullerene' after the famous architect of geodesmic domes Richard Buckminster Fuller. Their structural hypothesis, confirmed in 1990 with the assistance of Taylor<sup>7</sup> and by Krätschmer and Huffman and co-workers,<sup>8</sup> would earn the co-discoverers of [60]fullerene, Kroto, Smalley and Curl, the Nobel Prize in chemistry in 1996.<sup>2</sup>

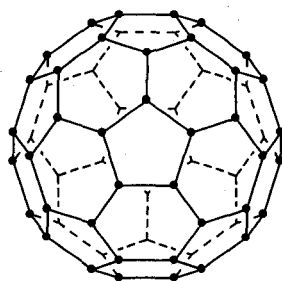


**Figure 3.** The cage structure of [60]fullerene has truncated icosahedral ( $I_h$ ) symmetry.

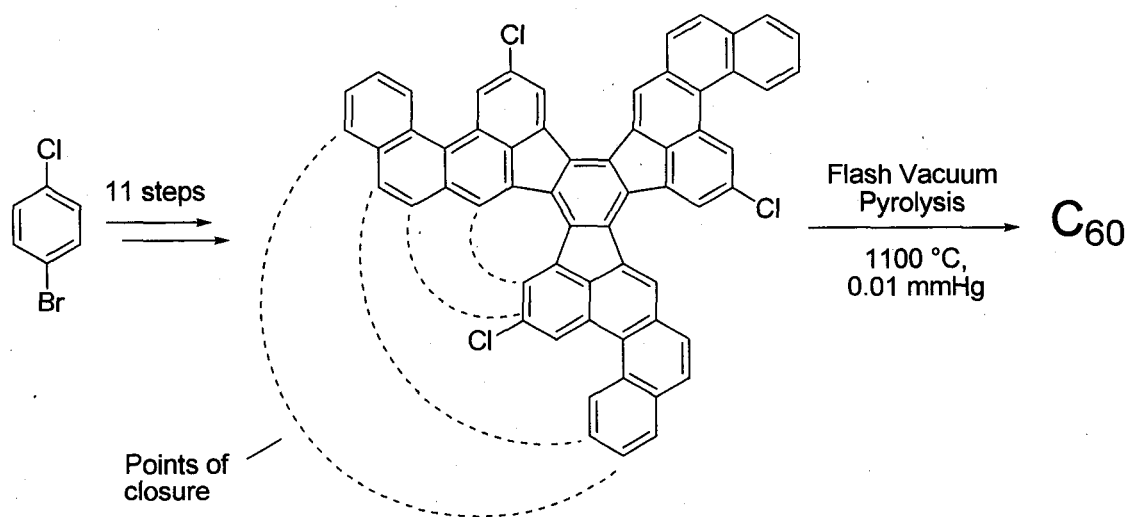
Since the successful identification of [60]fullerene, numerous other higher or giant fullerenes ( $C_n > 70$ ) having closed-cage structures have been isolated from graphite vaporization. The most common<sup>9</sup> of these are  $C_{76}$ ,<sup>10</sup>  $C_{78}$ ,<sup>11,12,13,14</sup> and  $C_{84}$ ,<sup>13,14,15</sup> while other larger fullerenes including  $C_{82}$ ,  $C_{90}$ ,  $C_{94}$  and  $C_{96}$  have also been reported.<sup>16,17</sup>

### 1.2.2 Synthesis of [60]Fullerene

As mentioned earlier, Kroto, Smalley and Curl first found optimal conditions for [60]fullerene formation. The first macroscopic generation of [60]fullerene was published five years later by Krätschmer and Huffman using a carbon arc procedure.<sup>8a</sup> More recently, Nano-C, Inc. has licensed a flame synthesis technology for large scale production of fullerenes. The lone chemical synthesis of [60]fullerene was developed by Scott and co-workers in 2002.<sup>18</sup> They synthesized the strategically chlorinated

hydrocarbon of Scheme 1 in 11 steps. Under flash vacuum pyrolysis conditions the arms of the chlorinated hydrocarbon ‘stitch’ together to form [60]fullerene, at the exclusion of all other fullerenes, in modest yield (estimated 0.1-1%). Although low yielding, Scott’s approach stands as the only rational synthesis of [60]fullerene and demonstrates a novel approach to building highly curved polycyclic aromatic hydrocarbons.<sup>19,20</sup>

**Scheme 1.** Scott and co-workers’ rational synthesis of [60]fullerene.



### 1.2.3 Physical Properties of [60]Fullerene

[60]Fullerene is the most abundant and, consequently, the most studied of the fullerenes.<sup>2,21,22</sup> The 60 chemically equivalent sp<sup>2</sup>-hybridized carbon atoms are arranged as 5-membered rings surrounded on all sides by 6-membered rings, as is the case in corannulene<sup>23</sup> (Figure 4).



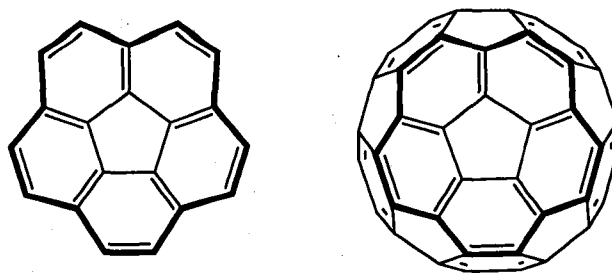


**Figure 4.** The carbon skeleton of corannulene (left) maps directly onto [60]fullerene (right).

This bonding pattern yields a truncated icosahedral cage composed of 12 pentagonal and 20 hexagonal rings with an overall diameter of 7 Å. Conspicuously, the geometric attributes of [60]fullerene ensure that no two 5-membered rings share an edge. Indeed, this geometrical motif is a prerequisite of fullerene stability and is recognized as the ‘isolated pentagon rule’.<sup>24</sup> [60]Fullerene is the smallest fullerene structure that can house isolated 5-membered rings.<sup>24c</sup> Another curious attribute of [60]fullerene is its propensity to spin in the solid state. The spherical nature of the cage permits room temperature rotational rates<sup>25</sup> in excess of  $10^9 \text{ s}^{-1}$  as measured by  $^{13}\text{C}$  NMR spectroscopy.<sup>25a</sup> This rapid rotation limits X-ray analysis of [60]fullerene to substituted derivatives only.

Although every atom in [60]fullerene is chemically equivalent, there are in fact two distinct bond types. They are the 6,6-bond and the 5,6-bond, where the former is the bond between two fused 6-membered rings and the latter is the bond adjoining 5- and 6-membered rings (Figure 5). The 6,6-bond is  $1.39 \text{ Å}$ <sup>26,27</sup> in length and appreciably shorter than the 5,6-bond, reported at both  $1.43 \text{ Å}$ <sup>26</sup> and  $1.46 \text{ Å}$ <sup>27</sup> in length. As a result, the 6,6-bond shows more double bond character while the 5,6-bond has more single bond character.

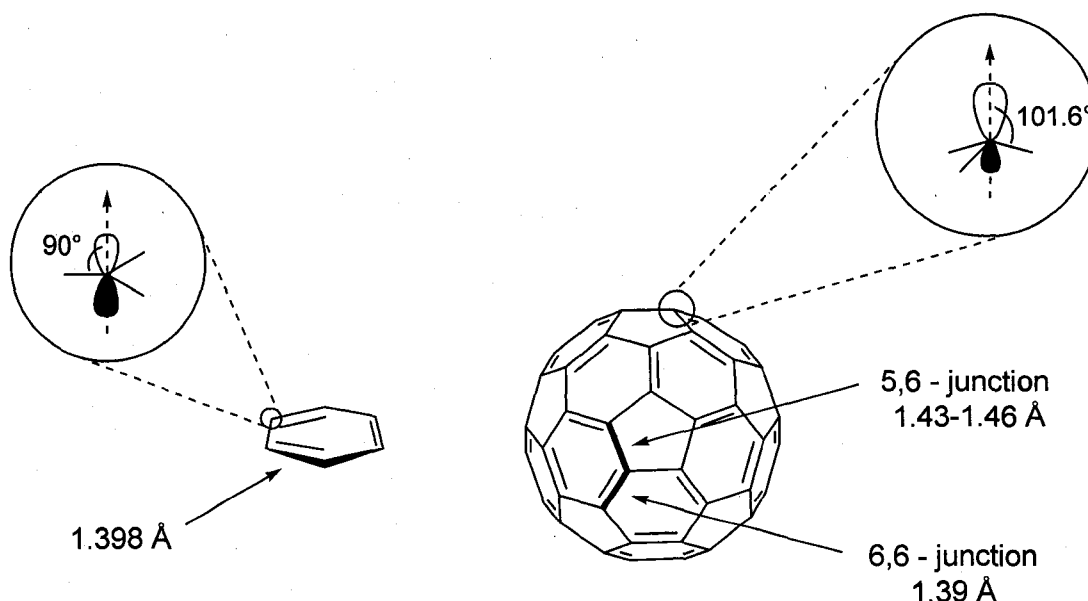


**Figure 5.** Bond lengths and pyramidalization in benzene (left) and [60]fullerene (right).

Although theorized as the gateway to superaromatic molecules,<sup>28</sup> [60]fullerene lacks key characteristics expected for an aromatic, let alone superaromatic, system.<sup>29</sup> While benzene shows special (*i.e.*, aromatic) stabilization and equal bond lengths,<sup>30</sup> [60]fullerene demonstrates no special stabilization, distinct bond length alternation, and increased reactivity. Indeed, [60]fullerene undergoes nucleophilic addition and cycloaddition reactions, chemistries akin to olefin reactivity as opposed to aromatic reactivity. The relative reactivity of [60]fullerene is attributed to the pyramidalization of the carbon atoms brought about by the curved nature of the cage (Figures 5 and 6).

The pyramidalization of [60]fullerene was first described mathematically by Haddon using his  $\pi$ -orbital axis vector (POAV) analysis.<sup>31</sup> It defines the degree of pyramidalization of an  $sp^2$ -hybridized carbon atom as  $\theta_{\sigma\pi} - 90^\circ$ , where  $\theta_{\sigma\pi}$  is the angle between the vectors of the p and  $sp^2$  orbitals (Figure 6). In planar aromatic hydrocarbons

the p and  $sp^2$  orbitals are orthogonal and, consequently, the pyramidalization angle is zero. For non-planar systems, curvature results in varying degrees of pyramidalization.

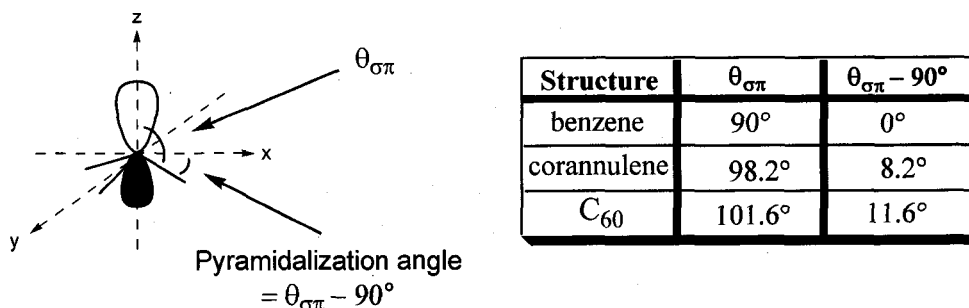


**Figure 6.** Haddon's pyramidalization; table of pyramidalization angles of select PAHs and [60]fullerene.

For the bowl-shaped conformation of corannulene, the pyramidalization angle is  $8.2^\circ$  at the 5-membered ring.<sup>32</sup> For [60]fullerene, the locked spheroidal nature of the cage imparts a pyramidalization angle of  $11.6^\circ$ .<sup>32</sup> This strong degree of pyramidalization of [60]fullerene results in hybridization of the carbon atoms such that the  $\pi$  orbitals take on some s-character and, in turn, greater p-character is exhibited in the  $\sigma$ -bond framework. The result is a 0.085 fraction of s-character in the  $\pi$ -orbitals, while the  $\sigma$ -bond framework consists of  $sp^{2.278}$  hybridized orbitals.<sup>31</sup>

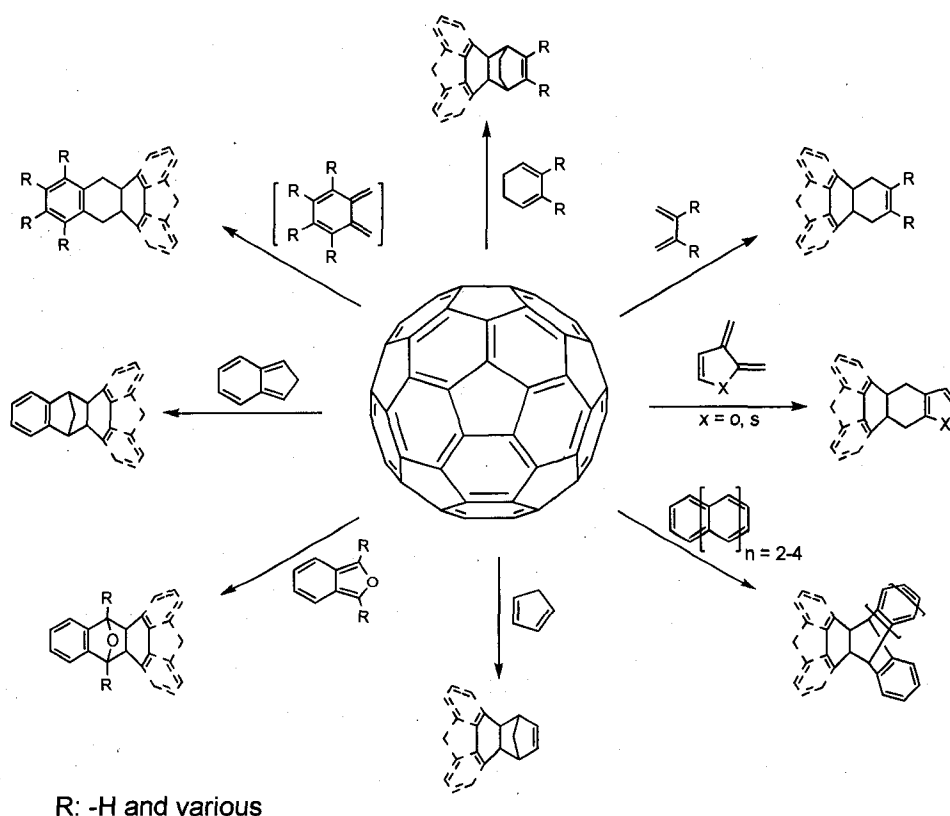
Lacking the kind of aromatic stabilization enjoyed by planar aromatic hydrocarbon systems, [60]fullerene shows enhanced reactivity. This reactivity is driven by the relief of strain. In fact, strain energy makes up approximately 80% of  $\Delta H_f^\circ$  for [60]fullerene.<sup>33</sup> For comparison,  $\Delta H_f^\circ$  for [60]fullerene is approximately 10 kcal/mol per carbon atom<sup>34</sup> while for diamond and graphite it is 0.4 and 0 kcal/mol per carbon atom, respectively. The reactions in which [60]fullerene engages to relieve this strain include hydrogenation, halogenation, nucleophilic and radical addition, as well as cycloaddition

reactions.<sup>2,21</sup> Of these chemistries, the Diels-Alder reactivity of [60]fullerene is of greatest relevance to this work.

#### 1.2.4 Diels-Alder Chemistry of [60]Fullerene

[60]Fullerene behaves more like an electron deficient olefin than an aromatic hydrocarbon, leading to its enhanced Diels-Alder reactivity. Predictably, cycloaddition occurs exclusively across the shorter 6,6-bond.<sup>35,36</sup> [60]Fullerene reacts with various dienes including butadienes,<sup>37</sup> 1,3-cyclohexadienes,<sup>37c,d</sup> *ortho*-quinodimethanes,<sup>36,38</sup> isobenzofurans<sup>39</sup> and isoindene,<sup>40</sup> cyclopentadiene,<sup>41,42,43</sup> acenes (see section 1.3.4.1), and exocyclic *ortho*-quinodimethane analogs of furans<sup>44</sup> and thiophenes<sup>45</sup> (Scheme 2).

**Scheme 2.** [60]Fullerene cycloadds to a variety of dienes.



Multiple diene additions to the surface of [60]fullerene are also possible. Hirsh, *et al.* performed a systematic analysis of the regiochemistry associated with polyadducts (Figure 7).<sup>46</sup> Addition of an addend to a functionalized [60]fullerene monoadduct of  $C_{2v}$  symmetry can proceed to generate 8 unique bisadducts.

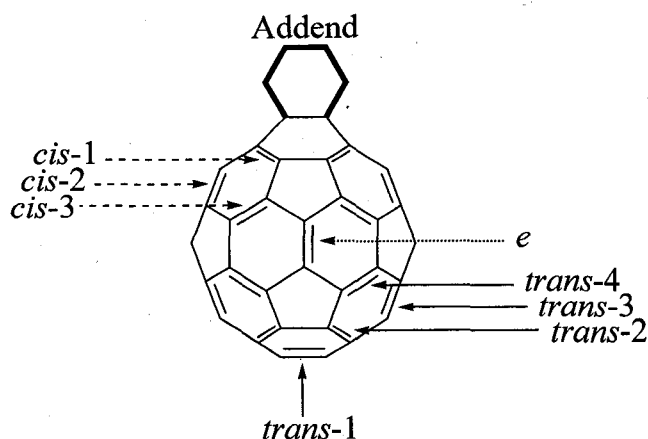
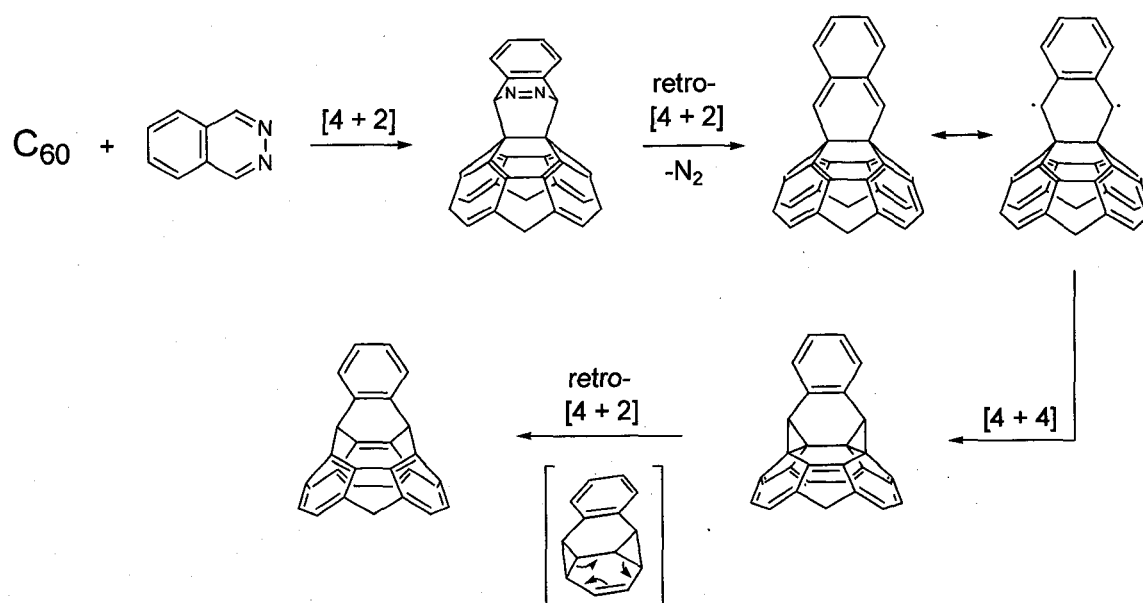


**Figure 7.** The eight distinct sites for addition to a  $C_{2v}$  [60]fullerene monoadduct.

Pang and Wilson reported a kinetics study of the cycloaddition of cyclopentadiene with both  $C_{60}$  and  $C_{70}$ .<sup>47</sup> The smaller fullerene reacts 7 times faster than the larger and multiple additions proceed across the surface of both  $C_{60}$  and  $C_{70}$ . In some cases the Diels-Alder adducts of [60]fullerene are labile, undergoing retro-Diels-Alder reaction at relatively low temperatures. This is the case for [60]fullerene adducts of anthracene<sup>42</sup> and isobenzofurans,<sup>39c,d</sup> which have been shown to undergo retro [4 + 2] reactions in solution at temperatures as low as 60 °C and 45 °C, respectively. On the other hand, Murata, *et al.*<sup>48,49</sup> used [4+2] cycloaddition adducts as gateways to open-cage fullerenes.<sup>50</sup> They used the cycloaddition adduct of [60]fullerene and phthalazine to generate, after multiple

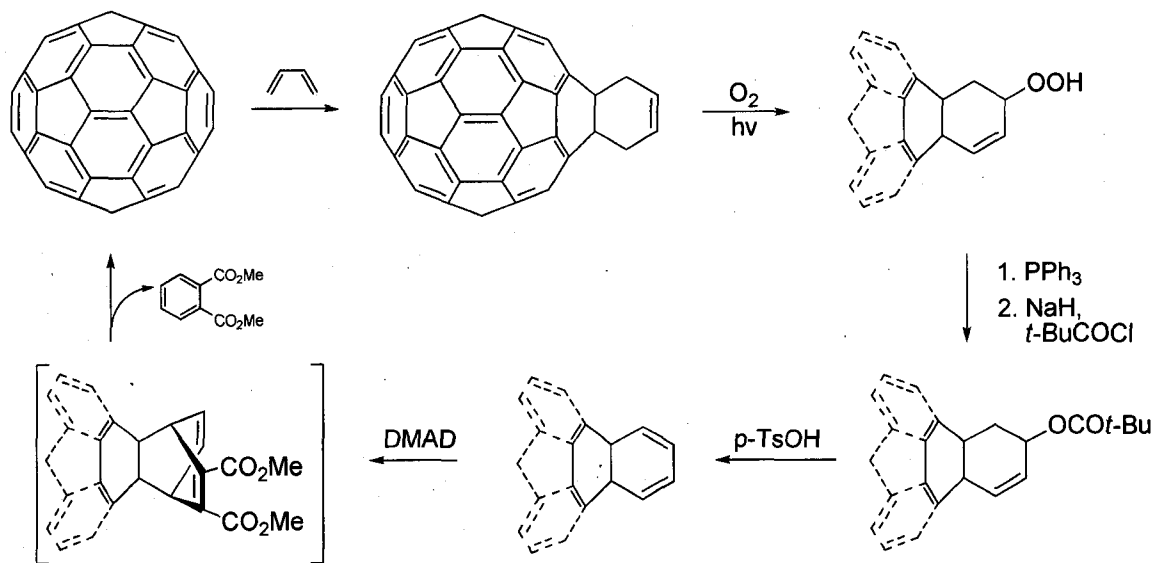
pericyclic reactions, an open-cage fullerene derivative with an 8-membered ring<sup>48a</sup> (Scheme 3).

**Scheme 3.** Murata and co-workers' synthesis of an open-cage fullerene.



Rubin and co-workers used Diels-Alder chemistry to successfully add and remove a carbocyclic fragment from [60]fullerene as part of solublizing/protecting scheme (Scheme 4).<sup>51</sup>

**Scheme 4.** Rubin and co-workers' carbocyclic protection/deprotection of [60]fullerene.



Nakamura, *et al.* synthesized a series of ortho-quinodimethane functionalized [60]fullerenes (Figure 8).<sup>52</sup> They found that the redox potentials, absorption spectra and fluorescence spectra of the adducts were virtually identical. Thus, they concluded that the electronic properties of the [60]fullerene moieties in all the adducts were independent of the addend makeup.

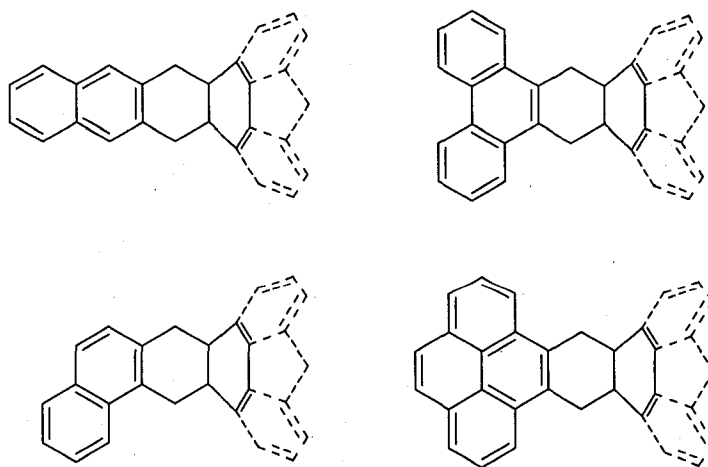
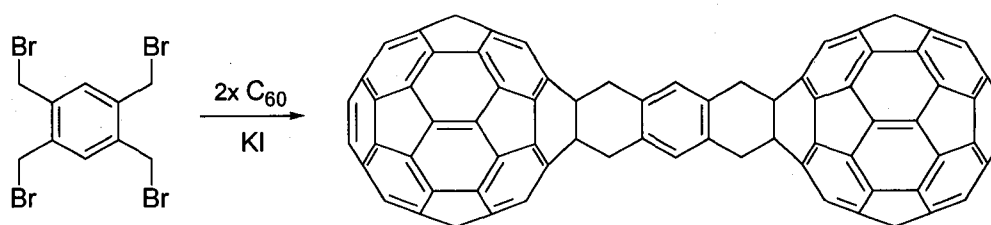


**Figure 8.** Nakamura and co-workers' *ortho*-quinodimethane benzolog adducts of [60]fullerene.

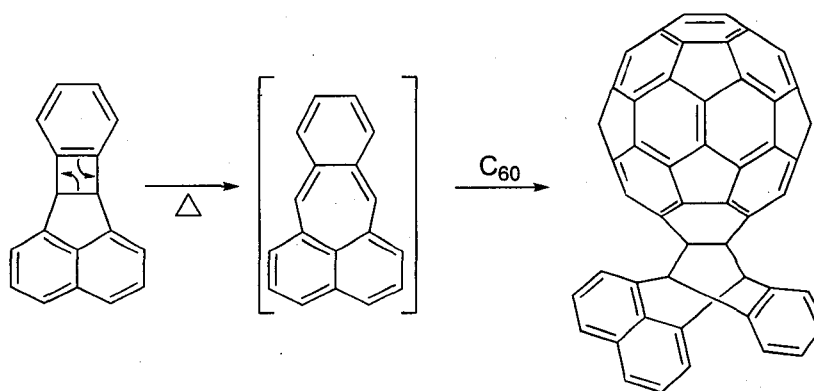
Müllen and co-workers also synthesized *ortho*-quinodimethane adducts of [60]fullerene, including a dumbbell shaped bis-*ortho*-quinodimethane adduct by treatment of tetrakis(bromomethyl)benzene with potassium iodide and an excess of [60]fullerene (Scheme 5).<sup>53</sup>

**Scheme 5.** Formation of bis[60]fullerene adduct of bis *o*-quinodimethane.



Taki, *et al.* reacted [60]fullerene with an exotic, in situ generated benzoacenaphthylene diene to yield the adduct (Scheme 6).<sup>54</sup>

**Scheme 6.** Taki and co-workers' trapping of an unusual acenaphthylene diene with [60]fullerene.





## 1.3 Acenes

### 1.3.1 Properties of Acenes

An acene is defined as a linear array of fused benzenoid rings (Figure 9).<sup>55</sup> Acenes are a subclass of the polycyclic aromatic hydrocarbon (PAH) family. A PAH is any hydrocarbon comprised of multiple, typically fused, aromatic rings. The sequential linear fusion of benzene rings that defines acenes is referred to as *cata*-annellation. Thus, tetracene is an example of *cata*-annelated anthracene and benzene. The name acene derives from the common suffix of its members, as in *anthracene*.

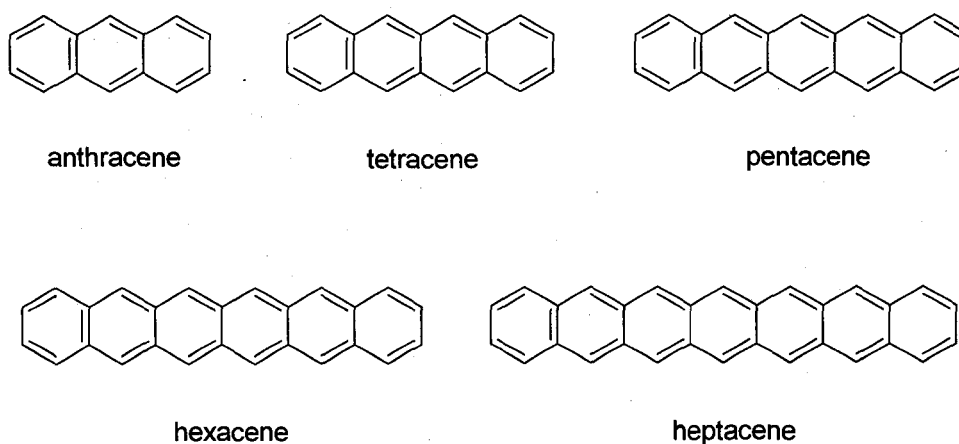


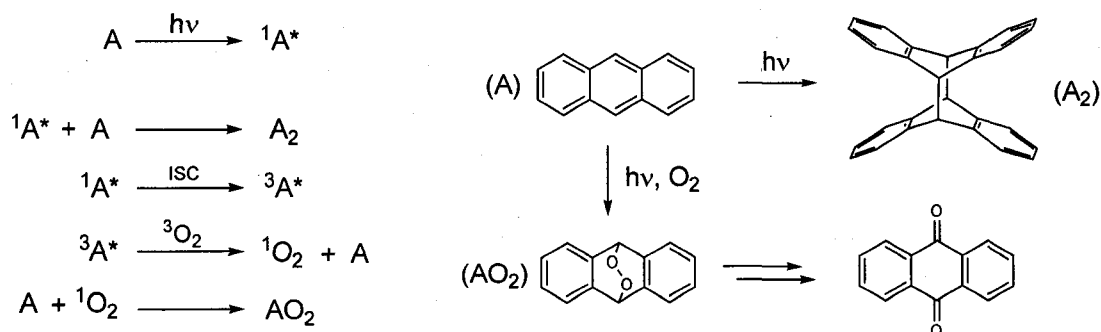
**Figure 9.** The structures of the known acenes.

Acenes vary in their properties. Anthracene is an off-white solid and the smallest and most stable of the acenes. Tetracene is a bright orange solid that solubilizes sparingly in common organic solvents. It is moderately reactive, bridging the reactivity gap between the comparatively stable anthracene and the reactive pentacene and hexacene. Pentacene is a blue solid which is virtually insoluble in organic solvents and readily

oxidizes in solution in the presence of light and air. Hexacene is green, oxidizes rapidly in solution, and is regarded as the largest isolable, well characterized acene.<sup>56,57</sup> Neckers and co-workers found that hexacene generated and trapped within a poly(methyl methacrylate) (PMMA) matrix persists for more than 12 hours under ambient conditions.<sup>57</sup> The largest of the reported acenes is heptacene. Its synthesis was claimed in two older reports,<sup>58,59</sup> both of which were later repudiated.<sup>60</sup> Neckers and co-workers successfully generated heptacene and found it incredibly reactive, adding oxygen immediately in solution and surviving for only 4 hours when generated within a PMMA matrix.<sup>61</sup>

Thus, acene stability decreases rapidly with annelation. The primary modes of acene degradation are photooxidation and photodimerization. Photooxidation is more common in large acenes while photodimerization is more frequently observed in smaller acenes. The photodimerization and photooxidation of anthracene were described in detail by Bowen and Tanner.<sup>62</sup> Photodimerization proceeds via addition of singlet excited state anthracene to ground state anthracene, addition proceeding across the central acene rings (Scheme 7).<sup>63</sup> The photodimer has been synthesized in common organic solvents<sup>64</sup> as well as supercritical CO<sub>2</sub><sup>65</sup> and is reversible.<sup>66</sup> While photodimerization dominates under deoxygenated conditions, photooxidation prevails in oxygenated solutions.<sup>67</sup> Photooxidation results eventually in formation of the quinone but proceeds first by the addition of singlet oxygen to ground state anthracene (Scheme 7). As described by Katz and co-workers, this *endo*-peroxide then cleaves at the oxygen-oxygen bond, rearranges to 9-hydroxyanthrone, and finally loses hydrogen to yield the quinone.<sup>68</sup>

**Scheme 7.** The photodimerization and photooxidation of anthracene.



The reactivity of large acenes ( $\geq 6$  rings) severely limits their experimental study. Consequently, a number of computational papers have been published to address the nature and properties of large acenes. Schleyer, *et al.* concluded that the inner rings of acenes are more, not less, aromatic than benzene itself, based on nucleus independent chemical shift (NICS) values.<sup>69</sup> The experimentally observed regioselective cycloaddition of dienophiles across these inner rings is rationalized as “due to the smaller aromaticity loss during reactions of the central rings.” Houk and Bendikov used density functional theory (DFT) to predict that hexacene and larger acenes would exist as open-shell ground state singlets and exhibit behavior akin to two polyacetylene chains linked by elongated bonds.<sup>70,71</sup>

### 1.3.2 Synthesis of Acenes

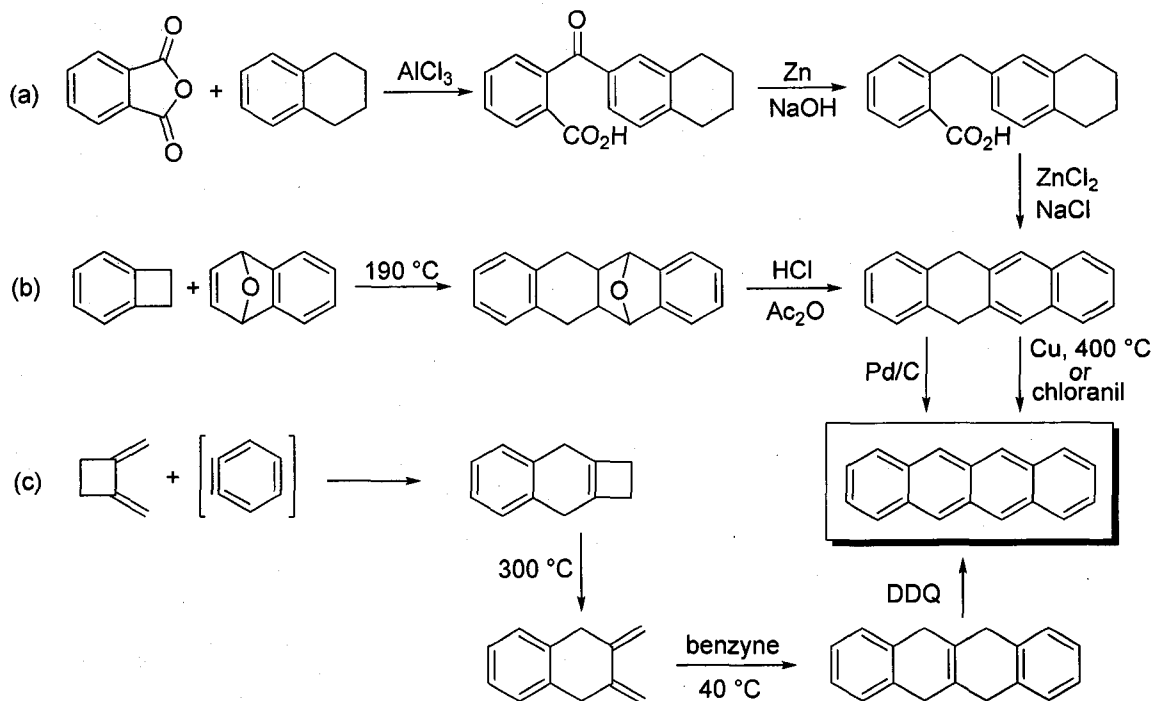
The syntheses of acenes, along with numerous other PAHs, were first developed and summarized by Erich Clar.<sup>72</sup> Clar’s syntheses typically begin with Friedel-Crafts acylation followed by ring-closures, reductions and oxidations. Since Clar’s pioneering work, Diels-Alder chemistry has been used extensively in the formation of acenes. As

[4+2] cycloaddition reactions form 6-membered rings, Diels-Alder chemistry lends itself well to acene synthesis.

### 1.3.2.1 Tetracene Syntheses

The first synthesis of tetracene, performed by Clar, begins with the condensation of phthalic anhydride with tetralin via Friedel-Crafts acylation (Scheme 8a).<sup>73</sup> The resulting keto-acid was reduced with zinc in basic media and then converted, using a  $\text{ZnCl}_2/\text{NaCl}$  melt, to 5,12-dihydrotetracene. Preparation of the tetracene target was accomplished via either choranyl oxidation or heating in the presence of copper.

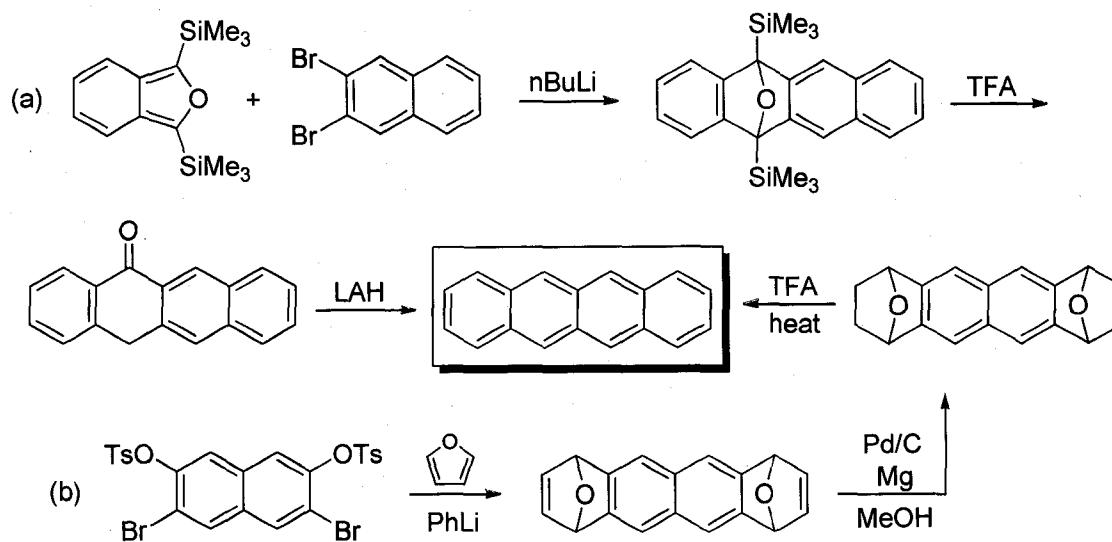
**Scheme 8.** Syntheses of tetracene. (a) Clar's original synthesis of tetracene; (b) Hart and Lou's synthesis of tetracene; (c) Thummel, Carvey and Nutakulalso's synthesis of tetracene.



Since Clar's original work, Diels-Alder chemistries have dominated tetracene syntheses. Hart and Luo reacted *o*-quinodimethane, generated *in situ* from benzocyclobutene, with 1,4-epoxynaphthalene to generate the Diels-Alder product (Scheme 8b).<sup>74</sup> This adduct was then sequentially dehydrated in HCl/Ac<sub>2</sub>O and oxidized with palladium on carbon to yield the desired tetracene. Thummel, Cravey and Nutaku also synthesized tetracene utilizing benzyne (Scheme 8c).<sup>75</sup> The researchers reacted benzyne with 1,2-methylenecyclobutane to generate, after thermal ring opening, 1,4-dihydro-*o*-naphthodimethane. Addition of the diene to another equivalent of benzyne yielded 5,6,11,12-tetrahydrotetracene which was converted to tetracene via 2,3-dichloro-5,6-dicyano-*p*-benzoquinone (DDQ) oxidation.

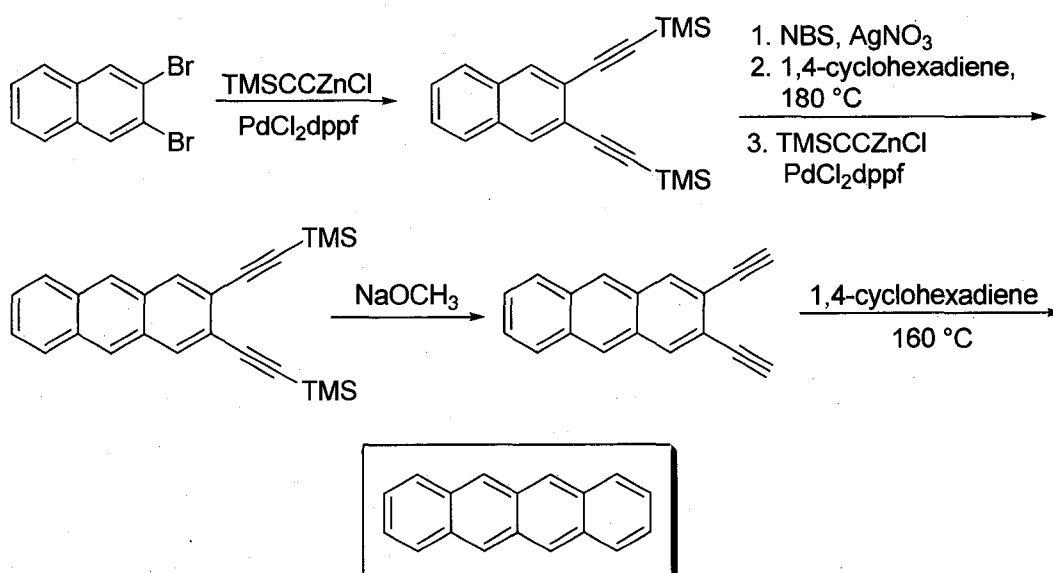
Furanoids have also been used to synthesize tetracene (Scheme 9). Rickborn, Netka and Crump reacted 1,3-di(trimethylsilyl)isobenzofuran with transient naphthalene

**Scheme 9.** Syntheses of tetracene. (a) Rickborn and co-workers' synthesis of tetracene; (b) Gribble and co-workers' synthesis of tetracene.



to generate 5,12-di(trimethylsilyl)-5,12-epoxytetracene (Scheme 9a).<sup>76</sup> Treatment of this adduct with trifluoroacetic acid resulted in 5(12*H*)-naphthacenone. Subsequent lithium aluminum hydride reduction/dehydration yielded tetracene. Gribble, Perni and Onan utilized arynes and furans to synthesize a number of PAHs, including tetracene (Scheme 9b).<sup>77</sup> After dual cycloaddition of furan to transient bisnaphthalynes, the diepoxide was hydrogenated and then dehydrated to yield tetracene. In a rare break from Diels-Alder based synthetic strategies, Bowles and Anthony used a reiterative Bergman cyclization<sup>78</sup> technique to synthesize tetracene (Scheme 10).<sup>79</sup>

**Scheme 10.** Bowles and Anthony's reiterative synthesis of tetracene.

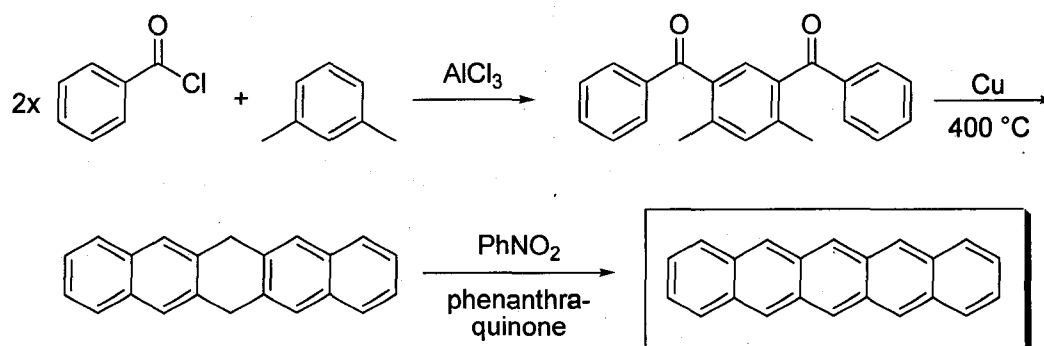


### 1.3.2.2 Pentacene Syntheses

Pentacene has garnered much interest due to its material electronic properties.<sup>80</sup> Accordingly, pentacene syntheses are abundant.<sup>55</sup> The original synthesis was performed by Clar, beginning with a dual Friedel-Crafts acylation of *m*-xylene using benzoyl

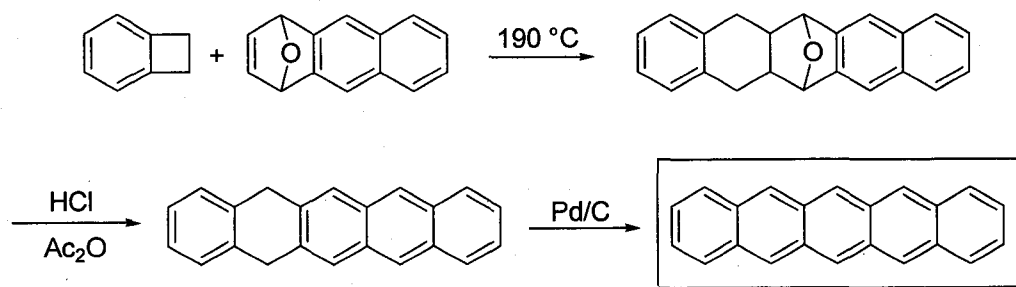
chloride to produce an alkylated diketone (Scheme 11).<sup>81</sup> Heating of the diketone in the presence of copper led to 6,13-dihydropentacene. Subsequent dehydrogenation yielded the target pentacene.

**Scheme 11.** Clar's original synthesis of pentacene.



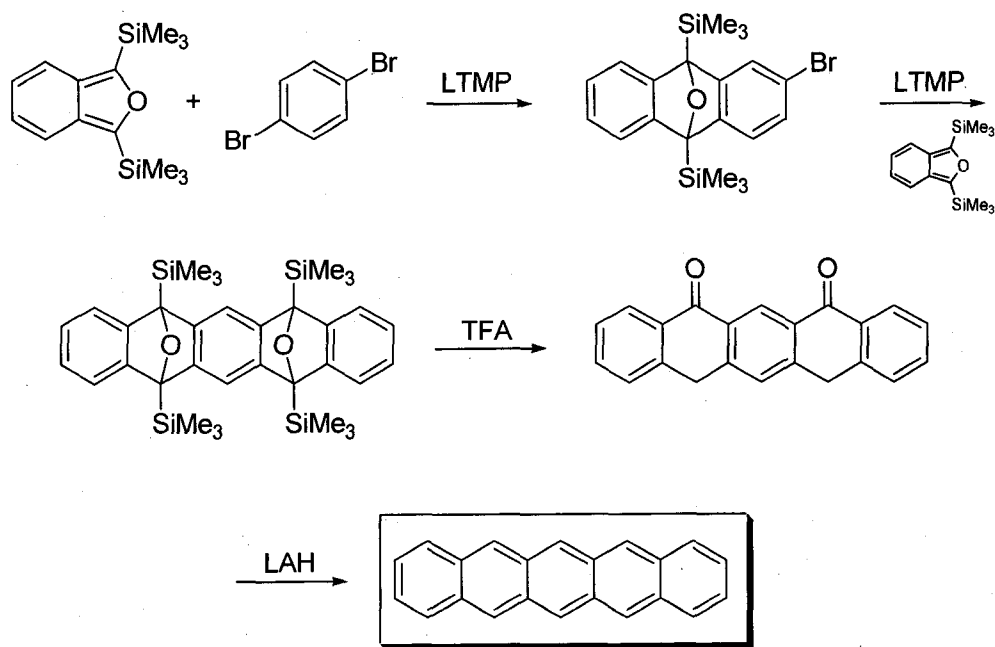
Hart and Luo synthesized pentacene in a fashion similar to their synthesis of tetracene (Scheme 8b) starting from benzocyclobutene and 1,4-epoxyanthracene (Scheme 12).<sup>74</sup> Rickborn, Netka and Crump also synthesized pentacene in a manner analogous to

**Scheme 12.** Hart and Luo's synthesis of pentacene.



their synthesis of tetracene (Scheme 9a), starting from 1,3-di(trimethylsilyl)isobenzofuran and the bisbenzyne precursor 1,4-dibromobenzene (Scheme 13).<sup>76</sup>

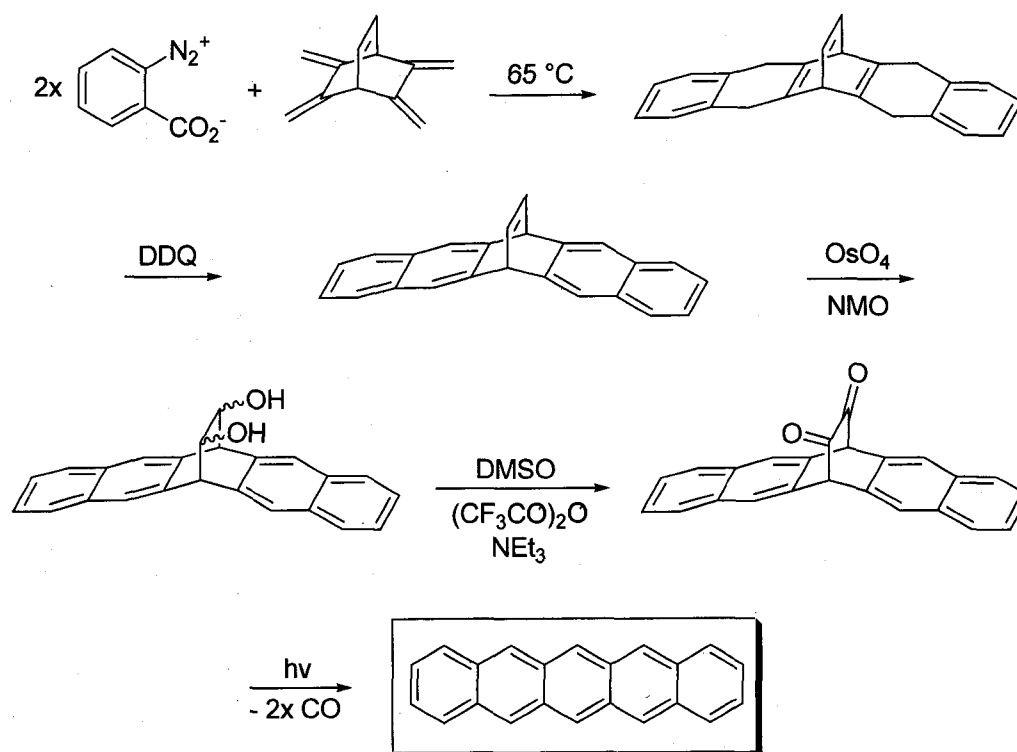
**Scheme 13.** Rickborn, Netka and Crump's synthesis of pentacene.



Recently Yamashita, Ogawa and Ono synthesized pentacene from a photochemical precursor (Scheme 14).<sup>82</sup> Addition of two equivalents of benzyne to a tetramethylene barrelene yielded, after DDQ oxidation, the 6,13-acetylene bridged pentacene. Sequential OsO<sub>4</sub> and Swern oxidations yielded the  $\alpha$ -diketone. This dione was then converted to pentacene via photolytic extrusion of carbon monoxide.

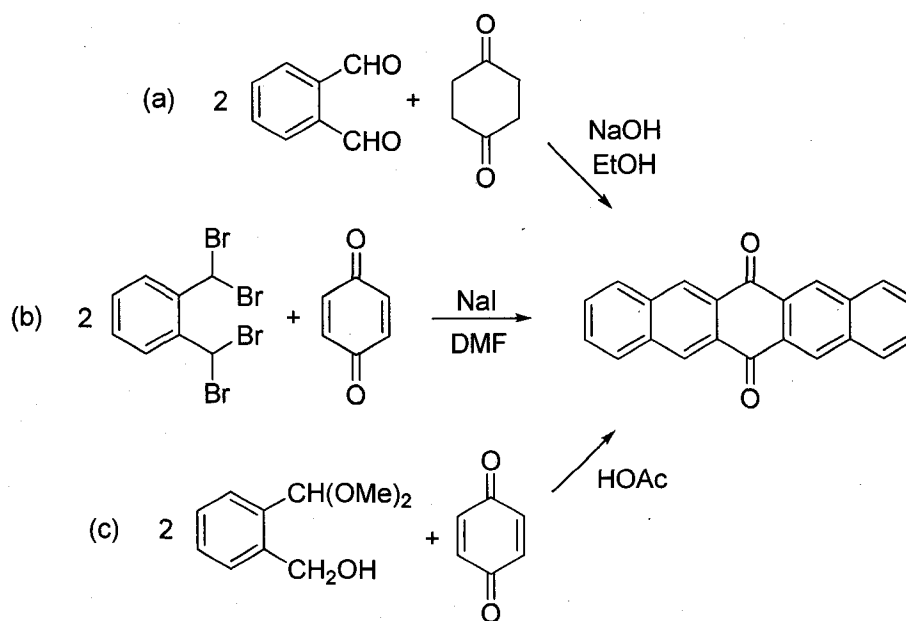


**Scheme 14.** Yamashita and co-workers' synthesis of pentacene via a photochemical precursor.



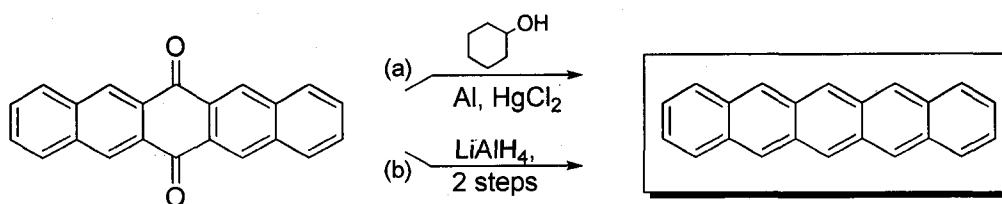
Currently the most common route to pentacene proceeds through 6,13-pentacenequinone. This quinone is a popular precursor due to the ease of its synthesis (Scheme 15) and the possibility of adding functionality to the 6,13 positions in subsequent synthetic steps.

**Scheme 15.** Known syntheses of 6,13-pentacenequinone.



Multiple short, high yielding routes to this quinone are known, including the tandem aldol condensation of commercially available phthalaldehyde and 1,4-cyclohexanedione (Scheme 15a),<sup>83,84</sup> reaction between commercially available  $\alpha,\alpha,\alpha',\alpha'$ -tetrakis(bromomethyl)*o*-xylene and *p*-benzoquinone (Scheme 15b)<sup>85,86</sup> and dual isobenzofuran addition to *p*-benzoquinone (Scheme 15c).<sup>87</sup> Likewise routes from 6,13-pentacenequinone to pentacene are also known (Scheme 16).

**Scheme 16.** Known syntheses of pentacene from 6,13-pentacenequinone.

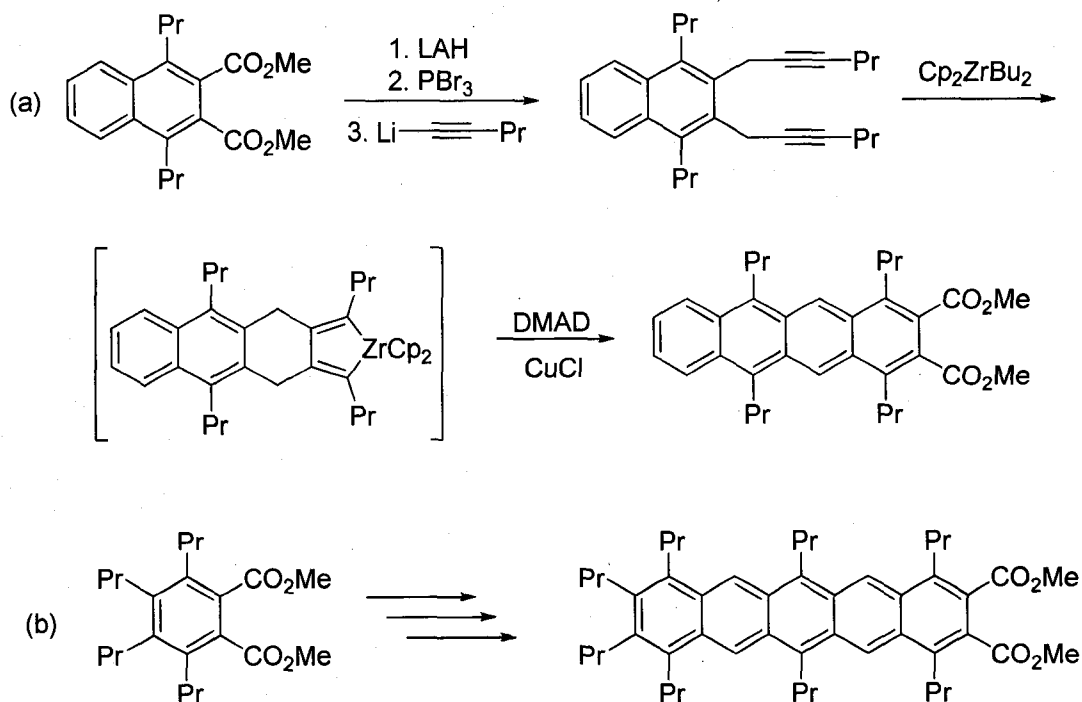


These include a Meerwein-Pondorf-Verley reduction (Scheme 16a)<sup>88</sup> and a sequential lithium aluminum hydride reduction technique (Scheme 16b).<sup>84</sup>

### 1.3.3 Substituted Acenes

Substituted acenes have received much attention as either stabilized or soluble alternatives to the unsubstituted parent. Wong and co-workers synthesized 2,3,9,10-tetrakis(trimethylsilyl)pentacene which showed increased solubility over pentacene but increased reactivity as well.<sup>89</sup> Takahashi, *et al.* developed a repetitive homologation technique to synthesize alkyl-substituted tetracene (Scheme 17a) and pentacene (Scheme 17b).<sup>90</sup>

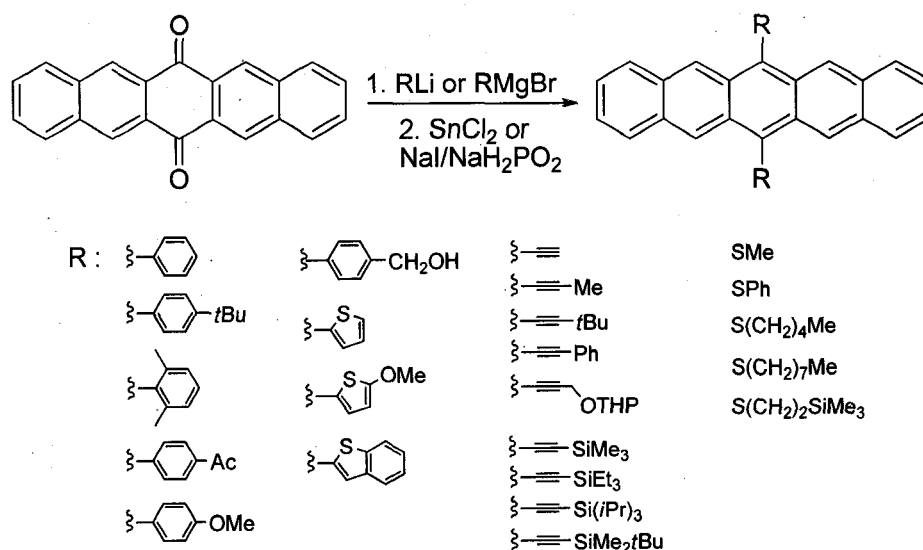
**Scheme 17.** Takahashi and co-worker's repetitive homologation technique to synthesize alkyl-substituted tetracene (a) and pentacene (b).



The substituents were found to improve both the solubility and stability of the corresponding acenes.

Numerous 6,13-disubstituted pentacenes have been synthesized from 6,13-pentacenequinone (Scheme 18). The first 6,13-disubstituted pentacene was 6,13-diphenylpentacene, synthesized by Allen and Bell in 1942.<sup>91</sup> Since then an array of analogs have been prepared with aryl groups,<sup>85,92,93</sup> thiophene groups,<sup>93</sup> and numerous ethynyl groups.<sup>85,94</sup> These syntheses are typically accomplished by sequential organometallic insertion and aromatization. In the case of thioethers, a slightly different approach from the corresponding thiols was used.<sup>95</sup>

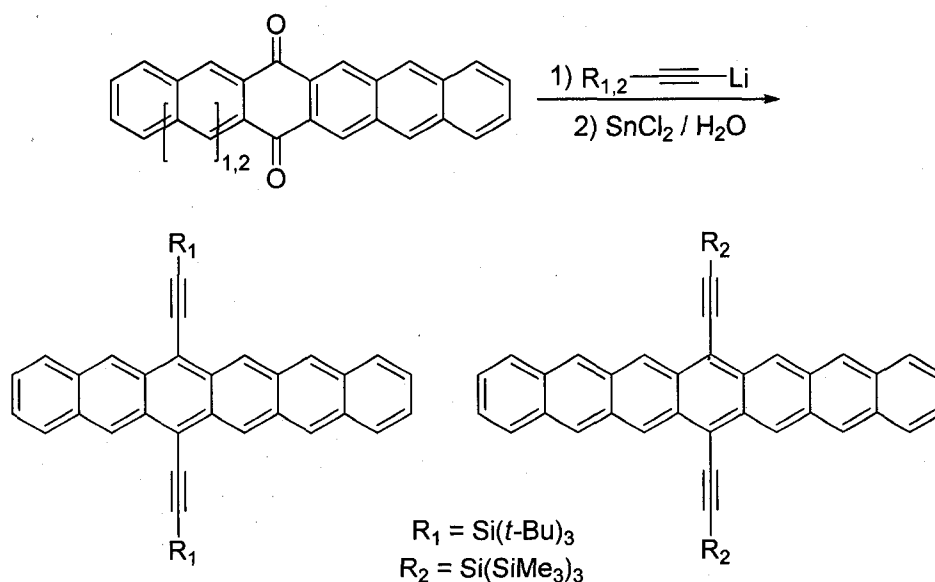
**Scheme 18.** Some of the known 6,13-disubstituted pentacenes derived from 6,13-pentacenequinone.



Miller, Mack and Briggs noted that ethynyl-substituted pentacenes showed increased stability.<sup>96</sup> Later, Anthony and co-workers prepared numerous silylethynyl-substituted acenes, all of which showed improved stability over their parent acenes.<sup>94,97</sup>

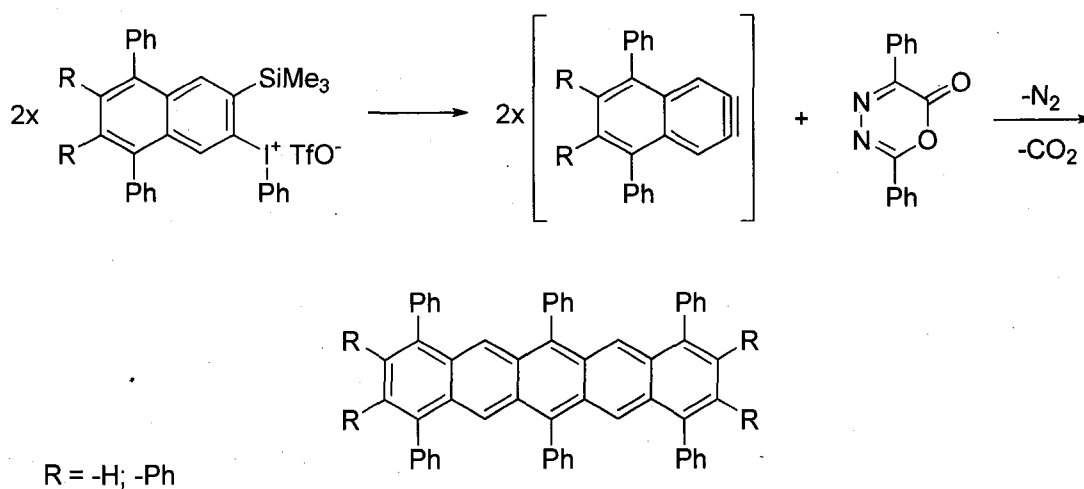
Indeed, silylethynyl substituted hexacene and heptacene have been isolated and characterized (Scheme 19).<sup>98</sup> While solutions of 6,15-bis(tri-*tert*-butylsilylethynyl)hexacene decomposed slowly in the presence of light and air, the solid was stored for months in the dark without noticeable degradation. In contrast, 7,16-bis(tris(trimethylsilyl)silylethynyl)heptacene decomposed within a day in solution. NMR and EPR spectroscopy of the heptacene suggest a closed-shell ground state configuration.

**Scheme 19.** Anthony and co-workers' syntheses of 6,15-bis(tri-*tert*-butylsilylethynyl)hexacene (left) and 7,16-bis(tris(trimethylsilyl)silylethynyl)heptacene (right).



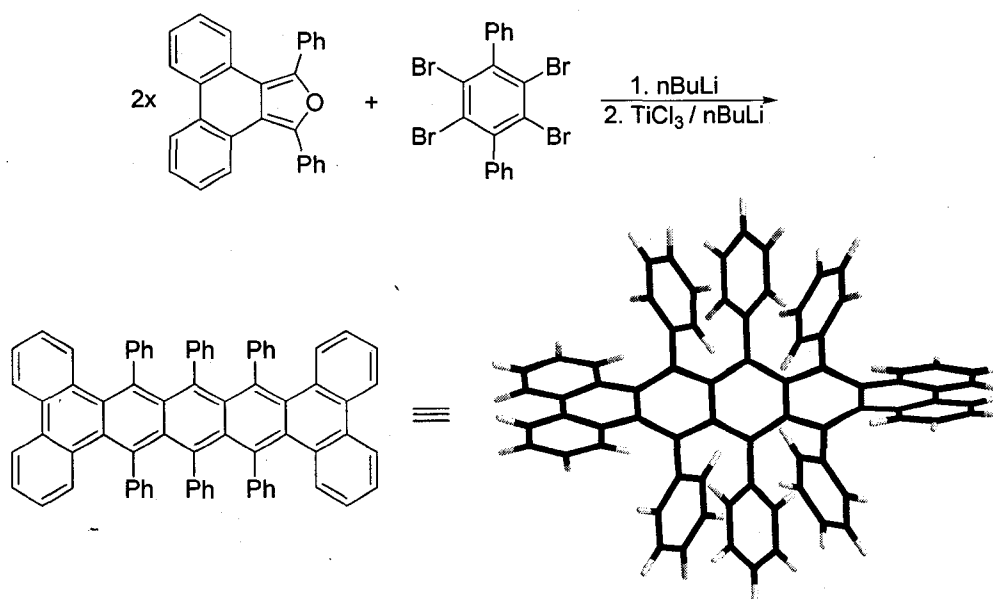
A series of phenyl-substituted pentacenes with a variety of substitution patterns were synthesized by Nuckolls and co-workers.<sup>99</sup> Novel systems included 6-phenylpentacene as well as hexaphenylpentacene and decaphenylpentacene (Scheme 20). The decaphenylpentacene in particular exhibited 'good electrical properties'.

**Scheme 20.** Nuckolls and co-workers' synthetic approach to phenyl-substituted acenes.



Pascal and co-workers synthesized a series<sup>100</sup> of bent benzannelated acenes bearing phenyl substituents, culminating in a pentacene derivative with a 144° end-to-end twist, the most twisted polycyclic aromatic hydrocarbon reported (Scheme 21).<sup>100c</sup>

**Scheme 21.** Pascal's benzannelated hexaphenyl pentacene, with an end-to-end twist of 144°.

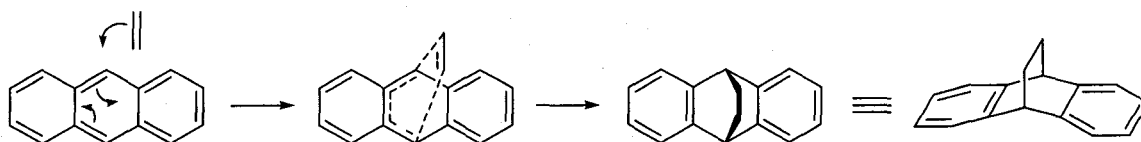


Despite the strong deformation from planarity, the acene was shown to be quite stable under ambient conditions and showed increased stability over less substituted, yet less twisted analogs.<sup>101</sup>

#### 1.3.4 Diels-Alder Chemistry of Acenes

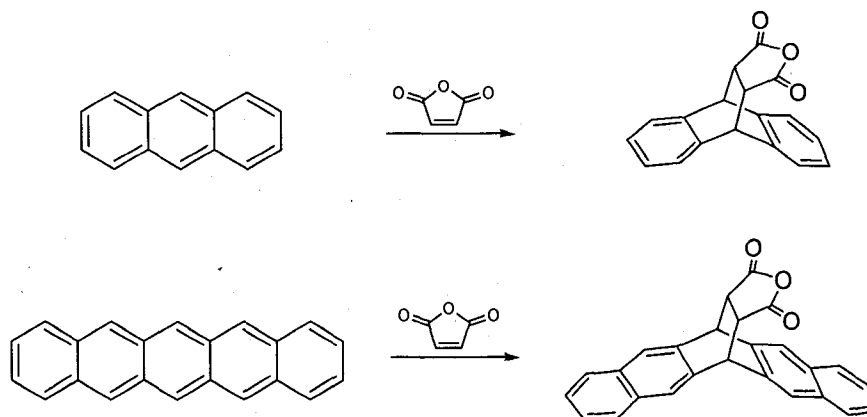
Acenes react as dienes in Diels-Alder cycloaddition reactions, adding dienophiles across aromatic rings in a 1,4 fashion (Scheme 22). Cycloaddition is a favorable reaction in part because it divides the acene into smaller, more stable acene moieties.

**Scheme 22.** Generic Diels-Alder reaction between anthracene and ethylene.



In the 1930's Erich Clar published a series of papers outlining the regioselective Diels-Alder reactivity of various acenes with maleic anhydride.<sup>102</sup> Maleic anhydride cycloadds to anthracene and pentacene exclusively across the central 9,10 and 6,13 carbon positions, respectively (Scheme 23).

**Scheme 23.** Diels-Alder adducts of maleic anhydride and anthracene (top) and pentacene (bottom).



Clar also showed that acene reactivity increases with annelation. From his results, Clar formulated his aromatic sextet theory which successfully explained the chemical and physical properties of acenes and other polyarenes.<sup>72</sup> In 1980, Biermann and Schmidt published an exhaustive kinetics study of the relative Diels-Alder reaction rates of a plethora of acenes and benzologs<sup>103a</sup> as well as phenes and starphenes<sup>103b</sup> (Table 1). Increased acene cycloaddition rates coincided with annelation, verifying the trend observed by Clar.

**Table 1.** Second order rate constants, normalized rate constants and relative rate constants associated with the addition of maleic anhydride to acenes.<sup>103a</sup>

Compound	$k_2 \times 10^3 \text{ (L M}^{-1} \text{ s}^{-1}\text{)}$	Sites <sup>a</sup>	Normalized <sup>b</sup> $k_2 \times 10^3$	Relative $k_2$
anthracene	2.27	1	2.27	1
tetracene	94.2	2	47.1	21
pentacene	1,640	1	1,640	723
hexacene	6,570	2	3,290	1,450

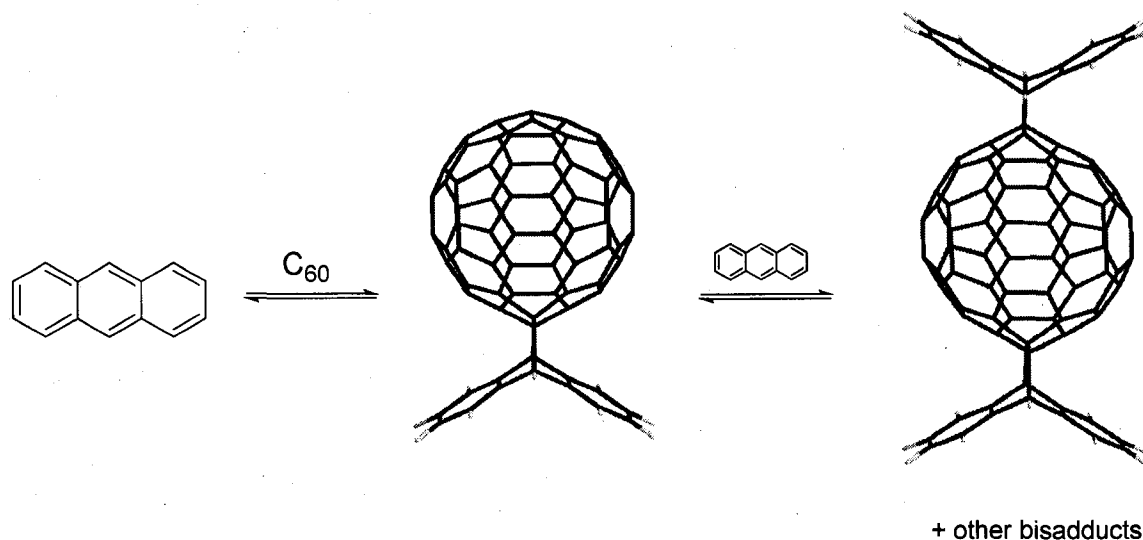
<sup>a</sup>Number of Diels-Alder reactive rings. <sup>b</sup>Rate constant divided by number of reactive sites.



#### 1.3.4.1 Diels-Alder Reactivity of Acenes with [60]Fullerene

As with other dienophiles, [60]fullerene undergoes Diels-Alder cycloadditions with acenes.<sup>104</sup> Addition is relegated to the central most ring of the acene, with a few exceptions (*vide infra*, Scheme 27). As is the case for other dienes, multiple acene additions to the fullerene surface are observed.<sup>105</sup> Thus, [60]fullerene adds to anthracene solely across the central 9,10 carbons to yield both mono- and bisadducts (Scheme 24).

**Scheme 24.** [60]Fullerene cycloadds to anthracene across the central ring to yield both mono- bisadducts.



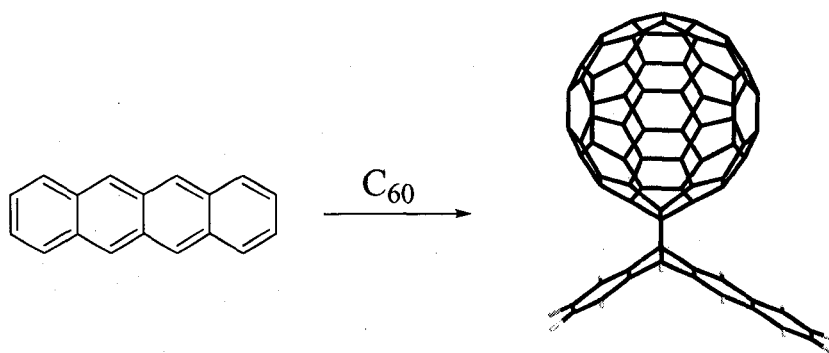
Schlueter, *et al.* isolated and fully characterized the 1:1 adduct of [60]fullerene and anthracene in 13% yield by heating a mixture of [60]fullerene and anthracene in toluene at 110 °C for 3 days.<sup>106</sup> Polyadducts were also isolated but not fully characterized. Tsuda, *et al.* reported 25% isolated yield of the monoadduct by heating a 1:1.2 mixture of [60]fullerene and anthracene at 80 °C for 12 hours.<sup>42</sup> When the reaction was rerun at progressively higher temperatures the researchers observed a steady decrease in the isolated yields of monoadduct. Komatsu, *et al.* isolated the monoadduct in

39% yield by heating a mixture of [60]fullerene and anthracene in molten naphthalene (200 °C) for 48 hours.<sup>107</sup> Cruz, Hoz and Langa used microwave irradiation to synthesize the monoadduct in 35% yield after just 15 minutes, a marked improvement in reaction time over previous procedures.<sup>108</sup> The monoadduct was also synthesized by mechanochemical means. Komatsu and co-workers reacted [60]fullerene with 1.2 equivalents of anthracene in a high-speed vibrating mill for 1 hour.<sup>105</sup> Under high-speed vibrational milling conditions, a solvent free mixture of material is rapidly (3500 rpm) shaken in a steel capsule with a steel milling ball. Under these conditions, mechanical energy is the driving force for reaction. The researchers isolated the monoadduct in 55% yield, along with a mixture of bisadducts in 19% yield.

Most recently, Sarova and Berberan-Santos performed a detailed kinetic study of the addition of [60]fullerene to anthracene.<sup>109</sup> They concluded that, while addition was reversible in the temperature range from 22 °C to 63 °C, the rate of addition of [60]fullerene to anthracene far exceeded the rate of retro-Diels-Alder reaction.

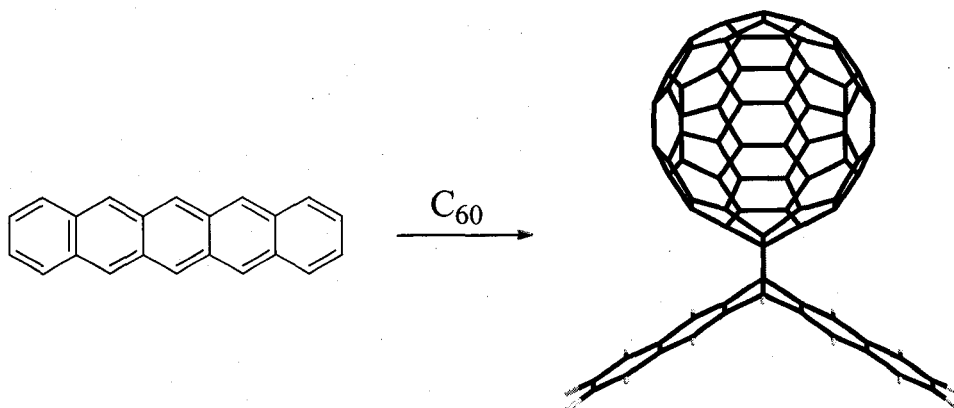
Only two reports are published for the addition of [60]fullerene to tetracene (Scheme 25). Komatsu and co-workers reacted the two using high-speed vibrational milling and isolated the monoadduct in 61% yield.<sup>105</sup> Sarova and Berberan-Santos' kinetic study also included the addition of [60]fullerene to tetracene. They found tetracene reacts much faster than does anthracene and saw no evidence of retro-[4 + 2] reaction up to 59 °C.<sup>109</sup>

**Scheme 25.** [60]Fullerene cycloadds to tetracene across either of the two inner aromatic rings.



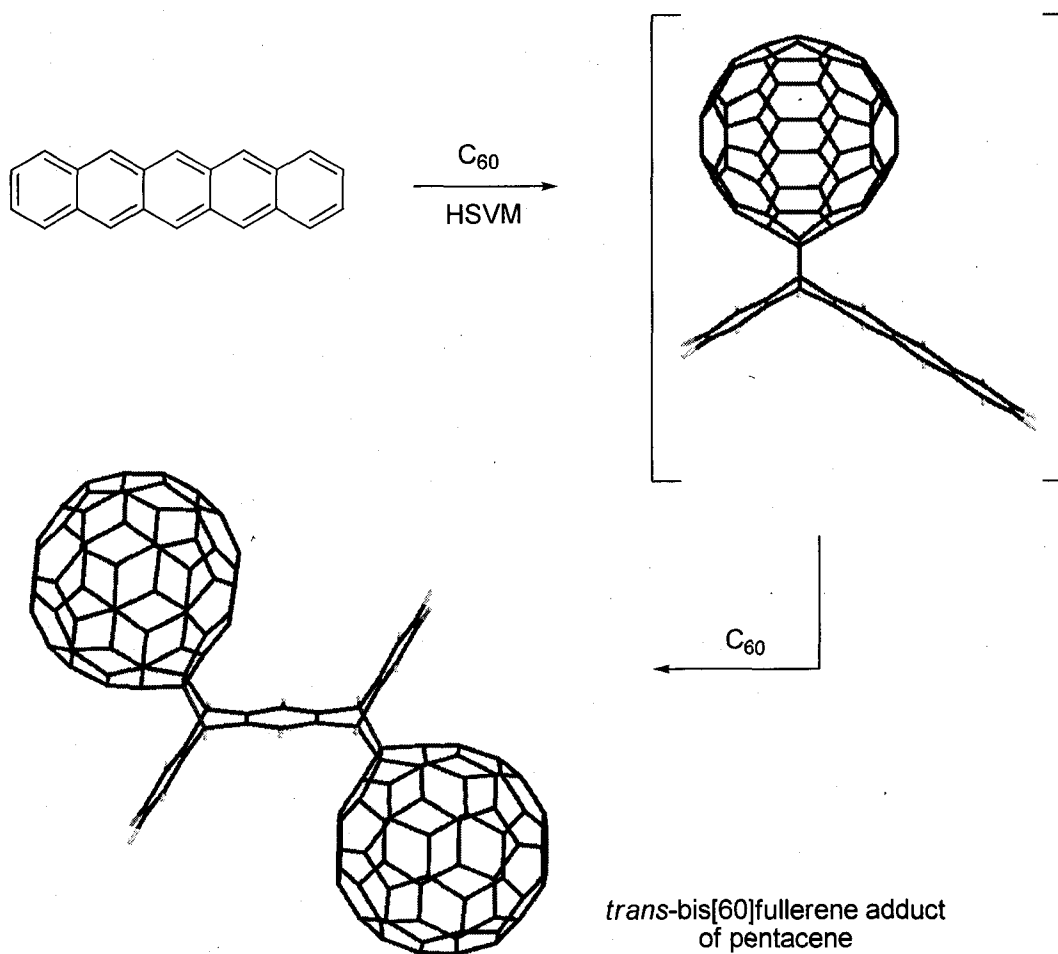
The cycloaddition of [60]fullerene to pentacene is also known (Scheme 26). Miller and Mack reported the addition of [60]fullerene to pentacene in toluene at 110 °C. Only the monoadduct, in which [60]fullerene adds across the central 6,13 ring, was observed.<sup>110</sup>

**Scheme 26.** Miller and Mack found that [60]fullerene cycloadds to pentacene solely across the central 6,13 positions in the solution phase.



Komatsu and co-workers reacted a 1:1 mixture of [60]fullerene and pentacene using high-speed vibrational milling and isolated both the mono[60]fullerene adduct and a single bis[60]fullerene adduct (Scheme 27).<sup>105</sup> This is remarkable as there are no other

**Scheme 27.** Komatsu and co-workers' synthesis of bis[60]fullerene-pentacene adduct. The researchers proposed formation of the *trans*-bis[60]fullerene adduct of pentacene.

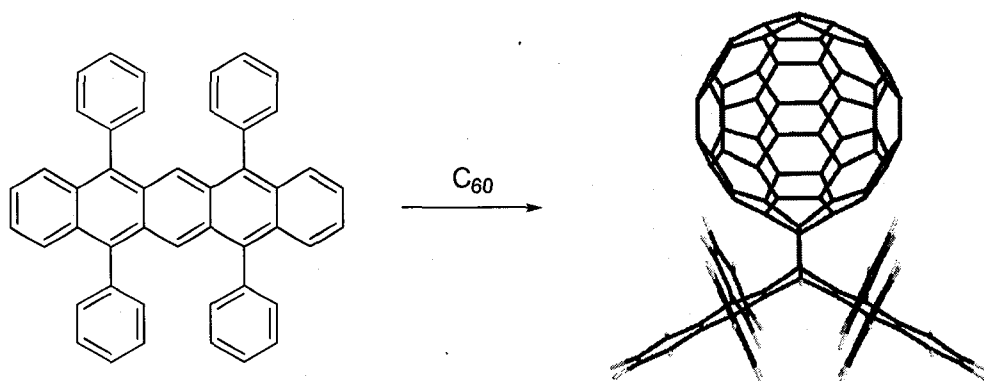


examples of dual  $[4 + 2]$  cycloaddition of any dienophile across unsubstituted pentacene. Furthermore, the authors reported formation of only one of the two possible bis[60]fullerene adduct diastereomers. Unable to distinguish between the diastereomers, Komatsu *et al.* proposed that the *trans*-bis[60]fullerene adduct is formed rather than the corresponding *cis* isomer. Subsequent work by Miller and co-workers (*vide infra*, Scheme 29) casts doubt on this assignment.

### 1.3.4.2 Diels-Alder Reactivity of Phenyl Substituted Acenes with [60]Fullerene

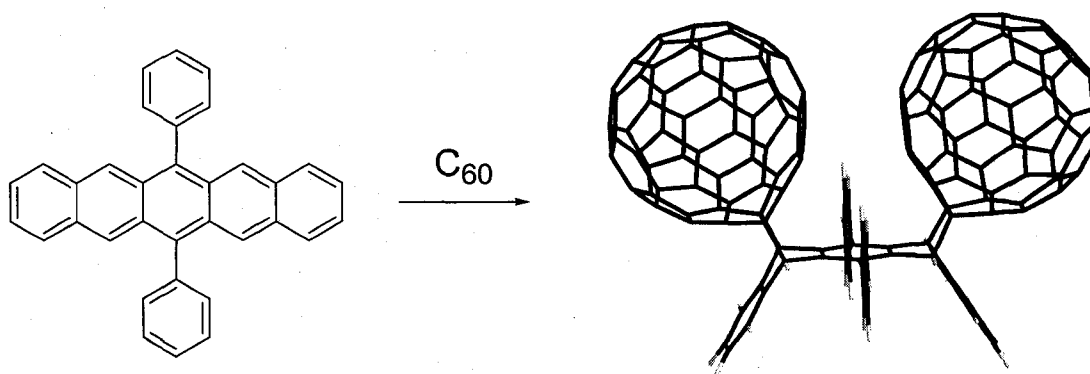
As stated earlier, [60]fullerene adds to pentacene solely across the central ring under solution phase conditions. Despite steric congestion, 5,7,12,14-tetraphenylpentacene also reacts with [60]fullerene across the 6,13 carbons to form the monoadduct (Scheme 28).<sup>111</sup>

**Scheme 28.** Cycloaddition of [60]fullerene to 5,7,12,14-tetraphenylpentacene.



In the case of 6,13-diphenylpentacene, however, [60]fullerene addition does not take place across the central ring. The phenyl substituents on the 6,13 carbons act to sterically hinder cycloaddition across the central ring. Instead, two equivalents of [60]fullerene add across the 5,14 and 7,12 positions of 6,13-diphenylpentacene in a highly diastereoselective *syn* fashion (Scheme 29).<sup>112</sup>

**Scheme 29.** The two-fold cycloaddition of [60]fullerene to 6,13-diphenylpentacene proceeds in a *cis* fashion.



Favorable  $\pi$ - $\pi$  interactions between the [60]fullerene addends drive formation of the *cis*-bis[60]fullerene adduct.<sup>113</sup> This *cis*-bisadduct is favored under both kinetic and thermodynamic conditions. Favorable  $\pi$ - $\pi$  interactions between the [60]fullerene addend of the monoadduct and incoming [60]fullerene dienophile lead to the kinetically favored product. The *cis*-bis[60]fullerene adduct is preferred thermodynamically as a result of  $\pi$ - $\pi$  interactions in the ground state. Indeed, 6,8,15,17-tetraphenylheptacene generated in situ reacts with three equivalents of [60]fullerene to yield solely the all *syn* trisadduct.<sup>114</sup>

## CHAPTER 2

### 4,7-DIPHENYLISOBENZOFURAN: A USEFUL INTERMEDIATE FOR THE CONSTRUCTION OF PHENYL- SUBSTITUTED ACENES

#### 2.1 Introduction

One useful strategy to synthesize phenyl-substituted pentacenes involves the Diels-Alder reaction between phenyl-substituted isobenzofuran and *p*-benzoquinone.<sup>115</sup> Isobenzofurans are long recognized as useful dienes in Diels-Alder cycloadditions.<sup>116</sup> The parent isobenzofuran was first postulated by Wittig and Pohmer,<sup>117</sup> and then later experimentally verified as a transient species by Fieser and Haddadin<sup>118</sup> via Diels-Alder trapping studies. Since its discovery, isobenzofuran and its substituted derivatives<sup>119</sup> have proven to be important synthetic intermediates in a variety of transformations.<sup>120</sup>

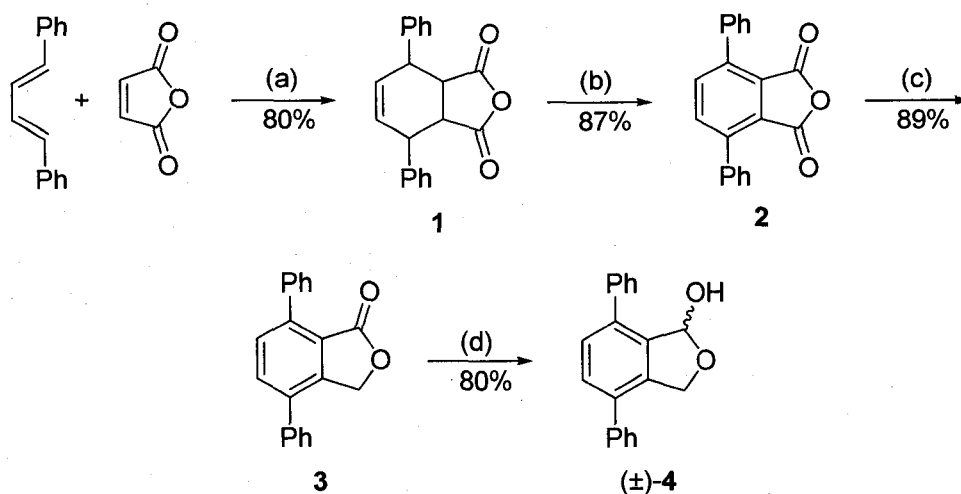
As isobenzofurans are often reactive and unstable species, save for some 1- and 1,3-substituted examples,<sup>121,122</sup> the construction of stable precursors is essential. 1-Hydroxy and 1-alkoxyphthalans are well established as convenient precursors to isobenzofurans.<sup>123,124,125,126,127</sup> Here, the synthesis of compounds **1-3**, precursors to previously unknown ( $\pm$ )-4,7-diphenyl-1-hydroxyphthalan, ( $\pm$ )-**4**, are described. It is further demonstrated that compound ( $\pm$ )-**4** readily converts to 4,7-diphenylisobenzofuran, **5**. It is also shown that reactive **5** is a versatile intermediate for the synthesis of phenyl-

substituted three, four and five-ring acene compounds. The reaction between **5** and *p*-benzoquinone is especially interesting as it yields the unprecedented *exo,exo anti* dual cycloaddition product **16b** on the way to 1,4,8,11-tetraphenylpentacene **22**.

## 2.2 Synthesis of 4,7-Diphenyl-1-hydroxyphthalan ((±)-**4**)

Lactol ((±)-**4**) is synthesized in four steps starting from commercially available reactants (Scheme 30). Cycloaddition of 1,4-diphenyl-1,3-butadiene with maleic anhydride is performed following the procedure of Kuhn and Wagner-Jauregg<sup>128</sup> to yield 3a,4,7,7a-tetrahydro-4,7-diphenylphthalic anhydride, **1**, in 80% yield.

**Scheme 30<sup>a</sup>**. Synthesis of ((±)-**4**) from 1,4-diphenylbutadiene and maleic anhydride.



<sup>a</sup> Reagents and conditions: (a) xylenes, 140 °C, 15 h; (b) DDQ, toluene, 111 °C, 18 h; (c) Zn, HOAc, 100 °C, 17 h; (d) DIBAL-H, dichloromethane, -60 °C, 70 min.

Subsequent aromatization of **1** with two equivalents of 2,3-dichloro-5,6-dicyano-*p*-benzoquinone (DDQ) in refluxing toluene gives the known 4,7-diphenylphthalic anhydride,<sup>129,130,131</sup> **2** in 87% yield. Using a modified Yang-Zhu reduction,<sup>132</sup> the



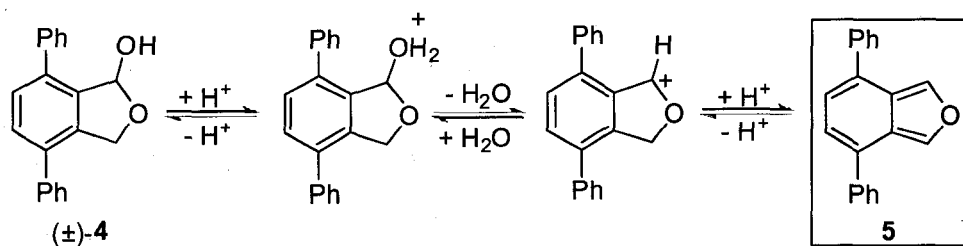
diphenylphthalide **3**<sup>133</sup> is synthesized in 89% yield. Conversion of **3** to the previously unknown hydroxyphthalan ( $\pm$ )-**4** was accomplished in 80% yield using Rodrigo's conditions.<sup>134</sup>

Lactol ( $\pm$ )-**4** is a stable white solid. Literature precedents exist for solution phase equilibria between similar hemiacetals and their corresponding aldehyde-alcohol ring-opened tautomers.<sup>135</sup> In the case of ( $\pm$ )-**4**, however, only the hemiacetal is observed by <sup>1</sup>H and <sup>13</sup>C NMR spectroscopies (See appendix for this and all other NMR spectra, organized by compound number).

### **2.3 In Situ Formation and Reactivity of 4,7-diphenylisobenzofuran (5): Construction of Three and Four-ring Acene Derivatives**

Hydroxyphthalan ( $\pm$ )-**4** is a stable and convenient precursor to 4,7-diphenylisobenzofuran **5**. Glacial acetic acid is an effective solvent/catalyst for the *in situ* generation of **5**, as is a mixture of *p*-TsOH in toluene. Glacial acetic acid is, however, preferred as it is observed that subsequent cycloaddition products precipitate cleanly from this solution in good yields. An E1 mechanism for the formation of isobenzofuran from alkoxy precursors in acidic media has been reported<sup>136</sup> and is analogous to that shown in Scheme 31.

Scheme 31. Acid catalyzed formation of transient **5** from lactol ( $\pm$ )-**4**.



### 2.3.1 Reactivity of 4,7-Diphenylisobenzofuran with Maleic Anhydride

Upon forming **5** in glacial acetic acid, its reactivity with maleic anhydride was studied. Both endo and exo products (Scheme 32) form under all conditions tested (Table 2). The exo product, **6b**, is highly favored in boiling acetic acid.

Table 2. Reactions between **5** and maleic anhydride.

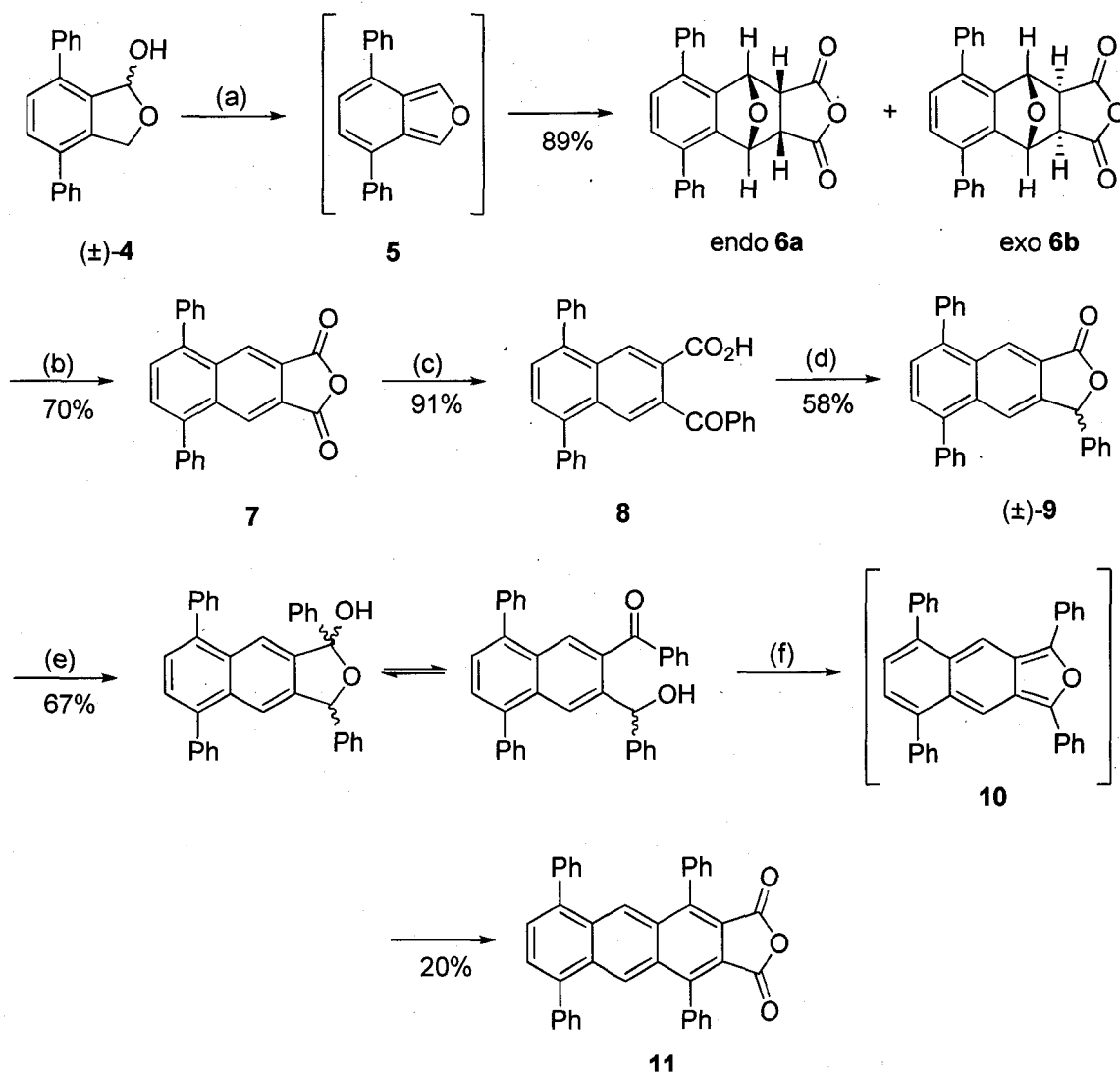
Exp.	( $\pm$ )- <b>4</b> : MA <sup>a</sup>	Reagents/Temp.	Time	endo <b>6a</b> : exo <b>6b</b> <sup>b</sup>
1	1 : 1.2	HOAc/118 °C	24 h	1 : 16.5
2	1 : 1.4	HOAc, Ac <sub>2</sub> O/50 °C	1 h	1 : 1
3	1 : 1.5	HOAc, Ac <sub>2</sub> O/35 °C	1 h	1 : 1

<sup>a</sup>MA is maleic anhydride. <sup>b</sup>Endo:exo ratios are calculated from <sup>1</sup>H NMR integrations of crude product mixtures.

The high temperature reactivity of **5** with maleic anhydride mimics that of the parent isobenzofuran which forms nearly the same ratio of endo:exo products at similar (~130°C) temperatures.<sup>137</sup> <sup>1</sup>H-<sup>1</sup>H NMR coupling, or lack thereof, between the methine protons at the sites of cycloaddition (oxabicyclo substructure) differentiates endo **6a** from exo **6b**.<sup>123,124,138,139</sup> The aliphatic methine protons of the oxabicyclo substructure of the endo diastereomer produce an AA'XX' pattern in the <sup>1</sup>H NMR spectrum. In the exo

isomer **6b**, the analogous protons are fixed with a dihedral angle that approaches 90°, thereby diminishing vicinal  $^1\text{H}$ - $^1\text{H}$  coupling. Consequently, the aliphatic methine protons in **6b** give rise to two singlets rather than two multiplets.

**Scheme 32<sup>a</sup>.** Synthesis of tetraphenylanthracene **11** from lactol ( $\pm$ )-**4**.



<sup>a</sup> Reagents and conditions: (a) maleic anhydride, HOAc, Ac<sub>2</sub>O, 118 °C, 2 h; (b) *p*-TsOH, toluene, Dean-Stark trap, 111 °C, 4 d; (c) PhH, AlCl<sub>3</sub>, 80 °C, 20 h; (d) NaBH<sub>4</sub>, NaOH, EtOH, H<sub>2</sub>O, 25 °C, 6 d; (e) PhMgBr, THF, 0 °C, 1 h; (f) maleic anhydride, *p*-TsOH, PhH, Dean-Stark trap, 80 °C, 24 h.

Optimal conditions for the formation of previously unknown **6a** and **6b** are illustrated in Scheme 32. The mixture may be dehydrated using *p*-TsOH to form anhydride **7**<sup>140</sup> which is then subjected to modified<sup>114</sup> Cava conditions<sup>141</sup> to form previously unknown keto-acid **8**. Reducing **8** with borohydride produces racemic lactone (±)-**9** in modest yield. Phenylation of (±)-**9** produces a mixture of lactols which coexist with their ring-opened keto-ol forms according to <sup>1</sup>H and <sup>13</sup>C NMR spectra. Previously unknown 1,3,5,8-tetraphenylisonaphthofuran, **10**, forms upon dehydration of the lactol and is trapped in situ with maleic anhydride to generate, after further dehydration, 4,6,9,11-tetraphenylanthra[2,3-*c*]furan-1,3-dione **11**. Compound **11**, a new acene derivative, is a stable yellow solid that exhibits strong fluorescence.

### 2.3.2 Reactivity of 4,7-Diphenylisobenzofuran with 1,4-Naphthoquinone

The reactivity between **5** and 1,4-naphthoquinone was also studied (Scheme 33). Similar to the trend observed with maleic anhydride, the reaction between **5** and 1,4-naphthoquinone favors endo product **12a** at lower temperatures and exo product **12b** at elevated temperatures (Table 3).

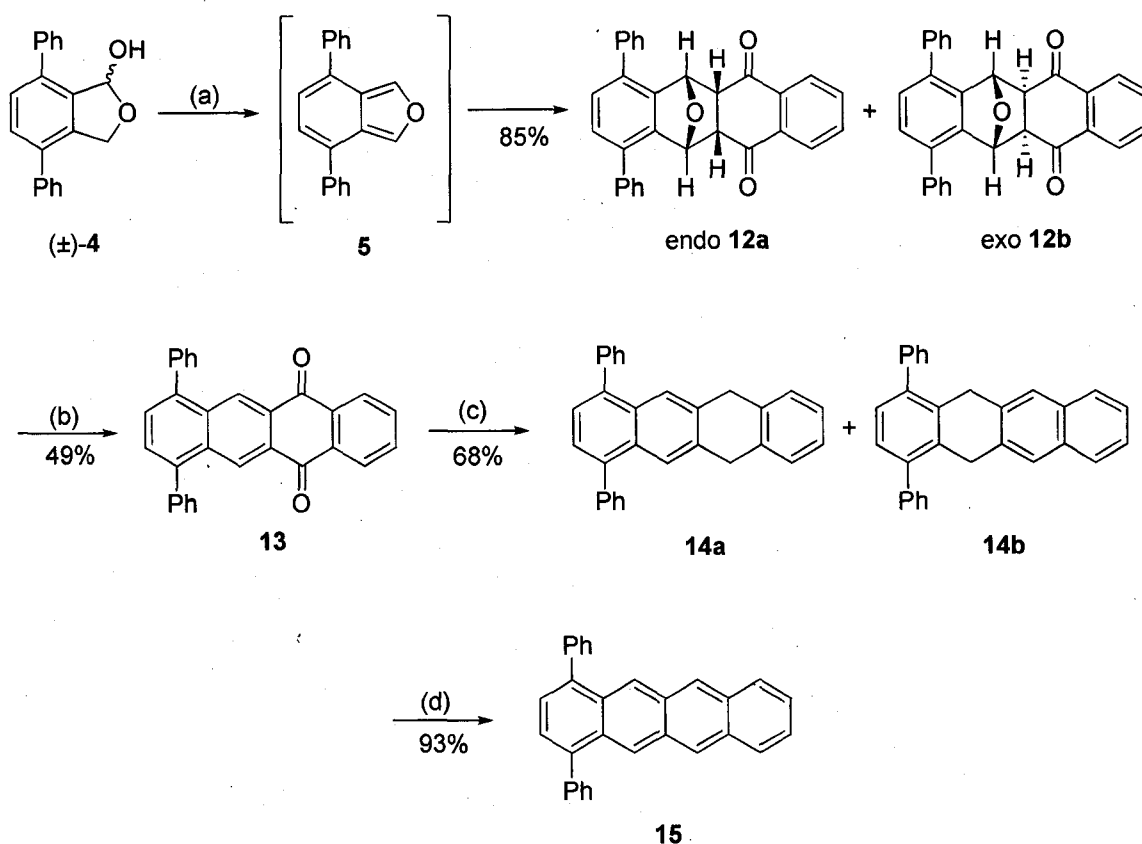
**Table 3.** Reactions between **5** and 1,4-naphthoquinone.

Exp.	(±)- <b>4</b> : 1,4-NQ <sup>a</sup>	Reagents/Temp.	Time	endo <b>12a</b> : exo <b>12b</b> <sup>b</sup>
4	1 : 1.2	HOAc/118 °C	18 h	N/A <sup>c</sup>
5	1 : 1.1	HOAc, Ac <sub>2</sub> O/100 °C	5 h	1 : 3 <sup>d</sup>
6	1 : 1.1	HOAc, Ac <sub>2</sub> O/90 °C	2 h	1.1 : 1
7	1 : 1.1	HOAc, Ac <sub>2</sub> O/75 °C	2 h	1.5 : 1
8	1 : 1	HOAc, Ac <sub>2</sub> O/50 °C	1 h	1.7 : 1

<sup>a</sup>1,4-NQ is 1,4-naphthoquinone. <sup>b</sup>Endo:exo ratios are calculated from <sup>1</sup>H NMR integrations of crude product mixtures. <sup>c</sup>Dehydration of **12a** and **12b** to form **13** is facile under these reaction conditions. No **12a** or **12b** is observed by NMR. <sup>d</sup>Trace **13** is also observed.

The mixture of **12a** and **12b** is readily dehydrated to 1,4-diphenyltetracene-6,11-quinone, **13**, which is then transformed to a mixture of dihydrodiphenyltetracenes, **14a** and **14b**, via an HI-HOAc reduction.<sup>114</sup> Finally, a Pd/C dehydrogenation produces previously unknown 1,4-diphenyltetracene, **15**, in excellent yield.

Scheme 33<sup>a</sup>. Synthesis of 1,4-diphenyltetracene from 4,7-diphenyl-1-hydroxyphthalan.



<sup>a</sup> Reagents and conditions: (a) 1,4-naphthoquinone, HOAc, 60°C, 2 h; (b) H<sub>2</sub>SO<sub>4</sub>, HOAc, 70°C, 1 h; (c) HI (55-58%), HOAc, 118°C, N<sub>2</sub>, dark, 4 d; (d) 10% Pd/C, 1,2-dichlorobenzene, 180°C, N<sub>2</sub>, dark, 3 d.

### 2.3.3 Unusual Diastereoselectivity in the Reaction Between

#### 4,7-Diphenylisobenzofuran (**5**) and *p*-Benzoquinone.

The two-fold cycloaddition of any isobenzofuran or isonaphthofuran with *p*-benzoquinone is reported for only three furanoid species: 1,3-diphenylisobenzofuran<sup>111,115</sup> 5,6-bis(trimethylsilyl)isobenzofuran,<sup>142</sup> and 1,3-diphenylisonaphthofuran.<sup>114</sup> In each case, a single diastereomer is formed. This sole product is invariably reported to be the endo,exo *syn* diastereomer arising from consecutive endo and exo cycloadditions of two isoacenofurans across opposite faces of the quinone (Figure 10). The initial two-fold cycloaddition product arising from the reaction between isobenzofuran itself and *p*-benzoquinone was formed but not isolated on the path leading to pentacene-6,13-quinone, a molecule more easily synthesized via alternative routes.<sup>83,84,85,86</sup>

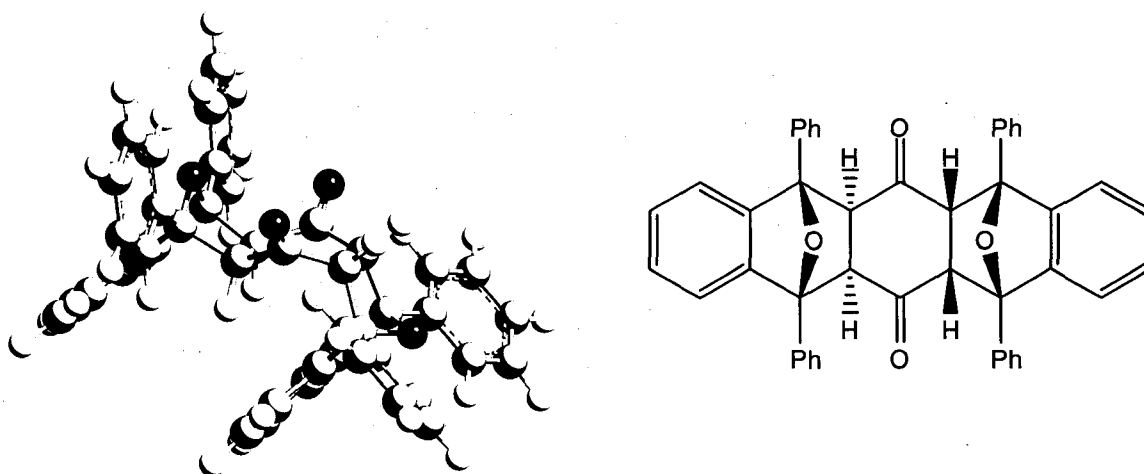


**Figure 10.** Left: MMFF optimized geometry of the endo,exo *syn* dual cycloaddition product arising from the reaction between 2 equivalents of 1,3-diphenylisobenzofuran and *p*-benzoquinone. Right: ChemDraw structure of the same compound. *Syn* describes the relative positions of the two oxygen bridges.

Interestingly, there are a total of six different diastereomers that could form upon the two-fold cycloaddition of **5** to *p*-benzoquinone (Figure 11). These arise from two different combinations each of either endo,endo or endo,exo or exo,exo cycloadditions.

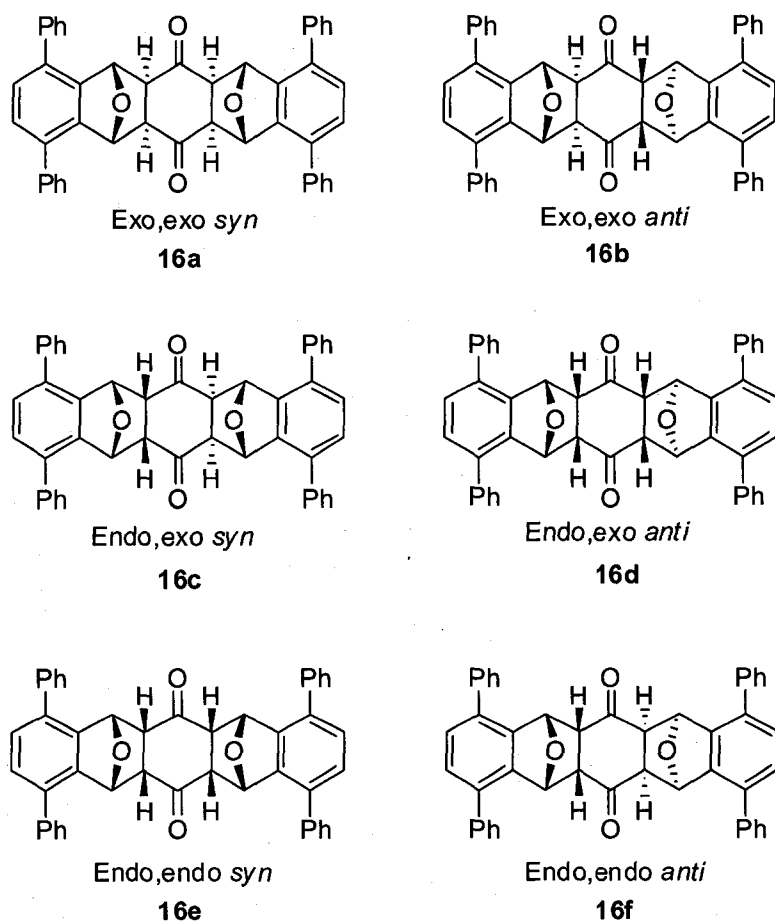
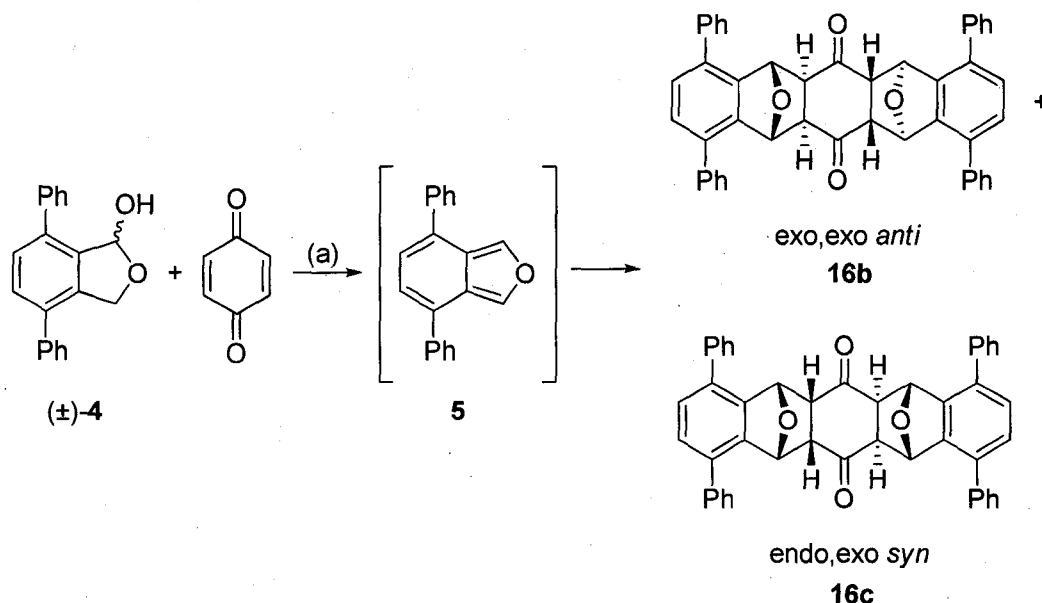


**Figure 11.** The six possible diastereomers that can form in the dual cycloaddition of **5** to *p*-benzoquinone.

Based upon literature precedents, we expected exclusive formation of the endo,exo *syn* isomer **16c**. However, when (±)-**4** and *p*-benzoquinone are reacted in glacial acetic acid (Scheme 34), we observe formation of both the expected **16c** as well as the exo,exo *anti* diastereomer **16b**. Isomer **16c** is slightly favored at lower temperatures while **16b** is dominant at higher temperatures (Table 3). In fact, **16b** forms in excellent yield and with 100% diastereoselectivity in boiling glacial acetic acid. Neither **16b** nor **16c** is especially soluble in acetic acid as both readily precipitate from cooled solutions.

Scheme 34<sup>a</sup>. Formation of **16b** and **16c** from (±)-**4**.



<sup>a</sup> Reagents and conditions: (a) HOAc, heat; see Table 4.

Table 4. Reactions Between **5** and *p*-Benzoquinone

Exp.	(±)- <b>4</b> : <i>p</i> -benzoquinone	Reagents/Temp.	Time	Yield	<b>16b</b> : <b>16c</b> <sup>a</sup>
9	2.1 : 1	HOAc/118 °C	8 h	90%	<b>16b</b> <sup>b</sup>
10	2.1 : 1	HOAc/90 °C	15 h	82%	5 : 1
11	2.1 : 1	HOAc/70 °C	5 h	89%	1 : 1.5

<sup>a</sup> Ratios of **16b**:**16c** are calculated from <sup>1</sup>H NMR integrations of precipitate product mixtures.

<sup>b</sup> Isomer **16c**, if formed at all, is not detected by <sup>1</sup>H NMR spectroscopy.

### 2.3.3.1 Structural Analysis of **16c**

The existence of both endo and exo stereochemistries on the oxabicyclo moieties of **16c** is revealed by the presence of both coupled and non-coupled aliphatic methine signals (see analysis of **6a** and **6b** above). The <sup>1</sup>H NMR data, however, do not distinguish *syn* from *anti* stereochemistries, *i.e.*, **16c** from **16d**. The endo,exo product is assigned a *syn* stereochemistry, *i.e.* **16c**, based solely upon literature precedent involving other endo,exo isomers of this type.<sup>111,114,115,142</sup>



### 2.3.3.2 Structural Analysis of 16b

Because **16b** is formed with 100% diastereoselectivity in boiling glacial acetic acid, a rigorous stereochemical analysis is warranted. The lack of coupling between the protons on the oxabicyclo moieties firmly establishes the exo,exo nature of **16b** but does not distinguish between *syn* and *anti* stereochemistries, *i.e.*, **16a** from **16b**. Both the  $C_{2h}$  symmetric exo,exo *anti* isomer **16b** and the  $C_{2v}$  symmetric exo,exo *syn* isomer **16a** (Figure 12) are consistent with the  $^1\text{H}$  NMR data. These structures arise from dual exo

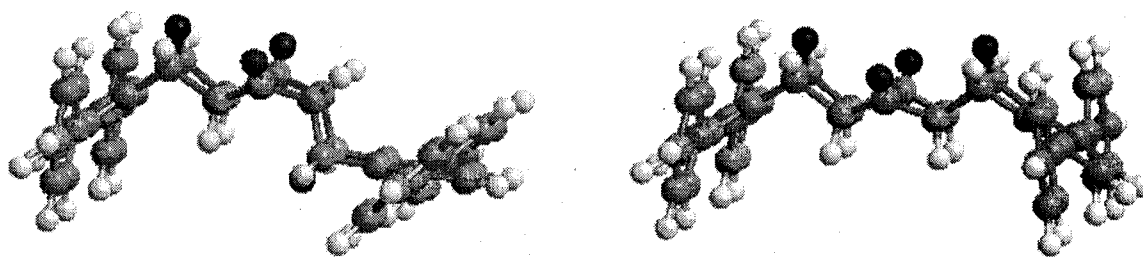


**Figure 12.** Isolated dual cycloaddition product exo,exo *anti* **16b** (left) and theoretical dual cycloaddition product exo,exo *syn* **16a** (right). MMFF optimized geometries

cycloadditions across either the opposite faces or the same face of *p*-benzoquinone, respectively. There is no literature precedent involving a dual cycloaddition product of this type. In order to assign either *syn* or *anti* stereochemistry, an attempt was made, without success, to grow X-ray quality crystals. An attempt was also made, without success, to prepare both a 2,4-dinitrophenylhydrazone derivative and the corresponding bis-dimethyl acetal. It was hoped that a 2,4-dinitrophenylhydrazone derivative would readily crystallize while the bis-dimethyl acetal would enable an NMR elucidation of *syn* versus *anti* stereochemistry. Finally, the single exo,exo product was successfully converted into a mixture of alcohols using a sodium borohydride reduction. This

conversion permitted the unambiguous assignment of *anti* stereochemistry to the exo,exo product, *i.e.* **16b**, as described below.

### 2.3.3.3 Analysis of Borohydride Reduction Products of **16b**

Reduction of hypothetical exo,exo *syn* isomer **16a** would produce up to three different diols (**17a-c**) while reduction of exo,exo *anti* **16b** produces two different diols (**18a** and **18b**) as illustrated in Figure 13. The expected  $^1\text{H}$  NMR signals associated with each of the central aliphatic substructures (Figure 14) are diagnostic. This diagnostic

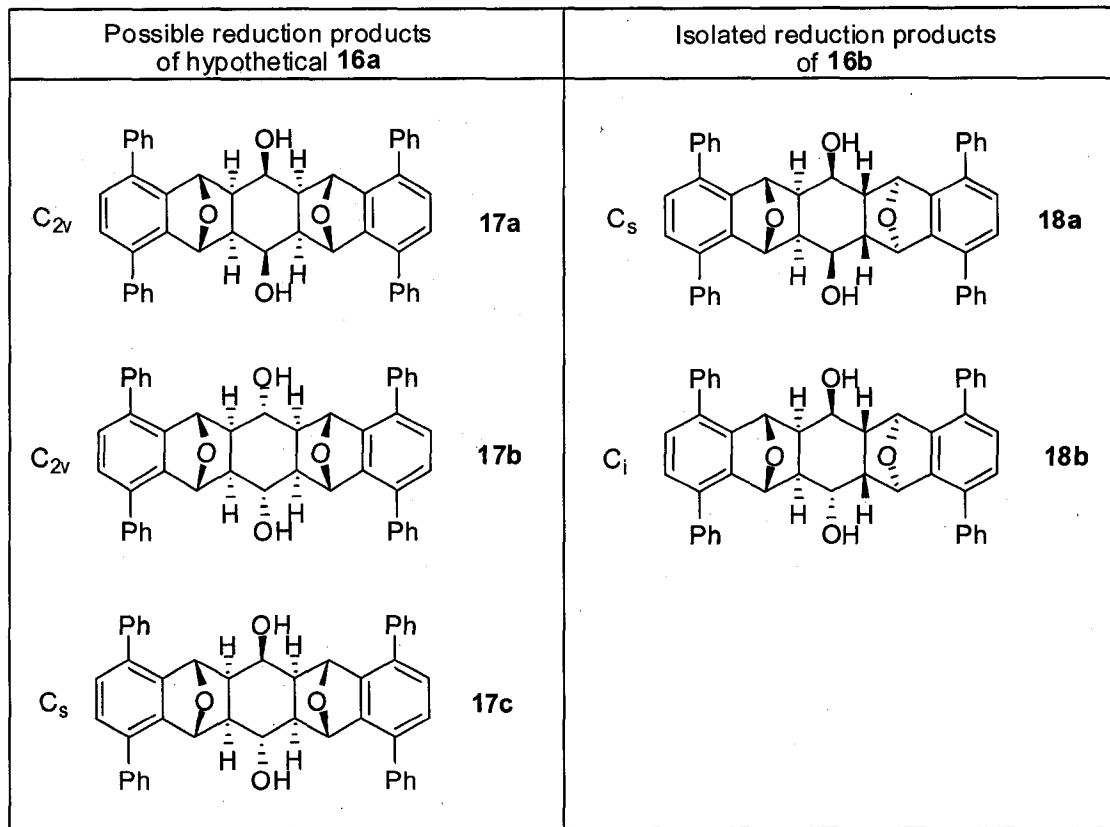


**Figure 13.** Left column: the three possible products arising from borohydride reduction of the hypothetical exo,exo *syn* **16a**. Right column: the two products formed during the borohydride reduction of exo,exo *anti* **16b**. The time-averaged symmetries associated with each structure are identified.

region possesses four types of protons including three unique methine protons ( $H_I$ ,  $H_{II}$ ,  $H_{III}$ ) and one alcohol proton ( $H_{IV}$ ). The diagnostic region includes a central cyclohexane ring that prefers in all cases a boat conformation due to constraining bicyclo addends.

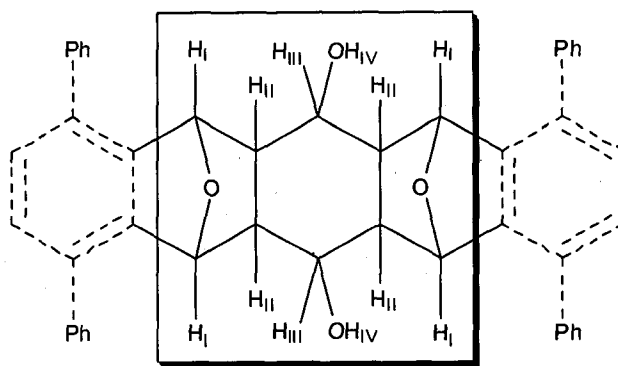


**Figure 14.** The central aliphatic diagnostic region for hypothetical structures **17a-c** and isolated molecules **18a-b**.

This strong preference for boat conformations is corroborated by molecular models and force-field calculations. For each of these structures, the number of  $^1\text{H}$  NMR resonances expected in the aliphatic diagnostic region is a function of both molecular symmetry and the rate of boat-to-boat inversions (Table 5). As such,  $^1\text{H}$  NMR spectroscopy alone can distinguish structures **17a-c** from structures **18a-b**.

**Table 5.** Expected  $^1\text{H}$  NMR spectra for compounds **17a-c** and **18a-b**.

Compound	Relationship between boat forms <sup>1</sup>	Maximum number of $^1\text{H}$ NMR signals <sup>2</sup>	
		fast inversion	Slow inversion
<b>17a</b>	CD	4	8 (2 x 4)
<b>17b</b>	CD	4	8 (2 x 4)
<b>17c</b>	CD	8	16 (2 x 8)
<b>18a</b>	CD	6	12 (2 x 6)
<b>18b</b>	CE	6	12 (1 x 12)

<sup>1</sup>CD: conformational diastereomers; CE: conformational enantiomers. <sup>2</sup>Number of  $^1\text{H}$  NMR signals in the aliphatic diagnostic region (see text). Inversion refers to boat-to-boat inversions of the central cyclohexane ring. Fast and slow inversions are relative to the NMR timescale.

The borohydride reduction of **16b** yields a crude product that is separated into two distinct bands on a silica preparative TLC plate using chloroform and ethyl acetate (10:1) as eluent. Careful characterization of these bands reveals each to be a single product, one **18a** and one **18b** (Figures 13 and 15), isolated in an approximate 1:1 ratio.

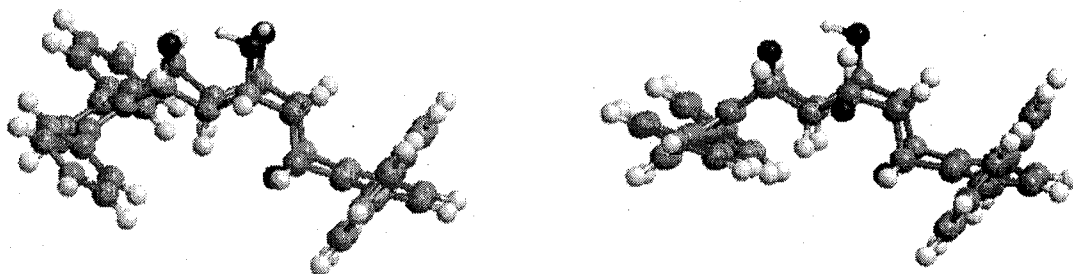


**Figure 15.** Diols **18a** (left) and **18b** (right) shown in boat conformations as predicted by molecular models and MMFF. MMFF optimized geometries.

The  $^1\text{H}$  NMR spectrum ( $\text{CDCl}_3$ ) for the slow eluting band is consistent with  $C_s$  symmetric **18a** as a single conformational diastereomer that is slow to invert on the NMR timescale (Table 5). It exhibits two  $^1\text{H}$  NMR resonances for the type  $\text{H}_\text{I}$  protons, two resonances for the type  $\text{H}_\text{II}$  protons, one resonance for the type  $\text{H}_\text{III}$  protons, and one resonance for the

type H<sub>IV</sub> protons. The assignment for the alcohol proton resonances was confirmed by deuterium exchange with D<sub>2</sub>O. This six resonance pattern is inconsistent with structures **17a-c** (Table 5) thereby confirming the assignment of **16b**. The observed preference of **18a** for one of two possible conformational diastereomers is corroborated by MMFF calculations. In one boat form, both hydroxyl groups of **18a** are pseudo-axial enabling two distinct intramolecular hydrogen bonding interactions (Figure 15). In the other boat form, the hydroxyl groups are pseudo-equatorial and do not enjoy any intramolecular hydrogen bonding. At the MMFF level, the boat form with pseudo-axial hydroxyl groups is 1.2 kcal/mol more stable.

<sup>1</sup>H NMR spectra for the fast eluting band are consistent with **18b** as a mixture of indistinguishable conformational enantiomers that are slow to ring invert on the NMR timescale (Table 5). At ambient temperature, the <sup>1</sup>H NMR spectrum (CDCl<sub>3</sub>) of **18b** reveals twelve unique resonances in the aliphatic diagnostic region (four for the type H<sub>I</sub> protons, four for the type H<sub>II</sub> protons, two for the type H<sub>III</sub> protons, and two for the type H<sub>IV</sub> protons), each integrating for one proton. As before, the assignments for the alcohol protons resonances was confirmed by deuterium exchange with D<sub>2</sub>O. Ten resonances are observed in the aliphatic diagnostic region of the corresponding <sup>13</sup>C NMR spectrum.

Variable temperature NMR spectroscopy corroborates the analysis. Thus, diol **18b** was dissolved in *o*-dichlorobenzene-*d*<sub>4</sub> and 400 MHz <sup>1</sup>H NMR spectra were recorded at progressively increasing temperatures. As illustrated in Figure 16, the type H<sub>I</sub> protons of **18b** give rise to four <sup>1</sup>H NMR singlets between 5.3 and 6.0 ppm at room temperature. At elevated temperatures, boat-to-boat interconversions become more rapid on the NMR timescale and consequently the two high field and the two low field singlets are observed

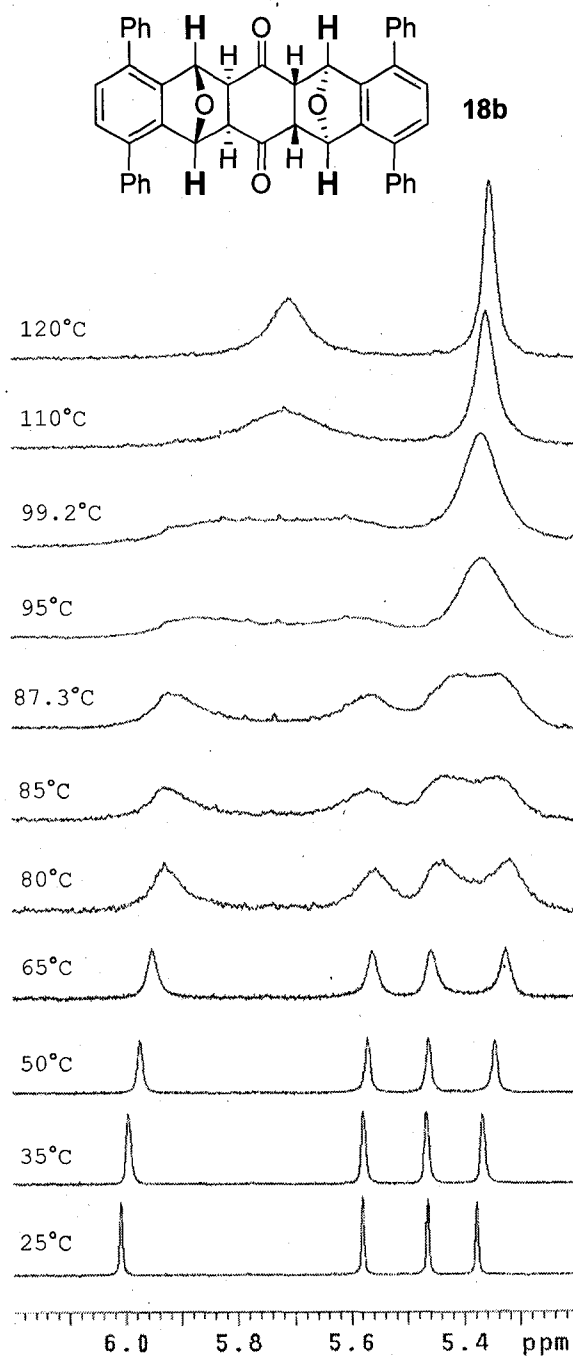


**Figure 16.** Variable Temperature NMR spectra of the type  $H_1$  protons of **18b**.

to coalescence at 87.3 °C and 99.2 °C, respectively. These signals ultimately sharpen into two singlets at higher temperatures at which point **18b** exhibits  $C_2$  symmetry on the NMR

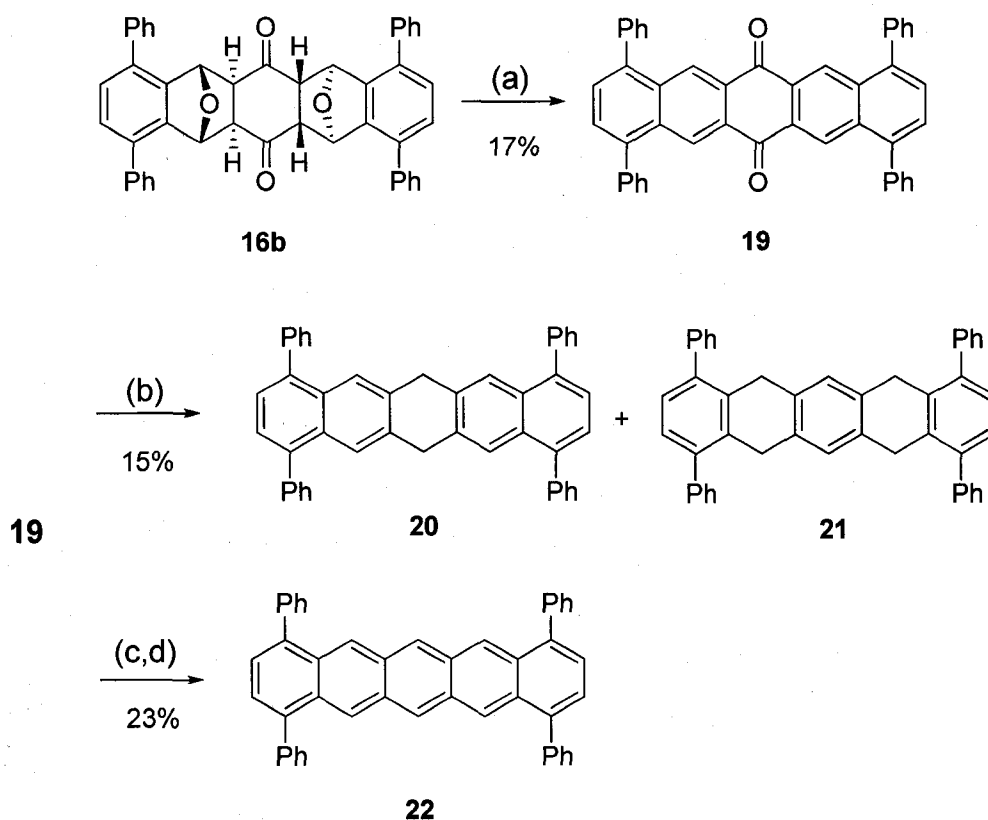
timescale. From the dynamic NMR data of **18b**, we calculate boat-to-boat inversion barrier to be  $18.1 \pm 0.2$  kcal/mol at 87.3 °C and  $17.7 \pm 0.2$  kcal/mol at 99.2 °C. The error is based on  $\pm 3$  °C gradient within the probe. An alternative interpretation is possible in which the assignments for **18a** and **18b** are switched, but it is highly unlikely. Thus, were the fast eluting band assigned the more polar structure **18a**, the room temperature  $^1\text{H}$  NMR spectrum of this compound would have to be interpreted as due to a 50:50 mixture of conformational diastereomers that are slow to invert on the NMR timescale. However, the previously mentioned MMFF calculations indicate an energetic preference for one conformational diastereomer, all but negating the possibility of a 50:50 mixture.

#### 2.3.4 Construction of a New Pentacene from **16b**

Compound **16b** is dehydrated using *p*-TsOH to give quinone **19** in modest yield (Scheme 35). Attempts to reduce **19** in a boiling mixture of hydriodic acid in acetic acid, conditions used to successfully reduce a plethora of acenequinones to hydrogen protected acenes,<sup>143</sup> met with little success. While reduction of **19** with hydriodic acid in acetic acid does produce a mixture of **20** and **21**, the yield never exceeds 15% with recovery of nearly all the starting quinone. Because compound **19** shows very poor solubility in acetic acid, the reduction was attempted in a 50/50 v/v mixture of acetic acid/chloroform with hydriodic acid. Interestingly, only the dihydro product **20** was observed, but in still lower overall reduction yields than before. An alternative conversion of **19** to **22** was found in which **19** is reduced with borane in refluxing toluene to a mixture of **20** and **22** in good crude yield.<sup>144</sup> The crude mixture is fully converted to **22** with 10% Pd/C in 1,2-dichlorobenzene at 180 °C. Compound **22** shows good solubility in carbon disulfide and,

like other pentacenes, appears blue in both solid form and in solution. The stability of **22** is also similar to that of other pentacenes. It should be stored as a solid under nitrogen in the absence of light at cool temperatures.

Scheme 35<sup>a</sup>. Synthesis of 1,4,8,11-tetraphenylpentacene, **22**.



<sup>a</sup> Reagents and conditions: (a) *p*-TsOH, PhH, Dean-Stark trap, 80°C, 1 d; (b) HI, HOAc, 118 °C, N<sub>2</sub>, dark, 5 d; (c) BH<sub>3</sub>-THF, Tol, 110 °C, N<sub>2</sub>, dark, 1 d; (d) 10% Pd/C, 1,2-dichlorobenzene, 180 °C, N<sub>2</sub>, dark, 1.5 d.

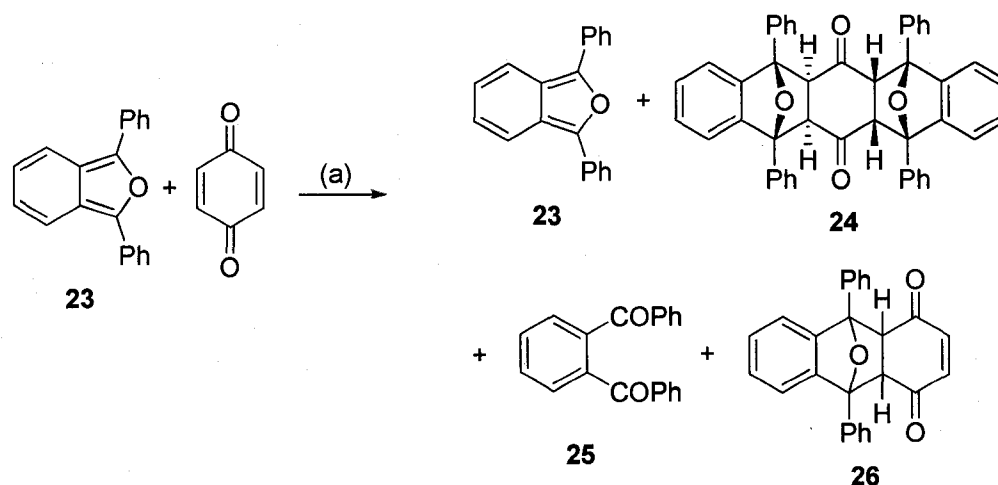
#### 2.4 A Re-Examination of the Reaction Between 1,3-Diphenylisobenzofuran (**23**) and *p*-Benzoquinone.

The highly diastereoselective formation of *exo,exo anti* **16b** was unexpected because in all previously studied dual cycloaddition reactions between isoacenofurans



and *p*-benzoquinone, a single endo,exo *syn* product was reported.<sup>111,114,115,142</sup> Surprisingly, there are only three reports describing the dual cycloaddition of commercially available 1,3-diphenylisobenzofuran, **23**, across *p*-benzoquinone, each conducted under a very limited set of conditions.<sup>145</sup> We sought to determine if alternative reaction conditions would change the diastereoselectivity associated with the dual cycloaddition between **23** and *p*-benzoquinone. As illustrated in Table 6, we studied this reaction using a variety of solvent systems and temperatures, most of which have never been reported. Reactions were run in both protic and aprotic solvents and at temperatures ranging from 25 °C to 140 °C (Scheme 36). It has been reported that the endo,exo *syn*

**Scheme 36<sup>a</sup>**. The addition of 1,3-diphenylisobenzofuran to *p*-benzoquinone yields only one type of dual cycloaddition product.



<sup>a</sup> Reagents and conditions: (a) various; see Table 6.

product undergoes retro Diels-Alder reactions under relatively mild conditions. At elevated temperatures, the reactions are presumed to be reversible. In all cases, the only dual cycloaddition product observed is the known endo,exo *syn* diastereomer **24** (Figure 11, Scheme 36, Table 6). Because 4,7-diphenylisobenzofuran **5** shows greatest

**Table 6.** Survey of reactions between **23** and *p*-benzoquinone under various conditions.

Exp.	<b>23</b> : BQ <sup>a</sup>	Reagents / Temp (°C) / Time (h)	Precipitate Product Ratios <sup>b</sup>			
			<b>23</b>	<b>24</b>	<b>25</b>	<b>26</b> <sup>c</sup>
12	2.1	HOAc / 50 / 1	32	100	145	0
13	2.0	HOAc / 70 / 1	450	100	1580	0
14	2.3	HOAc / 90 / 2	100	0	110	0
15	2.1	HOAc, Ac <sub>2</sub> O / 118 / 16	100	0	120	0
16	2.2	EtOH / 78 / 1	0	100	0	0
17	2.0	4 HOAc, EtOH / 108 / 1	0	100	0	trace
18	2.1	21 HOAc, EtOH / 108 / 1	0	100	0	trace
19	2.1	210 HOAc, EtOH / 108 / 1	0	100	0	trace
20	2.0	HOAc, CHCl <sub>3</sub> (50:50 v/v) / 50 / 1	16	100	46	0
21	2.0	HOAc, CHCl <sub>3</sub> (50:50 v/v) / 85 / 1	83	0	100	0
22	2.1	CHCl <sub>3</sub> / 25 / 17	50	100	65	trace
23	2.0	CHCl <sub>3</sub> / 61 / 1	trace	100	10	5
24	2.0	CHCl <sub>3</sub> / 61 / 17	trace	100	10	8
25	2.1	Toluene / 111 / 18	0	100	36	14
26	2.1	Xylenes / 140 / 16	0	100	58	8

<sup>a</sup>BQ is *p*-benzoquinone. <sup>b</sup>Relative ratios of **23-26** present in precipitate collected, normalized to 100 for most abundant species. <sup>c</sup>A single mono addition adduct is observed by <sup>1</sup>H NMR spectroscopy.

diastereoselectivity toward formation of *exo,exo anti* **16b** in boiling acetic acid (Table 6), we studied the corresponding reaction involving 1,3-diphenylisobenzofuran **23**. However, as illustrated in Table 6 (Exp. 12-15), **23** degrades to 1,2-dibenzoylbenzene, **25**, in hot acetic acid. Thus, compound **23** with its 1,3-diphenyl substitution pattern is considerably more prone to hydrolysis than compound **5** which possesses a 4,7-diphenyl substitution pattern. In fact, the hydrolysis of **23** to **25** accompanies most of the reactions studied, to

varying degrees. While good yields of **24** could be achieved in chloroform, toluene and xylenes, the best solvent for the clean formation of **24** is ethanol.

## CHAPTER 3

### A STUDY OF THE DIELS-ALDER CYCLOADDITIONS BETWEEN ARYL SUBSTITUTED ACENES AND [60]FULLERENE

#### 3.1 Introduction

In our acene-fullerene research, we have synthesized phenyl-substituted acenes for the strategic purpose of directing [60]fullerene cycloadditions to predetermined rings along the acene backbone. In the absence of substituents, [60]fullerene will preferentially cycloadd across the centermost ring of the acene. When phenyl substituents are located at these positions, [60]fullerene cycloaddition is directed to adjacent rings of the acene. Thus, the phenyl substituents impart the regiochemistry of [60]fullerene cycloaddition. While this effect is largely driven by steric resistance, we made the interesting observation that [60]fullerene cycloaddition across phenyl substituted acenes is often more facile than addition across the corresponding unsubstituted acene. That is, the presence of phenyl substituents is believed, in some cases, to hasten the rate of [60]fullerene cycloaddition.

To further probe the influence of phenyl substituents on the cycloaddition of [60]fullerene across phenyl substituted acenes, we studied the Diels-Alder reactions between [60]fullerene and both 1,4-diphenyltetracene, **15**, and 1,4,8,11-tetraphenylpentacene, **22** (Figure 17). In the case of **15**, [60]fullerene addition can occur

across one of two chemically nonequivalent rings while in the case of **22**, [60]fullerene can cycloadd across either the central ring or those rings flanking the terphenyl moieties. As elaborated below, we believe that aryl CH–fullerene  $\pi$  interactions are influencing these cycloadditions.

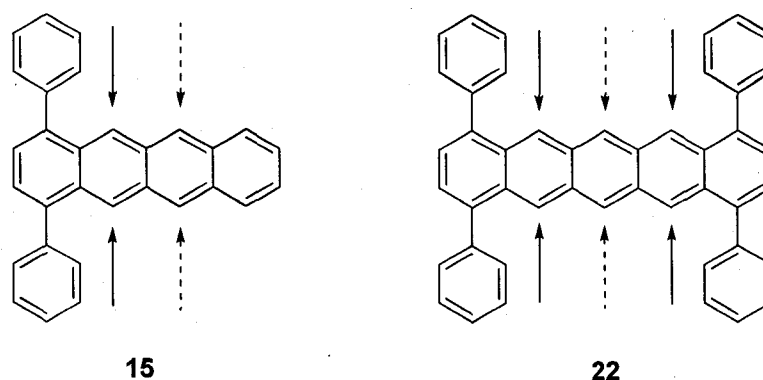


**Figure 17.** Compounds **15** and **22** each have two chemically distinct ring types across which Diels-Alder cycloaddition can occur.

Non-covalent interactions including van der Waals forces, dipole-dipole interactions, and hydrogen bonding play an important role in chemical reactions and supramolecular chemistry.<sup>146</sup> A less known but still important non-bonding interaction is the CH/ $\pi$  interaction.<sup>147</sup> First suggested by Tarmes in 1952 to explain the interaction between benzene and chloroform,<sup>148</sup> CH/ $\pi$  interactions are the weakest of all hydrogen bonds, estimated to have an enthalpy of less than 1 kcal mol<sup>-1</sup>.<sup>147</sup> More recently, Shibasaki, *et al.* experimentally determined the interaction energy of benzene-methane in the gas phase to be 1.03-1.13 kcal mol<sup>-1</sup>.<sup>149</sup> Traditionally, a CH/ $\pi$  interaction has been viewed as one between a slightly acidic CH hydrogen and a  $\pi$  base.<sup>147</sup> From an orbital perspective, this would indicate an interaction between the HOMO on the  $\pi$  donor and a  $\sigma^*$  on the hydrogen donor. Examples include the benzene dimer which adopts a T-shaped conformation in the solid state<sup>150</sup> and the benzene-chloroform complex<sup>151</sup> in which the

relatively acidic hydrogen on chloroform associates with the benzene  $\pi$ -system. Nakagawa and Fujiwara analyzed chemical shifts of the methyl protons in a number of substituted toluene molecules in both  $\text{CCl}_4$  and benzene solvent. They found that the magnitudes of the difference in chemical shifts (i.e., greater shielding in benzene solvent than in  $\text{CCl}_4$ ) were a function of the acidity of the methyl groups, which they explained as evidence for CH/ $\pi$  interactions between the methyl hydrogens and benzene.<sup>152</sup> In this and other traditional CH/ $\pi$  interactions, the interacting orbitals are presumably a  $\sigma^*$  of the H-donor and a  $\pi$  of the H-acceptor.

Recently, Nishio and coworkers made a compelling case that fullerenes routinely participate in CH/ $\pi$  interactions.<sup>153</sup> They surveyed the Cambridge Crystallographic Database and found numerous examples in which the fullerene  $\pi$  system is located within 3 Å of a CH donor. Often, a CH-fullerene distance was observed at or below 2.9 Å, as low as 2.5 Å. For example, Olmstead, *et al.* found that ethyl substituents in porphyrin-[60]fullerene complexes preferentially orient in the crystal structure such that they lie within the van der Waals distance of the [60]fullerene cage.<sup>154</sup>

Here we consider the possible role of aryl CH-fullerene  $\pi$  interactions in the Diels-Alder cycloadditions involving [60]fullerene and either **15** or **22**. We synthesized **15** and a series of related 1,4-diaryl-substituted tetracenes and studied the regiochemistries of their Diels-Alder reactions with [60]fullerene and other dienophiles under both kinetically and thermodynamically controlled reaction conditions. In all cases, [60]fullerene shows a greater selectivity for cycloaddition across the 5,12 carbons of 1,4-diaryltetracenes compared to other dienophiles. In conjunction with our experimental results, we performed computational studies to help clarify the regioselective addition of

[60]fullerene across 1,4-diaryltetracenes. We also studied the Diels-Alder reactions between **22** and [60]fullerene, as well as other dienophiles. We observe formation of both mono- and bisadducts with [60]fullerene (i.e., one and two [60]fullerene additions respectively), while other dienophiles are far more selective for mono addition. Computational investigations were designed to shed light on the observed selectivity. Direct evidence for CH/ $\pi$  interactions was obtained from a careful examination of  $^1\text{H}$  NMR chemical shift data. Finally, we surveyed the Cambridge Crystallographic Database to find examples of aryl-fullerene CH/ $\pi$  interactions in which the CH/ $\pi$  distance is 2.5 to 3.2 Å. This survey led us to understand the nature of phenyl CH donors that are inclined to participate in aryl CH–fullerene  $\pi$  interactions. Our combined results suggest that aryl CH–fullerene  $\pi$  interactions play a significant role in fullerene-acene chemistry. However, these interactions may not involve fullerene  $\pi$  and CH  $\sigma^*$  orbitals, as per a normal CH/ $\pi$  interaction. Instead, we raise the interesting possibility that aryl CH–fullerene  $\pi$  interactions may involve  $\pi^*$  orbitals on [60]fullerene and  $\sigma$  orbitals on the aryl CH donors. This unique type of CH/ $\pi$  interaction could be termed an *inverse electron demand* CH/ $\pi$  interaction but more work will be required to verify the participating orbitals.

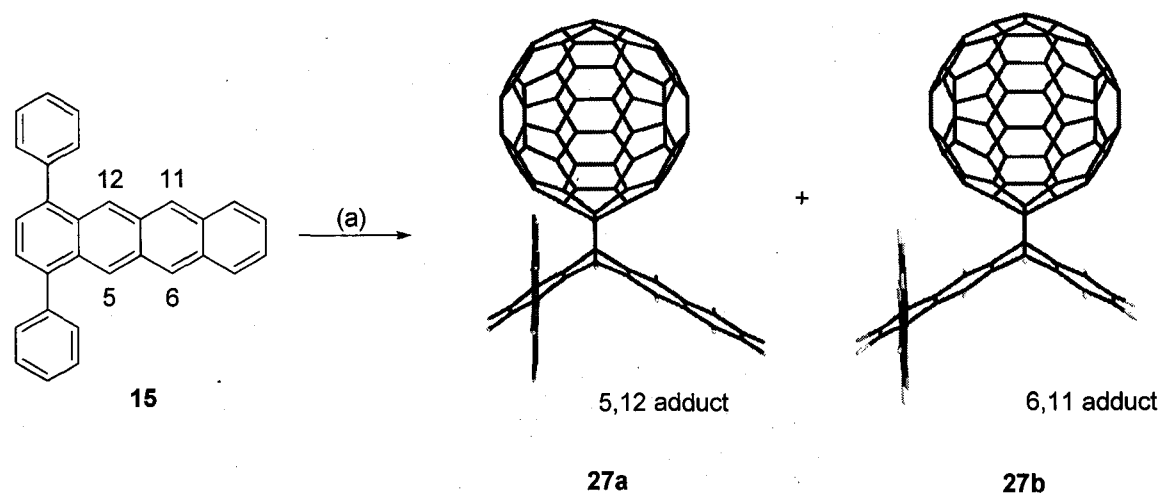
### 3.2 Diels-Alder Reactions Between 1,4-Diphenyltetracene, **15**, and [60]Fullerene

Compound **15** was synthesized as illustrated in Scheme 33 of Chapter 2. It serves as a simple platform on which to study the effects of phenyl substituents on acene-[60]fullerene cycloaddition chemistries. While tetracene adds [60]fullerene across one of its two equivalent internal rings, compound **15** has two chemically distinct rings across

which [60]fullerene can cycloadd (Scheme 37). Addition across the 5,12 carbons located adjacent to the terphenyl moiety produces **27a** while cycloaddition across the 6,11 carbons yields **27b**. We investigated the regioselective addition of [60]fullerene across **15** under both kinetically and thermodynamically controlled reaction conditions (Table 7).

Under kinetically controlled conditions (i.e., 50 °C), [60]fullerene shows preferential cycloaddition across the 5,12 carbons over the 6,11 carbons to yield **27a** and **27b** in a ratio of 2.6 : 1, respectively. Heating a mixture of **27a** and **27b** to 50 °C in the presence of excess maleic anhydride yielded no reaction, suggesting that [60]fullerene cycloaddition is indeed irreversible at 50 °C.

**Scheme 37<sup>a</sup>**. Diels-Alder cycloaddition between **15** and [60]fullerene.



<sup>a</sup> Reagents and conditions: (a) [60]fullerene, heat; see Table 7.

**Table 7.** Kinetic and thermodynamic reaction conditions for [60]fullerene cycloaddition to **15**.

Exp.	<b>15</b> : C <sub>60</sub>	Conditions <sup>a</sup>	Time	Yield	<b>27a</b> : <b>27b</b> <sup>b</sup>
1	1 : 1.2	PhH, 50 °C	1.5 h	71%	2.6 : 1
2	1 : 1.2	<i>o</i> -DCB <sub>d4</sub> , 180 °C	15 m (1 h)	68%	7.6 : 1 (7.5 : 1)

<sup>a</sup>All reactions performed under N<sub>2</sub> in the absence of light. <sup>b</sup>Ratios are calculated from <sup>1</sup>H NMR integrations of crude product mixtures.



Under thermodynamic conditions (i.e., 180 °C), the addition proceeds with still greater regioselectivity, favoring **27a** in a ratio of 7.6 : 1 (Table 7). From this ratio we find a Gibbs free energy difference,  $\Delta G^\circ(453\text{ K})$ , of 1.8 kcal mol<sup>-1</sup>. Thermodynamic equilibrium was achieved under the reaction conditions utilized as verified in the following manner. A sample of **27a** and **27b** was heated to 180 °C for 15 minutes in the presence of excess maleic anhydride. Under these conditions, complete substitution of [60]fullerene addends with maleic anhydride was observed. Also, no significant change in the ratio of **27a** and **27b** is observed when the addition of [60]fullerene to **15** is performed at 180 °C for either 15 minutes or 1 hour. Thus, rapid equilibration is achieved at 180 °C.

While <sup>1</sup>H NMR spectroscopy is useful to determine the relative amounts of **27a** and **27b**, it proves inadequate to differentiate between **27a** and **27b**. Indeed, each isomer produces <sup>1</sup>H NMR signals which are qualitatively consistent with either **27a** or **27b**. To discriminate between the isomers, we used Nuclear Overhauser Effect Spectroscopy (NOESY1D). Careful analysis of **27a** and **27b** reveals that each isomer should give rise to unique NOE enhancement patterns during selective excitation of the bridgehead methine protons at the site of cycloaddition (Figure 18).

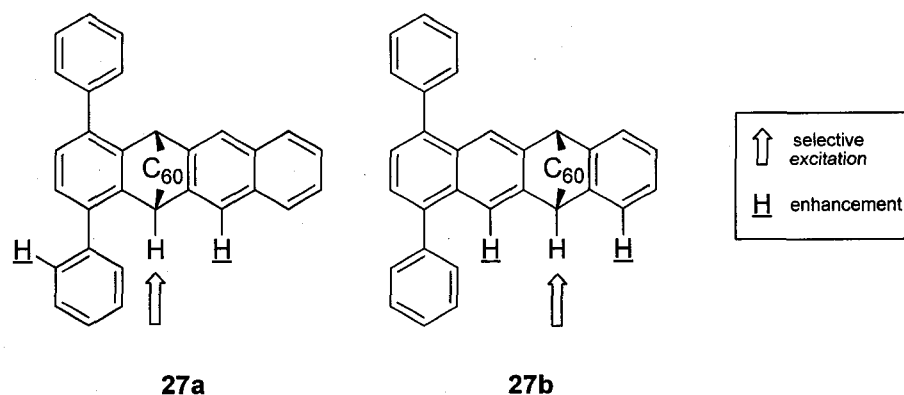


**Figure 18.** The 5,12 and 6,11 cycloaddition adducts of **15** are distinguished by NOE spectroscopy.

Selective excitation of the bridgehead methine protons of **27a** should result in the enhancement of aromatic X protons and also the four *ortho* protons of the phenyl substituents. Selective excitation of the bridgehead methine protons on **27b** should result in the enhancement of aromatic X protons and one half of an aromatic AA'MM' multiplet. Figure 19 shows the  $^1\text{H}$  NMR spectrum and NOESY1D spectra of the mixture of **27a** and **27b**. In the NOESY1D spectra, signals that are selectively excited appear as inverse phase peaks while protons of close spatial proximity to the excited proton rise from the baseline. Selective excitation of the bridgehead methine protons of the minor product results in enhancement of aromatic X and AA' signals. This enhancement pattern, as well as the enhancement patterns of the remaining NOE spectra for the minor product, are uniquely consistent with the 6,11 addition product (i.e., **27b**).

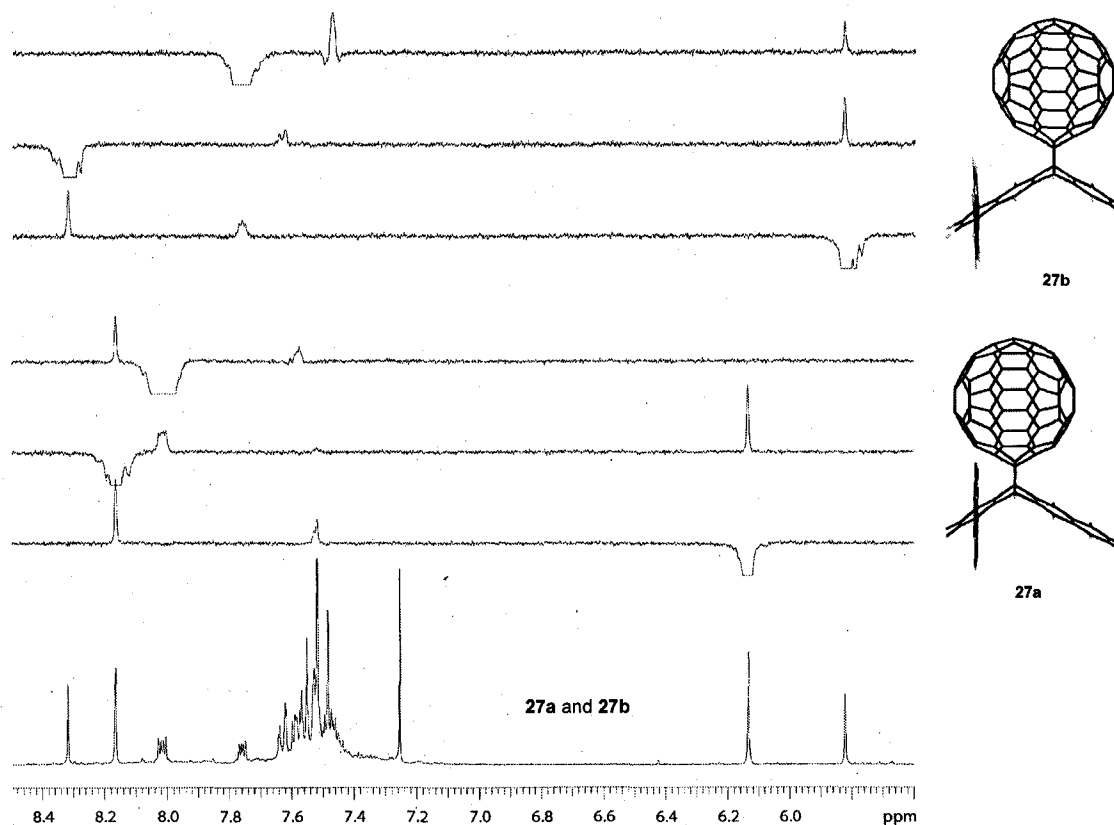


**Figure 19.**  $^1\text{H}$  NMR spectrum for a mixture of **27a** and **27b** and NOE spectra for **27a** (bottom) and **27b** (top).

Likewise, the complementary enhancement spectra for selective excitation of the major product are uniquely consistent with 5,12 addition (i.e., **27a**). Thus, the isomers are unambiguously assigned with NOE spectroscopy. This NOE technique has proven quite valuable. It has been utilized to not only discriminate **27a** and **27b**, but all 5,12 and 6,11 adduct isomers of every dienophile utilized in this study save for a single set of regioisomers, as noted in Table 10. These NOE spectra can be found in their entirety in the Appendix.

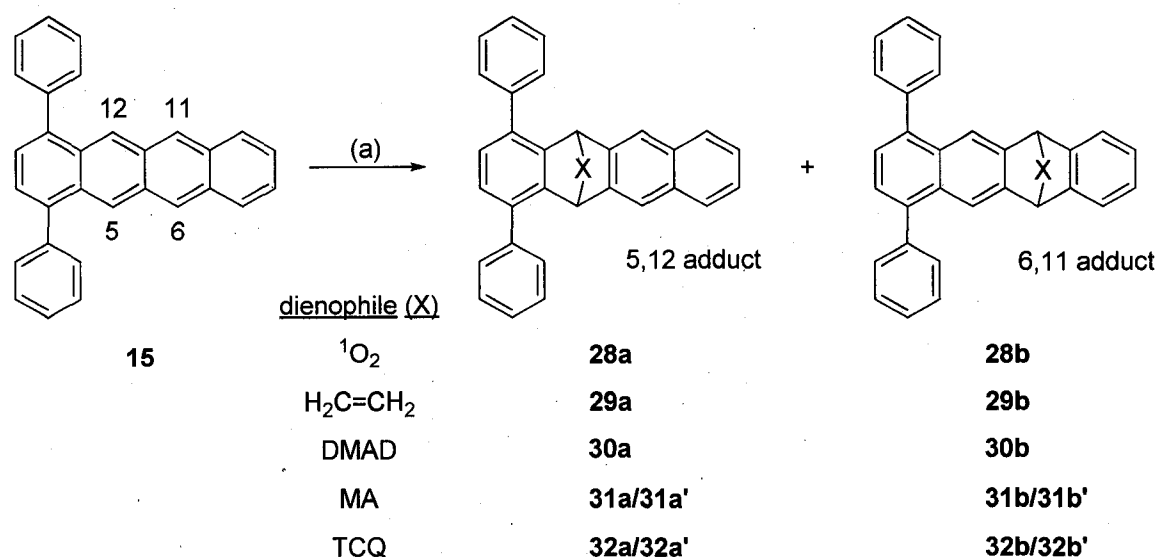
The regioselective addition of [60]fullerene to **15** across the more sterically demanding 5,12 carbons under both kinetic and thermodynamic conditions is surprising. In order to understand this result, we need to consider the intrinsic reactivity of the two

internal rings in **15** and also the ground state energies of **27a** and **27b**. In this manner, we hope to ascertain to what degree, if any, CH/ $\pi$  interactions influence the regioselective addition.

### 3.3 Diels-Alder Reactions Between **15** and Other Dienophiles Under Kinetically Controlled Reaction Conditions

To better understand the intrinsic reactivity of **15**, the acene was reacted with a range of additional dienophiles: singlet oxygen ( $^1\text{O}_2$ ), ethylene, dimethyl acetylenedicarboxylate (DMAD), maleic anhydride (MA) and tetrachloroquinone (TCQ) (Scheme 38). The results are summarized in Table 8.

Scheme 38<sup>a</sup>. Diels-Alder cycloaddition between **15** and various dienophiles.



<sup>a</sup> Reagents and conditions: (a) various; see Table 8.

**Table 8.** Reactions between **15** and various dienophiles run under kinetic (Exp. 3-7) and thermodynamic (Exp. 8) conditions.

Exp.	X	<b>15</b> : X	Conditions <sup>a</sup>	Time	5,12 : 6,11 <sup>b</sup>
3	<sup>1</sup> O <sub>2</sub>	--	CDCl <sub>3</sub> , ambient <sup>c</sup>	20 h	1.7 : 1
4	ethylene	--	160 psi, Tol, bomb, 175 °C <sup>c</sup>	3 d	1.9 : 1
5	DMAD	1 : 27	<i>o</i> -DCB <sub>d4</sub> , 180 °C <sup>c</sup>	15 m	2.1 : 1
6	MA	1 : 1.1	<i>o</i> -DCB <sub>d4</sub> , 180 °C <sup>c</sup>	1 h	1 : 1.2 <sup>d</sup>
7	TCQ	1 : 1.2	<i>o</i> -DCB <sub>d4</sub> , 125 °C <sup>c</sup>	1 h	1 : 2.3 <sup>d</sup>
8	TCQ	1 : 1.1	<i>o</i> -DCB <sub>d4</sub> , 180 °C <sup>c</sup>	15 m (1 h)	1.7 : 1 (1.9 : 1) <sup>d</sup>

<sup>a</sup>All reactions performed under N<sub>2</sub> in the absence of light, except in the case of oxygen. <sup>b</sup>Ratios are calculated from <sup>1</sup>H NMR integrations of crude product mixtures. <sup>c</sup>Kinetic reaction conditions. <sup>d</sup>A mixture of four diastereomers; see text. <sup>e</sup>Thermodynamic reaction conditions.

### 3.3.1 Synthesis and Characterization of Diels-Alder Adducts **28-32**

For addition of singlet oxygen to **15** to form **28a** and **28b** (Exp. 3, Table 8), the acene was dissolved in 1.5 mL of CDCl<sub>3</sub> in an open vial and the solution left open to the atmosphere under ambient lighting. As discussed in Section 1.3.1, Scheme 7, acenes react with singlet oxygen to yield dioxo bridged cycloaddition adducts. The reaction proceeds with total conversion of **15** to **28a** and **28b**. These products were characterized by <sup>1</sup>H NMR spectroscopy and distinguished from one another by NOESY1D in an analogous manner as described above for **27a** and **27b** (see Appendix for these and related spectra, organized by compound number).

In the case of ethylene cycloaddition across **15**, decidedly more severe reaction conditions were applied. Literature precedent exists for ethylene addition to tetracenes and these reactions involved elevated pressure and temperature.<sup>155</sup> As such, **15** was combined with toluene in a steel bomb and the apparatus pressurized with ethylene to 160

psi, sealed, and heated in a sand bath to 175 °C (Exp. 4, Table 8). The crude product mixture was characterized by  $^1\text{H}$  NMR spectroscopy. The 5,12 and 6,11 addition isomers were distinguished by NOESY1D (see Appendix).

The Diels-Alder adducts **30a** and **30b** were synthesized by heating a mixture of DMAD and **15** in *o*-dichlorobenzene- $d_4$  to 180 °C (Exp. 5, Table 8). When DMAD and **15** were heated to 80 °C in benzene for only 16 hours, trace quantities of the Diels-Alder adducts **30a** and **30b** were observed, demonstrating a relatively high barrier for DMAD addition to **15**. Adducts **30a** and **30b** were isolated as a mixture and characterized by  $^1\text{H}$ ,  $^{13}\text{C}$ , NOESY1D and HSQC NMR spectroscopies (see Appendix).

Maleic anhydride was reacted with **15** at 180 °C to yield a mixture of 4 diastereomers, **31a**, **31a'**, **31b** and **31b'**. The increased number of Diels-Alder products is a consequence of the fact that maleic anhydride can cycloadd in both endo and exo fashions across either the 5,12 or the 6,11 rings of **15**. The 5,12 and 6,11 addition products can be distinguished by NOESY1D (see Appendix). However, distinction between the 5,12 endo and 5,12 exo products and also between the 6,11 endo and 6,11 exo products requires NOESY2D (Figures 20 and 21). Analysis of NOESY2D spectra is analogous to that of COSY spectra, where cross peaks correspond to mutual NOE enhancements. Because the 5,12/6,11 nature of the molecules giving rise to the methine proton signals at the site of cycloaddition (type  $\text{H}_{\text{II}}$  protons) can be assigned by NOESY1D, examination of the cross peaks in the NOESY2D spectra associated with these proton resonances and those of the methine protons of the maleic anhydride rings (type  $\text{H}_{\text{I}}$  protons) elucidates the 5,12/6,11 nature of the type  $\text{H}_{\text{I}}$  protons (Figure 20). A careful examination of the NOESY2D cross peaks between type  $\text{H}_{\text{I}}$  protons and protons

of the acene backbone reveal the endo/exo nature of each molecule (Figure 21). For the 5,12 isomers, a cross peak for the type H<sub>I</sub> protons and an aromatic X is consistent with the exo configuration (i.e., **31a'**) while a cross peak with the ortho protons of a phenyl substituent is consistent with the endo configuration (i.e., **31a**). For the 6,11 isomers, a cross peak for the type H<sub>I</sub> protons and an aromatic X is also consistent with the exo configuration (i.e., **31b'**) while a cross peak with an AA' multiplet is consistent with the endo configuration (i.e., **31b**). Due to coincidental overlap some of these correlations cannot be observed. However, from Figure 22 it is observed that the upfield type H<sub>I</sub> proton signal of the 5,12 isomers correlates to an aromatic X, identifying it as the 5,12 exo product (**31a'**). Consequently, the downfield type H<sub>I</sub> proton signal must be the 5,12 endo product (**31a**).

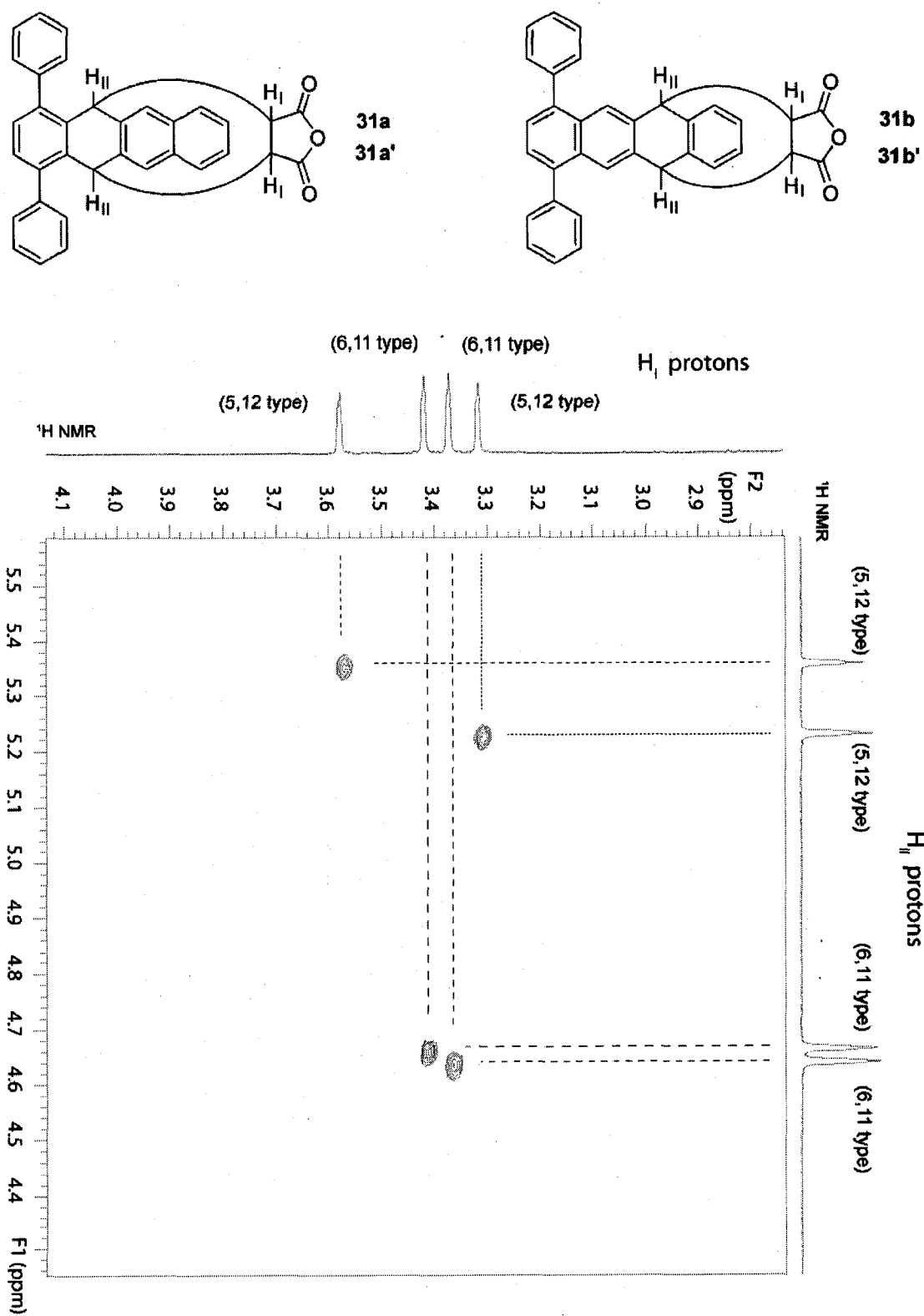
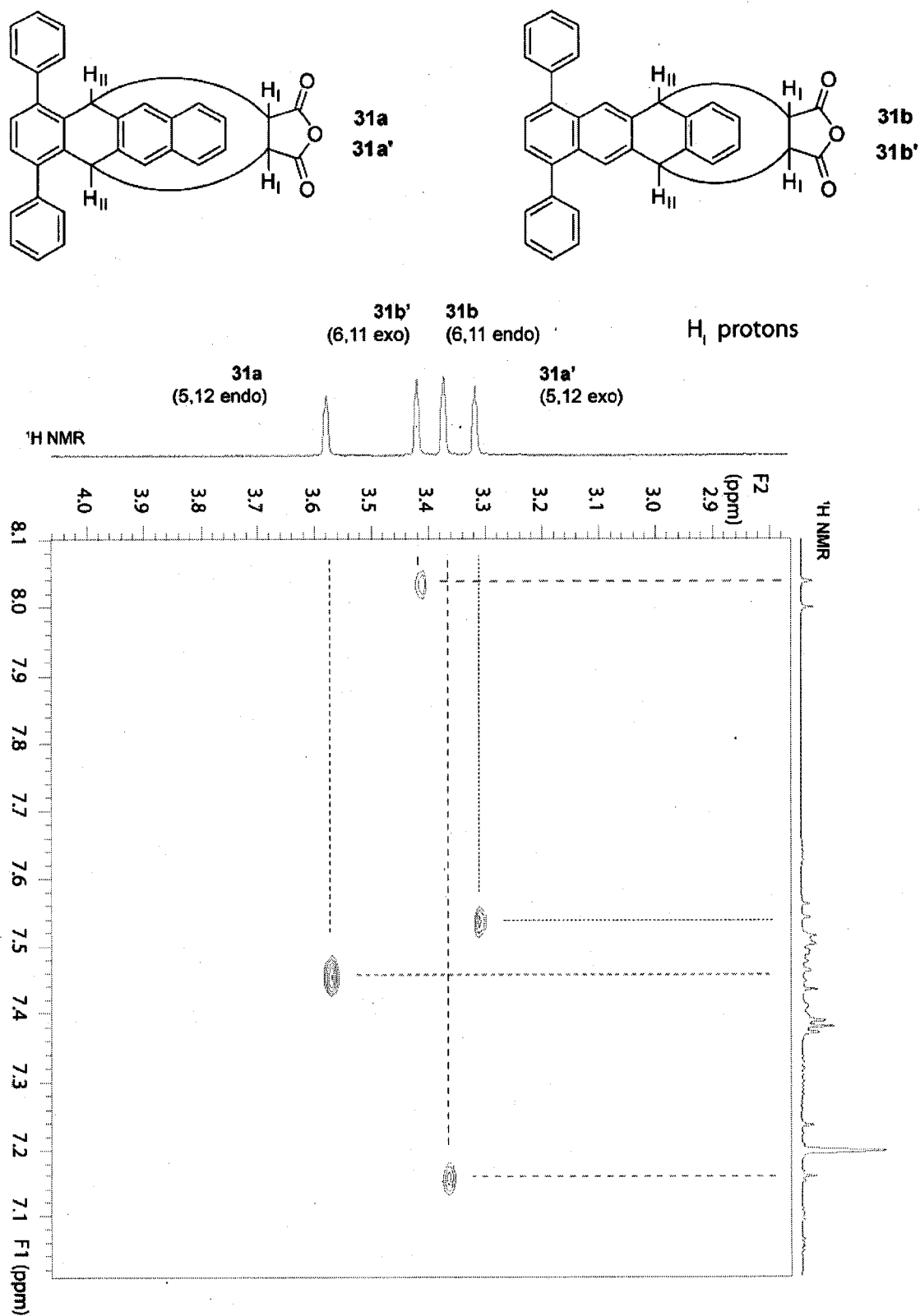


Figure 20. NOESY2D spectrum of type  $H_I$  and  $H_{II}$  protons of 31a-31b'.





**Figure 21.** NOESY2D spectrum of type  $H_I$  and aromatic protons of **31a-31b'**.

For isomers **31b** and **31b'**, the downfield type H<sub>I</sub> proton signal shows a correlation to an aromatic X, identifying it as the 6,11 exo product (**31b'**). Consequently, the upfield type H<sub>I</sub> proton signal must be the 6,11 endo product (**31b**). Thus, careful examination of the NOESY1D and NOESY2D spectra of a mixture of **31a**, **31a'**, **31b** and **31b'** reveals the relative endo/exo nature of each. The ratio of **31a** : **31a'** : **31b'** : **31b** (i.e., 5,12 endo : 5,12 exo : 6,11 exo : 6,11 endo) is 1 : 1.15 : 1.22 : 1.29, respectively.

Cycloaddition of TCQ to **15** did not occur at temperatures of 50 °C, 75 °C or 100 °C over spans of 1 hour each. Not until the reactants were heated to 125 °C for 1 hour was cycloaddition observed with approximately 20% conversion of the acene. Like maleic anhydride, TCQ can and does cycloadd in both endo and exo fashions across both the 5,12 and 6,11 rings of **15** to yield adducts **32a**, **32a'**, **32b** and **32b'**. While the 5,12 and 6,11 adducts are discernible by NOESY1D, the endo/exo nature of the adducts cannot be determined, to the best of our knowledge, by any NMR technique.

### 3.3.2 Irreversible/Reversible Nature of Reactions Between **15** and Various Dienophiles, Experiments 3-8

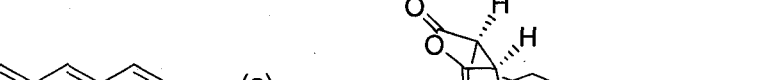
With only one exception (Exp. 8, Table 8; TCQ at 180 °C), all of the cycloadditions described in Table 8 are believed to have occurred in an irreversible fashion. The dioxo bridged acene adducts **28a** and **28b**, for example, do not undergo retro-Diels-Alder reaction. Rather, the O-O bond cleaves irreversibly to form acenequinones. When **15** and ethylene were heated together at 260 °C for 2 days we saw no change in the ratio of products associated with reaction at 175 °C for 3 days. In other cases, for example the DMAD adducts **30a** and **30b**, a lack of reversibility was

demonstrated by heating the product mixture to 180 °C in the presence of excess maleic anhydride, where no reaction was observed. Maleic anhydride adducts **31a**, **31a'**, **31b** and **31b'** also showed no reaction when heated to 180 °C in the presence of excess DMAD. However, when a sample of the TCQ adducts **32a**, **32a'**, **32b** and **32b'** were heated to 180 °C in the presence of excess maleic anhydride, complete substitution of the TCQ addends by maleic anhydride was observed, thus indicating reversible formation of these products at 180 °C.

### 3.3.3 Summary of Results for Reactions of **15** Run Under Kinetically Controlled Conditions

Under kinetically controlled reaction conditions (Exp. 3-7, Table 8),  $^1\text{O}_2$ , ethylene and DMAD all favor 5,12 cycloaddition, although to a lesser extent than [60]fullerene (Exp. 1, Table 7). This shows that the 5,12 ring is intrinsically favored over the 6,11 ring of **15**. Interestingly, though, this selectivity is reversed when the larger dienophiles maleic anhydride and TCQ are reacted with **15** under kinetically controlled conditions (Exp. 6-7, Table 8). These larger dienophiles can add in both an endo and an exo fashion. The formation of four diastereomers somewhat complicates the analysis but does not diminish the apparent significance of steric resistance in determining 5,12 : 6,11 regioselectivity. It is in this light that the 5,12 selectivity exhibited by the very large dienophile [60]fullerene seems especially odd. We are left to conclude that the kinetically controlled reaction involving [60]fullerene and **15** is special. It must involve a unique interaction that is absent in the other reactions studied, one that overrides the steric resistance associated with large dienophiles.

As described in section 3.3.1, no strong endo/exo selectivity is associated with the cycloaddition reaction between maleic anhydride and **15**. This led us to wonder whether unsubstituted tetracene would add maleic anhydride with any endo/exo selectivity. Remarkably, this important detail is neglected in all literature reports of the reaction.<sup>102b,103a,156</sup> As both exo and endo maleic anhydride-tetracene isomers **33a** and **33b** should be discernable by NOE spectroscopy, we investigated the reaction (Scheme 39). We found that exo addition is favored to endo in a ratio of 1.6 : 1. Heating a sample of **33a/33b** to 180 °C in the presence of an excess of DMAD yields no reaction, indicating that the reaction is irreversible under these conditions. Because we observed that the adducts **31a**, **31a'**, **31b** and **31b'** do not easily undergo cycloreversion (*vide infra*), we made no attempt to find the ratio of **33a** : **33b** under thermodynamic conditions.



73

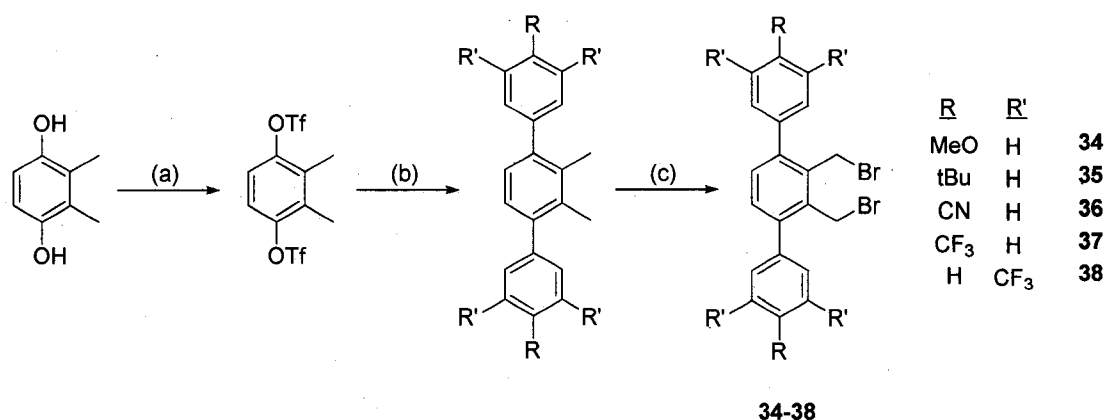
### 3.5 Synthesis and Diels-Alder Reactivity of 1,4-Diaryltetracenes 41-45

If the special regioselectivity associated with [60]fullerene cycloaddition is indeed due to CH/ $\pi$  interactions between [60]fullerene and the 1,4 phenyl substituents, then it should be possible to magnify or diminish this interaction through electronic modifications of the phenyl substituents. In order to probe substituent effects in the reaction between [60]fullerene and **15**, several *para* substituted and one bis(*meta*) substituted 1,4-diaryltetracene derivatives were synthesized and their Diels-Alder reactivities studied.

#### 3.5.1 Synthesis of Electron-rich and Electron-poor 1,4-Diaryltetracenes 41-45

Two slightly different synthetic routes to the desired 1,4-diaryltetracenes were developed. These relatively short, high yielding procedures are used to synthesize *p*-methoxy, *p*-terbutyl, *p*-cyano, *p*-trifluoromethyl and bis(*meta*) trifluoromethyl derivatives of 1,4-diphenyltetracene (Schemes 40, 41 and 42). Following synthesis of the series of

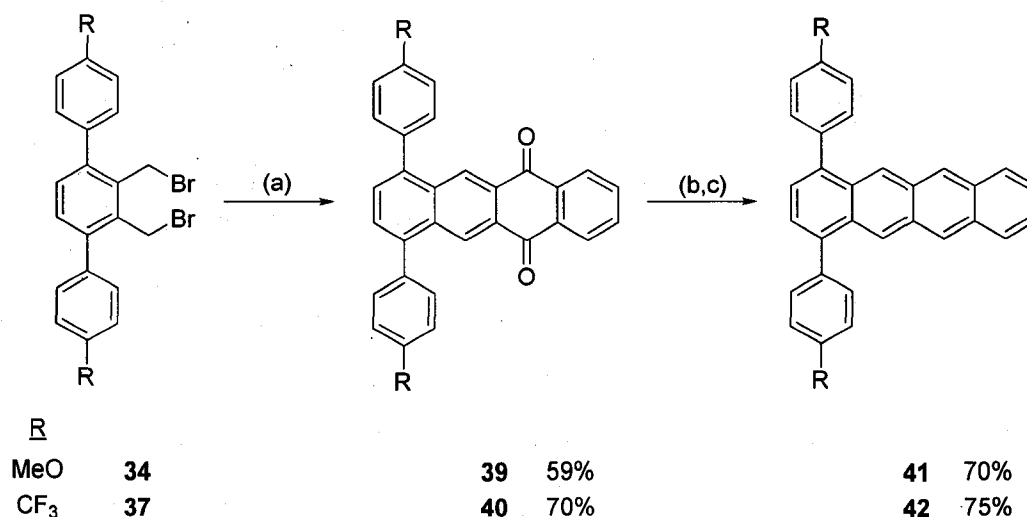
**Scheme 40<sup>a</sup>**. Synthesis of dibromomethyl terphenyl derivatives **34-38** as performed by Dr. Jazdyk.



<sup>a</sup> Reagents and conditions: (a) TfO<sub>2</sub>, pyridine, 25 °C, 1 h; (b) Pd(OAc)<sub>2</sub>, 2-dicyclohexylphosphino-2',6'-dimethoxy-1,1'-biphenyl (S-Phos), ArylB(OH)<sub>2</sub>, K<sub>3</sub>PO<sub>4</sub>, THF, 80 °C, 18-24 h; (c) NBS, BPO, CCl<sub>4</sub>, 77 °C, 14 h.

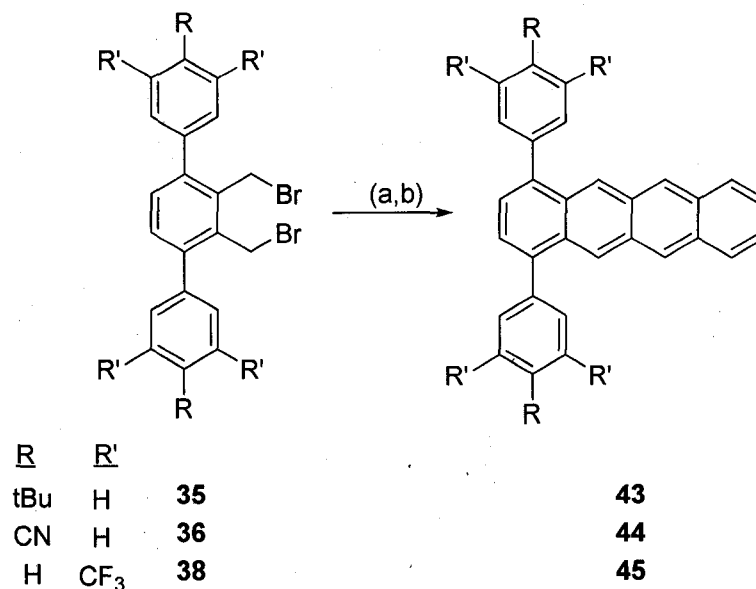
dibromomethylterphenyl derivatives **34-38** by Dr. Mikaël Jazdyk (Scheme 40), the derivatives **34** and **37** were first reacted with 1,4-naphthoquinone to yield the corresponding quinones **39** and **40** (Scheme 41). These were sequentially reduced with borane to a mixture of 6,11-dihydrotetracenes and aromatic tetracenes and then oxidized with palladium on carbon to give the target acenes **41** and **42**. The syntheses of acenes **43**, **44**, and **45** were performed by Dr. Jazdyk in two steps from the terphenyl compounds **35**, **36**, and **38**, respectively, using 1,4-epoxynaphthalene (Scheme 42). The color of compounds **41-45** range from orange to red-brown.

**Scheme 41<sup>a</sup>.** Synthesis of 1,4-diaryltetracene derivatives **41** and **42**.



<sup>a</sup> Reagents and conditions: (a) 1,4-naphthoquinone, KI, DMF, 125 °C, 18-24 h; (b) BH<sub>3</sub>-THF, Tol, 110 °C, N<sub>2</sub>, dark, 1 d; (c) 10% Pd/C, 1,2-dichlorobenzene, 180 °C, N<sub>2</sub>, dark, 4-7 d.

**Scheme 42<sup>a</sup>.** Synthesis of 1,4-diaryltetracene derivatives **43-45** as performed by Dr. Jazdyk.

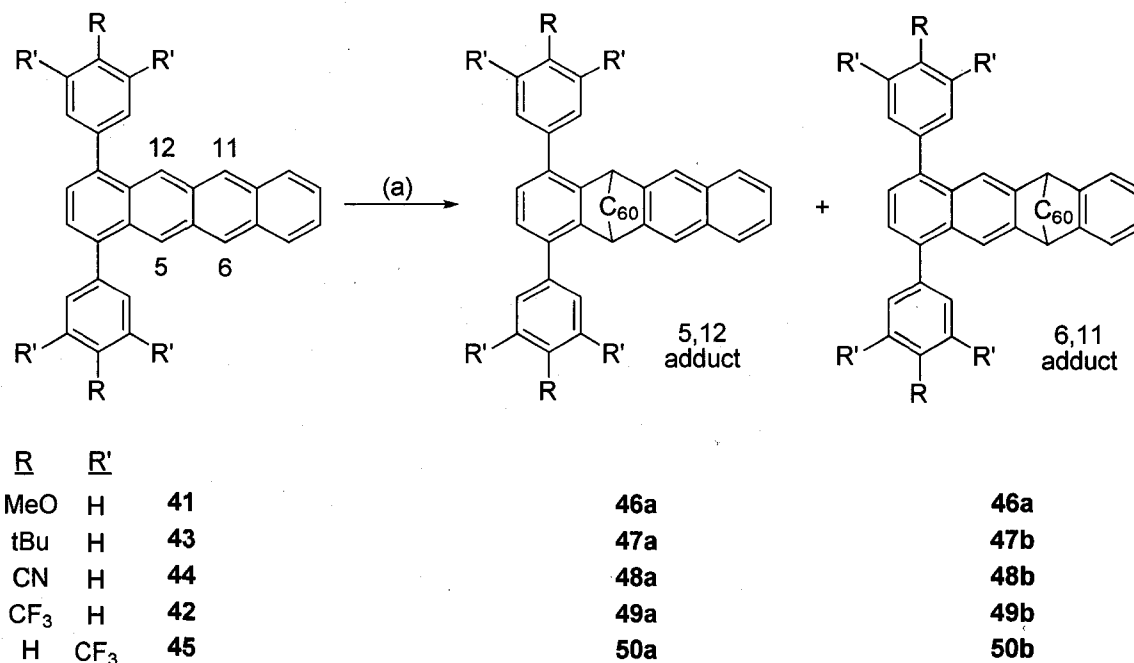


<sup>a</sup> Reagents and conditions: (a) 1,4-epoxynaphthalene, KI, DMF, 125 °C, 18-24 h; (b) 10% Pd/C, 1,2-dichlorobenzene, 180 °C, N<sub>2</sub>, dark, 4-7 d.

### 3.5.2 Diels-Alder Reactivity of 1,4-Diaryltetracenes **41-45** Under Kinetically Controlled Reaction Conditions

We investigated the regioselective addition of [60]fullerene across **41-45** under kinetically controlled reaction conditions. This investigation allowed us to study the impact of electron withdrawing and donating substituents on the regiochemistry of [60]fullerene addition. We observe that [60]fullerene cycloaddition across 1,4-diaryltetracenes **41-45** occurs with greater 5,12 regioselectivity for those reactions involving relatively electron-rich phenyl substituents. Scheme 43 and Table 9 illustrate the reactions and summarize the results. Greatest 5,12 addition selectivity is observed when strongly electron donating methoxy groups are utilized as substituents (see Exp. 9 in Table 9). Selectivity for 5,12 addition diminishes in the presence of strong electron withdrawing groups like cyano or trifluoromethyl (Exp. 11-13, Table 9).

**Scheme 43<sup>a</sup>.** Diels-Alder cycloaddition between 1,4-diaryltetracenes **41-45** and [60]fullerene run under kinetic conditions.



<sup>a</sup> Reagents and conditions: (a) [60]fullerene, PhH, 50 °C; see Table 9.

**Table 9.** Reactions between substituted 1,4-diaryltetracenes **41-45** and [60]fullerene run under kinetic conditions.

Exp.	Comp.	R, R'	acene : C <sub>60</sub>	Conditions <sup>a</sup>	Time	Yield <sup>b</sup>	5,12 : 6,11 <sup>c</sup>
9	<b>41</b>	MeO, H	1 : 1.2	PhH, 50 °C	1.5 h	75%	3.3 : 1
10	<b>43</b>	tBu, H	1 : 1.2	PhH, 50 °C	1.5 h	70%	1.9 : 1
1	<b>15</b>	H, H	1 : 1.2	PhH, 50 °C	1.5 h	71%	2.6 : 1
11	<b>44</b>	CN, H	1 : 1.2	PhH, 50 °C	1.5 h	78%	1.7 : 1
12	<b>42</b>	CF <sub>3</sub> , H	1 : 1.2	PhH, 50 °C	1.5 h	55%	1.5 : 1
13	<b>45</b>	H, CF <sub>3</sub>	1 : 1.2	PhH, 50 °C	1.5 h	64%	1.3 : 1

<sup>a</sup>All reactions performed under N<sub>2</sub> in the absence of light. <sup>b</sup>Isolated mixture of the 5,12 and 6,11 addition products. <sup>c</sup>Ratios are calculated from <sup>1</sup>H NMR integrations of crude product mixtures.



Hammett plots of 5,12 : 6,11 selectivity versus both  $\sigma_m$  and  $\sigma_p$  substituent constants (Figure 22) show poor correlations but confirm the general trend toward greater 5,12 selectivity in the presence of neutral or electron rich phenyl groups.

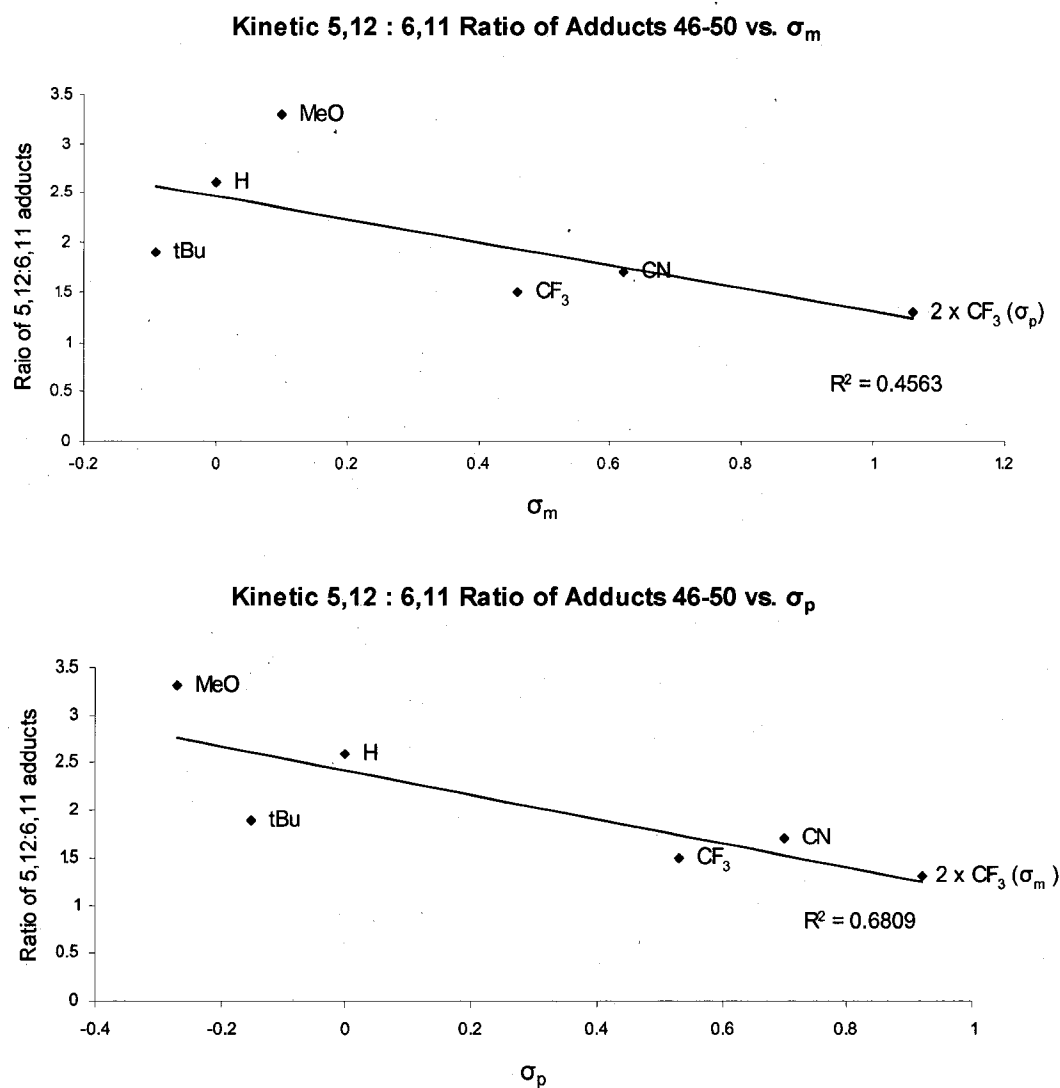
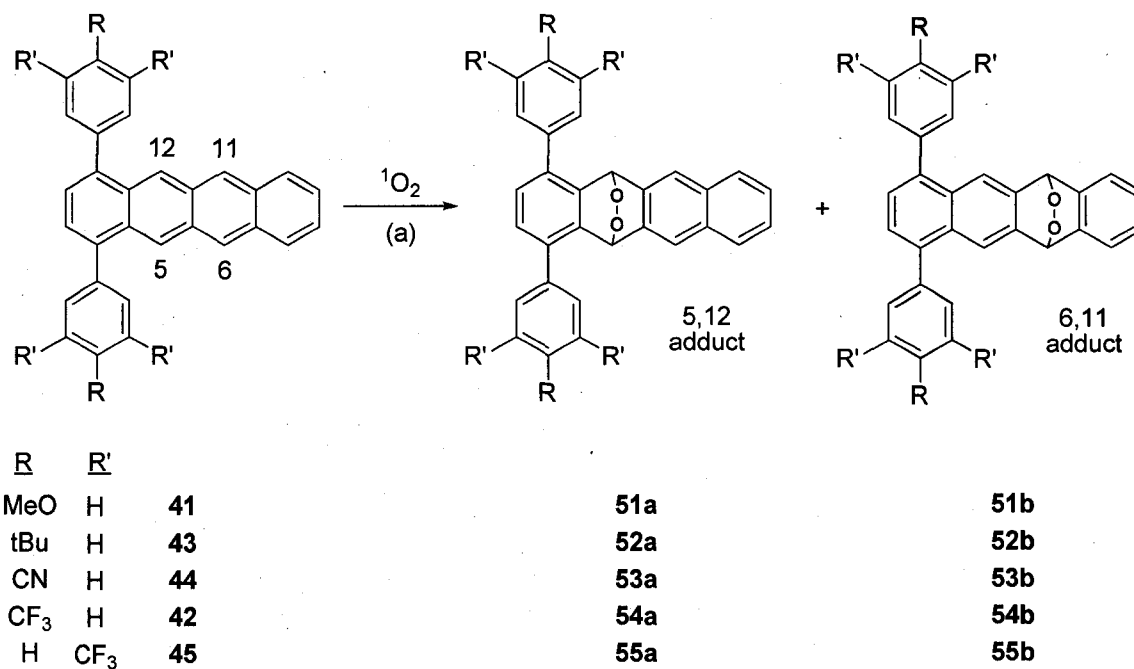


**Figure 22.** Hammett plots of 5,12 : 6,11 selectivities for [60]fullerene cycloaddition across **15** and **41-45** under kinetically controlled reaction conditions. The selectivities are plotted against both  $\sigma_m$  (top) and  $\sigma_p$  (bottom) substituent constants.

The diminished 5,12 : 6,11 selectivity in the presence of electron withdrawing substituents is seemingly inconsistent with the notion of traditional CH/ $\pi$  interactions in which the HOMO of the  $\pi$  system interacts with a  $\sigma^*$  orbital of the CH donor.<sup>147</sup> If this type of traditional CH/ $\pi$  interaction were at play, then electron donating groups would be expected to diminish regioselectivity by rendering the ortho phenyl protons less acidic and less apt to engage in CH/ $\pi$  interactions. Conversely, electron withdrawing groups would be expected to promote traditional CH/ $\pi$  interactions. We observe exactly the opposite behavior.

We also studied the reaction between compounds **41-45** and singlet oxygen (Scheme 44, Table 10). For these reactions, as with the addition of  $^1\text{O}_2$  with **15**, the tetracenes are dissolved in  $\text{CDCl}_3$  and the resulting solutions left open to the air in ambient light at room temperature. The results are summarized in Table 10. Singlet oxygen addition occurs with modest 5,12 selectivity in all cases but one, Experiment 18, in which two  $\text{CF}_3$  groups are located on each phenyl ring.

**Scheme 44<sup>a</sup>.** Diels-Alder cycloaddition between 1,4-diaryltetracenes **41-45** and singlet oxygen.



<sup>a</sup> Reagents and conditions: (a) CDCl<sub>3</sub>, ambient; see Table 10.

**Table 10.** Reactions between 1,4-diaryltetracenes **41-45** and singlet oxygen.

Exp.	Comp.	R , R'	Conditions	Time	5,12 : 6,11 <sup>a</sup>
14	<b>41</b>	MeO , H	CDCl <sub>3</sub> , ambient	18 h	1.5 : 1
15	<b>43</b>	tBu , H	CDCl <sub>3</sub> , ambient	20 h	1.6 : 1
3	<b>15</b>	H , H	CDCl <sub>3</sub> , ambient	20 h	1.7 : 1
16	<b>44</b>	CN , H	CDCl <sub>3</sub> , ambient	18 h	1.3 : 1 <sup>b</sup>
17	<b>42</b>	CF <sub>3</sub> , H	CDCl <sub>3</sub> , ambient	22 h	1.1 : 1
18	<b>45</b>	H , CF <sub>3</sub>	CDCl <sub>3</sub> , ambient	18 h	0.8 : 1

<sup>a</sup>Ratios are calculated from <sup>1</sup>H NMR integrations of crude product mixtures. <sup>b</sup>The 5,12 and 6,11 adduct signals are assigned based on chemical shifts rather than NOE analysis due to low solubility.

Hammett plots of 5,12 : 6,11 selectivity versus both  $\sigma_m$  and  $\sigma_p$  substituent constants (Figure 23) show better correlations than the corresponding [60]fullerene plots (Figure 22), indicating less complex reactions in which only the dienophilicities of the 5,12 and 6,11 rings dictate regioselectivity.

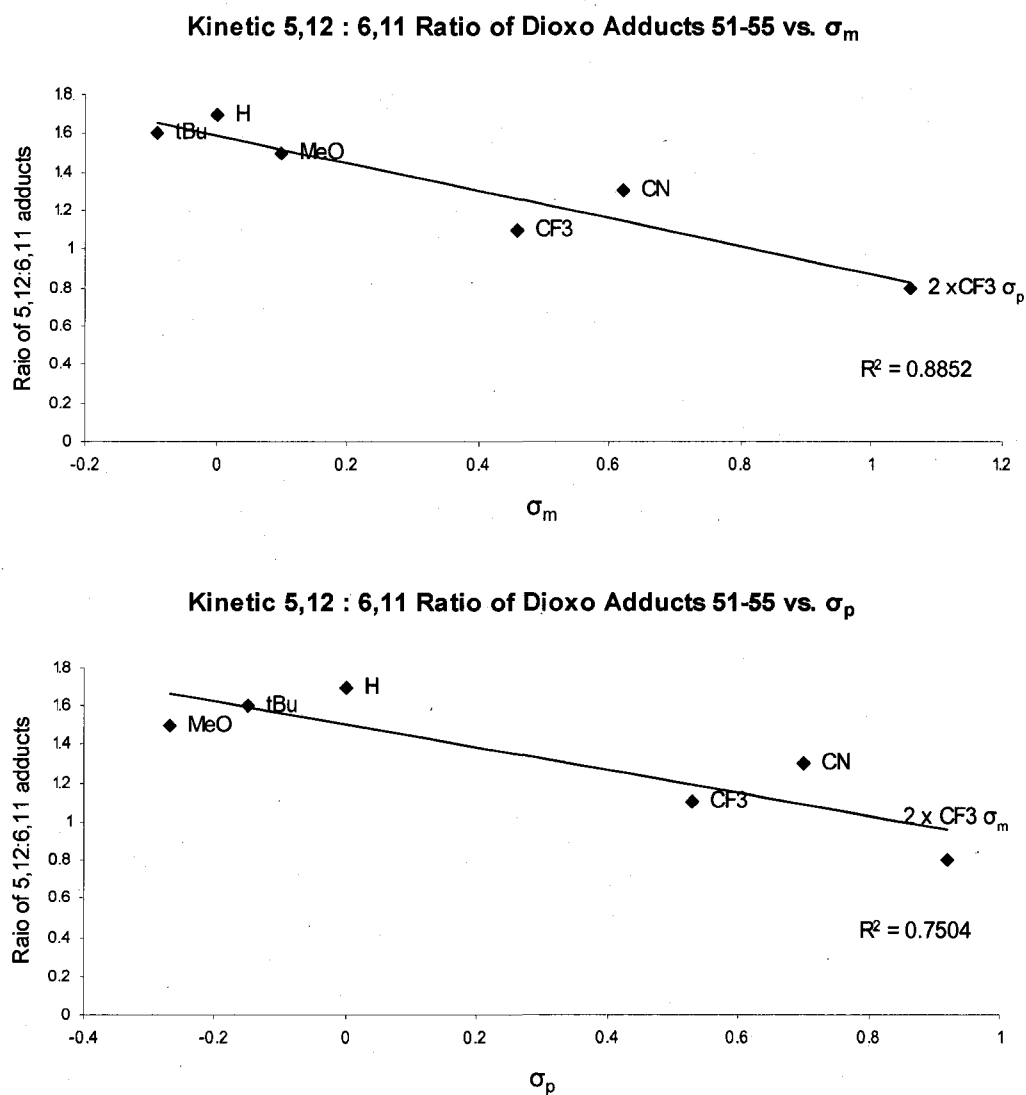


**Figure 23.** Hammett plots of 5,12 : 6,11 selectivities for  $^1\text{O}_2$  cycloaddition across **15** and **41-45**. The selectivities are plotted against both  $\sigma_m$  (top) and  $\sigma_p$  (bottom) substituent constants.

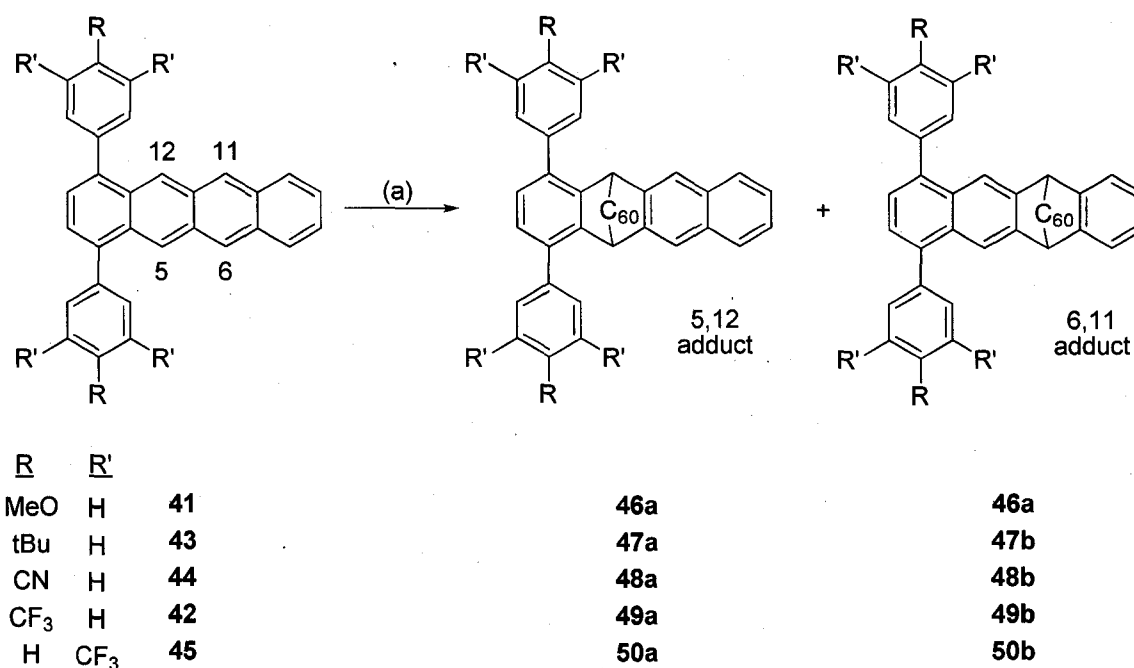
The results suggest that the 5,12 ring on 1,4-diphenyltetracene is inherently more Diels-Alder reactive than the 6,11 ring when neutral or electron donating substituents are present. When strong electron withdrawing groups are present, Diels-Alder cycloadditions across the 6,11 carbons becomes competitive. These conclusions are consistent with the notions that electron rich dienes are more reactive than electron poor dienes in Diels-Alder reactions, and that the 5,12 positions on compounds **41-45** are disproportionately influenced by electronic effects that originate on the 1,4 phenyl substituents. These conclusions also provide a qualitative understanding for the regioselectivity trend that is observed for both  $^1\text{O}_2$  (Table 10) and [60]fullerene (Table 9). However, these conclusions do not explain the enhanced 5,12 selectivity exhibited by [60]fullerene. Indeed, the relative size of [60]fullerene as compared to  $^1\text{O}_2$  would seem to suggest that steric resistance alone should diminish 5,12 selectivity for [60]fullerene, irrespective of the electronic nature of the phenyl substituents at the 1,4 positions. We conclude that a specific, favorable interaction between [60]fullerene and the phenyl substituents must be invoked in order to explain the enhanced 5,12 selectivity of [60]fullerene.

### **3.6 Thermodynamically Controlled Diels-Alder Reactions Involving **15** and **41-45****

Only two dienophiles, [60]fullerene and TCQ, are observed to add reversibly to **15** and could be studied under thermodynamically controlled reaction conditions. The Diels-Alder products arising from the reactions between **15** and all other dienophiles have proven robust, resisting cycloreversion at temperatures up to and including 180 °C. Under thermodynamic conditions, TCQ shows regioselective formation of 5,12 addition

products **32a/a'** over 6,11 addition products **32b/b'** in a ratio of 1.7 : 1 (Exp. 8, Table 8). Likewise, [60]fullerene also favors 5,12 addition under thermodynamic conditions, but with much greater selectivity (7.6 : 1, see Exp. 2 of Table 7). Upon reacting [60]fullerene with tetracenes **41-45** under thermodynamically controlled conditions (Scheme 45), the dienophile continued to show enhanced 5,12 selectivity. The data are summarized in Table 11.

**Scheme 45<sup>a</sup>**. Diels-Alder cycloaddition between 1,4-diaryltetracenes **41-45** and [60]fullerene run under thermodynamic conditions.



<sup>a</sup> Reagents and conditions: (a) [60]fullerene, *o*-DCB<sub>d4</sub>, 180 °C; see Table 11.

**Table 11.** Reactions between 1,4-diaryltetracenes **41-45** and [60]fullerene run under thermodynamic conditions.

Exp.	Comp.	R , R'	acene : C <sub>60</sub>	Conditions <sup>a</sup>	Time	5,12 : 6,11 <sup>b</sup>
19	<b>41</b>	MeO , H	1 : 1.2	<i>o</i> -DCB <sub>d4</sub> , 180 °C	15 m (1 h)	7.1 : 1 (7.2 : 1)
20	<b>43</b>	tBu , H	1 : 1.2	<i>o</i> -DCB <sub>d4</sub> , 180 °C	15 m (1 h)	6.3 : 1 (6.4 : 1)
2	<b>15</b>	H , H	1 : 1.2	<i>o</i> -DCB <sub>d4</sub> , 180 °C	15 m (1 h)	7.6 : 1 (7.5 : 1)
21	<b>44</b>	CN , H	1 : 1.2	<i>o</i> -DCB <sub>d4</sub> , 180 °C	15 m (1 h)	4.0 : 1 (4.2 : 1)
22	<b>42</b>	CF <sub>3</sub> , H	1 : 1.2	<i>o</i> -DCB <sub>d4</sub> , 180 °C	15 m (1 h)	3.7 : 1 (3.7 : 1)
23	<b>45</b>	H , CF <sub>3</sub>	1 : 1.2	<i>o</i> -DCB <sub>d4</sub> , 180 °C	15 m (1 h)	4.4 : 1 (4.4 : 1)

<sup>a</sup>All reactions performed under N<sub>2</sub> in the absence of light. <sup>b</sup>Ratios are calculated from <sup>1</sup>H NMR integrations of crude product mixtures.

The 5,12 : 6,11 ratio is plotted as a function of both  $\sigma_m$  and  $\sigma_p$  substituent constants in Figure 24, revealing only a weak correlation in both cases.

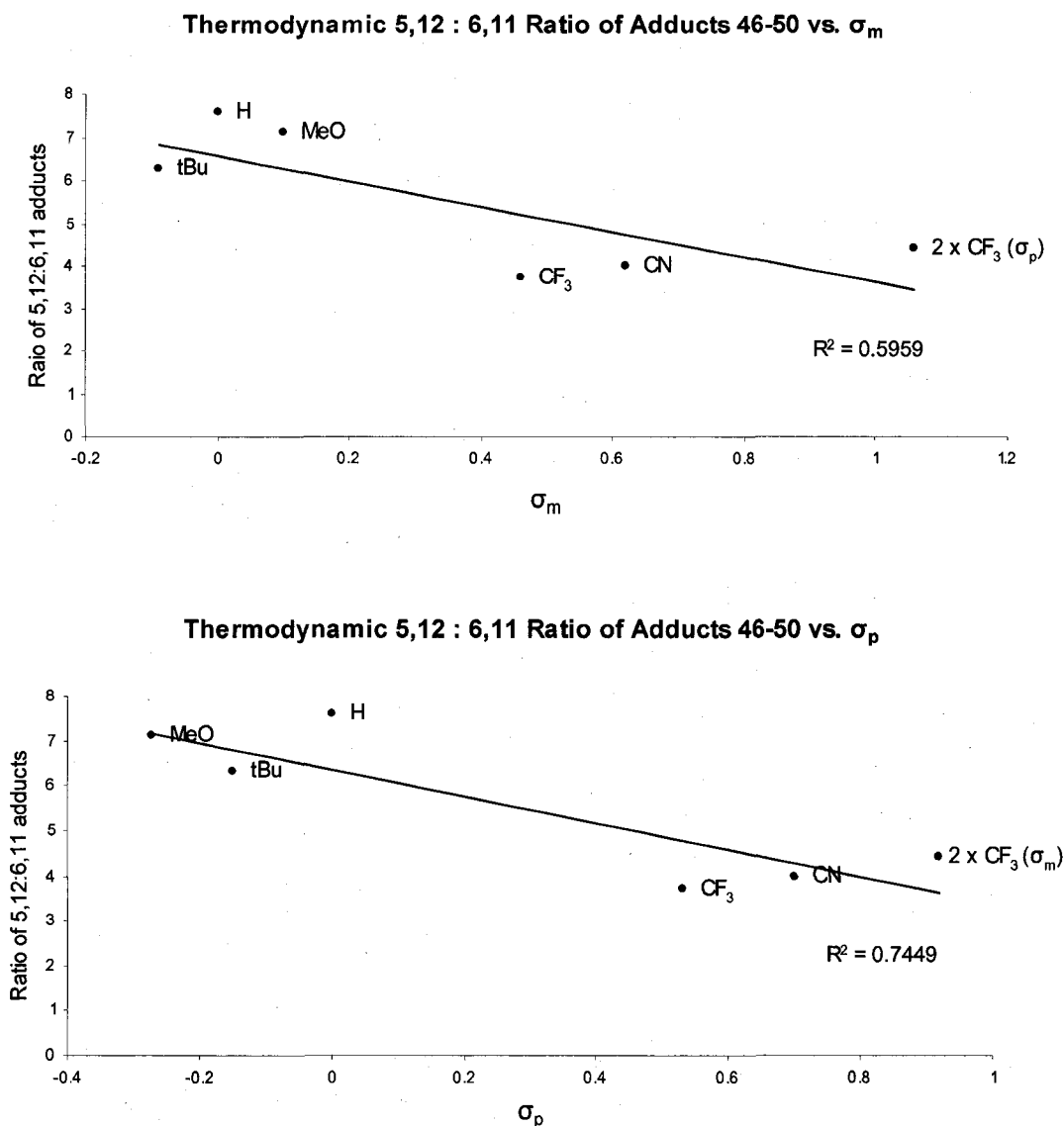


**Figure 24.** Hammett plots of 5,12 : 6,11 selectivities for [60]fullerene cycloaddition across **15** and **41-45** under thermodynamically controlled reaction conditions. The selectivities are plotted against both  $\sigma_m$  (top) and  $\sigma_p$  (bottom) substituent constants.

As was the case for reactions run under kinetically controlled reaction conditions, the greatest 5,12 selectivity is observed when electron donating substituents are present on the 1,4 phenyl groups. We believe this trend is influenced by factors other than CH/ $\pi$  considerations, namely greater thermodynamic stabilities for those fullerene-acene adducts that result from reactions involving electron rich dienes. However, a specific,



favorable ground state interaction between the [60]fullerene moiety and the phenyl substituents should be invoked in order to explain the substantially greater 5,12 selectivity exhibited by [60]fullerene as compared to tetrachloroquinone.

### 3.7 Ab Initio Calculations of Acenes and Acene Adducts

#### 3.7.1 Ab Initio Calculations of **15** and **45**

In order to better understand the impact of phenyl substituents on the acene  $\pi$ -system, B3LYP/6-31G(d) calculations were performed on **15** and **45**. Structure **15** was optimized from two starting geometries in which the dihedral angle of the phenyl substituents was set to 60° and 90°. Two local energetic minima were found, one in which the phenyl groups rotate slightly to 59.1° (**15'**) and one in which the phenyl groups remain orthogonal (90.5°) to the acene backbone (**15''**) (Figure 25). Structure **15'** shows a slight bend in the acene backbone and is 1.5 kcal mol<sup>-1</sup> lower in energy than **15''** which shows no backbone bending. DFT optimized structure **15'** was equipped with four trifluoromethyl groups and reoptimized with B3LYP/6-31G(d) to yield **45** (Figure 25). In this case the dihedral angle of the phenyl substituents was found to be 56°. Qualitatively, the influence of the phenyl substituents on the HOMOs is indiscernible. Thus, the enhanced 5,12 selectivity exhibited by dienophiles under kinetically controlled reaction conditions cannot be explained or predicted by a qualitative analysis of the computed HOMOs.

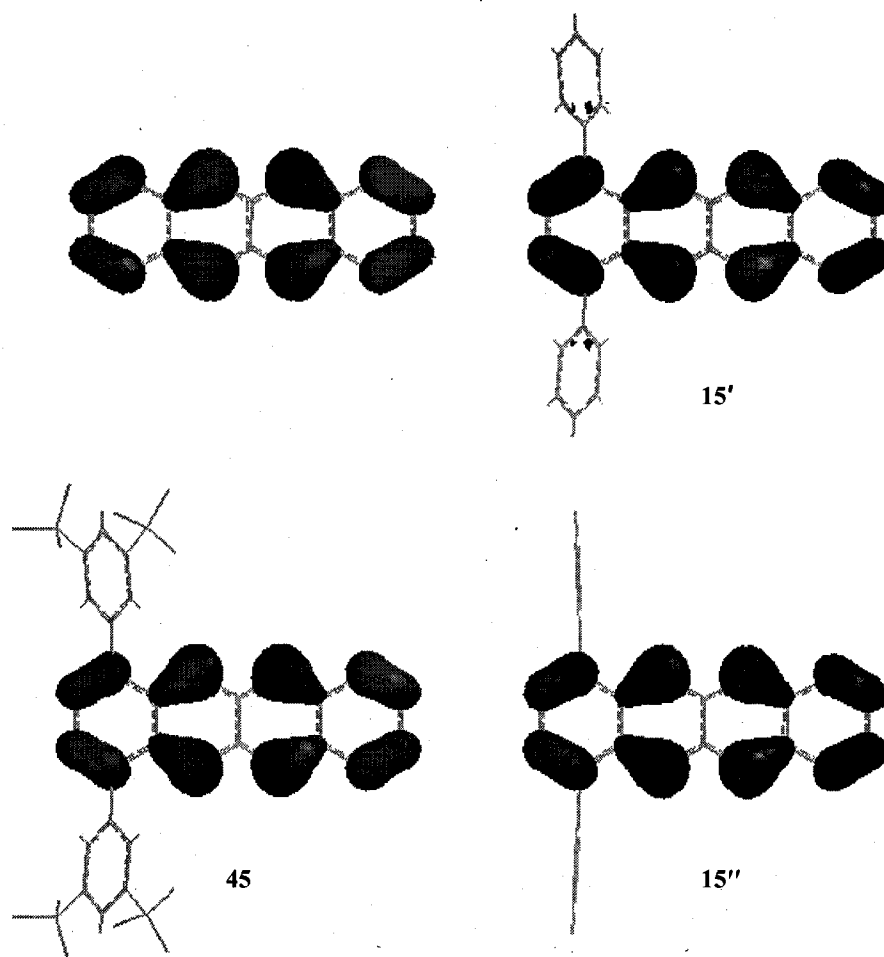


Figure 25. HOMOs of tetracene, 15', 15'' and 45 found at the B3LYP/6-31G(d) level of theory.

### 3.7.2 Ab Initio Calculations of the Ground State Energies of Ethylene Adducts of 15, 41 and 42

In order to investigate the impact of electron donating and electron withdrawing substituents on the ground state energies of Diels-Alder adducts that are not influenced by CH/ $\pi$  or other intramolecular interactions, we calculated the energies of several isomers that would form upon addition of ethylene across the 5,12 and 6,11 positions of 15, 41 and 42 (Figure 26, Table 12). At all levels of theory, the 5,12 addition isomers are of lower energy than the 6,11 addition isomers. Electron releasing and electron

withdrawing substituents have little or no impact on the relative energetics. Although the number of calculated structures is small, these results are seemingly inconsistent with the experimental trends summarized in Table 11.

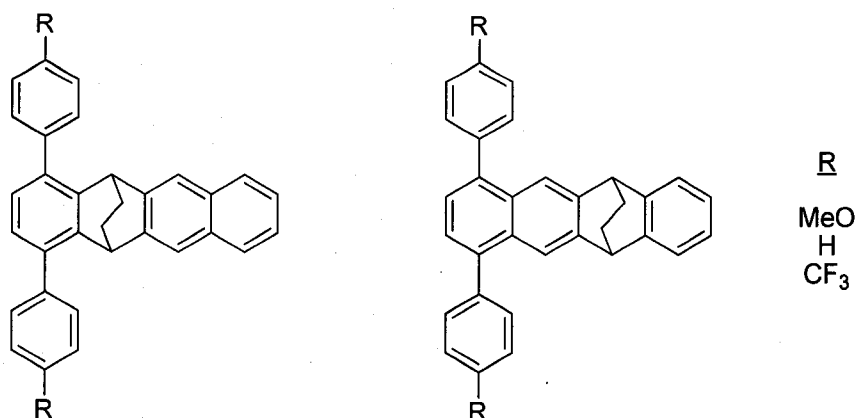


Figure 26. Ethylene adducts of **15**, **41** and **42**. See Table 12.

Table 12. Relative energies of ethylene adducts of 1,4-diaryltetracenes **15**, **41** and **42** calculated at various levels of theory<sup>a</sup>.

Acene	R	Adduct	MP2/6-311G(d) //B3LYP/6-31G(d)	B3LYP/6-31G(d)	AM1
			Relative energies (kcal mol <sup>-1</sup> )		
<b>15</b>	H	5,12	0	0	0
		6,11	1.6	1.2	1.2
<b>41</b>	MeO	5,12	0	0	0
		6,11	1.6	1.2	1.4
<b>42</b>	CF <sub>3</sub>	5,12	0	0	0
		6,11	1.4	1.0	1.2

<sup>a</sup>All calculations performed with Gaussian 03. All optimizations performed with phenyl substituents rotated away from the addend.

### 3.7.3 A Computational Examination of Compound **27a**

As the regioselective formation of **27a** is most pronounced under thermodynamic conditions, we calculated the energies of two associated conformers (Figure 27, Table

13). When **27a** is optimized at the AM1 level, two local minima are observed in which the phenyl substituents are rotated toward (**27a'**) or away (**27a''**) from the fullerene addend (Figure 27). At the AM1 level, conformer **27a'** is slightly higher in energy than **27a''** while the acene bend angle ( $\theta$ ) is the same for each (Table 9). The closest phenyl CH-[60]fullerene contact distance ( $d$ ) is much shorter in **27a'** (2.55 Å) than **27a''** (4.30 Å). The contact distance in the former is well within the range of van der Waals

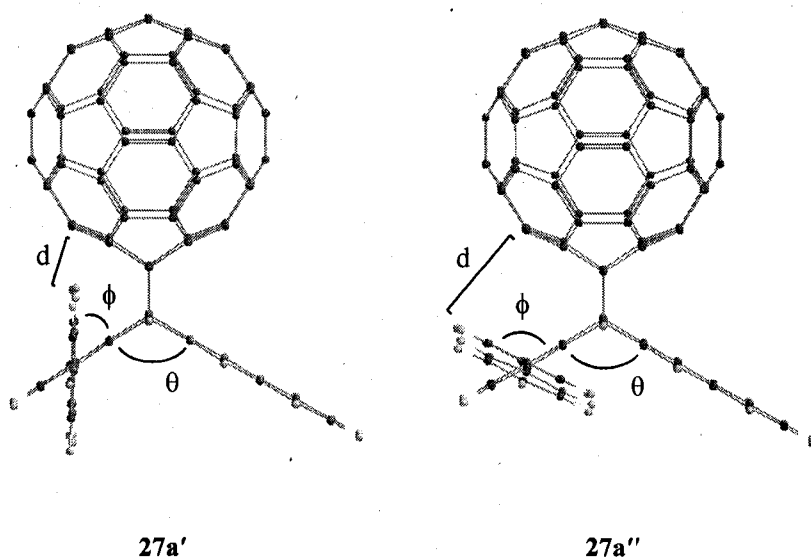


**Figure 27.** Conformation isomers **27a'** and **27a''** as found by AM1. See Table 13.

**Table 13.** Energetic and geometric properties of conformers **27a'** and **27a''** as found by AM1. All calculations performed using Spartan '03.

Measure	<b>27a'</b>	<b>27a''</b>
Rel. Energy	0.45 kcal mol <sup>-1</sup>	0
$\phi$	57°	126°
$\theta$	107°	107°
$d$	2.55 Å	4.30 Å

interactions. Similar calculations should be performed at higher levels of theory although these are complicated by the large number of atoms involved.

### 3.8 $^1\text{H}$ NMR Evidence for Aryl CH–Fullerene $\pi$ Interactions

Direct evidence for aryl CH–fullerene  $\pi$  interactions comes from a careful examination of the  $^1\text{H}$  NMR spectra for numerous fullerene-acene adducts. Although relatively few [60]fullerene-acene compounds with appropriately positioned phenyl substituents are known, [60]fullerene shielding of *syn* phenyl and especially *syn-ortho* protons is a common feature of those available for comparison. The *syn-ortho* protons on compounds **56**, **57**, **58** and **59** all exhibit substantial upfield shifts relative to their *anti-ortho* proton counterparts (Table 14). For example, the *cis*-bis[60]fullerene adduct of 6,13-diphenylpentacene, **56** (Figure 28), exhibits five separate phenyl  $^1\text{H}$  NMR signals indicating slow rotation of the phenyl groups on the NMR timescale.

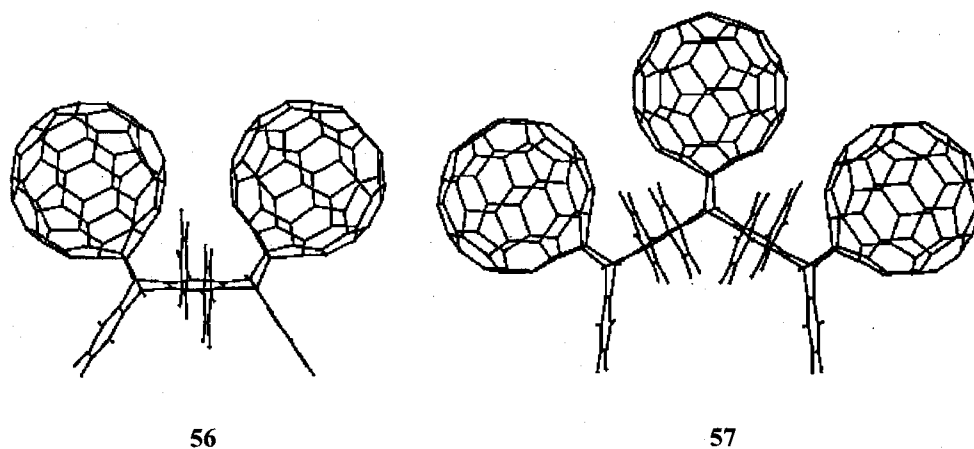
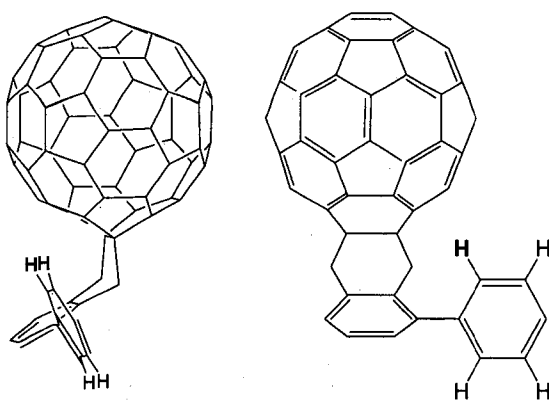


Figure 28. MM2 structures for compounds **56** and **57**.

One set of *ortho* protons on the phenyl substituents gives rise to a quasi-doublet at 7.09 ppm and is considerably shielded compared to the other set of *ortho* protons that give rise to a quasi-doublet at 7.65 ppm. We assign the shielded *ortho*  $^1\text{H}$  signal to the protons on **56** that are *syn* to the [60]fullerene moieties (Figure 29). These protons are shielded due to secondary anisotropic fields resulting from their proximity to the  $\pi$ -bonds on the [60]fullerene surface. An X-ray crystal structure has been reported for **56**.<sup>113b</sup> In it, the *syn-ortho* protons sit almost directly above and 2.96 Å removed from the nearest fullerene carbon atom, one that is formally part of a benzene ring substructure on the [60]fullerene surface.



**Figure 29.** Two views of a [60]fullerene-acene substructure with *ortho* and *meta* phenyl protons shown. The *syn-ortho* protons on **56**, **57**, **58** and **59** are approximately 3 Å removed from a [60]fullerene cage.

Likewise, the shielding of *syn-ortho* protons on tris[60]fullerene adduct **57** (Figure 28) is substantial. MM2 calculations, which very nearly reproduce the X-ray crystal structure for **56**, indicate the *syn-ortho* protons on **57** are only 3.0 Å removed from the nearest  $\text{sp}^2$  hybridized fullerene carbon atom.

An examination of the  $^1\text{H}$  NMR spectra for **58** and **59** (Figure 30) indicates that two [60]fullerene moieties are not required in order to observe shielded *syn-ortho*

protons. However, the extent of shielding is greater, as expected, when a *syn-ortho* proton is *syn* to two [60]fullerene moieties as in **56** and **57**. This is perhaps best gauged by comparing the chemical shift difference between *syn-ortho* and *anti-ortho* protons for each molecule ( $\Delta\delta_o$  values, Table 14).<sup>114</sup> Thus, compounds **56** and **57** with two [60]fullerenes surrounding each *syn-ortho* proton have  $\Delta\delta_o$  values that are roughly twice those of compounds **58** and **59**.

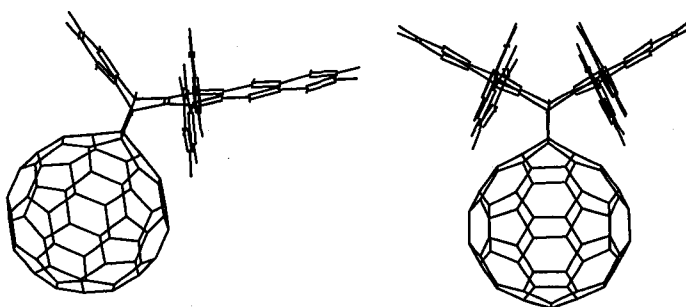


Figure 30. MM2 structures for compounds **58** (left) and **59** (right).

Table 14. <sup>1</sup>H NMR chemical shifts ( $\delta_o$ ) for *syn-ortho* and *anti-ortho* protons on [60]fullerene-acene compounds.

Compound	<i>syn ortho</i> $\delta_o^a$	<i>anti ortho</i> $\delta_o^a$	$\Delta\delta_o$ ( <i>anti</i> $\delta_o$ – <i>syn</i> $\delta_o$ ) <sup>a</sup>
<b>56</b>	7.09	7.65	0.56
<b>57</b>	6.86	7.46	0.60
<b>58</b>	7.32	7.61	0.29
<b>59</b>	7.01	7.38	0.37

<sup>a</sup>All spectra were recorded in CS<sub>2</sub>-CDCl<sub>3</sub> solvent.

A careful examination of the <sup>1</sup>H NMR spectra for the [60]fullerene adducts of 1,4-diphenyltetracene, **27a** and **27b**, suggests that these phenyl groups rotate quickly on the NMR timescale so no calculation of the chemical shift differences between *syn-ortho* and *anti-ortho* protons ( $\Delta\delta_o$ ) is possible. In fact, the *ortho* proton resonances are not even

resolved from a cluster of  $^1\text{H}$  NMR signals that appear between 7.42 and 7.66 ppm (Figure 19). However, as illustrated in Figure 19, NOESY1D spectra do provide chemical shift values for the *ortho* protons on **27a** and **27b** and they are 7.52 and 7.63 ppm, respectively. Not surprisingly, the *ortho* protons on **27a** appear at higher field than those on **27b** suggesting that the former protons lie close to and are effectively shielded by the [60]fullerene  $\pi$ -system. The  $\Delta\delta_o$  value here, representing the chemical shift difference between *ortho* protons on **27a** and **27b**, is 0.11 ppm. For comparison purposes, we consider the NOESY1D spectra of the 5,12 and 6,11 DMAD adducts of 1,4-diphenyltetracene, **30a** and **30b** (see Appendix with spectra organized by compound number). On **30a** and **30b**, the phenyl groups also rotate quickly on the NMR timescale such that only one resonance is observed for each set of *ortho* protons. The chemical shifts for the *ortho* protons on **30a** and **30b** are 7.49 and 7.48, respectively, with a corresponding  $\Delta\delta_o$  value of only 0.01 ppm. This small  $\Delta\delta_o$  value for DMAD adducts **30a** and **30b** confirms that the shielding of *ortho* protons in **27a** is in fact due to an interaction with the [60]fullerene  $\pi$ -system. The relatively small  $\Delta\delta_o$  value for the differences in *ortho* proton chemical shifts on **27a** and **27b** as compared to the analogous  $\Delta\delta_o$  values for *syn-ortho* and *anti-ortho* protons on compounds **58** and **59** is likely related to the different rates of rotation for the corresponding phenyl groups. Thus, whereas the shielding of *ortho* protons is confined to the *syn-ortho* protons on **58** and **59**, twice as many *ortho* protons are shielded in **27a** due to faster rotation of the phenyl substituents.



### 3.9 Survey of the Cambridge Crystallographic Database

To better understand the nature of phenyl CH donors that are inclined to participate in aryl CH/ $\pi$  interactions with [60]fullerene, we searched the Cambridge Crystallographic Database in search of aryl CH–[60]fullerene contacts in the range of 2.5 – 3.2 Å, as illustrated in Figure 31.

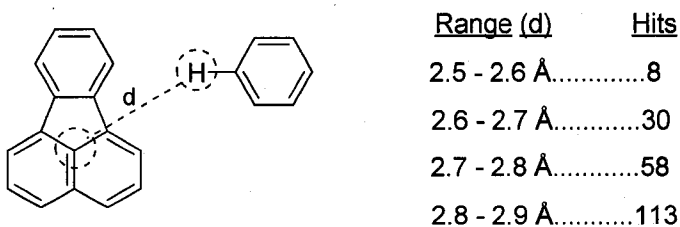


**Figure 31.** Structure and number of hits for Cambridge Crystallographic Database search.

Nishio previously performed a similar Cambridge Crystallographic Database search for CH/ $\pi$  interactions involving [60]fullerene through the year 2003.<sup>153</sup> He discovered numerous examples of relatively short CH – [60]fullerene distances (< 3.2 Å) involving both aliphatic and aromatic CH donors. He found that the greatest number of instances of close contact occur when the CH – fullerene distance is 2.9-3.0 Å. The search reported here is specific to aromatic CH donors and is complete for contributions made to the Cambridge Crystallographic Database through October of 2007. Interestingly, the instances of short contacts (< 2.9 Å) are dominated by phenyl rings bearing electron donating groups (Figure 32).

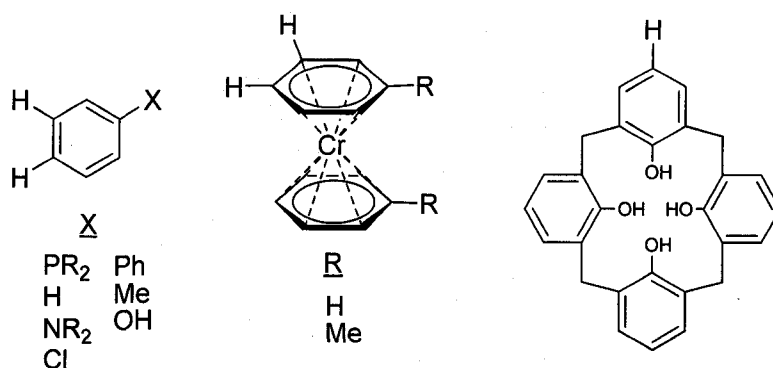


**Figure 32.** Some of the common aryl containing compounds in the Cambridge Crystallographic Database with close CH-[60]fullerene contacts in the range of 2.5-2.8 Å.

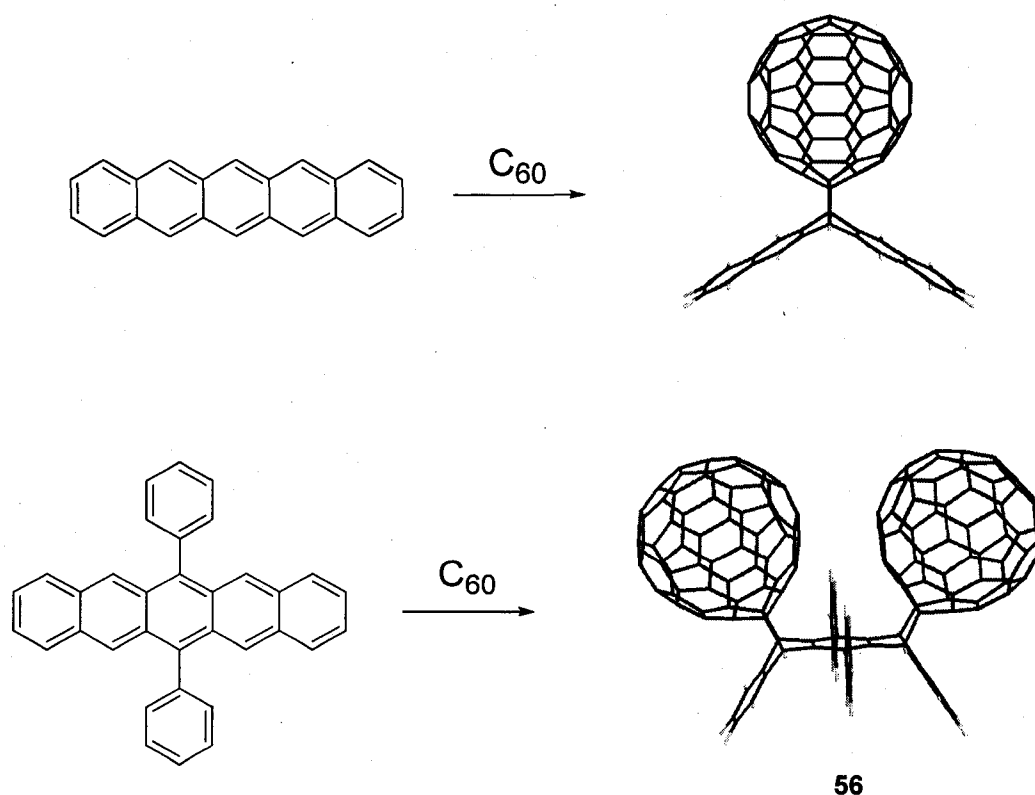
When instances of close contacts between [60]fullerene and aryl rings bearing  $\text{CF}_3$ ,  $\text{CN}$ , or  $\text{NO}_2$  substituents were specifically sought, only a single example involving benzonitrile was found. Chlorobenzene and 1,2-dichlorobenzene are common solvents for fullerene reactions. When instances of close contacts involving [60]fullerene and either chlorobenzene or 1,2-dichlorobenzene were specifically sought, only a few examples were found in which the CH-fullerene distance is less than or equal to 2.9 Å. We conclude that either aryl CH-fullerene  $\pi$  interactions favor electron rich aromatic rings or crystals incorporating [60]fullerene and electron poor aromatic rings are not properly represented in the Cambridge Crystallographic Database. It is tempting to accept the former conclusion, especially in light of the fact that [60]fullerene shows a greater 5,12 regioselectivity for those Diels-Alder reactions involving neutral and electron rich phenyl substituents on the 1,4-diaryltetracenes. This interpretation would require acceptance of a unique type of CH/ $\pi$  interaction, one that involves a  $\sigma$  orbital on the aryl CH donor and a  $\pi^*$  orbital on the [60]fullerene. More work is required before an *inverse electron demand* CH/ $\pi$  interaction of this type can be believed. Especially valuable would be high level *ab initio* calculations on **27a**.

### 3.10 Diels-Alder Reactivity of 1,4,8,11-Tetraphenylpentacene, 22

#### 3.10.1 Introduction

Given our assertion that aryl CH–fullerene  $\pi$  interactions impact the regioselectivities of [60]fullerene cycloadditions across 1,4-diaryltetracenes, it was wondered if 1,4,8,11 phenyl substituents on pentacene would alter its Diels-Alder chemistry. As mentioned in Chapter 1, [60]fullerene preferentially cycloadds across the center ring of pentacene (Scheme 46). In the case of 6,13-diphenylpentacene, **56**, [60]fullerene adds across the penultimate rings flanking the central ring in a

**Scheme 46.** Cycloaddition of [60]fullerene to pentacene and 6,13-diphenylpentacene.



diastereoselective *syn* fashion. In this case, the phenyl groups block cycloadditions across the central ring while  $\pi$ - $\pi$  stacking interactions between the [60]fullerene moieties lead to the selective *syn* addition. With no phenyl substituents at the 6,13 positions, 1,4,8,11-tetraphenylpentacene **22** would normally be expected to add dienophiles primarily across the 6,13 position in order to form Diels-Alder monoadducts. However, aryl CH-fullerene  $\pi$  interactions could conceivably alter this regiochemistry when [60]fullerene is utilized as dienophile.

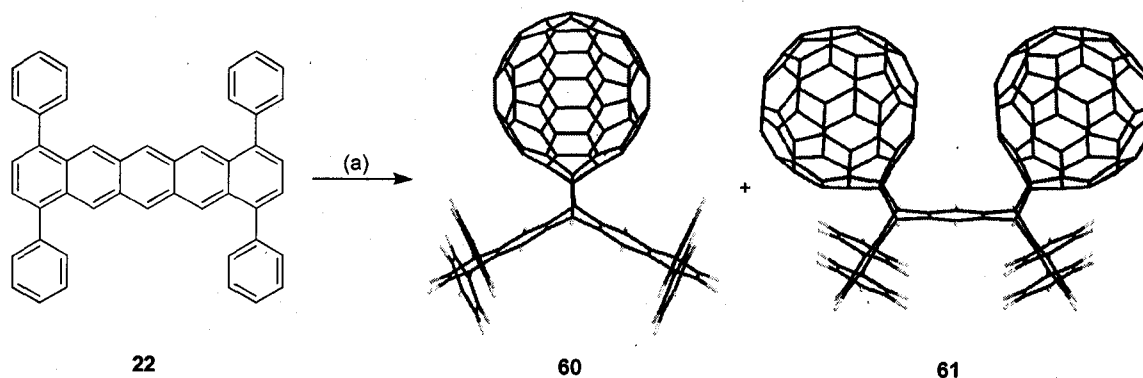
In order to study this interesting possibility, we synthesized and studied the Diels-Alder reactivity of **22** with [60]fullerene, singlet oxygen, maleic anhydride and DDQ. Compound **22** reacts with [60]fullerene to yield both the monoadduct **60** and a single bis[60]fullerene adduct, **61**, in a 4.3 : 1 ratio under kinetically controlled reaction conditions. In contrast, singlet oxygen, maleic anhydride and DDQ show highly selective 6,13 addition yielding far less or no 5,14 addition product.

### 3.10.2 Diels-Alder Reactivity of **22** with [60]Fullerene, $^1\text{O}_2$ , Maleic Anhydride, and DDQ

Compound **22** was synthesized according to Scheme 35 in Chapter 2. It reacts with 4.2 equivalents of [60]fullerene in benzene at 50 °C to afford a mixture of mono[60]fullerene adduct **60** and bis[60]fullerene adduct **61** in a 4.3:1 ratio, respectively (Figure 47, Table 15). From our work with similar fullerene-acene adducts of this type, it is unlikely that the formation of **60** or **61** is reversible under these conditions. While both *syn* and *anti* bisaddition are possible, we assign a *syn* stereochemistry to **61** based upon

precedence involving similar molecules including **56**. This assignment cannot be readily verified, however, as the *syn* and *anti* configurations are indistinguishable by  $^1\text{H}$  NMR spectroscopy.

**Scheme 47<sup>a</sup>**. Diels-Alder cycloaddition between [60]fullerene and **22**.



<sup>a</sup> Reagents and conditions: (a) [60]fullerene, heat; See Table 15.

**Table 15.** Diels-Alder cycloaddition between [60]fullerene and **22** run under kinetic conditions.

Exp.	<b>22</b> : C <sub>60</sub>	Conditions <sup>a</sup>	Time	Yield <sup>b</sup>	<b>60</b> : <b>61</b> <sup>c</sup>
24	1 : 4.2	PhH, 50 °C	1.5 h	73%	4.3 : 1

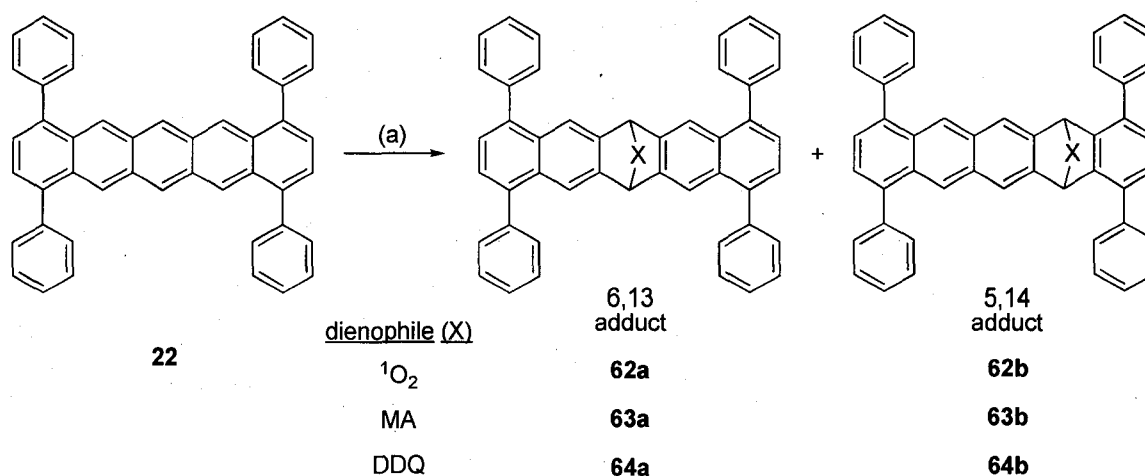
<sup>a</sup>All reactions performed under N<sub>2</sub> in the absence of light. <sup>b</sup>Yield based on pentacene reacted.

<sup>c</sup>Ratios are calculated from  $^1\text{H}$  NMR integrations of crude product mixtures.

For comparison purposes, **22** was also reacted with singlet oxygen, maleic anhydride (MA), and 2,3-dichloro-5,6-dicyano-*p*-benzoquinone (DDQ) (Scheme 48). The results are summarized in Table 16. Based upon prior results involving cycloadditions of similar dienophiles across **15**, it is believed that the reaction conditions shown in Table 16 lead to irreversible addition of dienophiles. Singlet oxygen addition to **22** occurs selectively across the 6,13 carbons leading to **62a**, with only trace formation of **62b**.

Maleic anhydride favors addition across the 6,13 positions of **22** but shows less regioselectivity than singlet oxygen. DDQ, on the other hand, shows the greatest regioselectivity for 6,13 addition across **22**. In this case, only the 6,13 isomer **64a** is observed.

**Scheme 48<sup>a</sup>**. Diels-Alder cycloaddition between **22** and singlet oxygen, maleic anhydride, and DDQ.



<sup>a</sup> Reagents and conditions: (a) various dienophiles, PhH, 50 °C; See Table 16.

**Table 16.** Diels-Alder reactions between **22** and singlet oxygen, maleic anhydride, and DDQ run under kinetic conditions.

Exp.	X	<b>22</b> : X	Conditions <sup>a</sup>	Time	6,13 : 5,14 <sup>b</sup>
25	$^1\text{O}_2$	--	PhH, 50 °C	45 min	25 : 1
26	MA	1 : 4.2	PhH, 50 °C	1.5 h	10 : 1
27	DDQ	1 : 4.2	PhH, 50 °C	1.5 h	<b>64a<sup>c</sup></b>

<sup>a</sup>All reactions performed under N<sub>2</sub> in the absence of light, except in the case of oxygen. <sup>b</sup>Ratios are calculated from <sup>1</sup>H NMR integrations of crude product mixtures. <sup>c</sup>Isomer **64b**, if formed at all, is not detected by <sup>1</sup>H NMR spectroscopy.

For both the maleic anhydride and DDQ adducts of **22**, the 6,13 and 5,14 cycloaddition isomers are not distinguishable by  $^1\text{H}$  NMR spectroscopy. However, NOESY1D does successfully distinguish the isomers (see Appendix for these and related spectra organized by compound number). Selective excitation of the bridgehead methine protons at the site of addition for both the maleic anhydride and DDQ adducts results in enhancement of two aromatic X signals. These enhancement patterns are only consistent with 6,13 cycloaddition products. In the case of maleic anhydride, only the major product was analyzed by NOESY1D. In the case of DDQ, the chemoselectivity of the dienophile was not investigated, but literature precedents<sup>157</sup> suggest that DDQ undergoes chemoselective cycloaddition reactions involving the cyano-bearing olefin. We presume this to be the case here as well.

Compared to singlet oxygen, maleic anhydride and DDQ, [60]fullerene shows a heightened propensity to cycloadd across the 5,14 and 7,12 positions of **22**. We attribute this selectivity to aryl CH–fullerene  $\pi$  interactions.

## CHAPTER 4

### CONCLUSIONS

The high yielding synthesis of 4,7-diphenyl-1-hydroxyphthalan ((±)-**4**) has been achieved and its facile conversion to 4,7-diphenylisobenzofuran (**5**) has been demonstrated. Separate reactions between **5** and maleic anhydride, 1,4-naphthoquinone and *p*-benzoquinone have been utilized to synthesize novel acenes **11**, **15** and **22**, respectively. In boiling glacial acetic acid, the reaction between **5** and *p*-benzoquinone produces an unprecedented *exo,exo anti* dual cycloaddition product, **16b**, in high yield and with 100% diastereoselectivity. The *exo,exo anti* structure of **16b** has been elucidated using a combination of <sup>1</sup>H NMR spectroscopy and a thorough stereochemical analysis of the corresponding borohydride-reduced diol species **18a** and **18b**. The reactivity between commercially available 1,3-diphenylisobenzofuran, **23**, and *p*-benzoquinone has been re-evaluated under a variety of reaction conditions including those utilized in the transformation of **5** to **16b**. In all cases studied, however, the only dual cycloaddition product formed was the known *endo,exo syn* adduct **24**.

[60] Fullerene undergoes regioselective cycloaddition across the 5,12 positions of 1,4-diphenyltetracene, **15**, and diaryltetracenes **41-45** under both kinetically controlled and thermodynamically controlled reaction conditions. For compounds **41-45**, it is observed that both neutral and electron donating substituents enhance regioselective



[60]fullerene addition across the 5,12 positions while electron withdrawing groups reduce 5,12 regioselectivity. NOESY (nuclear Overhauser effect spectroscopy) methods have been used to discriminate between the 5,12 and 6,11 cycloaddition regioisomers of **15** and **41-45**. The regiochemistry of [60]fullerene addition is compared and contrasted to that of other dienophiles including dimethyl acetylenedicarboxylate, ethylene, singlet oxygen, maleic anhydride, and tetrachloroquinone. In all cases, the enhanced 5,12 selectivity exhibited by [60]fullerene is special. It is not replicated by other dienophiles. In the case of 1,4,8,11-tetraphenylpentacene, **22**, [60]fullerene shows an unusual propensity for bis cycloaddition across the 5,14 and 7,12 positions under kinetically controlled reaction conditions. The dienophiles singlet oxygen, maleic anhydride, and 2,3-dichloro-5,6-dicyanobenzoquinone do not show the same selectivity for addition across the penultimate rings of **22** under similar reaction conditions.

The unusual tendency for [60]fullerene cycloaddition across acene rings that are adjacent to rings bearing phenyl substituents lead us to conclude that CH/ $\pi$  interactions play an important role in fullerene-acene chemistry. Direct evidence for aryl CH–fullerene  $\pi$  interactions comes from an examination of  $^1\text{H}$  NMR chemical shifts for the *ortho* phenyl protons in fullerene-acene adducts. A careful review of the Cambridge Crystallographic Database reveals numerous instances of aryl CH/fullerene contact distances within 3 Å. The tantalizing possibility that aryl CH-fullerene  $\pi$  interactions involve  $\pi^*$  orbitals on [60]fullerene and  $\sigma$  orbitals on the aryl CH donors, an *inverse electron demand* CH/ $\pi$  interaction, is suggested, but more work is needed to verify the interacting orbitals. High level *ab initio* calculations of **27a** and **27b** would be especially useful.

## CHAPTER 5

### EXPERIMENTAL SECTION

#### 5.1 General Methods

##### Melting Points

Melting points were recorded on a Uni-melt Thomas Hoover capillary melting point apparatus or a Mel-Temp II and are uncorrected.

##### NMR Spectra

$^1\text{H}$  NMR spectra were recorded on a Varian Mercury Plus 400 FT-NMR spectrometer or a Varian INOVA 500 FT-NMR spectrometer operating at 399.7491 MHz and 499.7733 MHz, respectively.

$^{13}\text{C}$  NMR spectra were recorded on a Varian Mercury Plus 400 FT-NMR spectrometer or a Varian INOVA 500 FT-NMR spectrometer operating at 100.5169 MHz and 125.6680 MHz, respectively.

$^{19}\text{F}$  NMR spectra were recorded on a Varian Mercury Plus 400 FT-NMR spectrometer or a Varian INOVA 500 FT-NMR spectrometer operating at 376.1411 MHz and 470.2582 MHz, respectively.

NOESY1D spectra were recorded on a Varian Mercury Plus 400 FT-NMR spectrometer (399.7491. MHz) using a DPGSE (Double Pulsed Field Gradient Spin Echo) pulse sequence for selective excitation. Relaxation delays were typically set to 8-10 s, acquisition times set to 3 s, and mixing times set to 0.5-1.2 ms.

### **Mass spectra**

High resolution mass spectra were recorded using Fast Atom Bombardment (FAB+) at the Notre Dame Mass Spectrometry facility.

### **Combustion analysis**

Combustion analysis was performed at Atlantic Microlab Inc. in Norcross, Georgia.

### **Chromatography**

Silica Gel (230-400 mesh) was obtained from Natland International Corporation.

Preparatory thin layer chromatography plates (20 cm<sup>2</sup> x 1000 µm) were obtained from Analtech, Inc.

## **5.2 Solvents**

*Note: All solvents were used without further purification unless otherwise noted.*

Acetic Acid was obtained from EMD.

Acetic Anhydride was obtained from EM Science.

Acetone was obtained from Pharmco.

Benzene was obtained from EMD.

Carbon Disulfide was obtained from EM Science.

Chloroform was obtained from Pharmco.

Deuterated NMR solvents were obtained from Cambridge Isotope Laboratories.

1,2-Dichlorobenzene was obtained from Acros.

Dichloromethane was obtained from EMD.

N,N-Dimethylformamide was obtained from EMD.

Ethanol was obtained from Pharmco.

Hexanes was obtained from EMD.

Methanol was obtained from EMD.

Tetrahydrofuran was obtained from EMD.

Toluene was obtained from EMD.

Xylenes was obtained from Pharmco.

### 5.3 Reagents

*Note: All reagents were used without further purification unless otherwise noted.*

Aluminum Chloride was obtained from Fisher Scientific.

Ammonium Chloride was obtained from Aldrich.

p-Benzoquinone was obtained from Acros and sublimed.

Calcium Chloride ( $\text{CaCl}_2$ ) was obtained from Fisher.

Diisobutylaluminum Hydride (DIBAL-H) was obtained from Aldrich.

2,3-Dichloro-5,6-dicyano-p-benzoquinone (DDQ) was obtained from Aldrich.

Dimethyl Acetylenedicarboxylate was obtained from TCI America.

1,4-Diphenyl-2,3-butadiene was obtained from Alfa Aesar.

1,3-Diphenylisobenzofuran was obtained from Acros.

Ethylene was obtained from Liquid Carbonic.

[60]Fullerene was obtained from M.E.R. Corp.

Hydriodic Acid (47%, stabilized) was obtained from Acros.

Hydriodic Acid (55-58%, unstabilized) was obtained from Alfa Aesar.

Hydrochloric Acid was obtained from EMD.

Magnesium Sulfate ( $\text{MgSO}_4$ ) was obtained from EMD.

Maleic Anhydride was obtained from Lancaster.

1,4-Naphthoquinone was obtained from Sigma-Aldrich and sublimed.

10% Pd on Carbon was obtained from Alfa Aesar.

Phenyllithium was obtained from Aldrich.

Phenyl Magnesium Bromide was obtained from Aldrich.

Potassium Iodide was obtained from EM Science.

Sodium Bicarbonate ( $\text{NaHCO}_3$ ) was obtained from Fisher Scientific.

Sodium Bisulfite ( $\text{NaHSO}_3$ ) was obtained from EM Science.

Sodium Borohydride ( $\text{NaBH}_4$ ) was obtained from Aldrich.

Sodium Chloride ( $\text{NaCl}$ ) was obtained from VWR.

Sodium Hydroxide ( $\text{NaOH}$ ) was obtained from Alfa Aesar.

Sulfuric Acid was obtained from J.T. Baker.

Tetracene was obtained from Acros.

2,3,5,6-Tetrachloro-*p*-benzoquinone was obtained from Aldrich.

*p*-Toluenesulfonic Acid was obtained from Aldrich and recrystallized from chloroform.

Zinc metal was obtained from Fisher Scientific.

## 5.4 Syntheses

Routine solvent evaporations were performed on a Büchi Rotavapor R-205 rotary evaporator with a Büchi V-500 vacuum pump unless otherwise noted.

**3a,4,7,7a-Tetrahydro-4,7-diphenylphthalic anhydride (1).** 1,4-diphenyl-2,3-butadiene (39.4 g, 0.191 mol) and maleic anhydride (20.5 g, 0.209 mol) were heated at 137-144 °C in xylenes (500 mL) for 15 hours. The solution was chilled and white crystalline precipitate filtered off to afford **1** (46.6 g, 80%). m.p. = 205-209 °C (lit. 207 °C<sup>158</sup>); <sup>1</sup>H NMR (500 MHz, CDCl<sub>3</sub>) δ (ppm): 3.74 (dd, 2H, *J* = 4.88, 2.44 Hz), 3.84 (d, 2H, *J* = 4.88 Hz), 6.55 (s, 2H), 7.34-7.39 (m, 6H), 7.41-7.45 (m, 4H); <sup>13</sup>C NMR (100 MHz, CDCl<sub>3</sub>) δ (ppm): 41.4, 47.7, 127.9, 128.8, 128.9, 132.3, 138.1, 169.9.

**4,7-Diphenylphthalic anhydride (2).** Adduct **1** (46.4 g, 0.152 mol) and DDQ (80.2 g, 0.353 mol) were combined in toluene (500 mL) and the red solution heated at 111 °C for 18 hours. The solvent was removed at reduced pressure and crude product rinsed with copious amounts of 95% ethanol to yield **2** (39.6 g, 87%). m.p. = 223-225 °C (lit. 220<sup>129</sup>, 224 °C<sup>130</sup>); <sup>1</sup>H NMR (500 MHz, CDCl<sub>3</sub>) δ (ppm): 7.50-7.54 (m, 6H), 7.57-7.60 (m, 4H), 7.85 (s, 2H); <sup>13</sup>C NMR (100 MHz, CDCl<sub>3</sub>) δ (ppm): 128.0, 128.7, 129.5, 135.2, 137.9, 142.2, 162.1 (coincidental overlap of two signals at 137.9 ppm).

**4,7-Diphenylphthalide (3).** Compound **2** (39.0 g, 0.130 mol) and zinc dust (85 g, 1.3 mol) were heated to 100 °C in glacial acetic acid (500 mL) for 17 hours with mechanical stirring. The solution was filtered hot and residual solids rinsed with hot

acetic acid and hot chloroform. The combined filtrate was concentrated at reduced pressure. The crude product was rinsed with methanol (25 mL) to yield **3** (33.3 g, 89%). m.p. = 170-172 °C (lit. 170-171<sup>159</sup>, 173-175°C<sup>133</sup>); <sup>1</sup>H NMR (400 MHz, CDCl<sub>3</sub>) δ (ppm): 5.38 (s, 2H), 7.43-7.59 (m, 11H), 7.72 (d, 1H, *J* = 7.8 Hz); <sup>13</sup>C NMR (100 MHz, CDCl<sub>3</sub>) δ (ppm): 68.7, 122.5, 128.1, 128.3, 128.64, 128.67, 129.4, 129.9, 131.8, 133.9, 136.0, 136.5, 137.7, 141.9, 145.7, 170.1.

**4,7-Diphenyl-1-hydroxyphthalan ((±)-4).** Compound **3** (3.57 g, 12.5 mmol) was dissolved in dry methylene chloride (175 mL) and the solution cooled to -60 °C. Diisobutyl aluminum hydride (15 mL of 1M solution, 15 mmol) was added drop wise to the stirring solution via syringe over 15 minutes. After 70 minutes, the reaction was quenched with aqueous sodium hydroxide (5 mL, 10% wt. solution) and the solution warmed to room temperature. To the solution was added water (50 mL) and carbon dioxide was bubbled through the solution until pH 7 was attained. The organic layer was separated and the aqueous layer extracted with dichloromethane (3 x 100 mL). The combined organic layers were dried (CaCl<sub>2</sub>) and solvent evaporated under ambient conditions to yield (±)-**4** (2.90 g, 80%). m.p. = 162 °C (dec.); <sup>1</sup>H NMR (500 MHz, CDCl<sub>3</sub>) δ (ppm): 2.84 (d, 1H, *J* = 6.35 Hz, disappears with D<sub>2</sub>O, OH), 5.08 (d, 1H, *J* = 13.18 Hz), 5.51 (dd, 1H, *J* = 13.18, 1.71 Hz), 6.63 (dd, 1H, *J* = 6.35, 1.71 Hz, collapses to doublet with D<sub>2</sub>O), 7.37-7.42 (m, 2H), 7.44-7.49 (m, 7H), 7.51 (d, 1H, *J* = 7.81 Hz), 7.64 (m, 2H); <sup>13</sup>C NMR (100 MHz, CDCl<sub>3</sub>) δ (ppm): 71.9, 101.1, 127.89, 127.95, 128.1, 128.8, 129.03, 129.7, 130.0, 135.4, 137.2, 137.8, 138.4, 139.5, 139.7 (coincidental overlap of two aromatic signals); HRMS (FAB) *m/z* = 288.1137, calcd *m/z* = 288.11503.

**Adducts of 4,7-diphenylisobenzofuran and maleic anhydride, (6a) and (6b).**

Compound ( $\pm$ )-**4** (2.11 g, 7.33 mmol) and maleic anhydride (0.81 g, 8.3 mmol) were heated to 118 °C in a solution of acetic acid (20 mL) and acetic anhydride (2 mL) for 2 hours. After cooling, water (2 mL) was added. The white precipitate was filtered off, rinsed with acetic acid (10 mL), and air-dried to yield a mixture of endo **6a** and exo **6b** (2.40 g, combined 89%). m.p. = 258-260 °C;  $^1\text{H}$  NMR (500 MHz,  $\text{CDCl}_3$ )  $\delta$  (ppm): 3.52 (exo adduct **6b**, s, 2H), 4.01 (endo adduct **6a**, m, 2H), 6.01 (exo adduct **6b**, s, 2H), 6.07 (endo adduct **6a**, m, 2H), 7.43-7.57 (endo **6a** and exo **6b**, m, 24H);  $^{13}\text{C}$  NMR (125 MHz,  $\text{CDCl}_3$ )  $\delta$  (ppm): 49.9, 50.5, 80.7, 82.6, 128.2, 128.3, 128.5, 128.8, 129.1, 129.5, 130.0, 134.8, 135.5, 138.3, 138.5, 140.0, 141.5, 167.4, 170.0 (coincidental overlap of two aromatic signals); HRMS (FAB)  $m/z$  = 369.1120 ( $\text{M} + \text{H}^+$ ), calcd  $m/z$  = 369.11268.

**5,8-diphenyl-naphthalene-2,3-dicarboxylic anhydride (7).**

*One pot synthesis from 4,7-diphenyl-1-hydroxyphthalan (( $\pm$ )-**4**) and maleic anhydride.*

Compound **4** (0.47 g, 1.6 mmol), maleic anhydride (0.18 g, 1.9 mmol) and *p*-toluenesulfonic acid monohydrate (1.8 g, 9.5 mmol) were heated to 111 °C in toluene (60 mL) with a Dean-Stark trap for 4 days. The crude reaction mixture was washed with saturated  $\text{NaHCO}_3$  (aq) (2 x 50 mL), water (1 x 50 mL), and brine (2 x 75 mL). The organic layer was dried ( $\text{CaCl}_2$ ) and concentrated at reduced pressure. The crude product was recrystallized from  $\text{HOAc}/\text{Ac}_2\text{O}$  to yield **7** (0.21 g, 36%).

*From 6a and 6b.* The adducts **6a** and **6b** (2.38 g, 6.45 mmol) were combined with freshly recrystallized ( $\text{CHCl}_3$ ) *p*-toluenesulfonic acid (3.65 g, 21.2 mmol) in toluene (90 mL) and



heated to 111 °C with a Dean-Stark trap for 4 days. The toluene was removed at reduced pressure, dichloromethane (50 mL) added, and the organic layer washed with saturated NaHCO<sub>3</sub> (aq) (2 x 85 mL), water (2 x 100 mL), and brine (2 x 75 mL). The organic layer was dried (CaCl<sub>2</sub>) and concentrated at reduced pressure. The residue was taken up in a solution of HOAc (30 mL) and Ac<sub>2</sub>O (5 mL) and the mixture heated to 118°C for 2 hours. The resulting solution was chilled overnight and the ensuing precipitate filtered off and rinsed with HOAc (15 mL) and water (40 mL) to yield yellow-green crystals of **7** (1.58 g, 70%). m.p. = 240-242 °C (lit. 235-236°C<sup>140</sup>); <sup>1</sup>H NMR (500 MHz, CDCl<sub>3</sub>) δ (ppm): 7.48-7.61 (m, 10H), 7.78 (s, 2H), 8.64 (s, 2H); <sup>13</sup>C NMR (100 MHz, CDCl<sub>3</sub>) δ (ppm): 125.8, 127.1, 128.7, 129.2, 130.2, 131.0, 135.3, 139.0, 142.9, 163.4; HRMS (FAB) *m/z* = 351.1023 (M + H<sup>+</sup>), calcd *m/z* = 351.10212.

**3-Benzoyl-5,8-diphenylnaphthalene-2-carboxylic acid (8).** Compound **7** (86 mg, 0.244 mmol) was dissolved in benzene (7 mL). To the stirring solution was added aluminum chloride (0.179 g, 1.34 mmol) in small portions at room temperature. The red solution was heated to 80 °C with a drying tube in place. After 20 hours, the solution was cooled to room temperature and a slurry of concentrated sulfuric acid (5 drops) in crushed ice added slowly. The organic layer was allowed to evaporate, the remaining aqueous solution filtered and product rinsed with water (20 mL) to yield pink solids. The solids were dried in an oven (75°C) for 2 hours yielding **8** (94 mg, 91%). m.p. = 226-228 °C; <sup>1</sup>H NMR (400 MHz, CDCl<sub>3</sub>) δ (ppm): 7.3-7.7 (m, 17H), 8.0 (s, 1H), 8.75 (s, 1H); <sup>13</sup>C NMR (100 MHz, CDCl<sub>3</sub>) δ (ppm): 125.8, 127.0, 128.1, 128.3, 128.6, 128.9, 129.0, 129.7, 130.2, 130.3, 131.5, 131.7, 133.2, 133.5, 137.6, 137.9, 139.6, 140.7, 141.7, 171.4, 197.1

(coincidental overlap of signals in the congested aromatic region); HRMS (FAB)  $m/z$  = 428.1433, calcd  $m/z$  = 428.14124.

**3,5,8-Triphenyl-3*H*-naphtho[2,3-*c*]furan-1-one ((±)-9).** Compound **8** (0.566g, 1.32 mmol) was added to a solution of sodium hydroxide (5.5 g) in 95% ethanol (100 mL) and water (20 mL). Sodium borohydride was added (0.303 g, 8.20 mmol) and the solution stirred for 3 days. The solution was then brought to pH 9 by addition of concentrated HCl. Sodium borohydride (0.127 g, 3.42 mmol) was again added and the solution stirred for an additional 3 days. The solution was acidified with concentrated HCl and filtered. The filtrate was concentrated under reduced pressure. Chloroform was added (50 mL) and the organic layer washed with saturated NaHCO<sub>3</sub> (aq) (2 x 50 mL), water (50 mL), and brine (50 mL). The organic layer was dried (CaCl<sub>2</sub>) and concentrated under reduced pressure to yield the crude product which was recrystallized from ethanol to yield (±)-**9** (0.316 g, 58%). m.p. = 169-172 °C; <sup>1</sup>H NMR (400 MHz, CDCl<sub>3</sub>) δ (ppm): 6.52 (s, 1H), 7.24-7.27 (m, 3H), 7.32-7.36 (m, 3H), 7.42-7.63 (m, 11H), 7.9 (s 1H), 8.66 (s, 1H); <sup>13</sup>C NMR (100 MHz, CDCl<sub>3</sub>) δ (ppm): 83.1, 120.8, 123.6, 126.3, 127.4, 127.7, 128.0, 128.2, 128.8, 129.0, 129.1, 129.5, 129.9, 130.2, 130.3, 132.6, 135.4, 137.3, 139.9, 140.1, 140.4, 142.3, 143.4, 170.7; HRMS (FAB)  $m/z$  = 413.1546 (M + H<sup>+</sup>), calcd  $m/z$  = 413.15415.

**4,6,9,11-Tetraphenylanthra[2,3-*c*]furan-1,3-dione (11).** Compound (±)-**9** (127 mg, 0.307 mmol) was dissolved in dry THF (10 mL). The solution was placed in an ice bath and a drying tube was attached to the vessel. Phenyl magnesium bromide (0.2 mL,

3M in Et<sub>2</sub>O) was added drop wise over three minutes. After 1 hour, the reaction was quenched with NH<sub>4</sub>Cl (aq) (3 mL). Diethyl ether (35 mL) was added and the solution washed with NaHCO<sub>3</sub> (aq) (50 mL), water (50 mL), and brine (50 mL). The organic layer was dried (CaCl<sub>2</sub>) and concentrated at reduced pressure at room temperature. The viscous liquid was triturated with hexanes and the resulting powder rinsed with hexanes (10 mL). The lactol (see Scheme 3) was air-dried to yield an off-white powder (101 mg, 67%). A benzene solution of this powder (36 mg, 0.07 mmol), maleic anhydride (29 mg, 0.30 mmol) and *p*-toluenesulfonic acid monohydrate (0.172 g, 0.903 mmol) was heated to 80 °C with a Dean-Stark trap for 24 hours. The organic layer was washed with saturated NaHCO<sub>3</sub> (aq) (20 mL), water (25 mL) and brined (25 mL). The organic layer was dried (CaCl<sub>2</sub>) and concentrated at reduced pressure. The crude solids were rinsed with acetone (15 mL) and the remaining solid air-dried to yield **11** (8 mg, 20%). m.p. = 336 °C (dec.); <sup>1</sup>H NMR (500 MHz, CDCl<sub>3</sub>) δ (ppm): 7.36-7.49 (m, 20H), 7.63 (s, 2H), 8.66 (s, 2H); <sup>13</sup>C NMR (125 MHz, CDCl<sub>3</sub>) δ (ppm): 120.7, 127.9, 128.45, 128.5, 128.6, 129.1, 130.0, 132.3, 132.7, 133.6, 139.4, 140.6, 144.4, 162.3 (coincidental overlap of two aromatic signals); HRMS (FAB) *m/z* = 553.1805 (M + H<sup>+</sup>), calcd *m/z* = 553.18037.

**Adducts of 4,7-diphenylisobenzofuran (5) and 1,4-naphthoquinone, (12a) and (12b).** Compound (±)-**4** (1.03 g, 3.56 mmol) and 1,4-naphthoquinone (0.568 g, 3.77 mmol) were heated to 60 °C in acetic acid (20 mL) for 2 hours. The solution was chilled in an ice bath, precipitate filtered, and solids rinsed with cold acetic acid (5 mL). The resulting white powder is a mixture of endo **12a** and exo **12b** cycloaddition adducts (1.30 g, 85% combined). m.p. = 222-223 °C; <sup>1</sup>H NMR (400 MHz, CDCl<sub>3</sub>) δ (ppm): 3.50 (exo

adduct **12b**, s, 2H), 3.64 (endo adduct **12a**, m, 2H), 5.94 (exo adduct **12b**, s, 2H), 6.25 (endo adduct **12a**, m, 2H), 7.24 (endo adduct **12a**, s, 2H), 7.32-7.34 (endo **12a**, m, 4H), 7.43-7.66 (endo **12a** and exo **12a**, m, 28H), 7.76 (exo adduct **12b**, m, 2H), 8.16 (exo adduct **12b**, m, 2H);  $^{13}\text{C}$  NMR (125 MHz,  $\text{CDCl}_3$ )  $\delta$  (ppm): 49.5, 51.7, 82.8, 85.2, 126.2, 127.4, 127.97, 127.99, 128.4, 128.7, 129.0, 129.2, 133.3, 133.9, 134.1, 134.6, 134.8, 135.6, 138.6, 138.7, 139.9, 143.1, 193.1, 195.4 (coincidental overlap of signals in the congested aromatic region); HRMS (FAB)  $m/z$  = 429.1489 ( $\text{M} + \text{H}^+$ ), calcd  $m/z$  = 429.14907.

**1,4-Diphenyltetracene-6,11-quinone (13).** Compound ( $\pm$ )-**4** (1.45 g, 5.02 mmol) and 1,4-naphthoquinone (0.871 g, 5.50 mmol) were heated to 70 °C in acetic acid (12 mL) for 2 hours. Five drops of concentrated sulfuric acid were added and the solution heated for an additional hour at 70°C. The solution was chilled in an ice bath and precipitate filtered off and rinsed with methanol (7 mL) to yield **13** as orange solids (1.00 g, 49%). m.p. = 282-285 °C;  $^1\text{H}$  NMR (500 MHz,  $\text{CDCl}_3$ )  $\delta$  (ppm): 7.52-7.59 (m, 10H), 7.70 (s, 2H), 7.79 (m, 2H), 8.33 (m, 2H), 9.01 (s, 2H);  $^{13}\text{C}$  NMR (125 MHz,  $\text{CDCl}_3$ )  $\delta$  (ppm): 127.6, 128.3, 128.7, 129.0, 129.7, 130.2, 130.4, 134.2, 134.4, 134.8, 139.6, 142.5, 183.2; HRMS (FAB)  $m/z$  = 411.1386 ( $\text{M} + \text{H}^+$ ), calcd  $m/z$  = 411.13850.

**1,4-Diphenyl-6,11-dihydrotetracene and 1,4-diphenyl-5,12-dihydrotetracene (14a and 14b).** Compound **13** (0.127 g, 0.308 mmol) was heated to 118 °C in a mixture of hydriodic acid (8 mL, 55-58%, unstabilized) and acetic acid (50 mL) under nitrogen in the dark for 3 days. The reaction was quenched with saturated  $\text{NaHSO}_3$  (aq) (10 mL).

Water (50 mL) was added and the aqueous mixture extracted with dichloromethane (50 mL). The organic extract was washed with saturated NaHSO<sub>3</sub> (aq) (30 mL), saturated NaHCO<sub>3</sub> (aq) (3 x 50 mL), water (50 mL) and brine (50 mL). The organic layer was dried (CaCl<sub>2</sub>) and concentrated at reduced pressure. The crude product (0.116 mg, 98% crude) was purified via silica column chromatography (benzene as eluent) to yield a mixture of **14a** and **14b** ( $R_f$  = 0.8, 80 mg, 68% combined). m.p. = 110-135 °C; <sup>1</sup>H NMR (500 MHz, CDCl<sub>3</sub>)  $\delta$  (ppm): 3.96 (s, 4H), 4.10 (s, 4H), 7.14 (m, 2H), 7.23 (m, 4H), 7.33 (m, 2H), 7.38 (s, 2H), 7.57 (s, 2H), 7.42-7.54 (m, 20H), 7.66 (m, 2H), 7.86 (s, 2H); <sup>13</sup>C NMR (125 MHz, CDCl<sub>3</sub>)  $\delta$  (ppm): 34.9, 37.0, 123.9, 125.0, 125.4, 126.1, 126.4, 127.2, 127.4, 127.6, 128.5, 129.8, 130.3, 131.0, 132.5, 135.5, 136.0, 136.4, 137.1, 139.4, 139.9, 141.3, 141.6 (coincidental overlap of signals in the congested aromatic region); HRMS (FAB)  $m/z$  = 382.1722, calculated  $m/z$  = 382.17215.

**1,4-Diphenyltetracene (15).** A mixture of **14a** and **14b** (60 mg, 0.157 mmol) and 10% Pd/C (65 mg) was heated to 180 °C in 1,2-dichlorobenzene (50 mL) under nitrogen in the dark for 3 days. The resulting solution was cooled, filtered to remove Pd/C, and the solid Pd/C rinsed with dichloromethane (15 mL). The combined organic filtrate was concentrated at reduced pressure under low-light conditions. The resulting orange-brown solids were dried on a vacuum pump to yield **15** (55 mg, 93%). m.p. = 214-217 °C; <sup>1</sup>H NMR (500 MHz, CDCl<sub>3</sub>)  $\delta$  (ppm): 7.36 (m, 2H), 7.39 (s, 2H), 7.54 (m, 2H), 7.59 (m, 4H), 7.68 (m, 4H), 7.93 (m, 2H), 8.56 (s, 2H), 8.75 (s, 2H); <sup>13</sup>C NMR (100 MHz, CDCl<sub>3</sub>)  $\delta$  (ppm): 125.4, 125.8, 125.9, 126.9, 127.8, 128.5, 128.7, 130.1, 130.5, 130.9, 131.9, 140.1, 141.2; HRMS (FAB)  $m/z$  = 380.1548, calcd  $m/z$  = 380.15650.

**1,4,8,11-Tetraphenyl-5,7,12,14-diendoxo-5a,6a,12a,13a-tetrahydropentacene-6,13-quinone (16b).** Lactol ( $\pm$ )-4 (1.75 g, 6.07 mmol) and freshly sublimed *p*-benzoquinone (0.315 g, 2.91 mmol) were heated to 118 °C in glacial acetic acid (35 mL) for 8 hours. The white precipitate was filtered, rinsed with HOAc (5 mL) and water (20 mL) and air dried to yield **16b** (1.70 g, 90%). m.p. = 293 °C (dec.);  $^1\text{H}$  NMR (500 MHz,  $\text{CDCl}_3$ )  $\delta$  (ppm): 3.37 (s, 4H), 6.03 (s, 4H), 7.42-7.49 (m, 16H), 7.53-7.56 (m, 8H);  $^{13}\text{C}$  NMR (125 MHz,  $\text{CDCl}_3$ )  $\delta$  (ppm): 55.1, 81.3, 127.9, 128.2, 129.1, 133.4, 138.7, 142.2, 205.2 (coincidental overlap of two aromatic signals). Anal. calcd for  $\text{C}_{46}\text{H}_{32}\text{O}_4$ : C, 85.16; H, 4.97. Found: C, 84.99; H, 4.86.

**Diols 18a and 18b.** Compound **16b** (38 mg, 0.059 mmol) and sodium borohydride (11 mg, 0.29 mmol) were heated to 66 °C in dry THF (50 mL) for 2.5 hours. The reaction was quenched with 4M HCl and concentrated at reduced pressure. The crude product was taken up in dichloromethane (40 mL) and the organic layer washed with saturated  $\text{NaHCO}_3$  (aq) (50 mL), water (50 mL), and brine (50 mL). The organic layer was dried ( $\text{CaCl}_2$ ) and concentrated at reduced pressure. The crude was purified via silica preparative plate chromatography (10% EtOAc in  $\text{CHCl}_3$  as eluent). Reduced products **18a** ( $R_f$  = 0.27, 11 mg, 28%) and **18b** ( $R_f$  = 0.42, 10 mg, 26%) were isolated.

**18a:** m.p. = 318 °C (dec.);  $^1\text{H}$  NMR (500 MHz,  $\text{CDCl}_3$ )  $\delta$  (ppm): 1.96 (OH, d, 2H,  $J$  = 4.64 Hz, disappears with  $\text{D}_2\text{O}$ ), 2.49 (m, 2H), 2.72 (m, 2H), 4.24 (bs, 2H), 5.42 (d, 2H,  $J$  = 0.98 Hz), 5.87 (s, 2H), 7.36-7.59 (m, 24H);  $^{13}\text{C}$  NMR (125 MHz,  $\text{CD}_2\text{Cl}_2$ )  $\delta$  (ppm): 46.0, 46.3, 69.1, 77.8, 81.0, 127.0, 127.1, 127.3, 127.4, 128.3, 128.4, 128.7, 128.8,

132.65, 132.70, 139.3, 143.5, 145.0; HRMS (FAB)  $m/z$  = 651.2524 (M - H), calcd  $m/z$  = 651.25353.

**18b**: m.p. = 290 °C (dec.);  $^1\text{H}$  NMR (500 MHz,  $\text{CDCl}_3$ )  $\delta$  (ppm): 2.09 (OH, d, 1H,  $J$  = 4.64 Hz, disappears with  $\text{D}_2\text{O}$ ), 2.48 (dd, 1H,  $J$  = 10.98, 8.54 Hz), 2.63-2.69 (m, 2H), 2.78 (dd, 1H,  $J$  = 8.17, 2.56 Hz), 3.67 (OH, d, 1H,  $J$  = 3.66 Hz, disappears with  $\text{D}_2\text{O}$ ), 4.59 (m, 1H, with  $\text{D}_2\text{O}$  converges to dd,  $J$  = 10.98, 5.61 Hz), 4.65 (m, 1H), 5.24 (s, 1H), 5.51 (s, 1H), 5.59 (s, 1H), 5.88 (s, 1H), 7.34-7.59 (m, 24H);  $^{13}\text{C}$  NMR (125 MHz,  $\text{CD}_2\text{Cl}_2$ )  $\delta$  (ppm): 42.5, 44.2, 45.3, 47.9, 69.7, 69.9, 78.2, 80.8, 81.0, 81.1, 127.02, 127.1, 127.3, 127.37, 127.43, 127.45, 127.47, 127.49, 128.28, 128.30, 128.33, 128.5, 128.8, 128.87, 128.9, 132.7, 132.8, 133.1, 139.1, 139.27, 139.30, 139.5, 142.2, 144.1, 144.8, 144.9; HRMS (FAB)  $m/z$  = 651.2553 (M - H), calcd  $m/z$  = 651.25353.

**1,4,8,11-Tetraphenylpentacene-6,13-quinone (19)**. Compound **16b** (0.26 g, 0.4 mmol) and *p*-toluenesulfonic acid (0.28 g, 1.61 mmol) were heated to 80 °C in benzene (25 mL) under nitrogen with a Dean-Stark trap for 24 hours. The benzene was removed at room temperature and crude black product washed with copious amounts of acetone to yield **19** (42 mg, 17%). m.p. = 458 °C (subl.);  $^1\text{H}$  NMR (500 MHz,  $\text{CDCl}_3$ )  $\delta$  (ppm): 7.48-7.58 (m, 20H), 7.00 (s, 4H), 9.02 (s, 4H);  $^{13}\text{C}$  NMR: Lack of solubility prohibits  $^{13}\text{C}$  NMR spectroscopy. HRMS failed to produce a molecular ion and elemental analysis failed due to incomplete combustion of carbon.

**1,4,8,11-Tetraphenyl-6,13-dihydropentacene (20)**. Compound **19** (119 mg, 0.194 mmol) was suspended in a mixture of HI (10 mL, 47%), glacial acetic acid (70

mL), and chloroform (70 mL). The solution was heated to 85 °C under nitrogen in the dark for 5 days. The solvent was concentrated to approximately 10 mL at reduced pressure and saturated NaHCO<sub>3</sub> (aq) added until bubbling ceased. The orange precipitate was then filtered and washed with saturated NaHCO<sub>3</sub> (aq) and water. The orange powder was taken up in boiling benzene (15 mL) and filtered, and the persistent precipitate washed with boiling benzene (2 x 10 mL). The combined benzene filtrate was concentrated and the crude product purified via silica preparative plate chromatography (45% hexanes in CHCl<sub>3</sub> as eluent) to yield **20** (2 mg, 1.6 %). m.p. = 348 °C (dec.); <sup>1</sup>H NMR (500 MHz, CDCl<sub>3</sub>) δ (ppm): 4.05 (s, 4H), 7.39 (s, 4H), 7.50-7.52 (m, 20H), 7.83 (s, 4H); <sup>13</sup>C NMR (125 MHz, CDCl<sub>3</sub>) δ (ppm): 37.04, 123.6, 126.0, 127.2, 128.3, 130.1, 130.9, 135.8, 139.3, 141.1; HRMS (FAB) *m/z* = 584.2509, calcd *m/z* = 548.25040.

**1,4,8,11-Tetraphenyl-5,7,12,14-tetrahydropentacene (21).** Compound **19** (52 mg, 0.085 mmol) was suspended in a mixture of HI (7.5 mL, 47%) and glacial acetic acid (150 mL). The solution was heated to 118 °C under nitrogen in the dark for 6 days. The solvent was concentrated to approximately 20 mL at reduced pressure and saturated NaHCO<sub>3</sub> (aq) added until bubbling ceased. The orange precipitate was then filtered and rinsed with water. The orange powder was taken up in boiling benzene (30 mL) and filtered, and the persistent precipitated washed with boiling benzene (30 mL). The combined benzene filtrate was concentrated to approximately 5-10 mL were upon a crystalline product precipitated from solution. This was filtered off and air dried to yield pure **21** (3 mg, 6%). The filtrate was concentrated and the crude product purified via silica preparative plate chromatography (10% hexanes in CH<sub>2</sub>Cl<sub>2</sub> as eluent) to yield a



mixture of **20** and **21** enriched in the former (5 mg, 10%). **21**:  $^1\text{H}$  NMR (400 MHz,  $\text{CDCl}_3$ )  $\delta$  (ppm): 4.05 (s, 4H), 7.39 (s, 4H), 7.50-7.52 (m, 20H), 7.83 (s, 4H);  $^{13}\text{C}$  NMR (125 MHz,  $\text{CDCl}_3$ )  $\delta$  (ppm): 34.1, 125.6, 126.9, 127.1, 128.2, 129.5, 135.3, 135.4, 139.7, 141.5.

**1,4,8,11-Tetraphenylpentacene (22).** Compound **19** (99 mg, 0.162 mmol) was suspended in dry toluene (115 mL) and chilled to 0 °C. To this stirring suspension, under nitrogen, was added drop wise  $\text{BH}_3$  in THF (2.5 mL, 1M) over 2 minutes. The solution was slowly brought to room temperature and heated to 111 °C in the dark for 15 hours. The reaction was quenched ( $\text{MeOH}$ , 3 mL) and washed with water (2 x 100 mL) and brine (1 x 75 mL). The organic layer was dried ( $\text{CaCl}_2$ ) and concentrated at reduced pressure under low-light to yield a mixture of 1,4,8,11-tetraphenyl-6,13-dihydropentacene and 1,4,8,11-tetraphenylpentacene. This crude material was taken up in 1,2-dichlorobenzene and 10% Pd/C (95 mg) added. The stirring solution was purged with nitrogen and subsequently heated to 180 °C in the dark for 36 hours. The resulting solution was filtered warm to remove Pd/C, and the solid Pd/C rinsed with dichloromethane (10 mL). The combined organic filtrate was concentrated at reduced pressure under low-light conditions. The resulting purple-blue solids were purified via silica column chromatography ( $\text{CS}_2$  as eluent) in the exclusion of light to yield **22** ( $R_f$  = 0.4, 22 mg, 23% overall).  $^1\text{H}$  NMR (500 MHz,  $\text{CS}_2\text{:C}_6\text{D}_6$ , 2:1)  $\delta$  (ppm): 7.14 (s, 4H), 7.36 (m, 4H), 7.42 (m, 8H), 7.52 (m, 8H), 8.22 (s, 2H), 8.54 (s, 4H);  $^{13}\text{C}$  NMR (125 MHz,  $\text{CDCl}_3$ )  $\delta$  (ppm): 125.4, 125.9, 127.1, 127.5, 128.5, 129.9, 130.1, 130.9, 139.5, 140.9.

**1,4-Diphenyltetracene-[60]fullerene adducts (27a and 27b).** Compound **15** (8 mg,  $2.10 \times 10^{-5}$  mol) and [60]fullerene (18 mg,  $2.50 \times 10^{-5}$  mol) were combined in benzene (20 mL) and the stirring solution heated to 50 °C under nitrogen in the dark for 1.5 hours. The solution was concentrated at reduced pressure and purified via silica column chromatography (CS<sub>2</sub> as eluent) to yield a mixture of isomers **27a** and **27b** ( $R_f$  = 0.6, 16.4 mg, 71%). <sup>1</sup>H NMR (500 MHz, CS<sub>2</sub>:CDCl<sub>3</sub>, 3:1)  $\delta$  (ppm): 5.71 (s, 2H, 6,11 adduct), 6.05, (s, 2H, 5,12 adduct), 7.38-7.55 (m, 28H, 5,12 and 6,11 adduct), 7.71 (m, 2H, 6,11 adduct), 7.90 (m, 2H, 5,12 adduct), 8.03 (s, 2H, 5,12 adduct), 8.21 (s, 2H, 6,11 adduct); <sup>13</sup>C NMR (125 MHz, CS<sub>2</sub>:CDCl<sub>3</sub>, 3:1)  $\delta$  (ppm): 54.7, 58.2, 71.8, 72.0, 122.6, 124.1, 125.9, 127.0, 127.3, 127.42, 127.44, 128.1, 128.2, 128.4, 128.6, 129.4, 130.2, 131.3, 132.8, 136.3, 136.8, 137.0, 138.93, 138.97, 139.0, 139.1, 139.6, 139.80, 139.83, 139.9, 140.0, 140.7, 141.2, 141.4, 141.5, 141.6, 141.81, 141.83, 141.86, 141.89, 142.0, 142.1, 142.4, 142.7, 142.9, 144.41, 144.43, 144.5, 145.1, 145.17, 145.2, 145.26, 145.3, 145.97, 146.0, 146.2, 146.26, 147.3, 155.0, 155.1, 155.15, 155.18 (coincidental overlap of signals in the congested aromatic region).

**1,4-Diphenyltetracene-[60]fullerene adducts (27a and 27b).** Compound **15** (8.6 mg,  $2.26 \times 10^{-5}$  mol) and [60]fullerene (19.5 mg,  $2.71 \times 10^{-5}$  mol) were combined in *ortho*-dichlorobenzene-*d*<sub>4</sub> (2 mL) and the stirring solution heated to 180 °C under nitrogen in the dark for 15 minutes. The solution was concentrated at reduced pressure and purified via silica column chromatography (CS<sub>2</sub> as eluent) to yield a mixture of isomers **27a** and **27b** ( $R_f$  = 0.6, 17 mg, 68%).

**1,4-Diphenyltetracene-oxygen adducts (28a and 28b).** Compound **15** (5.5 mg,  $1.5 \times 10^{-5}$ ) was dissolved in  $\text{CDCl}_3$  (1.5 mL) and exposed to ambient light and air for 20 hours. The sample was analyzed without further purification.  $^1\text{H}$  NMR (400 MHz,  $\text{CDCl}_3$ )  $\delta$  (ppm): 6.04 (s, 2H, 6,11 adduct), 6.42 (s, 2H, 5,12 adduct), 7.28 (m, 2H, 6,11 adduct), 7.37-7.41 (m, 4H, 5,12 and 6,11 adduct), 7.46-7.60 (m, 24H, 5,12 and 6,11 adduct), 7.86 (s, 2H, 5,12 adduct), 7.88 (m, 2H, 5,12 adduct), 7.93 (s, 2H, 6,11 adduct).

**1,4-Diphenyltetracene-ethylene adducts (29a and 29b).** Compound **15** (3.6 mg,  $9.5 \times 10^{-6}$ ) was dissolved in toluene (4 mL) and placed in a stainless steel bomb. The head space was purged with nitrogen and subsequently pressurized with ethylene to 150 psi. The vessel was heated at 175 °C for 3 days. The vessel was quenched and carefully opened to vent excess ethylene. The solution was concentrated and analyzed without further purification.  $^1\text{H}$  NMR (400 MHz,  $\text{CDCl}_3$ )  $\delta$  (ppm): 1.80 (m, 4H, 5,12 adduct), 1.78 (s, 4H, 6,11 adduct), 4.32 (bs, 2H, 6,11 adduct), 4.78 (bs, 2H, 5,12 adduct) 7.1-7.8 (m, 36H, 5,12 and 6,11 adduct).

**1,4-Diphenyltetracene-dimethyl acetylenedicarboxylate adducts (30a and 30b).** Compound **15** (4.3 mg,  $1.130 \times 10^{-2}$  mmol) and dimethylacetylene dicarboxylate (43 mg,  $3.03 \times 10^{-1}$  mmol) were combined in *ortho*-dichlorobenzene- $d_4$  (1.5 mL) and the stirring solution heated to 180°C under nitrogen in the dark for 15 minutes. The solution was concentrated at reduced pressure and purified via preparatory plate chromatography (toluene as eluent) to yield a mixture of **30a** and **30b** ( $R_f = 0.2$ , 1.5 mg, 25%).  $^1\text{H}$  NMR

(400 MHz, CDCl<sub>3</sub>)  $\delta$  (ppm): 3.76 (s, 6H, 6,11 adduct), 3.79 (s, 6H, 5,12 adduct), 5.47 (s, 2H, 6,11 adduct), 5.88 (s, 2H, 5,12 adduct), 7.02 (m, 2H, 6,11 adduct), 7.10 (s, 2H, 5,12 adduct), 7.35-7.41 (m, 6H, 5,12 and 6,11 adduct), 7.45-7.58 (m, 20H, 5,12 and 6,11 adduct), 7.65-7.7 (m, 4H, 5,12 adduct), 7.88 (s, 2H, 6,11 adduct); <sup>13</sup>C NMR (125 MHz, CDCl<sub>3</sub>)  $\delta$  (ppm): 49.0, 51.9, 52.4, 120.7, 122.3, 124.0, 125.8, 126.1, 126.79, 126.83, 127.3, 127.4, 127.6, 128.4, 128.5, 129.5, 130.1, 131.7, 137.5, 139.7, 139.8, 140.0, 140.1, 140.7, 141.0, 143.0, 146.1, 146.5, 165.83, 165.85 (coincidental overlap of two aromatic signals and two aliphatic signals at 52.4 ppm (see HSQC for details).

**1,4-Diphenyltetracene-maleic anhydride adducts (31a,31a',31b,31b').**

Compound **15** (5.1 mg,  $1.34 \times 10^{-5}$  mol) and maleic anhydride (1.4 mg,  $1.43 \times 10^{-5}$  mol) were combined in *ortho*-dichlorobenzene-*d*<sub>4</sub> (1 mL) and the stirring solution heated to 180°C under nitrogen in the dark for 1 hour. The vessel was quenched and the sample analyzed without further purification. <sup>1</sup>H NMR (400 MHz, *o*-DCB<sub>d4</sub>)  $\delta$  (ppm): 3.31 (m, 2H, 5,12 exo adduct), 3.38 (m, 2H, 6,11 endo adduct), 3.42 (m, 2H, 6,11 exo adduct), 3.58 (m, 2H, 5,12 endo adduct), 4.64 (m, 2H, 6,11 endo adduct), 4.66 (m, 2H, 6,11 exo adduct), 5.23 (m, 2H, 5,12 exo adduct), 5.36 (m, 2H, 5,12 endo adduct), 6.95 (m, 2H), 7.05 (m, 2H), 7.1 (m, 2H), 7.16 (m, 4H), 7.24 (m, 4H), 7.29 (m, 2H), 7.31 (m, 2H), 7.36-7.58 (m, 46H), 7.64 (m, 2H), 8.0 (s, 2H), 8.04 (s, 2H).

**1,4-Diphenyltetracene-tetrachloroquinone adducts (32a,32a',32b,32b').**

Compound **15** (3.2 mg,  $8.4 \times 10^{-3}$  mmol) and tetrachloroquinone (2.5 mg,  $1.02 \times 10^{-2}$  mmol) were combined in *ortho*-dichlorobenzene-*d*<sub>4</sub> (1 mL) and the stirring solution

heated to 125°C under nitrogen in the dark for 1 hour. The sample, a mixture of **15** and Diels-Alder products, was analyzed without further purification. <sup>1</sup>H NMR (400 MHz, *o*-DCB<sub>d4</sub>) δ (ppm): 5.10 (s, 2H, 6,11 adduct), 5.15 (s, 2H, 6,11 adduct), 5.61 (s, 2H, 5,12 adduct), 5.82 (s, 2H, 5,12 adduct).

**Tetracene-maleic anhydride adducts (33a and 33b).** Tetracene (5.2 mg, 2.28 x 10<sup>-5</sup> mol) and maleic anhydride (2.4 mg, 2.45 x 10<sup>-5</sup> mol) were combined in *ortho*-dichlorobenzene-*d*<sub>4</sub> (1 mL) and the stirring solution heated to 180°C under nitrogen in the dark for 1 hour. The vessel was quenched and the reaction analyzed without further purification. <sup>1</sup>H NMR (400 MHz, *o*-DCB<sub>d4</sub>) δ (ppm): 3.45 (m, 4H, endo and exo adduct), 4.78 (bs, 2H, exo adduct), 4.80 (bs, 2H, endo adduct), 7.06 (m, 2H, exo adduct), 7.11 (m, 2H, endo adduct), 7.25 (m, 2H, exo adduct), 7.6 (m, 4H, endo adduct), 7.39 (m, 2H, exo adduct), 7.5 (m, 2H, endo adduct), 7.53 (s, 2H, exo adduct), 7.54 (s, 2H, endo adduct), 7.42 (m, 2H, exo adduct).

**1,4-Di(*p*-methoxyphenyl)tetracene-6,11-quinone (39).** Compound **34** (1,4-di(*p*-methoxyphenyl)-2,3-dibromomethylbenzene) (351 mg, 0.740 mmol), sublimed 1,4-naphthoquinone (160 mg, 1.01 mmol) and potassium iodide (571 mg, 3.44 mmol) were combined in dimethylformamide (10 mL) and the stirring solution heated to 125 °C for 22 hours. Water (25 mL) was added and the precipitate filtered and rinsed with MeOH (130 mL) to yield **39** (206 mg, 59%). <sup>1</sup>H NMR (400 MHz, CDCl<sub>3</sub>) δ (ppm): 3.95 (s, 6H), 7.11 (m, 4H), 7.50 (m, 4H), 7.67 (s, 2H), 7.80 (m, 2H), 8.45 (m, 2H), 9.01 (s, 2H); <sup>13</sup>C

NMR (125 MHz, CDCl<sub>3</sub>)  $\delta$  (ppm): 55.6, 114.4, 127.6, 128.7, 129.5, 130.1, 131.4, 131.9, 134.2, 134.3, 134.7, 141.8, 159.7, 183.2.

**1,4-Di(*p*-trifluoromethylphenyl)tetracene-6,11-quinone (40).** Compound **37** (1,4-di(*p*-trifluoromethylphenyl)-2,3-dibromomethylbenzene) (507 mg, 0.917 mmol), sublimed 1,4-naphthoquinone (192 mg, 1.21 mmol) and potassium iodide (690 mg, 4.16 mmol) were combined in dimethylformamide (7 mL) and the stirring solution heated to 125 °C for 18 hours. Water (35 mL) was added and the precipitate filtered and rinsed with MeOH (30 mL) to yield **40** (341 mg, 70%). <sup>1</sup>H NMR (400 MHz, CDCl<sub>3</sub>)  $\delta$  (ppm): 7.69-7.71 (m, 6H), 7.82 (m, 2H), 7.88 (m, 4H), 8.35 (m, 2H), 8.91 (s, 2H); <sup>13</sup>C NMR (100 MHz, CDCl<sub>3</sub>)  $\delta$  (ppm): {120.3, 123.0, 125.7, 128.4 (q, <sup>1</sup>J = 272.3 Hz)}, {126.0, 126.04, 126.08, 126.11 (q, <sup>3</sup>J = 3.8 Hz)}, 127.7, 128.0, 130.15, 130.18, 130.6, {130.2, 130.6, 130.9, 131.2 (q, <sup>2</sup>J = 32.9 Hz)}, 133.8, 134.6, 141.6, 143.0, 182.9 (coincidental overlap of two aromatic signals); <sup>19</sup>F NMR (470 MHz, CDCl<sub>3</sub>)  $\delta$  (ppm): -65.68 (referenced to C<sub>6</sub>F<sub>6</sub> set at -164.90 ppm).

**1,4-Di(*p*-methoxyphenyl)tetracene (41).** Quinone **39** (51mg, 1.08 x 10<sup>-4</sup>) was dissolved in dry toluene (25 mL). To this stirring solution at 0 °C under nitrogen was added BH<sub>3</sub> in THF (1.8 mL, 1M) drop wise over 5 minutes. The solution was allowed to warm to room temperature and then heated to reflux for 22 hours under nitrogen and in the dark. The reaction was quenched (MeOH, 3 mL) and the organic layer washed with NaHCO<sub>3</sub> (aq) (50 mL), water (50 mL) and brine (50 mL). The organic layer was dried (CaCl<sub>2</sub>) and concentrated at reduced pressure to yield a mixture of 1,4-di(*p*-

methoxyphenyl)-6,11-dihydrotetracene and 1,4-di(*p*-methoxyphenyl)tetracene (47 mg, 98% crude). The mixture was combined with 10% Pd/C (120 mg) in 1,2-dichlorobenzene (50 mL) and heated to 180°C under nitrogen in the dark for 6 days. The resulting solution was cooled, filtered to remove Pd/C, and the solid Pd/C rinsed with chloroform (10 mL). The combined organic filtrate was concentrated at reduced pressure under low-light conditions and purified via silica column chromatography (hexanes:DCM 2:1 as eluent) to yield **41** ( $R_f = 0.2$ , 33 mg, 70%).  $^1\text{H}$  NMR (400 MHz,  $\text{CDCl}_3$ )  $\delta$  (ppm): 3.94 (s, 6H), 7.11 (m, 4H), 7.35-7.37 (m, 2H), 7.59 (m, 2H), 7.92 (m, 2H), 8.55 (s, 2H), 8.77 (s, 2H);  $^{13}\text{C}$  NMR (100 MHz,  $\text{CDCl}_3$ )  $\delta$  (ppm): 55.7, 114.2, 125.4, 125.7, 125.9, 126.8, 128.5, 130.1, 131.2, 131.5, 131.8, 133.6, 139.4, 159.4.

**1,4-Di(*p*-trifluoromethylphenyl)tetracene (42).** Compound **40** (88mg,  $1.60 \times 10^{-4}$ ) was dissolved in dry toluene (25 mL). To this stirring solution at 0 °C under nitrogen was added  $\text{BH}_3$  in THF (2.5 mL, 1M) drop wise over 5 minutes. The solution was allowed to warm to room temperature and then heated to 111 °C for 20 hours under nitrogen and in the dark. The reaction was quenched (MeOH, 3 mL) and the organic layer washed with  $\text{NaHCO}_3$  (aq) (50 mL), water (75 mL) and brine (75 mL). The organic layer was dried ( $\text{CaCl}_2$ ) and concentrated to yield a mixture of 1,4-di(*p*-trifluoromethylphenyl)-6,11-dihydrotetracene and 1,4-di(*p*-trifluoromethylphenyl)tetracene (80 mg, 96% crude). The mixture was combined with 10% Pd/C (53 mg) in 1,2-dichlorobenzene (30 mL) and heated to 180°C under nitrogen in the dark for 7 days. The resulting solution was cooled, filtered to remove Pd/C, and the solid Pd/C rinsed with dichloromethane (15 mL). The combined organic filtrate was concentrated at reduced pressure under low-light

conditions and purified via silica column chromatography (hexanes:DCM 2:1 as eluent) to yield **42** (60 mg, 75%).  $^1\text{H}$  NMR (400 MHz,  $\text{CDCl}_3$ )  $\delta$  (ppm): 7.38-7.41 (m, 4H), 7.78 (m, 4H), 7.86 (m, 4H), 7.95 (m, 2H), 8.58 (s, 2H), 8.65 (s, 2H);  $^{13}\text{C}$  NMR (125 MHz,  $\text{CDCl}_3$ )  $\delta$  (ppm): {121.3, 123.5, 125.7, 127.8 (q,  $^1J = 272.6$  Hz)}, {125.72, 125.75 (app. d,  $^3J = 3.8$  Hz)}, 125.78, 126.9, 128.5, {129.7, 130.0, 130.2, 130.5 (q,  $^2J = 32.6$  Hz)}, 130.2, 130.3, 130.7, 132.2, 139.4, 144.7 (coincidental overlap of signals in the congested aromatic region);  $^{19}\text{F}$  NMR (376 MHz,  $\text{CDCl}_3$ )  $\delta$  (ppm): -65.52 (referenced to  $\text{C}_6\text{F}_6$  set at -164.90 ppm).

**1,4-Di(*p*-methoxyphenyl)tetracene-[60]fullerene adducts (**46a** and **46b**).**

Compound **41** (6.6 mg,  $1.50 \times 10^{-5}$  mol) and [60]fullerene (13 mg,  $1.80 \times 10^{-5}$  mol) were combined in benzene (7 mL) and the stirring solution heated to 50°C under nitrogen in the dark for 1.5 hours. The solvent was removed at reduced pressure and the crude material purified via silica column chromatography ( $\text{CS}_2$  as eluent) to yield a mixture of the isomers **46a** and **46b** ( $R_f = 0.1$ , 13 mg, 75%).  $^1\text{H}$  NMR (400 MHz,  $\text{CS}_2:\text{CDCl}_3$ , 5:3)  $\delta$  (ppm): 3.85 (5,12 adduct, s, 6H), 3.87 (6,11 adduct, s, 6H), 5.73 (6,11 adduct, s, 2H), 6.08 (5,12 adduct, s, 2H), 6.95 (5,12 adduct, d, 4H), 7.0 (6,11 adduct, d, 4H), 7.33-7.36 (5,12 adduct, m, 6H), 7.43 (6,11 adduct, d, 4H), 7.50 (5,12 adduct, m, 2H), 7.71 (6,11 adduct, m, 2H), 7.91 (5,12 adduct, m, 2H), 8.04 (5,12 adduct, s, 2H), 8.24 (6,11 adduct, s, 2H);  $^{13}\text{C}$  NMR (100 MHz,  $\text{CS}_2:\text{CDCl}_3$ , 5:3)  $\delta$  (ppm): 55.1, 55.3, 55.4, 58.7, 72.3, 72.5, 114.3, 114.4, 123.1, 124.5, 126.3, 126.7, 127.5, 127.8, 128.5, 128.7, 130.9, 131.6, 132.0, 132.8, 133.2, 133.5, 136.8, 137.2, 137.4, 138.9, 139.2, 139.4, 139.5, 139.7, 140.1, 140.25 (shoulder), 140.3, 141.7, 141.9, 141.93, 142.0, 142.25, 142.27 (shoulder), 142.31, 142.35,



142.42, 142.47 (shoulder), 142.50, 142.8, 143.1, 143.15, 143.2, 143.3, 144.86, 144.91, 145.57, 145.60 (shoulder), 145.62, 145.65, 145.67 (shoulder), 145.8, 146.4, 146.5, 146.66, 146.69, 147.8, 155.5, 155.6, 155.62 (shoulder), 155.7, 159.3 (coincidental overlap of signals in the congested aromatic region).

**1,4-Di(*p*-tertbutylphenyl)tetracene-[60]fullerene adducts (47a and 47b).**

Compound **43** (7.3 mg,  $1.48 \times 10^{-5}$  mol) and [60]fullerene (12.8 mg,  $1.78 \times 10^{-5}$  mol) were combined in benzene (8 mL) and the stirring solution heated to 50°C under nitrogen in the dark for 1.5 hours. The solution was concentrated at reduced pressure and purified via silica column chromatography (CS<sub>2</sub> as eluent) to yield a mixture of the isomers **47a** and **47b** ( $R_f$  = 0.7, 12 mg, 70%). <sup>1</sup>H NMR (500 MHz, CS<sub>2</sub>:C<sub>6</sub>D<sub>6</sub>, 10:1) δ (ppm): 1.39 (s, 9H, 5,12 adduct), 1.40 (s, 9H, 6,11 adduct), 5.64 (s, 2H, 6,11 adduct), 6.15 (s, 2H, 5,12 adduct), 7.3-7.5 (m, 24H, 5,12 and 6,11 adduct), 7.62 (m, 2H, 6,11 adduct), 7.81 (m, 2H, 5,12 adduct), 7.94 (s, 2H, 5,12 adduct), 8.25 (s, 2H, 6,11 adduct); <sup>13</sup>C NMR (125 MHz, CDCl<sub>3</sub>) δ (ppm): 31.47, 31.51, 34.69, 34.72, 54.7, 58.1, 72.2, 72.3, 122.9, 124.3, 125.45, 125.52, 126.06, 126.13, 127.2, 127.5, 128.2, 128.4, 129.2, 129.9, 131.4, 132.9, 136.6, 136.8, 137.1, 137.16, 137.21, 138.0, 139.0, 139.2, 139.58, 139.64, 139.76, 139.83, 139.9, 141.62, 141.64, 141.97, 142.02, 142.1, 142.16, 142.24, 142.27, 142.33, 142.5, 142.9, 143.0, 144.59, 144.61, 144.63, 145.2, 145.3, 145.38, 145.40, 145.44, 145.5, 145.7, 146.1, 146.15, 146.18, 146.36, 146.39, 146.4, 147.54, 147.56, 150.23, 150.25, 155.5, 155.56, 155.62, 155.7 (coincidental overlap in the congested aromatic region).

**1,4-Di(*p*-cyanophenyl)tetracene-[60]fullerene adducts (48a and 48b).**

Compound **44** (5.4 mg,  $1.25 \times 10^{-5}$  mol) and [60]fullerene (10.8 mg,  $1.5 \times 10^{-5}$  mol) were combined in benzene (7 mL) and the stirring solution heated to 50°C under nitrogen in the dark for 1.5 hours. The solution was concentrated at reduced pressure and purified via silica column chromatography (CS<sub>2</sub> as eluent) to yield a mixture of the isomers **48a** and **48b** ( $R_f$  = 0.1, 11.2 mg, 78%). <sup>1</sup>H NMR (400 MHz, CDCl<sub>3</sub>) δ (ppm): 5.84 (s, 2H, 6,11 adduct), 6.0 (2, 2H, 5,12 adduct), 7.49-7.54 (m, 4H), 7.55 (s, 2H), 7.61-7.66 (m, 6H), 7.72 (m, 4H), 7.80 (m, 2H), 7.84-7.89 (m, 8H), 8.03 (m, 2H), 8.16 (s, 2H), 8.17 (s, 2H); <sup>13</sup>C NMR (125 MHz, CDCl<sub>3</sub>:CS<sub>2</sub>, 4:1) δ (ppm): 54.9, 58.4, 71.8, 72.0, 112.3, 112.6, 118.0, 118.2, 122.3, 124.6, 126.6, 127.0, 127.2, 128.0, 128.2, 128.4, 130.3, 131.0, 132.5, 132.6, 133.1, 136.4, 136.9, 137.1, 137.3, 138.2, 138.4, 139.2, 139.7, 140.05, 140.11, 140.2, 140.3, 140.6, 140.9, 141.6, 141.7, 141.8, 141.95, 142.02, 142.09, 142.14, 142.70, 142.72, 142.2, 142.8, 143.0, 143.1, 143.2, 144.4, 144.7, 144.8, 145.07, 145.11, 145.2, 145.3, 145.47, 145.53, 145.57, 145.60, 146.3, 146.4, 146.5, 146.6, 147.7, 154.5, 154.7, 155.0 (coincidental overlap of signals in the congested aromatic region).

**1,4-Di(*p*-trifluoromethylphenyl)tetracene-[60]fullerene adducts (49a and**

**49b).** Compound **42** (7.3 mg,  $1.41 \times 10^{-5}$  mol) and [60]fullerene (12 mg,  $1.67 \times 10^{-5}$  mol) were combined in benzene (7 mL) and the stirring solution heated to 50°C under nitrogen in the dark for 1.5 hours. The solution was concentrated at reduced pressure and purified via silica column chromatography (CS<sub>2</sub> as eluent) to yield a mixture of the isomers **49a** and **49b** ( $R_f$  = 0.6, 9.5 mg, 55%). <sup>1</sup>H NMR (400 MHz, CS<sub>2</sub>:CDCl<sub>3</sub>, 2:1) δ (ppm): 5.75 (s, 2H, 6,11 adduct), 6.0 (s, 2H, 5,12 adduct), 7.46 (m, 4H, 5,12 and 6,11 adduct), 7.51 (s,

2H, 5,12 adduct), 7.55 (m, 2H, 5,12 adduct), 7.60 (m, 4H, 5,12 adduct), 7.68-7.80 (m, 14H, 5,12 and 6,11 adduct), 7.91 (m, 2H, 5,12 adduct), 8.04 (s, 2H, 5,12 adduct), 8.18 (s, 2H, 6,11 adduct);  $^{13}\text{C}$  NMR (100 MHz,  $\text{CS}_2:\text{CDCl}_3$ , 2:1)  $\delta$  (ppm): 55.1, 58.6, 72.1, 72.3, 122.7, 124.7, 125.9 (m), 126.1 (m), 126.4, 127.1, 127.4, 128.1, 128.5, 128.6, 130.1, 130.3, 130.4, 130.6, 130.9, 131.5, 133.3, 136.7, 137.2, 137.3, 137.5, 138.7, 139.6, 139.8, 140.2, 140.3, 140.4, 140.44, 141.3, 141.87, 141.94, 142.1, 142.26, 142.31, 142.35, 142.37, 142.5, 142.88, 142.94, 143.2, 143.3, 143.4, 143.9, 144.5, 144.86, 144.89, 145.2, 145.45, 145.49, 145.54, 145.67, 145.71, 145.73, 145.75, 145.77, 145.8, 146.5, 146.6, 146.7, 146.8, 147.8, 154.97, 155.0, 155.1, 155.3 (coincidental overlap of signals in the congested aromatic region).

**1,4-Di(bis-*m*-trifluoromethylphenyl)tetracene-[60]fullerene adducts (50a and 50b).** Compound **45** (8.2 mg,  $1.25 \times 10^{-5}$  mol) and [60]fullerene (10.8 mg,  $1.5 \times 10^{-5}$  mol) were combined in benzene (7 mL) and the stirring solution heated to 50°C under nitrogen in the dark for 1.5 hours. The solution was concentrated at reduced pressure and purified via silica column chromatography ( $\text{CS}_2$  as eluent) to yield a mixture of the isomers **50a** and **50b** ( $R_f = 0.7$ , 11 mg, 64%).  $^1\text{H}$  NMR (400 MHz,  $\text{CS}_2:\text{CDCl}_3$ , 1:1)  $\delta$  (ppm): 5.80 (s, 2H, 6,11 adduct), 5.87 (s, 2H, 5,12 adduct), 7.49 (m, 2H), 7.54 (s, 2H), 7.56 (m, 2H), 7.59 (s, 2H), 7.78 (m, 2H), 7.92-8.04 (m, 16H), 8.11 (s, 2H);  $^{13}\text{C}$  NMR (125 MHz,  $\text{CS}_2:\text{CDCl}_3$ , 1:1)  $\delta$  (ppm): 55.3, 58.6, 71.9, 72.2, 122.1, 122.2, 124.9, 126.5, 127.3, 127.6, 128.3, 128.6, 129.9, 130.5, 131.3, 132.5, 132.7, 133.3, 136.6, 137.0, 137.3, 137.5, 137.6, 138.0, 138.4, 140.2, 140.4, 140.58, 140.64, 140.9, 141.4, 141.9, 142.0, 142.06, 142.09, 142.25, 142.29, 142.3, 142.4, 142.7, 142.9, 143.0, 143.2, 143.3, 142.4, 144.8, 144.88,

144.92, 145.2, 145.3, 145.38, 145.41, 145.5, 145.6, 145.72, 145.74, 145.8, 145.9, 146.48, 146.52, 146.7, 146.76, 146.79, 147.85, 147.89, 154.3, 154.5, 154.8, 155.2 (coincidental overlap of signals in the congested aromatic region).

**1,4-Di(*p*-methoxyphenyl)tetracene-oxygen adducts (51a and 51b).** Compound **41** (4 mg,  $9.1 \times 10^{-6}$  mol) was dissolved in CDCl<sub>3</sub> (1 mL) and exposed to light and air for 18 hours. The sample was analyzed without further purification. <sup>1</sup>H NMR (400 MHz, CDCl<sub>3</sub>) δ (ppm): 3.92 (s, 12H, 5,12 and 6,11 adduct), 6.05 (s, 2H, 6,11 adduct), 6.42 (m, 2H, 5,12 adduct), 7.05-7.11 (m, 8H, 5,12 and 6,11 adduct), 7.28 (m, 2H, 6,11 adduct), 7.34 (s, 2H, 5,12 adduct), 7.38-7.45 (m, 12H, 5,12 and 6,11 adduct), 7.52 (m, 2H, 5,12 adduct), 7.84 (s, 2H, 5,12 adduct), 7.87 (m, 2H, 5,12 adduct), 7.94 (s, 2H, 6,11 adduct).

**1,4-Di(*p*-tertbutylphenyl)tetracene-oxygen adducts (52a and 52b).** Compound **43** (5.1 mg,  $1.0 \times 10^{-5}$  mol) was dissolved in CDCl<sub>3</sub> (1 mL) and exposed to light and air for 22 hours. The sample was analyzed without further purification. <sup>1</sup>H NMR (400 MHz, CDCl<sub>3</sub>) δ (ppm): 1.47 (s, 18H, 5,12 adduct), 1.58 (s, 18H, 6,11 adduct), 6.08 (2, 2H, 6,11 adduct), 6.48 (s, 2H, 5,12 adduct), 7.28 (m, 4H), 7.36-7.60 (m, 22H, 5,12 and 6,11 adduct), 7.88-7.91 (m, 4H, 5,12 adduct), 8.0 (s, 2H, 6,11 adduct).

**1,4-Di(*p*-cyanophenyl)tetracene-oxygen adducts (53a and 53b).** Compound **44** (6.1 mg,  $1.4 \times 10^{-5}$  mol) was dissolved in CDCl<sub>3</sub> (1 mL) and exposed to light and air for 18 hours. The sample was analyzed without further purification. <sup>1</sup>H NMR (400 MHz, CDCl<sub>3</sub>) δ (ppm): 6.05 (s, 2H, 6,11 adduct), 6.3 (s, 2H, 5,12 adduct), 7.31 (m, 2H, 5,12

adduct), 7.40-7.44 (m, 4H, 5,12 and 6,11 adduct), 7.49 (s, 2H, 6,11 adduct), 7.55-7.65 (m, 10H, 5,12 and 6,11 adduct), 7.8-7.9 (m, 14H, 5,12 and 6,11 adduct).

**1,4-Di(*p*-trifluoromethylphenyl)tetracene-oxygen adducts (54a and 54b).**

Compound **42** (4.5 mg,  $8.7 \times 10^{-3}$  mmol) was dissolved in  $\text{CDCl}_3$  (1 mL) and exposed to light and air for 22 hours. The sample was analyzed without further purification.  $^1\text{H}$  NMR (400 MHz,  $\text{CDCl}_3$ )  $\delta$  (ppm): 6.06 (s, 2H, 6,11 adduct), 6.34 (s, 2H, 5,12 adduct), 7.30 (m, 2H, 5,12 adduct), 7.40-7.44 (m, 4H, 5,12 and 6,11 adduct), 7.49 (s, 2H, 6,11 adduct), 7.55 (m, 2H, 5,12 adduct), 7.58-7.64 (m, 8H, 5,12 and 6,11 adduct), 7.8-7.9 (m, 14H, 5,12 and 6,11 adduct).

**1,4-Di(bis-*m*-trifluoromethylphenyl)tetracene-oxygen adducts (55a and 55b).**

Compound **45** (6.4 mg,  $9.8 \times 10^{-6}$  mol) was dissolved in  $\text{CDCl}_3$  (1 mL) and exposed to light and air for 18 hours. The sample was analyzed without further purification.  $^1\text{H}$  NMR (400 MHz,  $\text{CDCl}_3$ )  $\delta$  (ppm): 6.10 (s, 2H, 6,11 adduct), 6.24 (s, 2H, 5,12 adduct), 7.32 (m, 2H, 6,11 adduct), 7.44 (m, 2H, 6,11 adduct), 7.49 (s, 2H, 5,12 adduct), 7.53 (s, 2H, 6,11 adduct), 7.59 (m, 2H, 5,12 adduct), 7.88 (s, 2H, 5,12 adduct), 7.9-7.96 (m, 10H, 5,12 and 6,11 adduct), 8.04, (m, 6H, 5,12 and 6,11 adduct).

**$\text{C}_{2v}$  symmetric [60]fullerene monoadduct of 1,4,8,11-tetraphenylpentacene and  $\text{C}_{2v}$  symmetric *cis*-bis[60]fullerene bisadduct of 1,4,8,11-tetraphenylpentacene (60 and 61).** Compound **22** (2.1 mg,  $3.6 \times 10^{-6}$ ) in benzene (5 mL) was added to a solution of [60]fullerene (11 mg,  $1.5 \times 10^{-5}$  mol) dissolved in benzene (12 mL). This

solution was purged with nitrogen and heated to 50 °C under nitrogen in the dark for 1.5 hours. The solution was concentrated at reduced pressure and purified via silica column chromatography (CS<sub>2</sub> as eluent) to yield **60** and **61** ( $R_f$  = 0.5, 3.8 mg, 73% based on reacted acene). <sup>1</sup>H NMR (400 MHz, CS<sub>2</sub>:C<sub>6</sub>D<sub>6</sub> 10:1)  $\delta$  (ppm): 5.60 (monoadduct, s, 2H), 6.12 (bisadduct, s, 4H), 7.34-7.5 (monoadduct and bisadduct, m, 48H), 7.90 (bisadduct, s, 2H), 8.20 (monoadduct, s, 4H); <sup>13</sup>C NMR (100 MHz, CDCl<sub>3</sub>:CS<sub>2</sub>, 1:1)  $\delta$  (ppm): 54.7, 58.0, 71.7, 72.3, 122.8, 123.2, 127.0, 127.3, 127.5, 128.1, 128.4, 128.5, 129.4, 130.2, 131.4, 136.3, 136.8, 137.1, 138.7, 138.9, 139.3, 139.65, 139.71, 139.8, 139.9, 140.0, 140.6, 141.2, 141.35, 141.43, 141.8, 141.9, 142.1, 142.2, 142.3, 142.7, 142.9, 144.4, 144.5, 144.97, 145.00, 145.1, 145.2, 145.27, 145.3; 146.0, 146.2, 146.3, 147.3, 154.8, 155.2 (coincidental overlap of signals in the congested aromatic region).

**1,4,8,11-Tetraphenylpentacene-oxygen monoadducts (62a and 62b).**

Compound **22** (1 mg,  $1.72 \times 10^{-6}$  mol) was dissolved in benzene (1.5 mL). The stirring solution was heated to 50°C under atmosphere and ambient lighting for 45 minutes, upon which time all purple-blue color was gone. The sample was analyzed without further purification. <sup>1</sup>H NMR (500 MHz, CDCl<sub>3</sub>)  $\delta$  (ppm): (**62a**) 6.06 (s, 2H), 7.45-7.54 (m, 24H), 7.91 (s, 4H).

**1,4,8,11-Tetraphenylpentacene-maleic anhydride monoadducts (63a and 63b).** Compound **22** (2.4 mg,  $4.1 \times 10^{-6}$  mol) and maleic anhydride (1.7 mg,  $1.7 \times 10^{-5}$  mol) were combined in benzene (1.5 mL). The stirring solution was purged with nitrogen and heated to 50°C under nitrogen in the dark for 1.5 hours. The reaction was analyzed

without further purification.  $^1\text{H}$  NMR (400 MHz,  $\text{CDCl}_3$ )  $\delta$  (ppm): (**63a**) 3.59 (m, 2H), 4.84 (m, 2H), 7.4-7.6 (m, 24H), 7.88 (s, 2H), 7.90 (s, 2H).

**1,4,8,11-Tetraphenylpentacene-DDQ monoadduct (64a).** Compound **22** (2.2 mg,  $3.8 \times 10^{-6}$  mol) and DDQ (3.6 mg,  $1.6 \times 10^{-5}$  mol) were combined in benzene (10 mL). The stirring solution was purged with nitrogen and heated to  $50^\circ\text{C}$  under nitrogen in the dark for 1.5 hours. The solution was concentrated at reduced pressure and purified via silica column chromatography ( $\text{CHCl}_3$  as eluent) to yield **64a** ( $R_f = 0.2$ , 2.5 mg, 81%).  $^1\text{H}$  NMR (400 MHz,  $\text{CDCl}_3$ )  $\delta$  (ppm): 5.01 (s, 2H), 7.38 (m, 4H), 7.48-7.56 (m, 20H), 7.77 (s, 2H), 8.15 (s, 2H).

## REFERENCES

1. *CRC Handbook of Chemistry and Physics, 86th Edition*; Lide, D. R., Ed.; CRC Press: New York, NY, 2005.
2. Taylor, R. *Lecture Notes on Fullerene Chemistry*; Imperial College Press: London, England, 1999.
3. Rohlffing, E. A.; Cox, D. M.; Kaldor, A. *J. Chem. Phys.* **1984**, *81*, 3322.
4. Goresy, E.; Donnay, G. *Science* **1968**, *161*, 363.
5. Kroto, H. W.; Heath, J. R.; O'Brien, S. C.; Curl, R. F.; Smalley, R. E. *Nature* **1985**, *318*, 162.
6. Smalley, R. E., Foreword of *Buckminsterfullerenes*; Billups, W. E.; Ciufolini, M. A., Eds.; VCH Publishers, Inc.: New York, NY, 1993, v-vii.
7. Taylor, R.; Hare, J. P.; Abdul-Sada, A. K.; Kroto, H. W. *J. Chem. Soc., Chem. Commun.* **1990**, 1423.
8. (a) Krätschmer, W.; Lamb, L. D.; Fostiropoulos, K.; Huffman, D. R. *Nature* **1990**, *347*, 354; (b) Wragg, J. L.; Chamberlain, J. E.; White, H. W.; Krätschmer, W.; Huffman, D. R. *ibid.* **1990**, *348*, 623.
9. Diederich, F.; Whetten, R. L. *Acc. Chem. Res.* **1992**, *25*, 119.
10. Ettl, R.; Chao, I.; Diederich, F.; Whetten, R. L. *Nature* **1991**, *353*, 149.
11. Diederich, F.; Whetten, R. L.; Thilgen, C.; Ettl, R.; Chao, I.; Alvarez, M. *Science* **1991**, *254*, 1768.
12. Taylor, R.; Langley, G. J.; Dennis, T. J. S.; Kroto, H. W.; Walton, D. R. M. *J. Chem. Soc., Chem. Commun.* **1992**, 1043.
13. Taylor, R.; Langley, G. J.; Avent, A. G.; Dennis, T. J. S.; Kroto, H. W.; Walton, D. R. M. *J. Chem. Soc., Perkin Trans. 2* **1993**, 1029.
14. Kikuchi, K.; Nakahara, N.; Wakabayashi, T.; Suzuki, S.; Shiromaru, H.; Miyake, Y.; Saito, K.; Ikemoto, I.; Kainosho, M.; Achiba, Y. *Nature* **1992**, *357*, 142.



15. Manolopoulos, D. E.; Fowler, P. W.; Taylor, R.; Kroto, H. W.; Walton, D. R. M. *J. Chem. Soc., Faraday Trans.* **1992**, *88*, 3117.
16. Diederich, F.; Ettl, R.; Rubin, Y.; Whetten, R. L.; Beck, R.; Alvarez, M.; Anz, S.; Sensharma, D.; Wudl, F.; Khemani, K. C.; Koch, A. *Science* **1991**, *252*, 548.
17. Kikuchi, K.; Nakahara, N.; Wakabayashi, T.; Honda, M.; Matsumiya, H.; Moriwaki, T.; Suzuki, S.; Shiromaru, H.; Saito, K.; Yamauchi, K.; Ikemoto, I.; Achiba, Y. *Chem. Phys. Lett.* **1992**, *188*, 177.
18. Scott, L. T.; Boorum, M. M.; McHahon, B. J.; Hagen, S.; Mack, J.; Blank, J.; Wegner, H.; deMeijere, A. *Science* **2002**, *295*, 1500.
19. For a review see: Scott, L. T. *Angew. Chem. Int. Ed. Eng.* **2004**, *43*, 4994.
20. Jackson, E. A.; Steinberg, B. D.; Bancu, M.; Wakamiya, A.; Scott, L. T. *J. Am. Chem. Soc.* **2007**, *129*, 484.
21. (a) *Buckminsterfullerenes*; Billups, W. E.; Ciufolini, M. A., Eds.; VCH Publishers, Inc.: New York, NY, 1993; (b) *Fullerenes: Chemistry, Physics, and Technology*; Kadish, K. M.; Ruoff, R. S., Eds.; John Wiley & Sons, Inc.: New York, NY, 2000; (c) *Fullerenes: From Science to Optoelectronic Properties*; Guldi, D. M.; Marin, N., Eds.; Developments in Fullerene Science; Kluwer Academic Publishers: Dordrecht, The Netherlands, 2002; Vol. 4.
22. For a review see *Acc. Chem. Res.* **1992**, *25*, 98-175.
23. (a) Barth, W. E.; Lawton, R. G. *J. Am. Chem. Soc.* **1966**, *88*, 380; (b) *ibid.* **1970**, *93*, 1730.
24. (a) Schmalz, T. G.; Seitz, W. A.; Klein, D. J.; Hite, G. E. *Chem. Phys. Lett.* **1986**, *130*, 203; (b) Zhang, Q. L.; O'Brien, S. C.; Heath, J. R.; Liu, Y.; Curl, R. F.; Kroto, H. W.; Smalley, R. E. *J. Phys. Chem.* **1986**, *90*, 525; (c) Kroto, H. W. *Nature* **1987**, *329*, 529; (d) Schmalz, T. G.; Seitz, W. A.; Klein, D. J.; Hite, G. E. *J. Am. Chem. Soc.* **1988**, *110*, 113; (e) Kroto, H. *Science* **1988**, *242*, 1139; (f) Zhang, B. L.; Wang, C. Z.; Ho, K. M. *Chem. Phys. Lett.* **1992**, *193*, 225.
25. (a) Yannoni, C. S.; Johnson, R. D.; Meijer, G.; Bethune, D. S.; Salem, J. R. *J. Phys. Chem.* **1991**, *95*, 9; (b) Tycko, R.; Haddon, R. C.; Dabbagh, G.; Glarum, S. H.; Douglass, D. C.; Mjjsce, A. M. *ibid.* **1991**, *95*, 518.
26. Hawkins, J. M.; Meyer, A.; Lewis, T. A.; Loren, S.; Hollander, F. J. *Science* **1991**, *252*, 312.

27. David, W. I. F.; Ibberson, R. M.; Matthewman, J. C.; Prassides, K.; Dennis, T. J. S.; Hare, J. P.; Kroto, H. W.; Taylor, R.; Walton, D. R. M. *Nature* **1991**, *353*, 147.
28. Haddon, R. C.; Brus, L. E.; Raghavachari, K. *Chem. Phys. Lett.* **1986**, *125*, 459.
29. Bühl, M.; Hirsh, A. *Chem. Rev.* **2001**, *101*, 1153.
30. Jeffery, G. A.; Ruble, J. R.; McMullan, R. K.; Pople, J. A. *Proc. R. Soc.* **1987**, *414*, 47.
31. (a) Haddon, R. C.; Scott, L. T. *Pure Appl. Chem.* **1986**, *58*, 137; (b) Haddon, R. C. *Acc. Chem. Res.* **1988**, *21*, 243; (c) *ibid.* **1992**, *25*, 127.
32. Haddon, R. C.; Brus, L. E.; Raghavachari, K. *Chem. Phys. Lett.* **1986**, *131*, 165.
33. Haddon, R. C. *Science* **1993**, *261*, 1545.
34. (a) Beckhaus, H.-D.; Rüchardt, C.; Kao, M.; Diederich, F.; Foote, C. S. *Angew. Chem. Int. Ed. Engl.* **1992**, *31*, 63; (b) Beckhaus, H.-D.; Verevkin, S.; Rüchardt, C.; Diederich, F.; Thilgen, C.; ter Meer, H.-U.; Mohn, H.; Müller, W. *ibid.* **1994**, *33*, 996.
35. Khan, S. I.; Oliver, A. M.; Paddon-Row, M. N.; Rubin, Y. *J. Am. Chem. Soc.* **1993**, *115*, 4919.
36. Diederich, F.; Jonas, U.; Gramlich, V.; Herrman, A.; Ringsdorf, H.; Thilgen, C. *Helv. Chim. Acta* **1993**, *76*, 2445.
37. (a) Kräulter, B.; Puchberger, M. *Helv. Chim. Acta* **1993**, *76*, 1626; (b) Metha, G.; Viswanath, M. B. *Synlett.* **1995**, 679; (c) Ohno, M.; Azuma, T.; Kojima, S.; Shirakawa, Y.; Eguchi, S. *Tetrahedron* **1996**, *52*, 4983; (d) Kräulter, B.; Maynollo, J. *Tetrahedron* **1996**, *52*, 5033; (e) Mattay, J.; Torres-Garcia, G.; Averdung, J.; Wolff, C.; Schlachter, I.; Luftmann, H.; Siedschlag, C.; Luger, P.; Ramm, M. *J. Phys. Chem. Solids* **1997**, *58*, 1929.
38. Illescas, B.; Martín, N.; Seoane, C. De la Cruz, P.; Langa, F.; Wudl, F. *Tetrahedron Lett.* **1995**, *36*, 8307.
39. (a) Nogami, T.; Tsuda, M.; Ishida, T.; Kurono, S.; Ohashi, M. *Fullerene Sci. Technol.* **1993**, *1*, 275; (b) Prato, M.; Suzuki, T.; Foroudian, H.; Li, Q.; Khemani, K.; Wudl, F.; Leonetti, J.; Little, R. D.; White, T.; Rickborn, B.; Yamago, S.; Nakamura, E. *J. Am. Chem. Soc.* **1993**, *115*, 1594; (c) Chuang, S.-C.; Sander, M.; Jarrosson, T.; James, S.; Rozumov, E.; Khan, S. I.; Rubin, Y. *J. Org. Chem.* **2007**, *72*, 2716; (d) Sander, M.; Jarrosson, T.; Chuang, S.-C.; Khan, S. I.; Rubin, Y. *ibid.*, 2724.
40. Puplovskis, A.; Kacens, J.; Neilands, O. *Tetrahedron Lett.* **1997**, *38*, 285.

41. Rotello, V. M.; Howard, J. B.; Yadav, T.; Conn, M. M.; Viani, E.; Giovane, L. M.; LaFleur, A. L. *Tetrahedron Lett.* **1993**, 34, 1561.
42. Tsuda, M.; Ishida, T.; Nogami, T.; Kurono, S.; Ohashi, M. *J. Chem. Soc., Chem. Commun.* **1993**, 1296.
43. Pang, L. S. K.; Wilson, M. A. *J. Phys. Chem.* **1993**, 97, 6761.
44. Ohno, M.; Koide, N.; Sato, H.; Eguchi, S. *Tetrahedron* **1997**, 53, 9075.
45. (a) Ohno, M.; Koide, N.; Eguchi, S. *Heterocyclic Commun.* **1995**, 1, 125; (b) Fernández-Paniagua, U. M.; Illescas, B. M.; Martín, N.; Seoane, C. *J. Chem. Soc., Perkin Trans. 1* **1996**, 1077.
46. Hirsch, A.; Lamparth, I.; Karfunkel, H. R. *Angew. Chem. Int. Ed. Engl.* **1994**, 33, 437.
47. Pang, L. S. K.; Wilson, M. A. *J. Phys. Chem.* **1993**, 97, 6761.
48. (a) Murata, Y.; Kato, N.; Komastu, K. *J. Org. Chem.* **2001**, 66, 7235; (b) Murata, Y.; Murata, M.; Komastu, K. *ibid.* **2001**, 66, 8187.
49. Inoue, H.; Yamaguchi, H.; Iwamatsu, S.; Uozaki, T.; Suzuki, T.; Akasaka, T.; Nagase, S.; Murata, S. *Tetrahedron Lett.* **2001**, 42, 895.
50. Rubin, Y. *Top. Curr. Chem.* **1999**, 199, 67.
51. An, Y.-Z.; Ellis, G. A.; Viado, A. L.; Rubin, Y. *J. Org. Chem.* **1995**, 60, 6353.
52. Nakamura, Y.; Minowa, T.; Tobita, S.; Shizuka, H.; Nishimura, J. *J. Chem. Soc., Perkin Trans. 2* **1995**, 2351.
53. Belik, P.; Gügel, A.; Spickermann, J.; Müllen, K. *Angew. Chem. Int. Ed. Engl.* **1993**, 32, 78.
54. Taki, M.; Takigami, S.; Watanabe, Y.; Nakamura, Y.; Nishimura, J. *Polym. J.* **1997**, 29, 1020.
55. Harvey, R. G. *Polycyclic Aromatic Hydrocarbons*; Wiley-VCH, Inc.: New York, NY, 1997.
56. Clar, E. *Chem. Ber.* **1939**, 72, 1817.
57. Mondal, R.; Adhikari, R. M.; Shah, B. K.; Neckers, D. C. *Org. Lett.* **2007**, 9, 2505.

58. Clar, E. *Chem. Ber.* **1942**, 75, 1330.
59. Bailey, W. J.; Liao, C. *J. Am. Chem. Soc.* **1955**, 77, 992.
60. Boggiano, B.; Clar, E. *J. Chem. Soc.* **1957**, 2681.
61. Mondal, R.; Shah, B. K.; Neckers, D. C. *J. Am. Chem. Soc.* **2006**, 128, 9612.
62. Bowen, E. J.; Tanner, D. W. *Faraday Trans.* **1955**, 51, 475.
63. Bouas-Laurent, H.; Desvergne, J. P. *Photochromism, Molecules and Systems*; Dürr, H.; Bouas-Laurent, H., Eds.; Elsevier: Amsterdam, The Netherlands, 1990.
64. Kaupp, G.; Teufel, E. *Chem. Ber.* **1980**, 113, 3669.
65. Bunker, C. E.; Rollins, H. W.; Gord, J. R.; Sun, Y.-P. *J. Org. Chem.* **1997**, 62, 7324.
66. Wei, K. S.; Livingston, R. *Photochem. Photobiol.* **1967**, 6, 229.
67. Zingg, S. P.; Sigman, M. E. *Photochem. Photobiol.* **1993**, 57, 453.
68. Lee-Ruff, E.; Kazarians-Moghaddam, H.; Katz, M. *Can. J. Chem.* **1986**, 64, 1297.
69. Schleyer, P. v R.; Manoharan, M.; Jiao, H.; Stahl, F. *Org. Lett.* **2001**, 3, 3643.
70. Bendikov, M.; Duong, H. D.; Starkey, K.; Houk, K. N.; Carter, E. A.; Wudl, F. *J. Am. Chem. Soc.* **2004**, 126, 7416.
71. Houk, K. N.; Lee, P. S.; Nendel, M. *J. Org. Chem.* **2001**, 66, 5517.
72. Clar, E. *Polycyclic Hydrocarbons*; Academic Press Inc.: London, England, 1964; Vols. 1 & 2.
73. Clar, E. *Chem. Ber.* **1942**, 75B, 1271.
74. Luo, J.; Hart, H. *J. Org. Chem.* **1987**, 52, 4833.
75. Thummel, R. P.; Cravey, W. E.; Nutakul, W. *J. Org. Chem.* **1978**, 43, 2473.
76. Netka, J.; Crump, S. L.; Rickborn, B. *J. Org. Chem.* **1986**, 51, 1189.
77. Gribble, G. W.; Perni, R. B.; Onan, K. D. *J. Org. Chem.* **1985**, 50, 2934.
78. Lockhart, T. P.; Comita, P. B.; Bergman, R. G. *J. Am. Chem. Soc.* **1981**, 103, 4082.

79. Bowles, D. M.; Anthony, J. E. *Org. Lett.* **2000**, *2*, 85.
80. Anthony, J. E. *Chem. Rev.* **2006**, *106*, 5028.
81. (a) Clar, E.; John, F. *Chem. Ber.* **1929**, *62*, 3021; (b) *ibid.* **1930**, *63*, 2967; (c) *ibid.* **1931**, *64B*, 981.
82. (a) Uno, H.; Yamashita, Y.; Kikuchi, M.; Watanabe, H.; Yamada, H.; Okujima, T.; Ogawa, T.; Ono, N. *Tetrahedron Lett.* **2005**, *46*, 1981; (b) Yamada, H.; Yamashita, Y.; Kikuchi, M.; Watanabe, H.; Okujima, T.; Uno, H.; Ogawa, T.; Ohara, K.; Ono, N. *Chem. Eur. J.* **2005**, *11*, 6212.
83. Ried, W.; Anthöfer, F. *Angew. Chem.* **1953**, *65*, 601.
84. Vets, N.; Smet, M.; Dehaen, W. *Tetrahedron Lett.* **2004**, *45*, 7287.
85. Mack II, J. Ph.D. dissertation, University of New Hampshire, Durham, NH, 2000.
86. Cava, M. P.; Deana, A. A.; Muth, K. *J. Am. Chem. Soc.* **1959**, *81*, 6458.
87. Smith, J. G.; Dibble, P. W. *J. Org. Chem.* **1983**, *48*, 5361.
88. Bruckner, V.; Karczag, A.; Körmendy, K.; Meszaros, M.; Tomasz, J. *Tetrahedron Lett.* **1960**, *1*, 5.
89. Chan, S. H.; Lee, H. K.; Wang, Y. M.; Fu, N. Y.; Chen, X. M.; Cai, Z. W.; Wong, H. N. C. *J. Chem. Soc., Chem. Commun.* **2005**, 66.
90. Takahashi, T.; Kitmaura, M.; Shen, B.; Nakajima, K. *J. Am. Chem. Soc.* **2000**, *122*, 12876.
91. Allen, C. F. H.; Bell, A. *J. Am. Chem. Soc.* **1942**, *64*, 1253.
92. Wolak, M. A.; Jang, B.-B.; Palilis, L. C.; Kafafi, Z. H. *J. Phys. Chem. B* **2004**, *108*, 5492.
93. Vets, N.; Smet, M.; Dehaen, W. *Synlett* **2005**, *2*, 217.
94. Anthony, J. E.; Eaton, D. L.; Parkin, S. R. *Org. Lett.* **2002**, *4*, 15.
95. Kobayashi, K.; Shimaoka, R.; Kawahata, M.; Yamanaka, M.; Yamaguchi, K. *Org. Lett.* **2006**, *8*, 2385.
96. Miller, G. P.; Mack, J.; Briggs, J. *Proc. Electrochem. Soc.* **2001**, *2001-11*, 202.

97. (a) Anthony, J. E.; Brooks, J. S.; Eaton, D. L.; Parkin, S. R. *J. Am. Chem. Soc.* **2001**, *123*, 9482; (b) Odom, S. A.; Parkin, S. R.; Anthony, J. E. *Org. Lett.* **2003**, *5*, 4245; (c) Payne, M. M.; Delcamp, J. H.; Parkin, S. R.; Anthony, J. E. *Org. Lett.* **2004**, *6*, 1609; (d) Swartz, C. R.; Parkin, S. R.; Bullock, J. E.; Anthony, J. E.; Mayer, A. C.; Malliaras, G. G. *Org. Lett.* **2005**, *7*, 3163.
98. Payne, M. M.; Parkin, S. R.; Anthony, J. E. *J. Am. Chem. Soc.* **2005**, *127*, 8028.
99. Miao, Q.; Chi, X.; Xiao, S.; Zeis, R.; Lefenfeld, M.; Siegrist, T.; Steigerwald, M. L.; Nuckolls, C. *J. Am. Chem. Soc.* **2006**, *128*, 1340.
100. (a) Pascal, R. A.; McMillian, W. D.; Engen, D. V. *J. Am. Chem. Soc.* **1986**, *108*, 5652; (b) Smyth, N.; Engen, D. V.; Pascal, R. A. *J. Org. Chem.* **1990**, *55*, 1937; (c) Lu, J.; Ho, D. M.; Vogelaar, N. J.; Kraml, C. M.; Pascal, R. A. *J. Am. Chem. Soc.* **2004**, *126*, 11168.
101. Schusten, I. I.; Craciun, L.; Ho, D. M.; Pascal, R. A. *Tetrahedron* **2002**, *58*, 8875.
102. (a) Clar, E. *Chem. Ber.* **1931**, *64*, 2194; (b) *ibid.* **1932**, *65*, 503.
103. (a) Biermann, D.; Schmidt, W. *J. Am. Chem. Soc.* **1980**, *102*, 3163; (b) *ibid.* **1980**, *102*, 3173; (c) see also: Hess, B. A.; Schaad, L. J.; Herndon, W. C.; Biermann, D.; Schmidt, W. *Tetrahedron* **1981**, *37*, 2983.
104. Briggs, J.; Miller, G. P. *C. R. Chimie* **2006**, *9*, 916.
105. Murata, Y.; Kato, N.; Fujiwara K.; Komatsu, K. *J. Org. Chem.* **1999**, *64*, 3483.
106. Schlueter, J. A.; Seaman, J. M.; Taha, S.; Cohen, H.; Lykke, K. R.; Wang, H. H.; Williams, J. M. *J. Chem. Soc., Chem. Commun.* **1993**, 972.
107. Komatsu, K.; Murata, Y.; Sugita, N.; Takeuchi, K.; Wan, T. S. M. *Tetrahedron Lett.* **1993**, *34*, 8473.
108. de la Cruz, P.; de la Hoz, A.; Langa, F. *Tetrahedron* **1997**, *53*, 2599.
109. Sarova, G. H.; Berberan-Santos, M. N. *Chem. Phys. Lett.* **2004**, *397*, 402.
110. Mack, J.; Miller, G. P. *Fullerene Sci. Technol.* **1997**, *5*, 607.
111. Miller, G. P.; Briggs, J. *Proc. Electrochem. Soc.* **2002**, 2002-12, 279.
112. Miller, G. P.; Mack, J. *Org. Lett.* **2000**, *2*, 3979.

113. (a) Miller, G. P.; Mack, J.; Briggs, J. *Org. Lett.* **2000**, *2*, 3983; (b) Miller, G. P.; Briggs, J.; Mack, J.; Lord, P. A.; Olmstead, M. M.; Blach, A. L. *Org. Lett.* **2003**, *5*, 4199.
114. Miller, G. P.; Briggs, J. *Org. Lett.* **2003**, *5*, 4203.
115. (a) Barnett, E. D. B. *J. Chem. Soc.* **1935**, 1326; (b) Allen, C. F. H.; Gates, J. W. *J. Am. Chem. Soc.* **1943**, *65*, 1502; (c) Oniciu, D. C.; Ghiviriga, I.; Iordache, F.; Istrate, D.; Dinulescu, I. G. *Rev. Roum. Chim.* **1992**, *37*, 1285.
116. Peters, O.; Friedrichsen, W. *Trends Heterocycl. Chem.* **1995**, *4*, 217.
117. Wittig, G.; Pohmer, L. *Chem. Ber.* **1956**, *89*, 1334.
118. (a) Fieser, L. F.; Haddadin, M. J. *J. Am. Chem. Soc.* **1964**, *86*, 2081; (b) *ibid.* *Can. J. Chem.* **1965**, *43*, 1599.
119. (a) Friedrichsen, W. *Adv. Heterocycl. Chem.* **1999**, *73*, 1; (b) Reck, S.; Friedrichsen, W. *Prog. Heterocycl. Chem.* **1997**, *9*, 117; (c) Rodrigo, R. *Tetrahedron* **1988**, *44*, 2093.
120. Wege, D. *Adv. Theor. Interesting Mol.* **1998**, *4*, 1.
121. Warrenner, R. N.; Shang, M.; Butler, D. N. *J. Chem. Soc., Chem. Commun.* **2001**, 1550.
122. Rodrigo, R.; Knabe, S. M. *J. Org. Chem.* **1986**, *51*, 3973.
123. Smith, J. G.; Kruger, G. *J. Org. Chem.* **1985**, *50*, 5759.
124. Smith, J. G.; Sandborn, R. E.; Dibble, P. W. *J. Org. Chem.* **1986**, *51*, 3762.
125. Naito, K.; Rickborn, B. *J. Org. Chem.* **1980**, *45*, 4061.
126. Tu, N. P. W.; Yip, J. C.; Dibble, P. W. *Synthesis* **1996**, *5*, 77.
127. Mikami, K.; Ohmura, H. *Org. Lett.* **2002**, *4*, 3355.
128. Kuhn, R.; Wagner-Jauregg, Th. *Chem. Ber.* **1930**, *63B*, 2662.
129. Bergmann, F. *J. Am. Chem. Soc.* **1942**, *64*, 176.
130. Weizmann, CH.; Bergmann, E.; Haskelberg, L. *J. Chem. Soc.* **1939**, 391.
131. Chardonens, L.; Bitsch, S. *Helv. Chim. Acta* **1972**, *55*, 1345.
132. Yang, C.-f.; Zhu, J.-l. *Huaxue Shijie* **2000**, *41*, 426.

133. Murakoka, O.; Tanabe, G.; Yamamoto, E.; Ono, M.; Minematsu, T.; Kimura, T. *J. Chem. Soc., Perkin Trans. 1* **1997**, 2879.
134. Keay, B. A.; Rodrigo, R. *Can. J. Chem.* **1985**, 63, 735.
135. Smith, J. G.; Deryn, E. F.; Munday, I. J.; Sandborn, R. E.; Dibble, P. W. *J. Org. Chem.* **1988**, 53, 2942.
136. Mir-Mohamad-Sadeghy, B.; Rickborn, B. *J. Org. Chem.* **1983**, 48, 2237.
137. Fier, S.; Sullivan, R. W.; Rickborn, B. *J. Org. Chem.* **1988**, 53, 2353.
138. Wiersum, U. E.; Mijs, W. J. *J. Chem. Soc., Chem. Commun.* **1972**, 347.
139. Halton, B.; Evans, D. A.; Warrenner, R. N. *Aust. J. Chem.* **1999**, 52, 1123.
140. Dufraisse, C.; Gigaudy, J.; Ricard, M. *Tetrahedron Suppl.* **1966**, 8 (Part II), 491.
141. (a) Cava, M. P.; VanMeter, J. P. *J. Am. Chem. Soc.* **1962**, 84, 2008; (b) *ibid. J. Org. Chem.* **1969**, 34, 538.
142. (a) Yick, C.-Y.; Chan, S.-H.; Wong, H. N. C. *Tetrahedron Lett.* **2000**, 41, 5957; (b) *ibid. Tetrahedron* **2002**, 58, 9413.
143. Athans, A. J.; Briggs, J. B.; Jia, W.; Miller, G. P. *J. Mater. Chem.* **2007**, 17, 2636.
144. Mondal, R.; Shah, B. K.; Neckers, D. C. *J. Org. Chem.* **2006**, 71, 4085.
145. The reaction was run separately in ethanol, alcohol, and benzene. The endo,exo *syn* product invariably precipitates from each of these solutions in high yields. See ref 115.
146. (a) Desiraju, G. R. *Chem. Commun.* **2005**, 2995; (b) *ibid. Acc. Chem. Res.* **2002**, 35, 565.
147. M. Nishio, M. Hirota and Y. Umezawa, *The CH/ $\pi$  Interaction: Evidence, Nature, and Consequences*, Wiley-VCH, New York, 1998.
148. Tamres, M. *J. Am. Chem. Soc.* **1952**, 74, 3375
149. Shibasaki, K.; Fujii, A.; Mikami, N.; Tsuzuki, S. *J. Phys. Chem. A* **2006**, 110, 4397.
150. Cox, E. G.; Cruickshank, D. W. J.; Smith, J. A. S. *Proc. Roy. Soc.* **1958**, A247, 1.
151. Reeves, L. W.; Schneider, W. G. *Can. J. Chem.* **1957**, 35, 251.



152. Nakagawa, N.; Fujiwara, S. *Bull. Chem. Soc. Jpn.* **1961**, *34*, 143.
153. Suezawa, H.; Yoshida, T.; Ishihara, S.; Umezawa, Y.; Nishio, M. *Cryst. Eng. Comm.*, **2003**, *5*, 514.
154. Olmstead, M. M.; Costa, D. A.; Maitra, K.; Noll, B. C.; Phillips, S. L.; van Calcar, P. M.; Balch, A. L. *J. Am. Chem. Soc.* **1999**, *121*, 7090.
155. (a) Meek, J. S.; Dewey, F. M.; Hanna, M. W. *J. Org. Chem.* **1967**, *32*, 69; (b) Meek, J. S.; Dewey, F. M. *J. Org. Chem.* **1970**, *35*, 1315.
156. (a) Allen, C. F. H.; Bell, A. *J. Am. Chem. Soc.* **1942**, *64*, 1253; (b) Gillet, I. *Bull. Soc. Chim. Fr.* **1950**, 1134.
157. (a) Hammam, A. S.; Hassan, M. A.; Fandy, R. F. *AFINIDAD* **2003**, *503*, 42; (b) Zhou, X.; Kitamura, M.; Shen, B.; Nakajima, K.; Takahashi, T. *Chem. Lett.* **2004**, *33*, 410.
158. Diels, O.; Alder, K. *Chem. Ber.* **1929**, *62*, 2081.
159. Smith, J. G.; Wikman, R. T. *Tetrahedron* **1974**, *30*, 2603.

# Miller Group 3

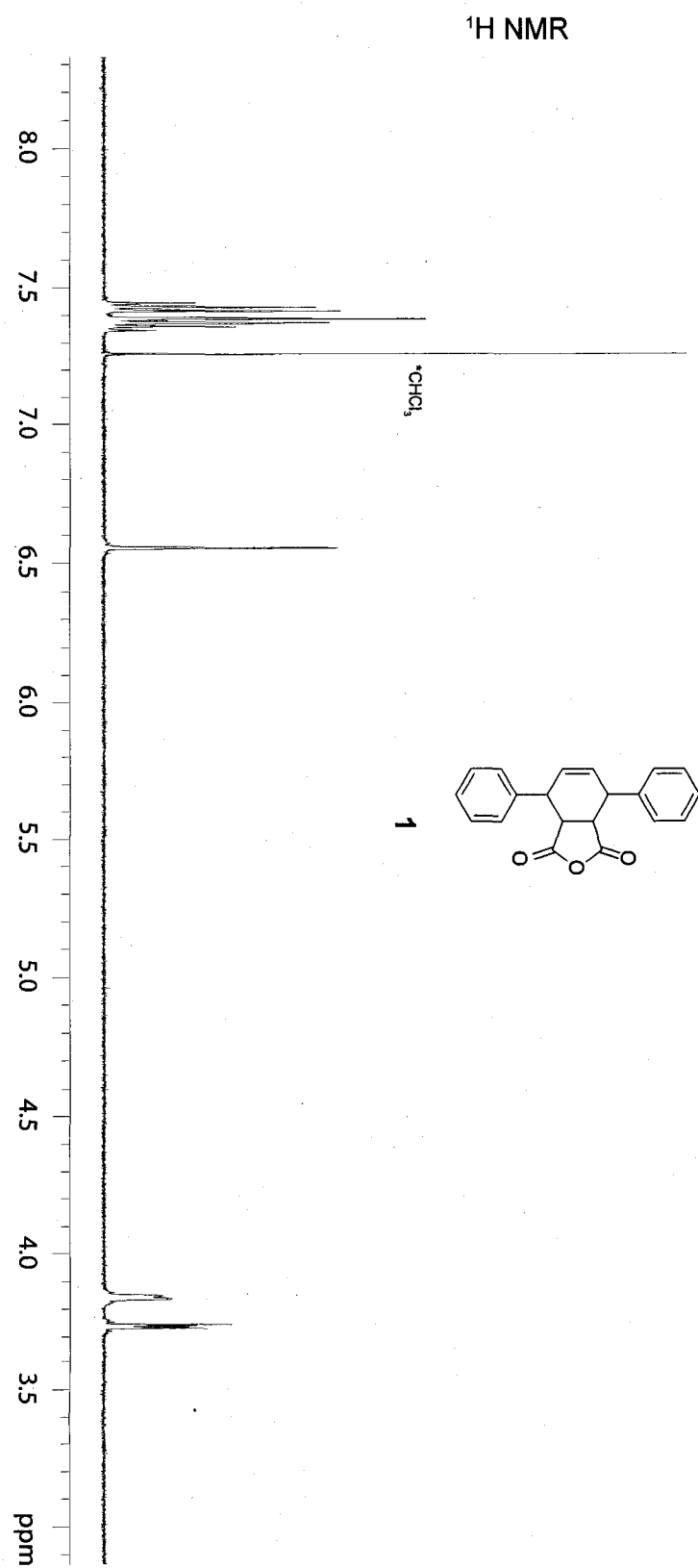
 Appendix5.pdf

 12/04/07 15:29

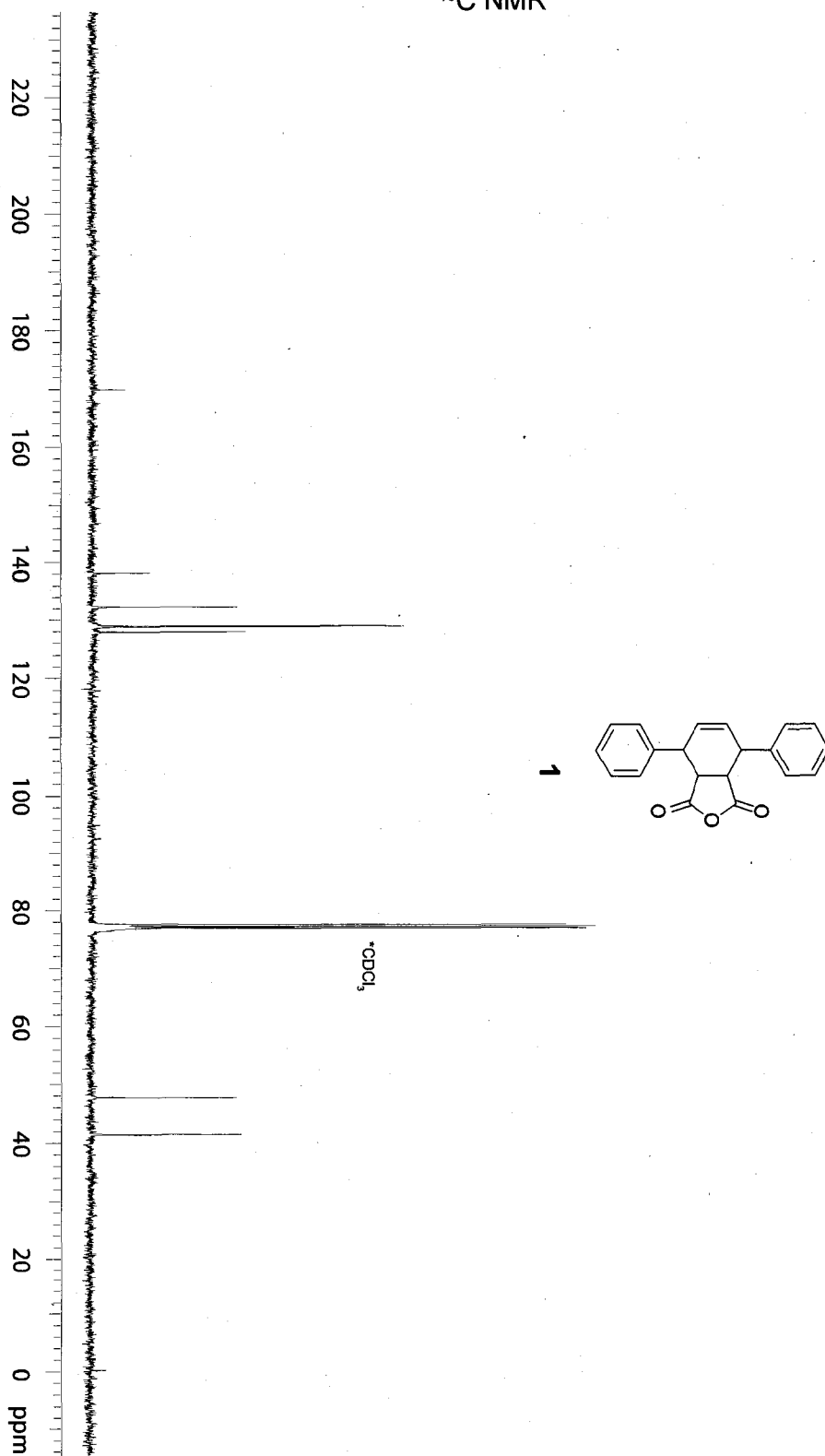


## APPENDIX

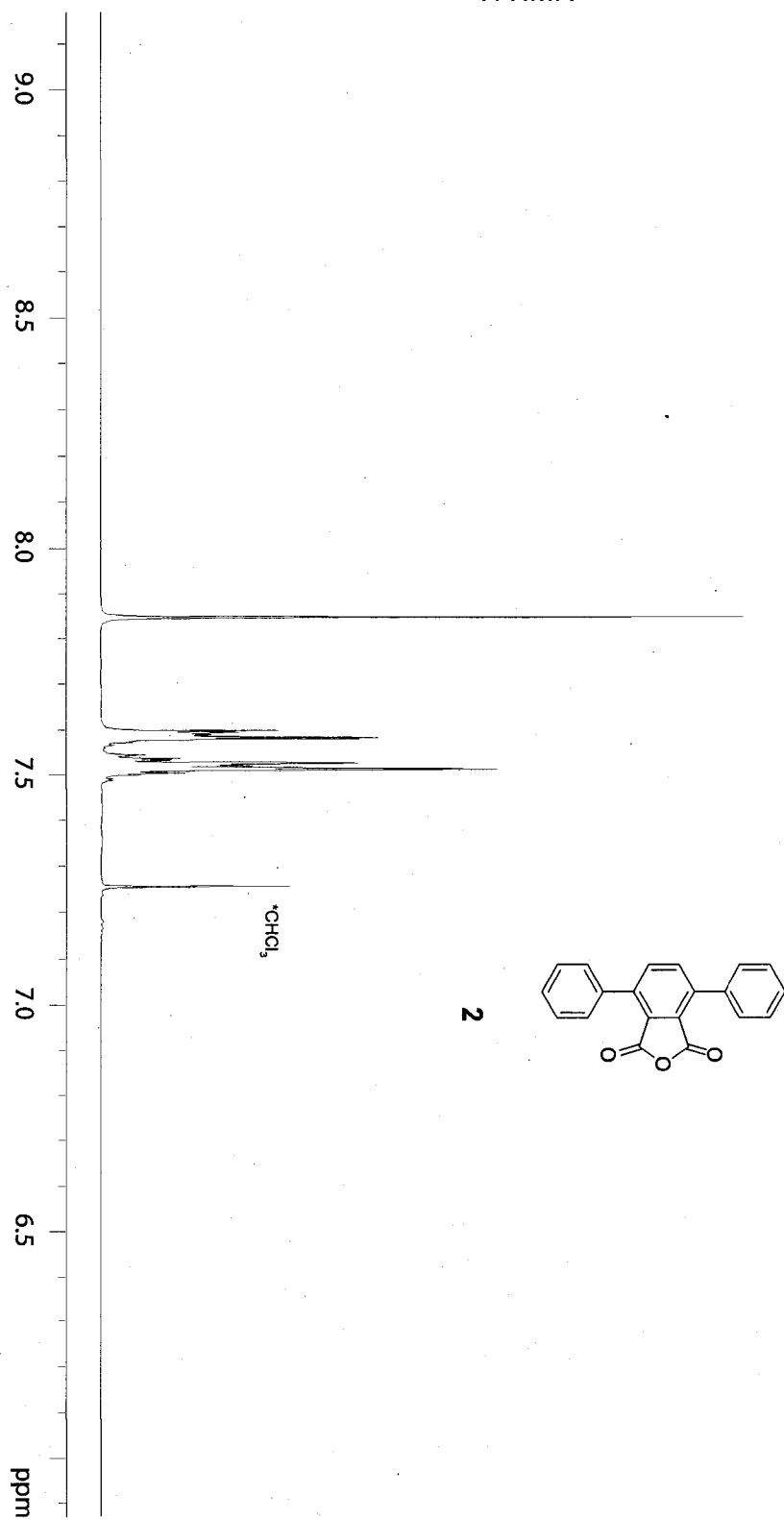
### NMR SPECTRA



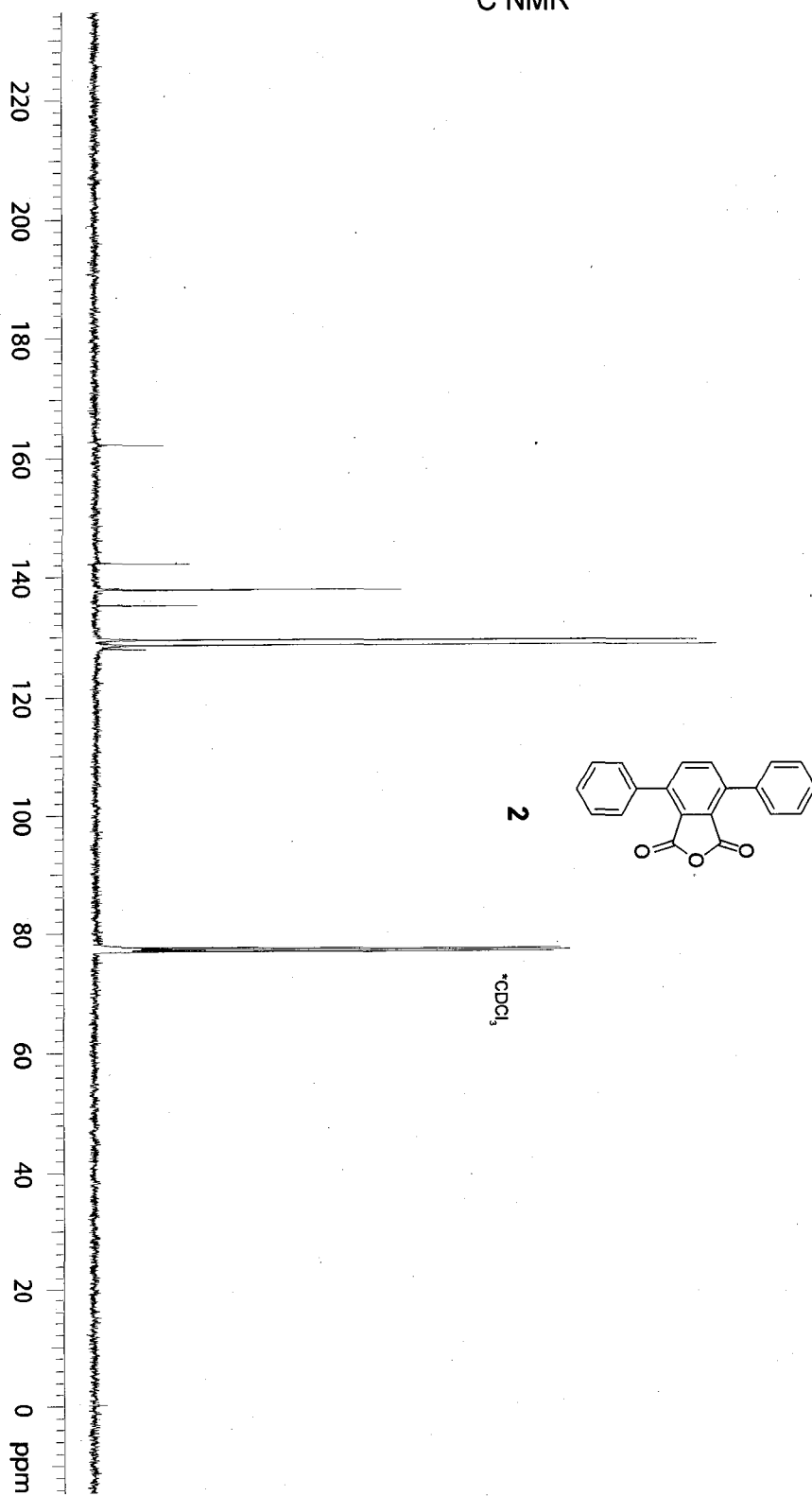
<sup>13</sup>C NMR



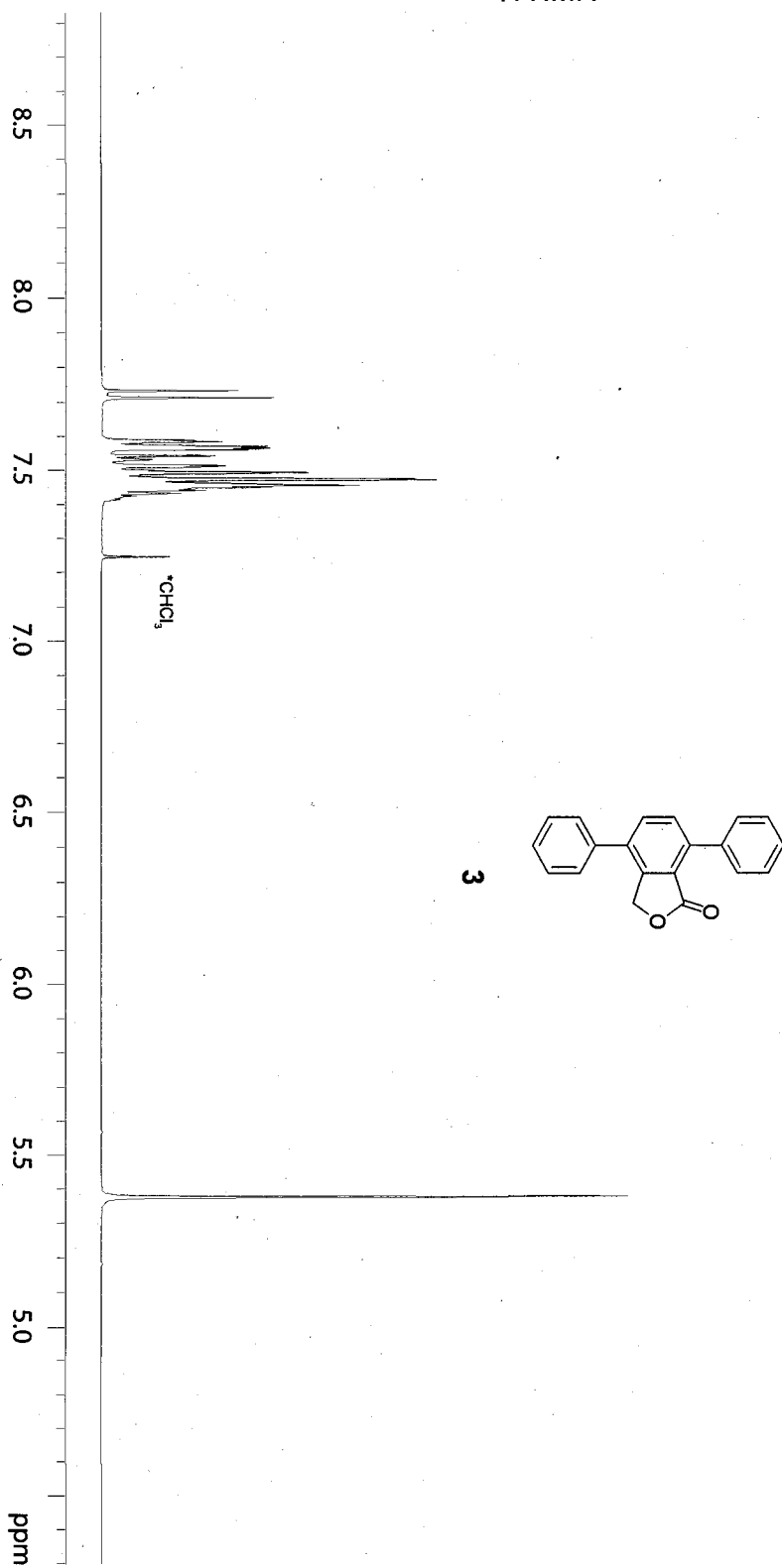
<sup>1</sup>H NMR



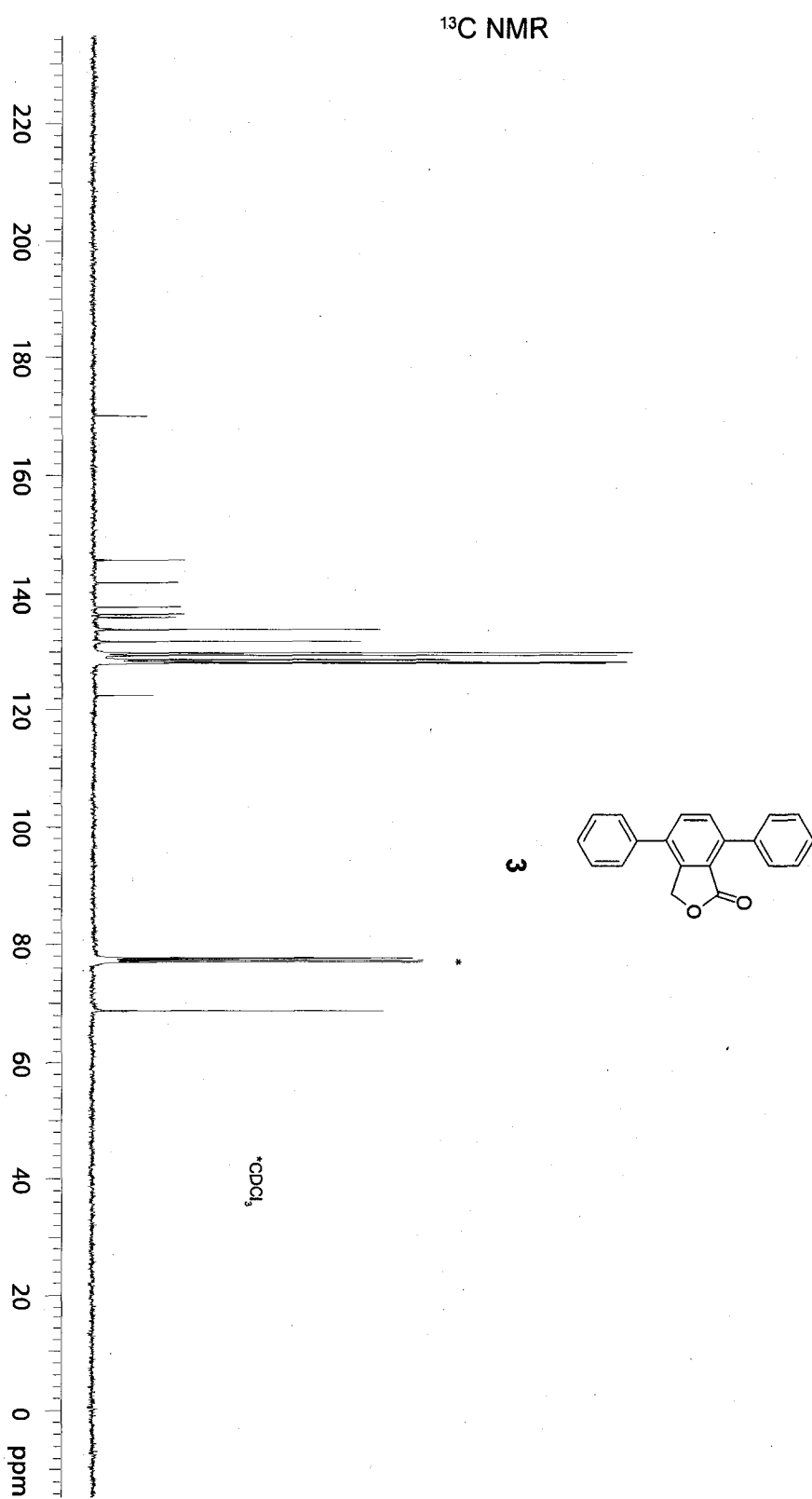
<sup>13</sup>C NMR



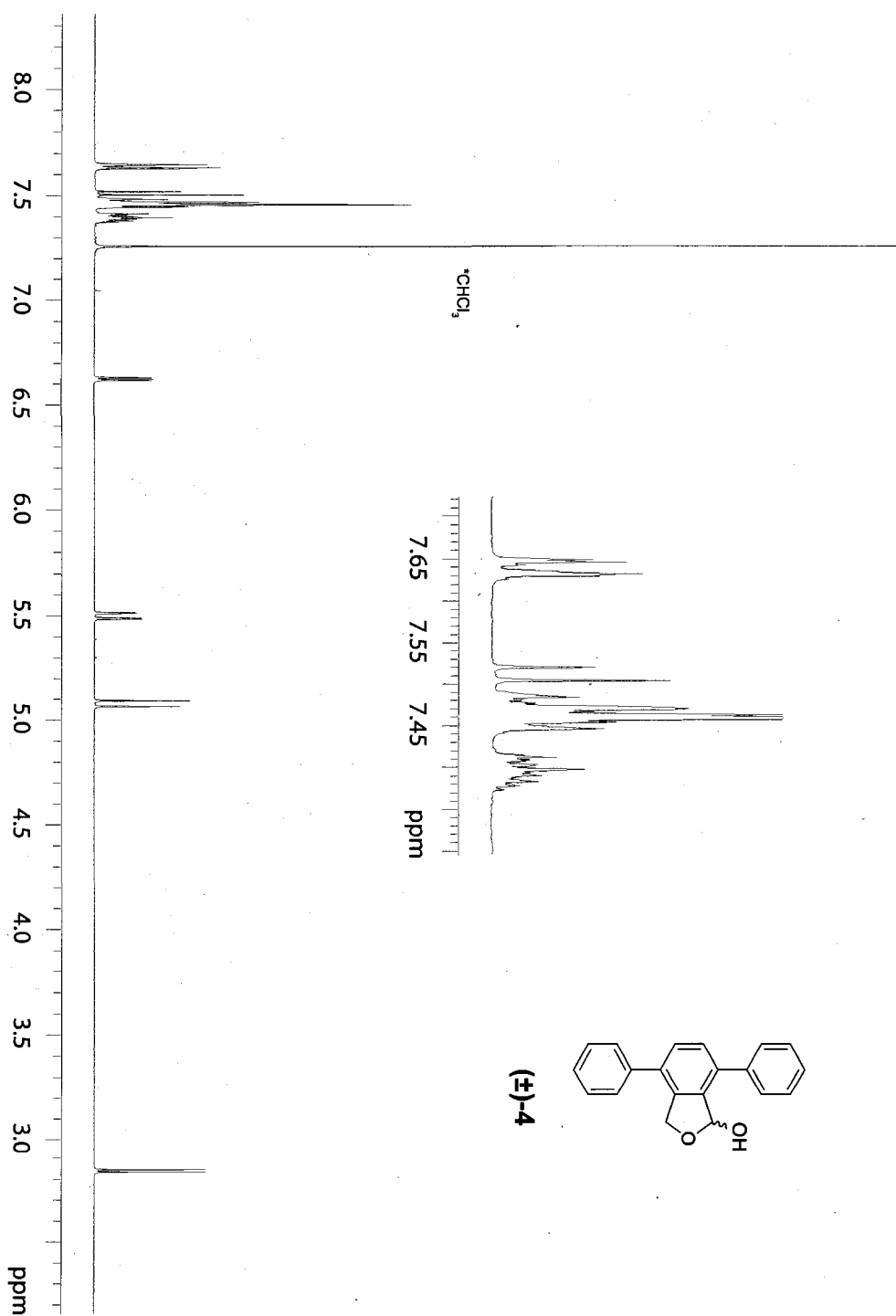
<sup>1</sup>H NMR



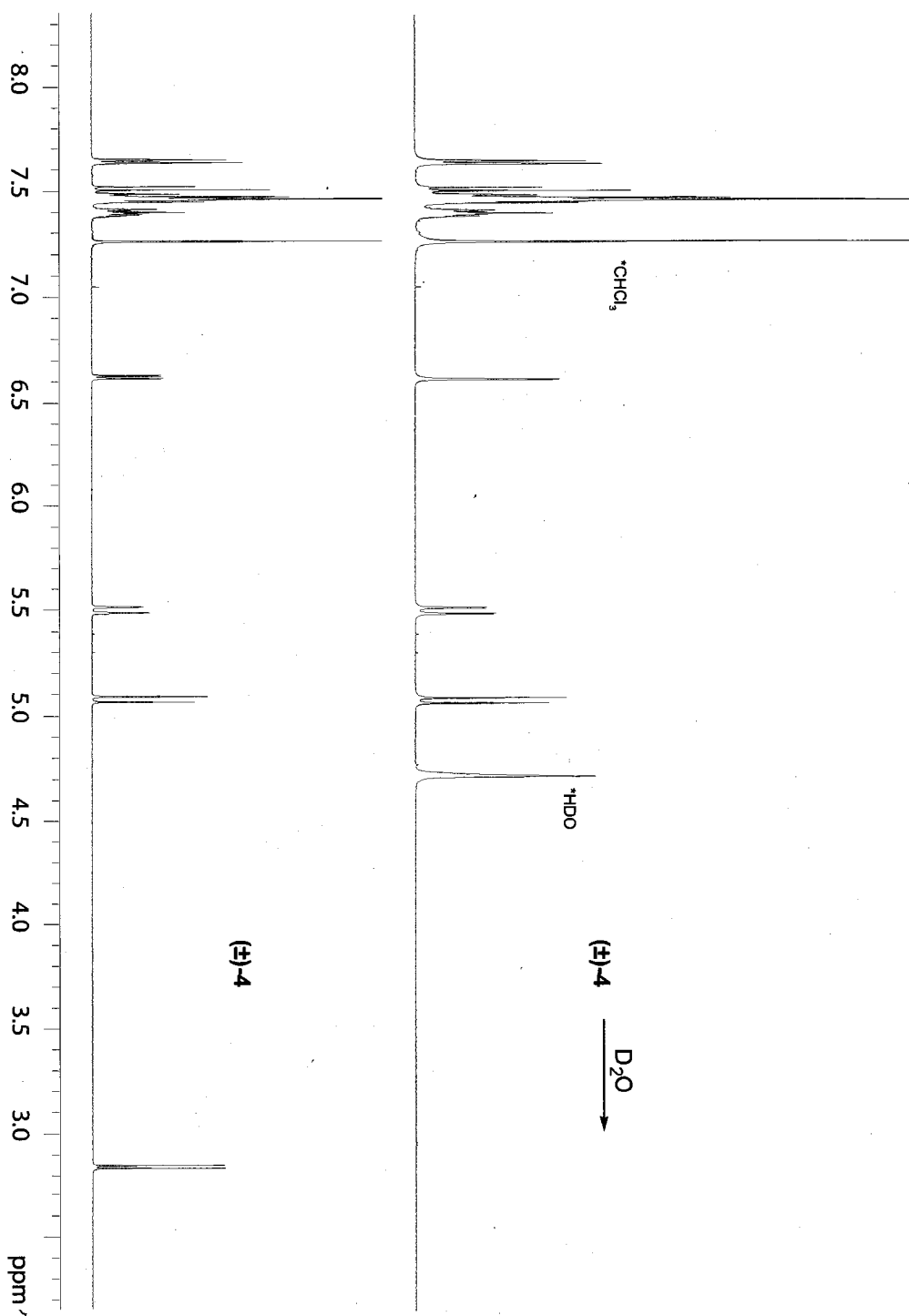




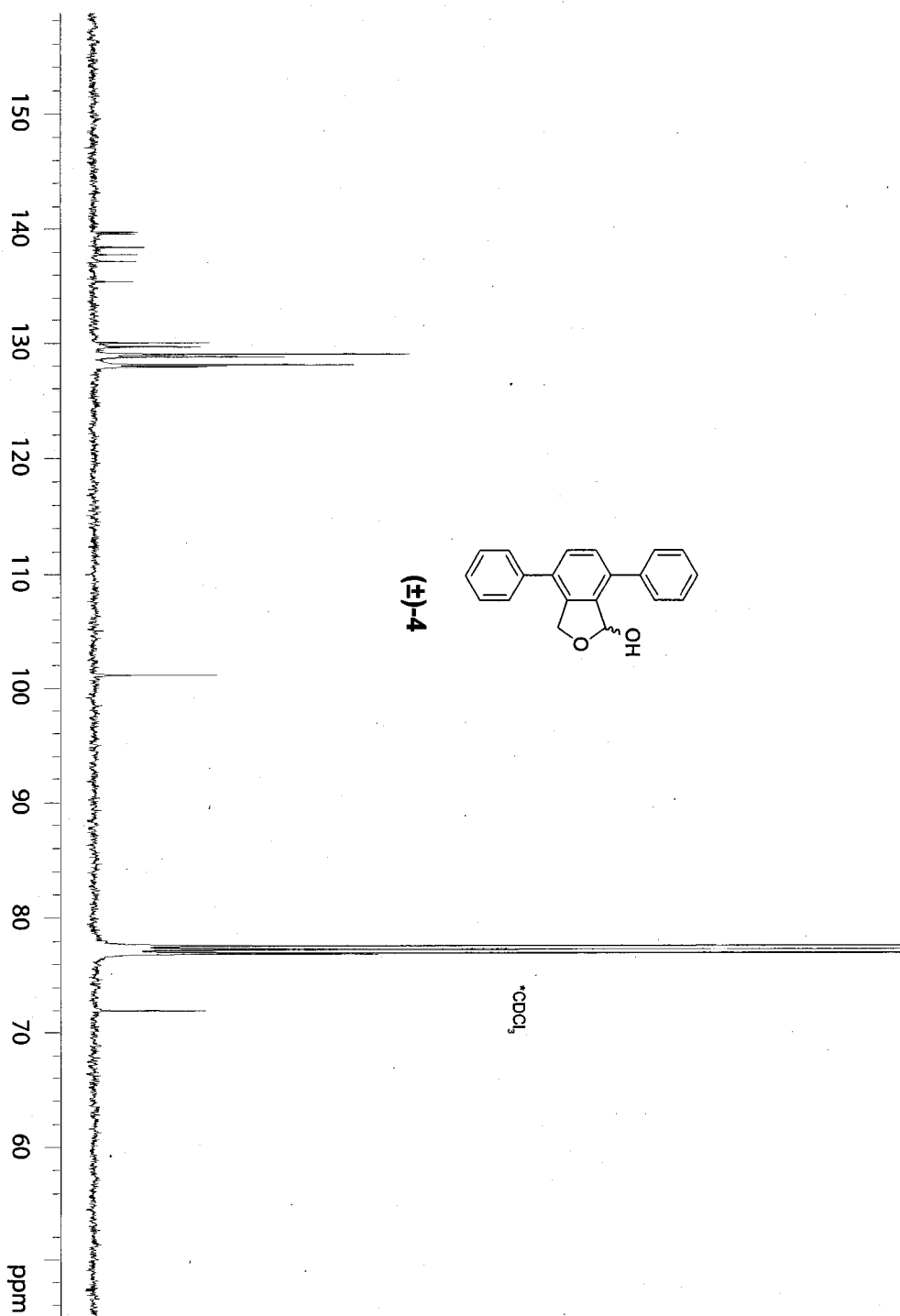
<sup>1</sup>H NMR



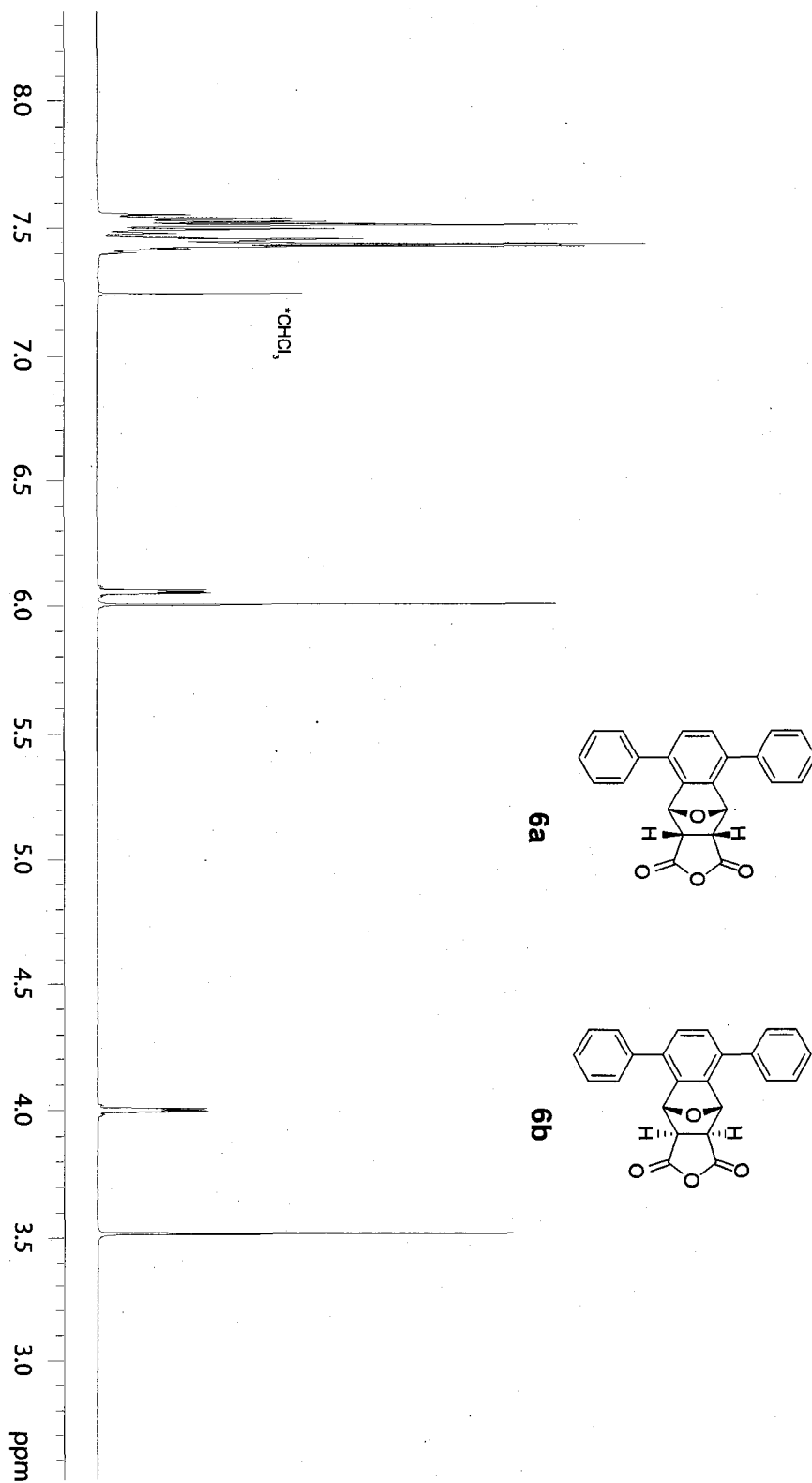
$^1\text{H}$  NMR

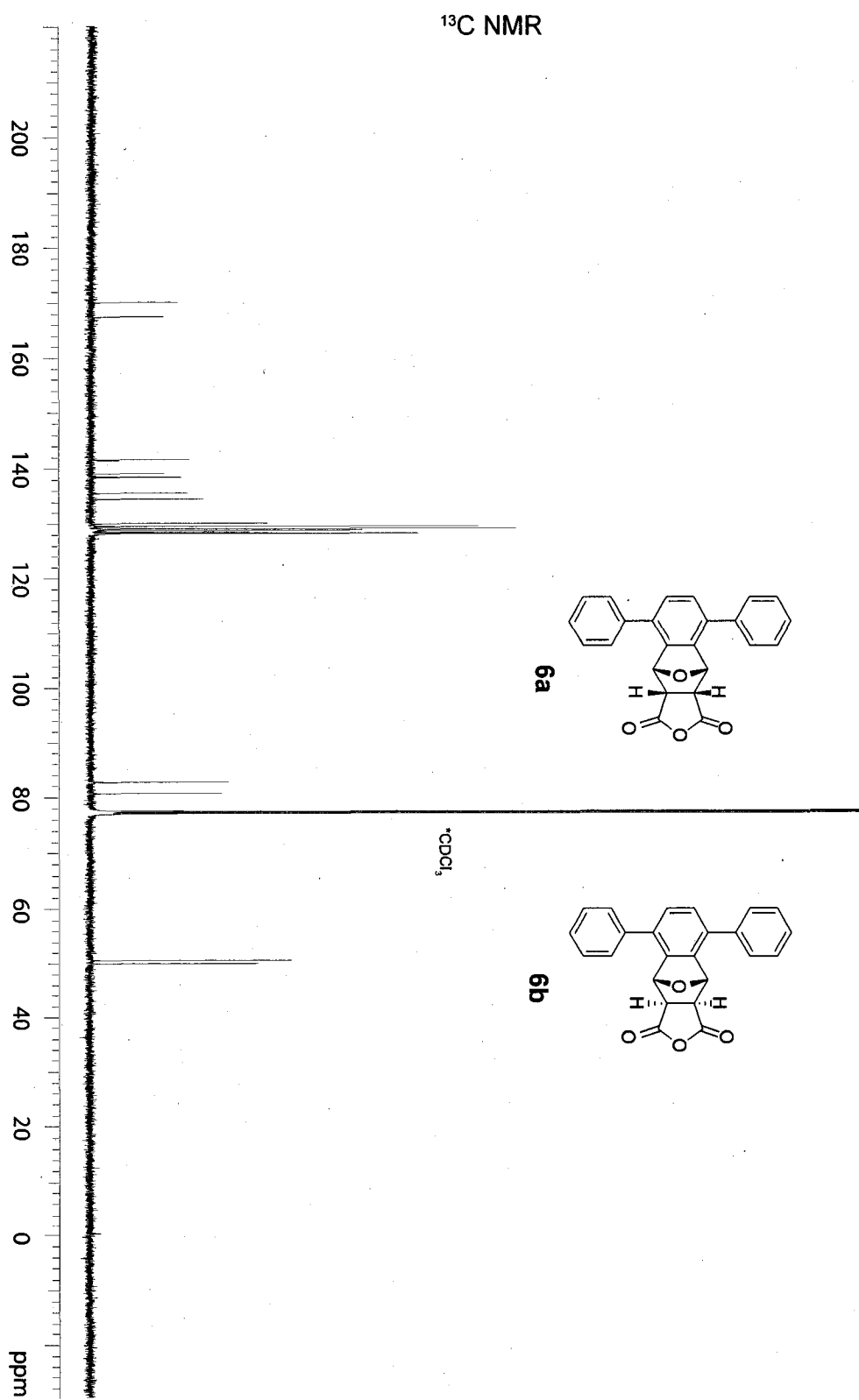


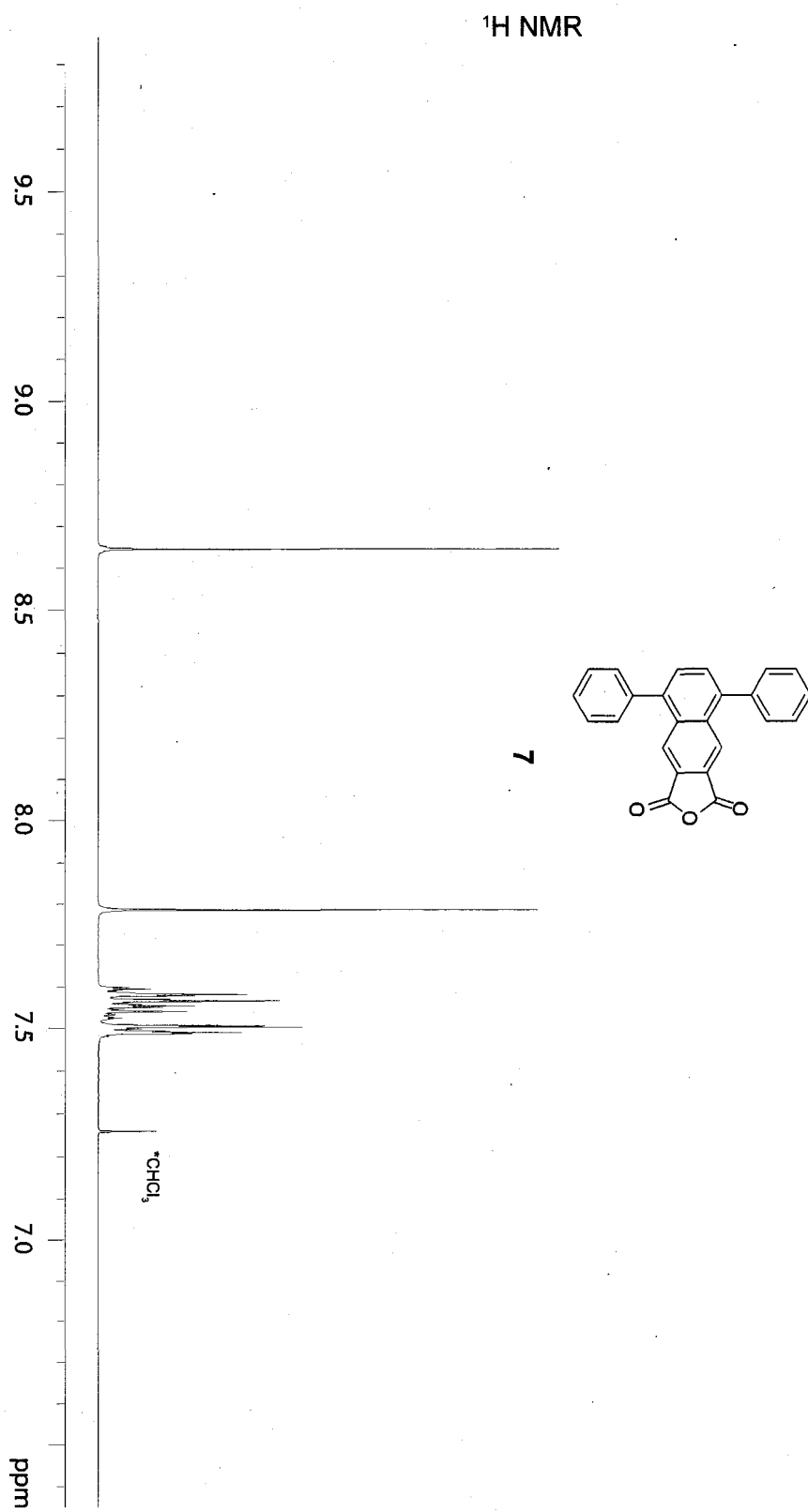
<sup>13</sup>C NMR



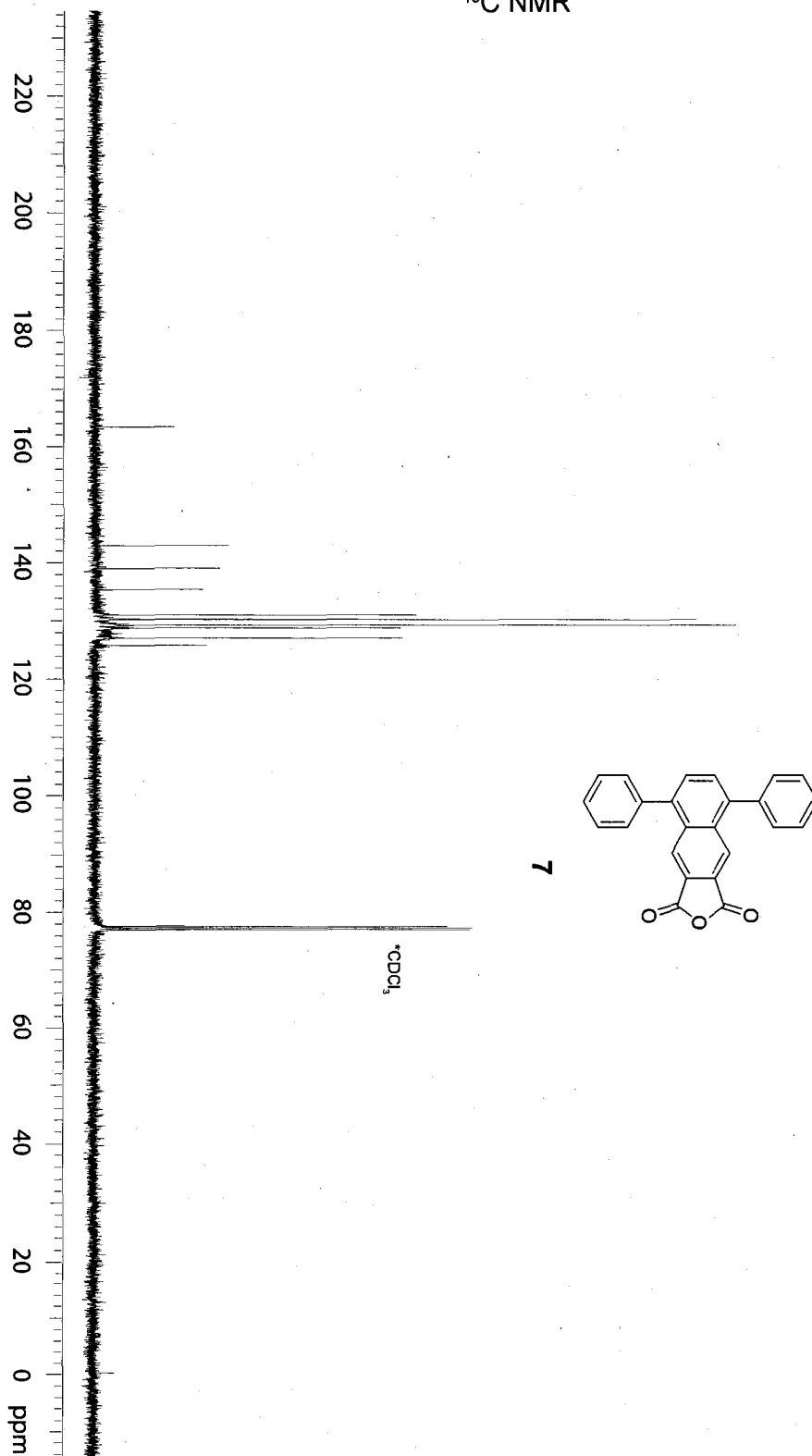
<sup>1</sup>H NMR





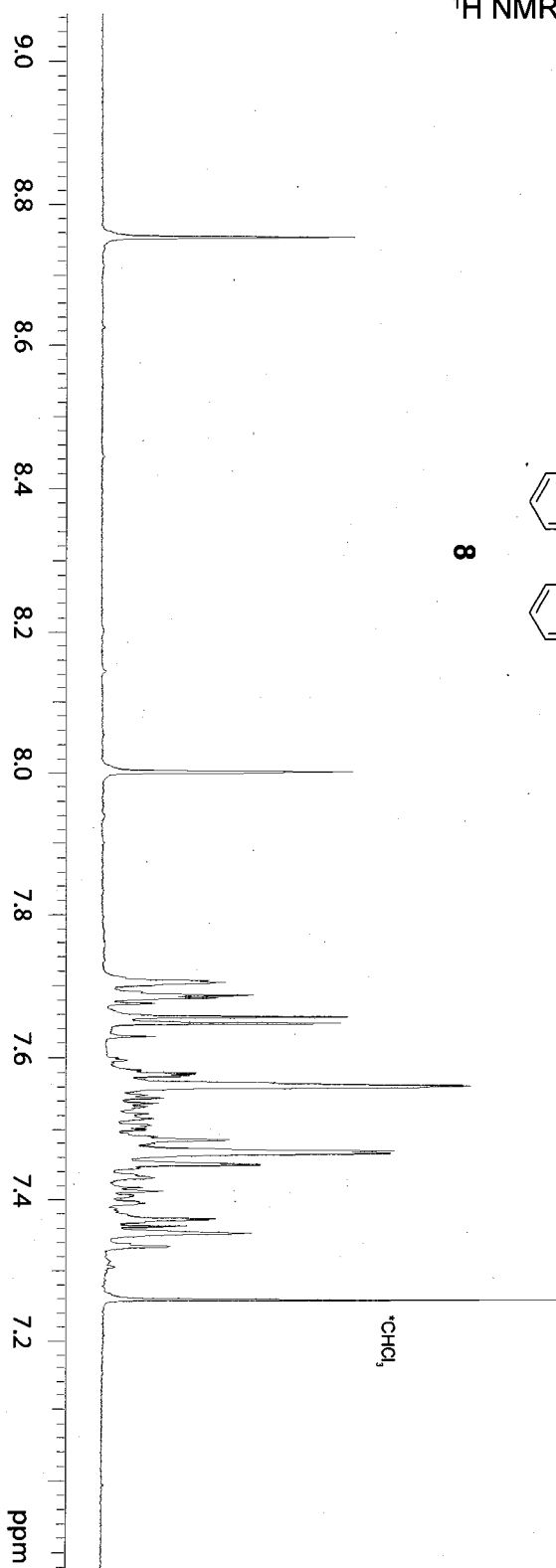


<sup>13</sup>C NMR

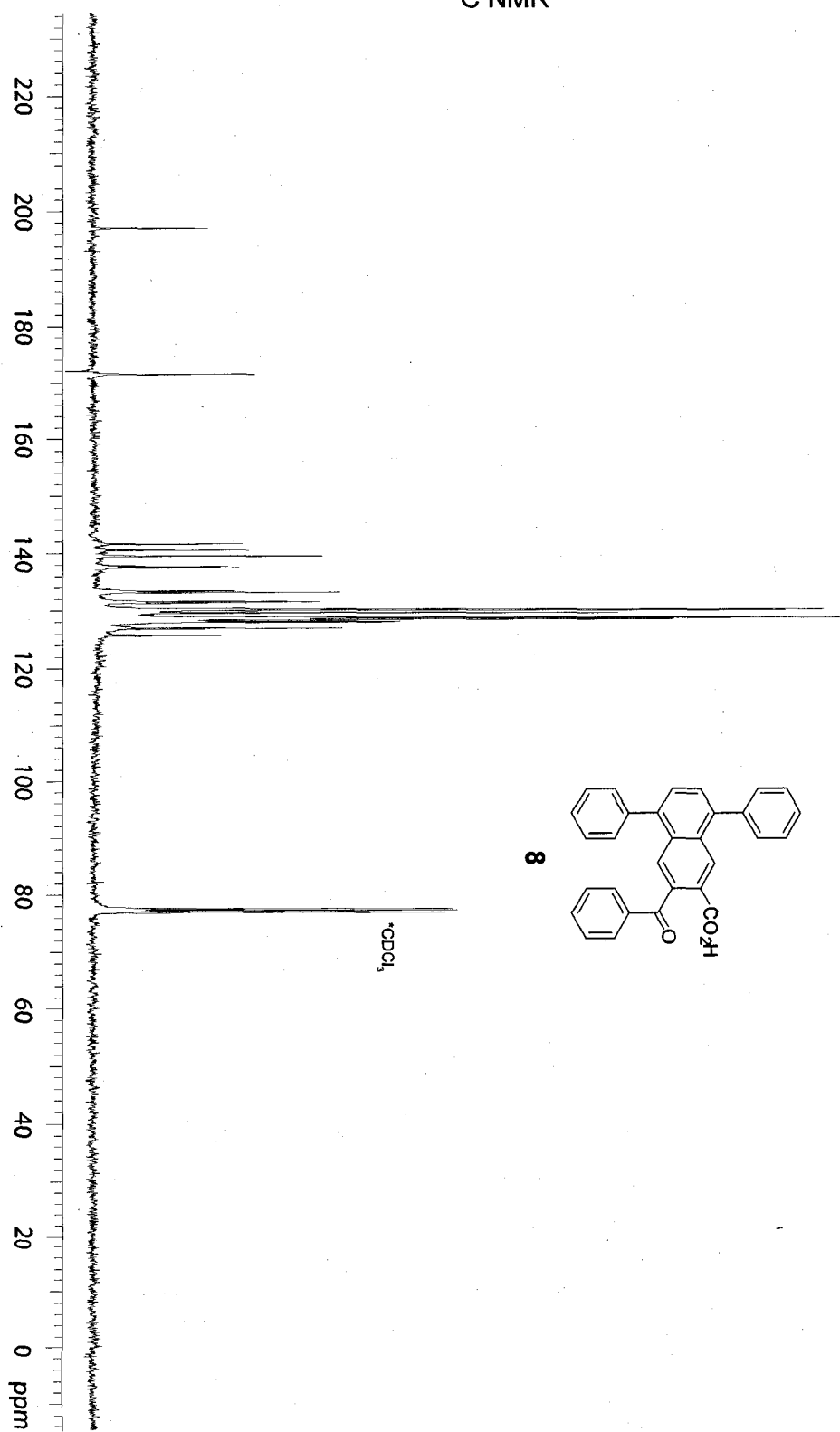


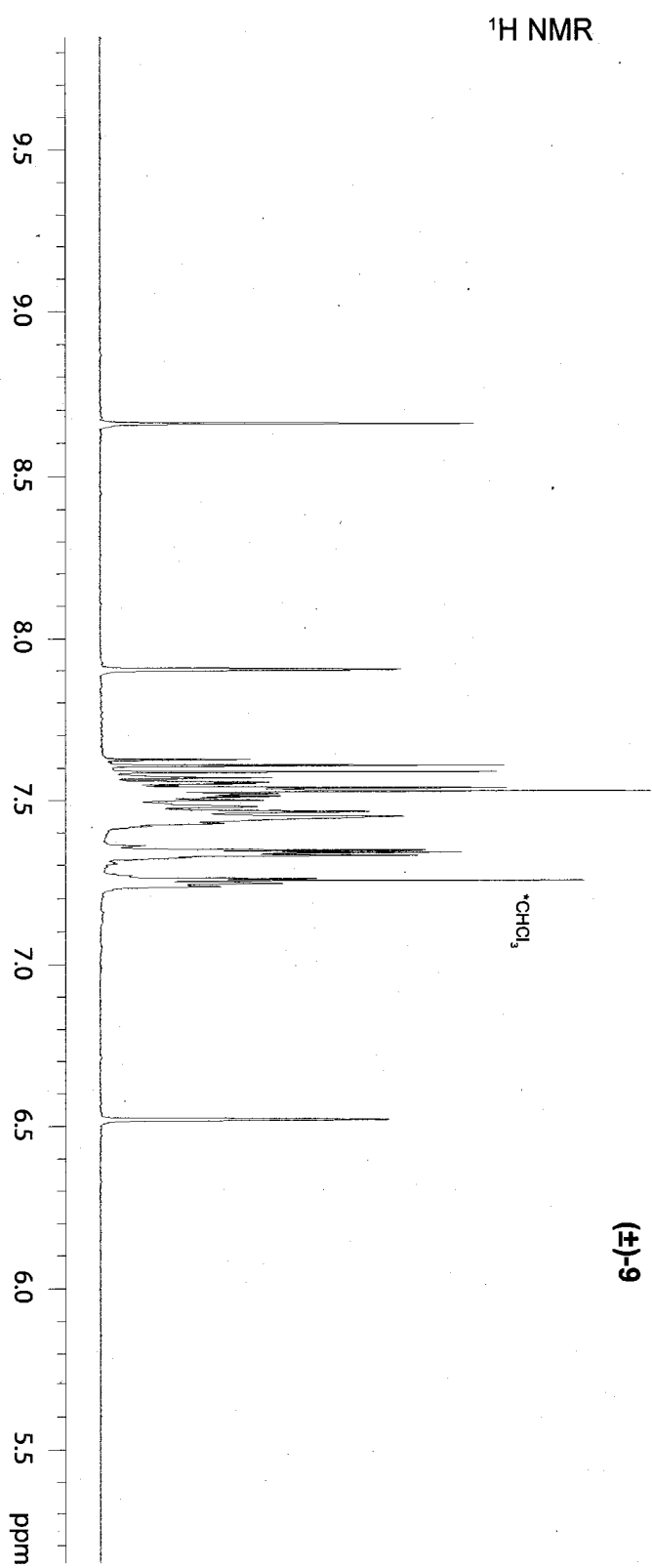


<sup>1</sup>H NMR

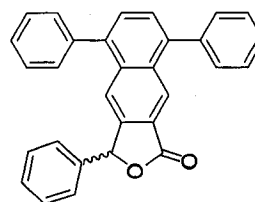


<sup>13</sup>C NMR

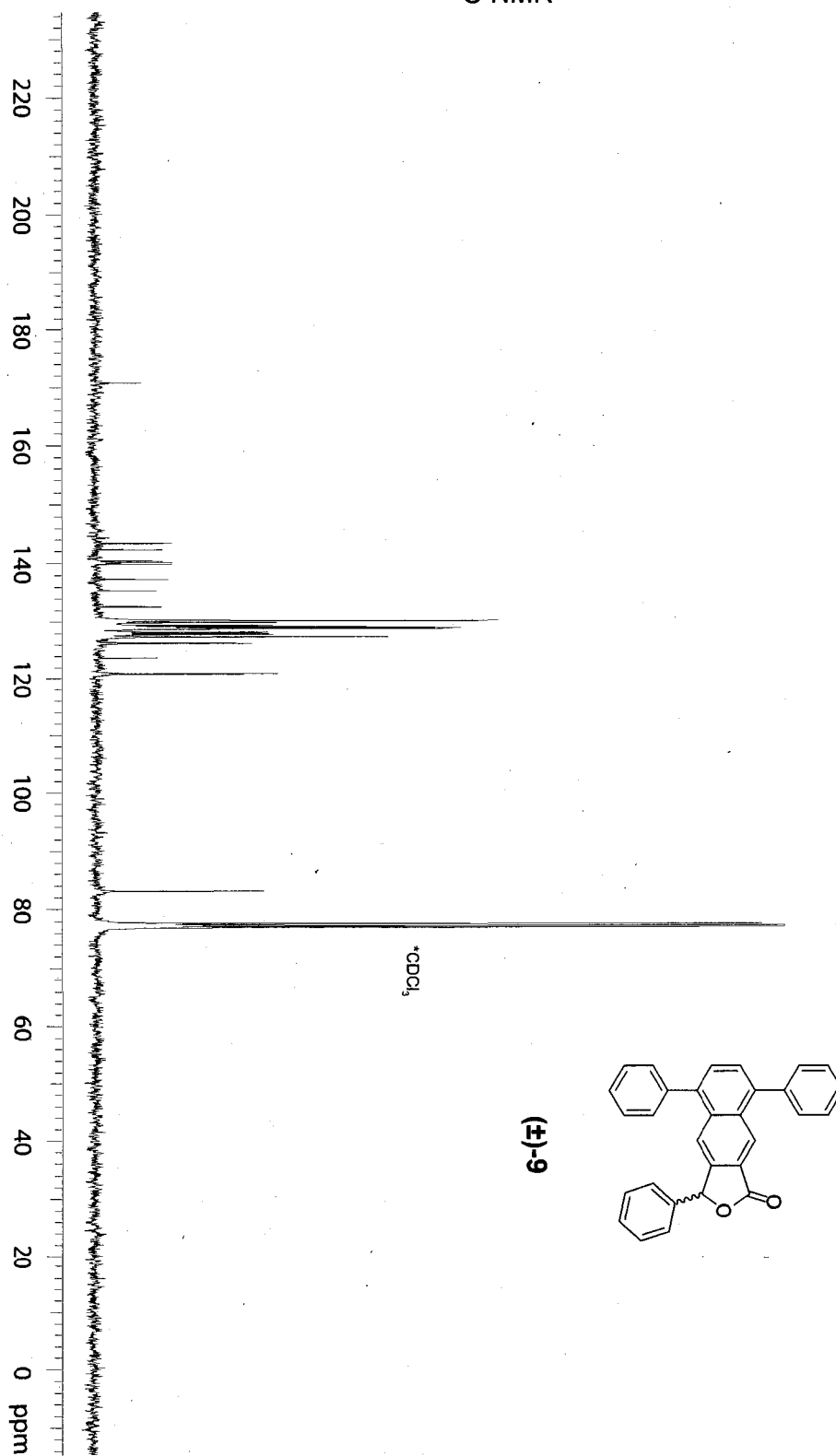


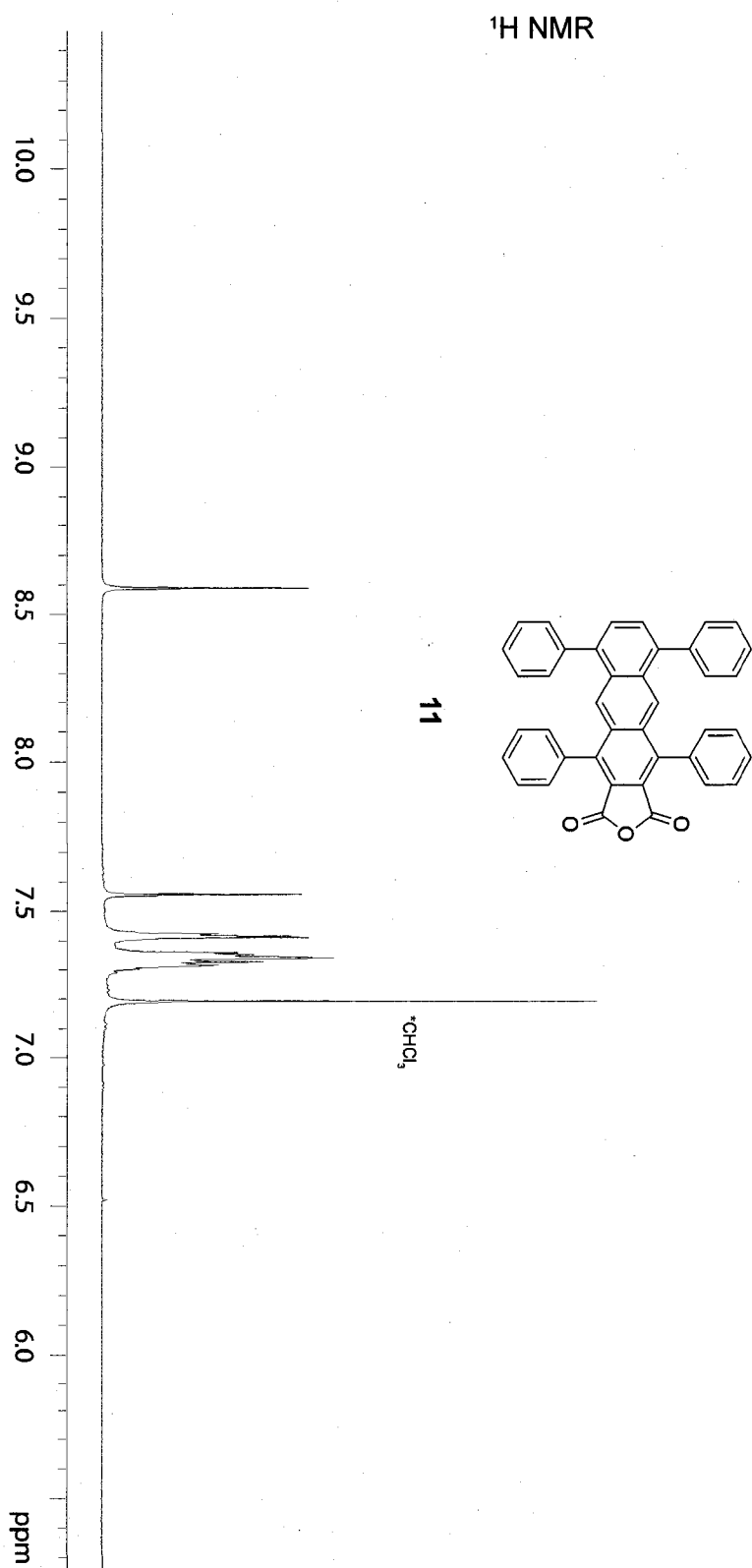


(±)-9

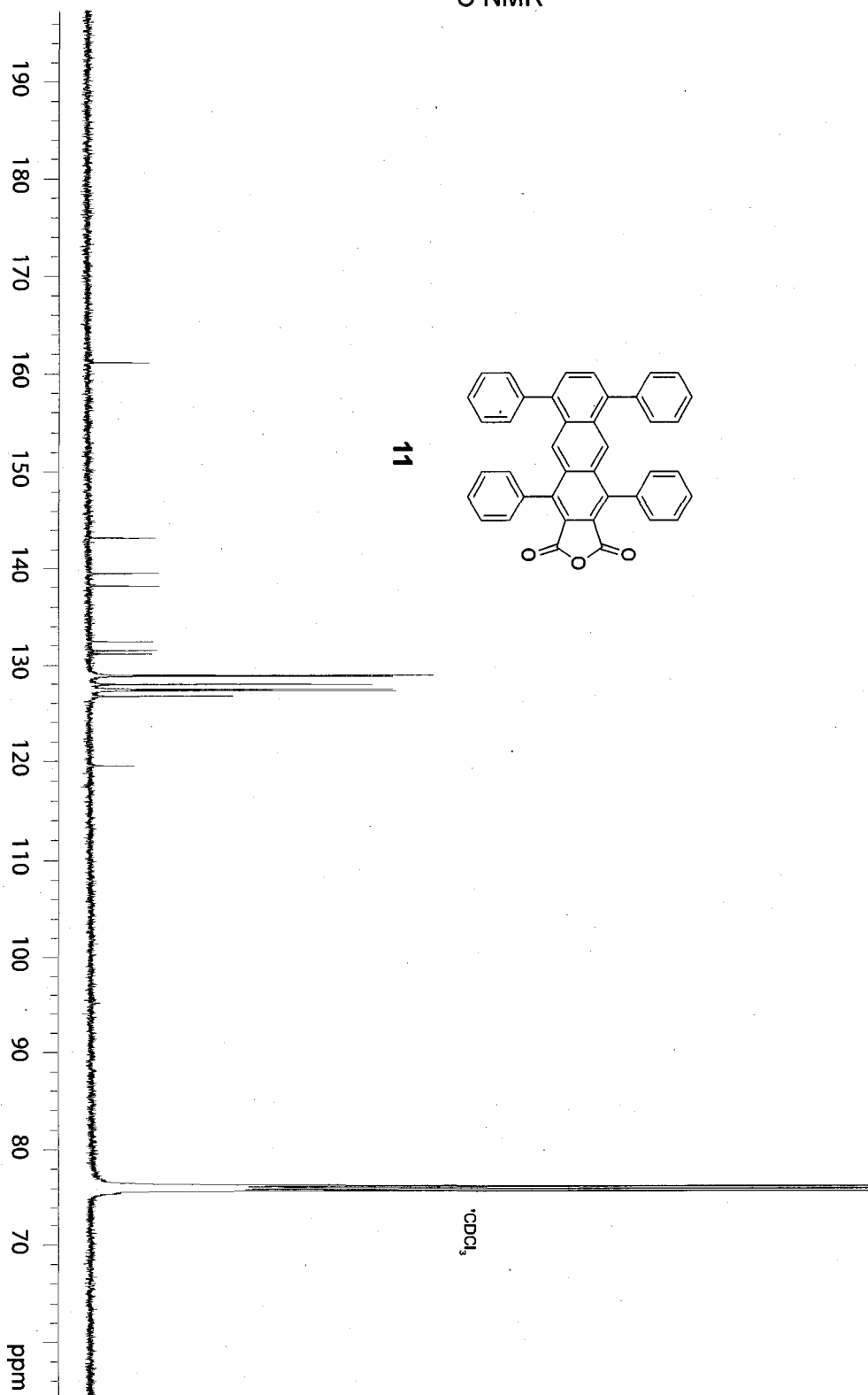


<sup>13</sup>C NMR

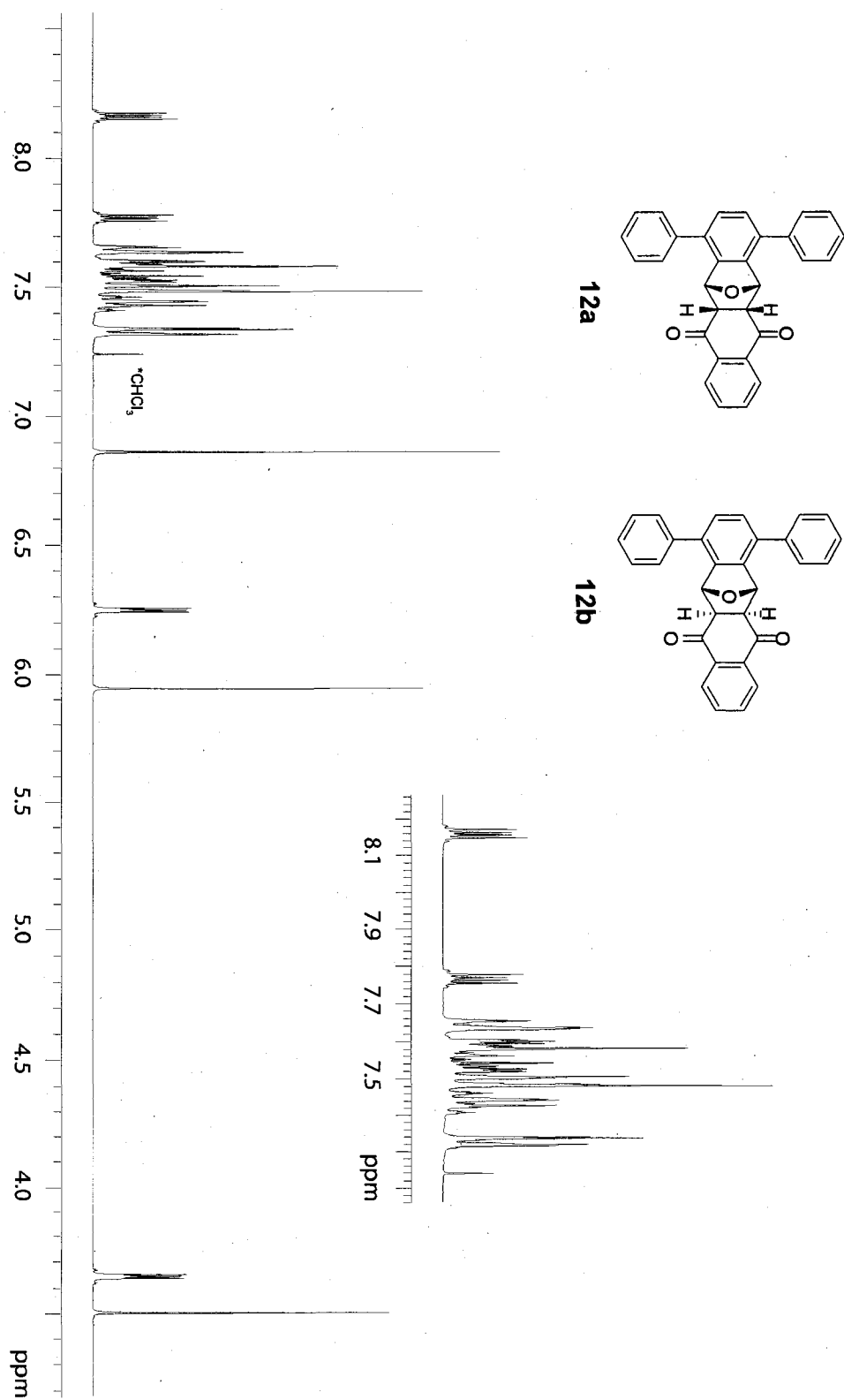


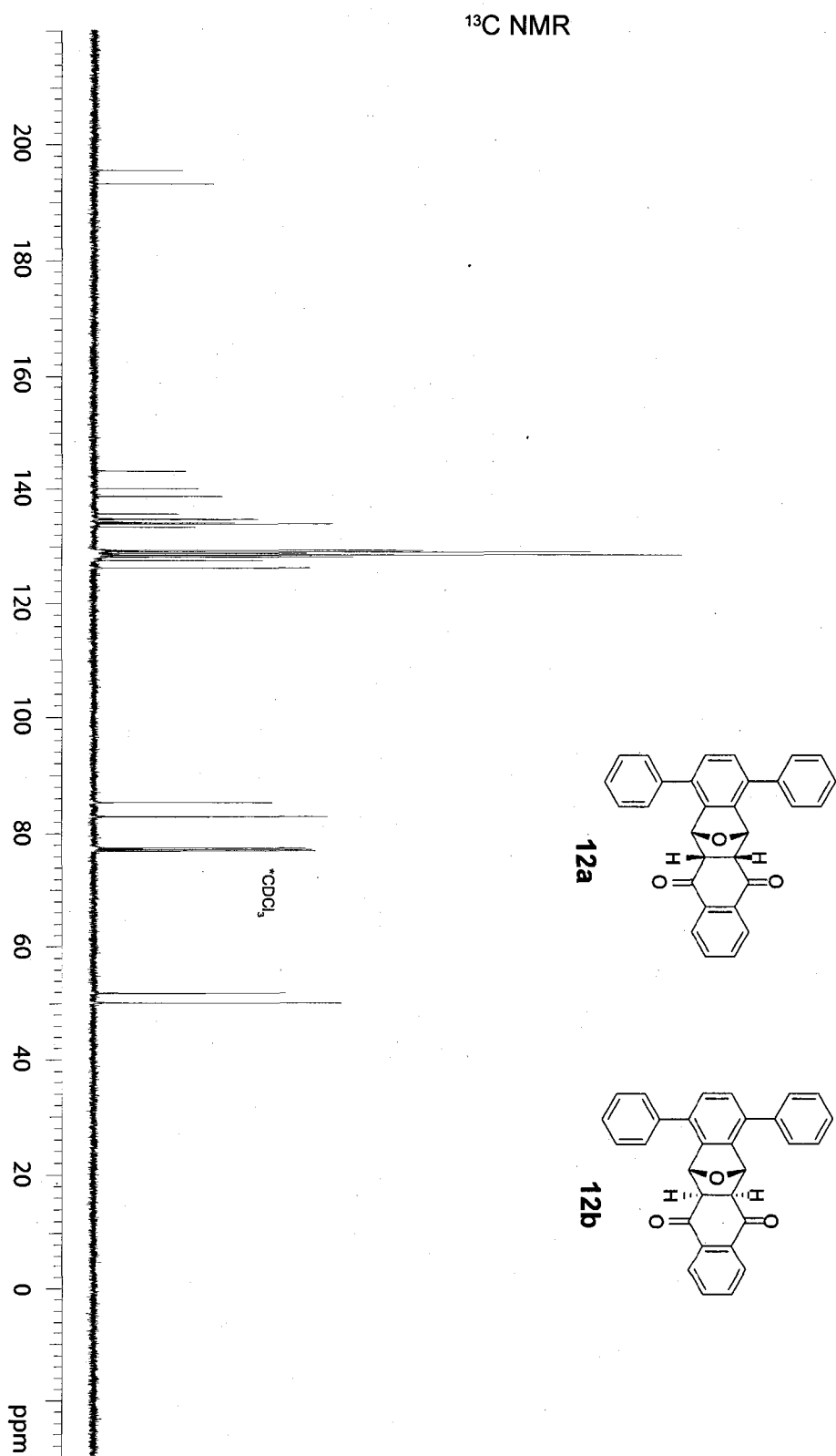


<sup>13</sup>C NMR



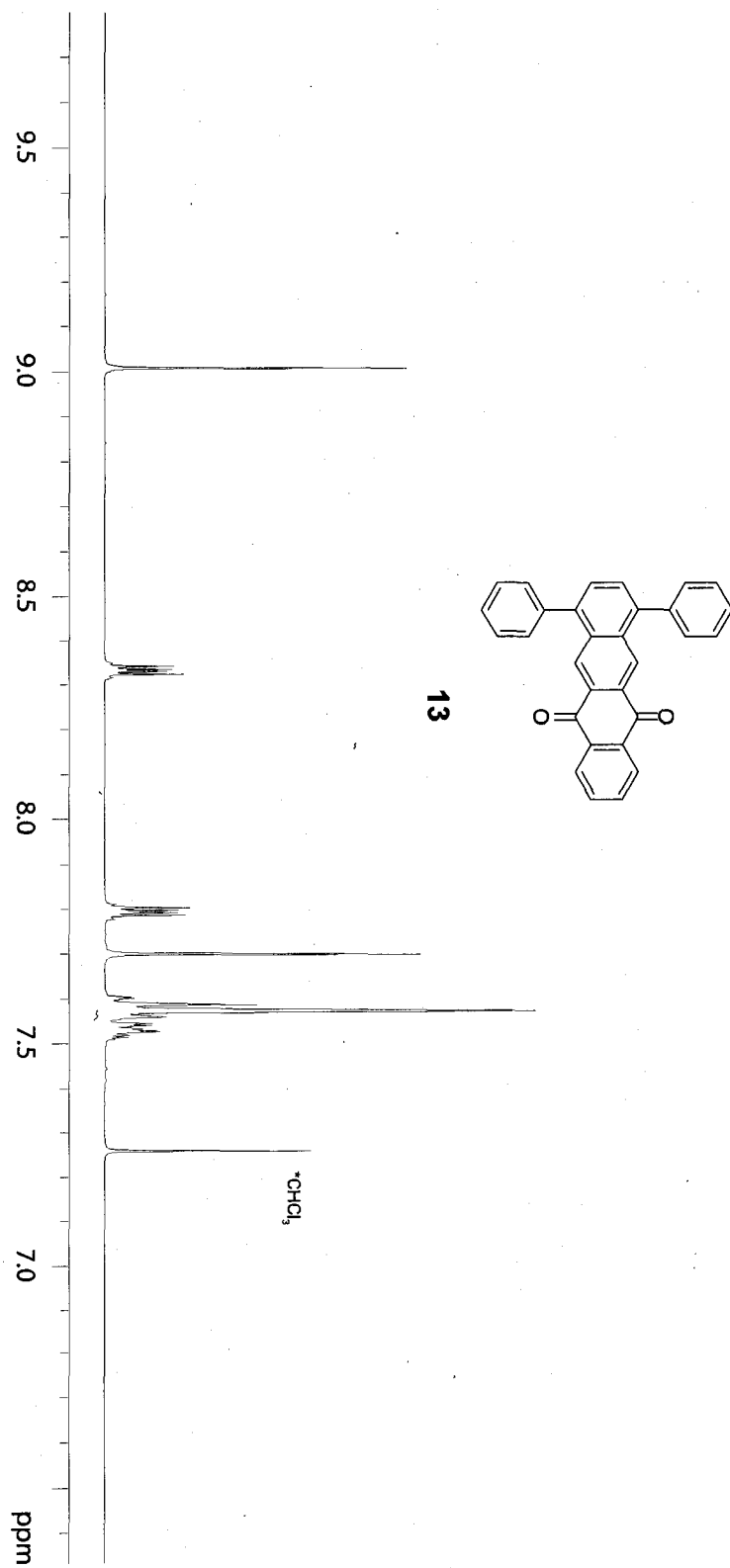
<sup>1</sup>H NMR

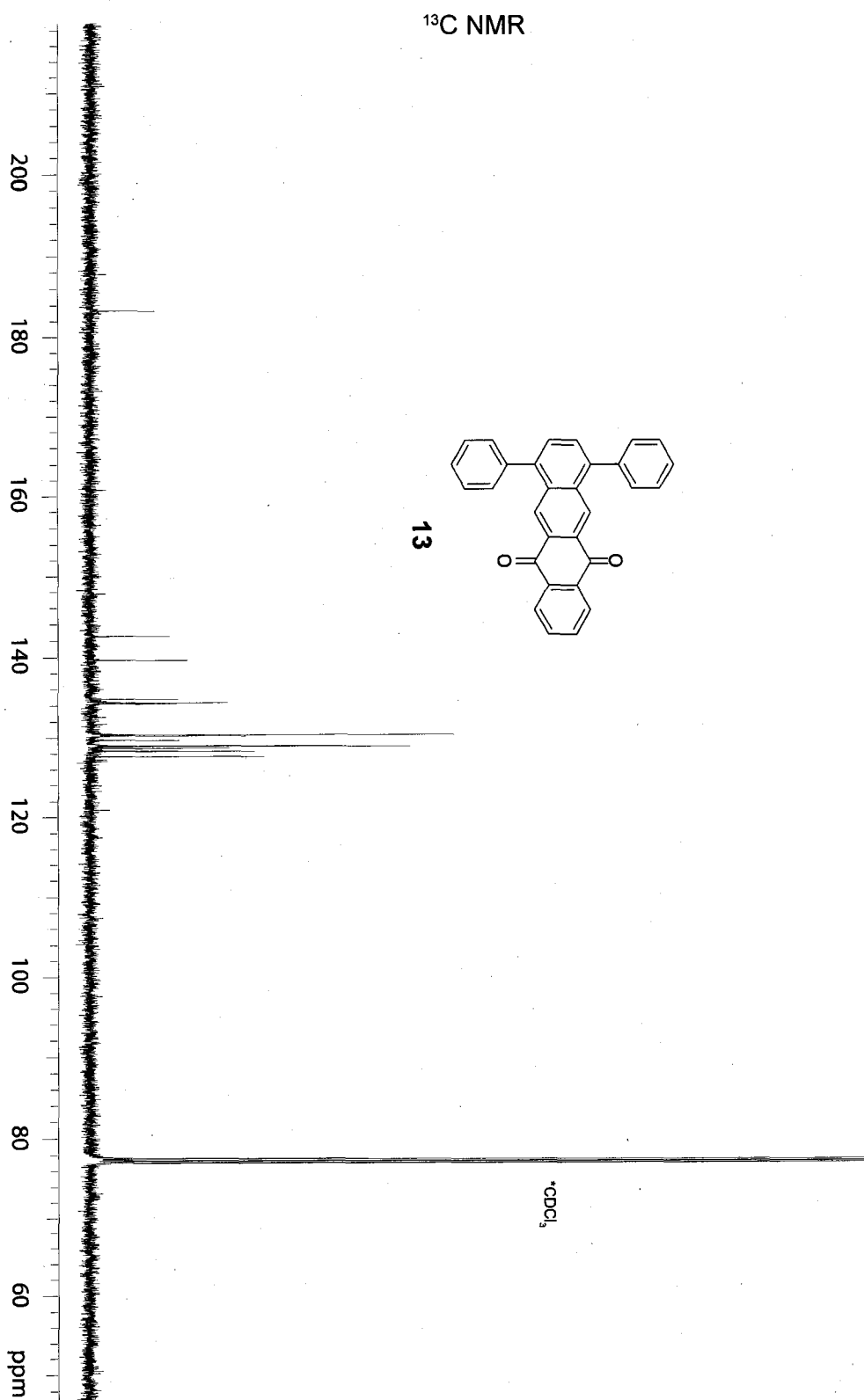


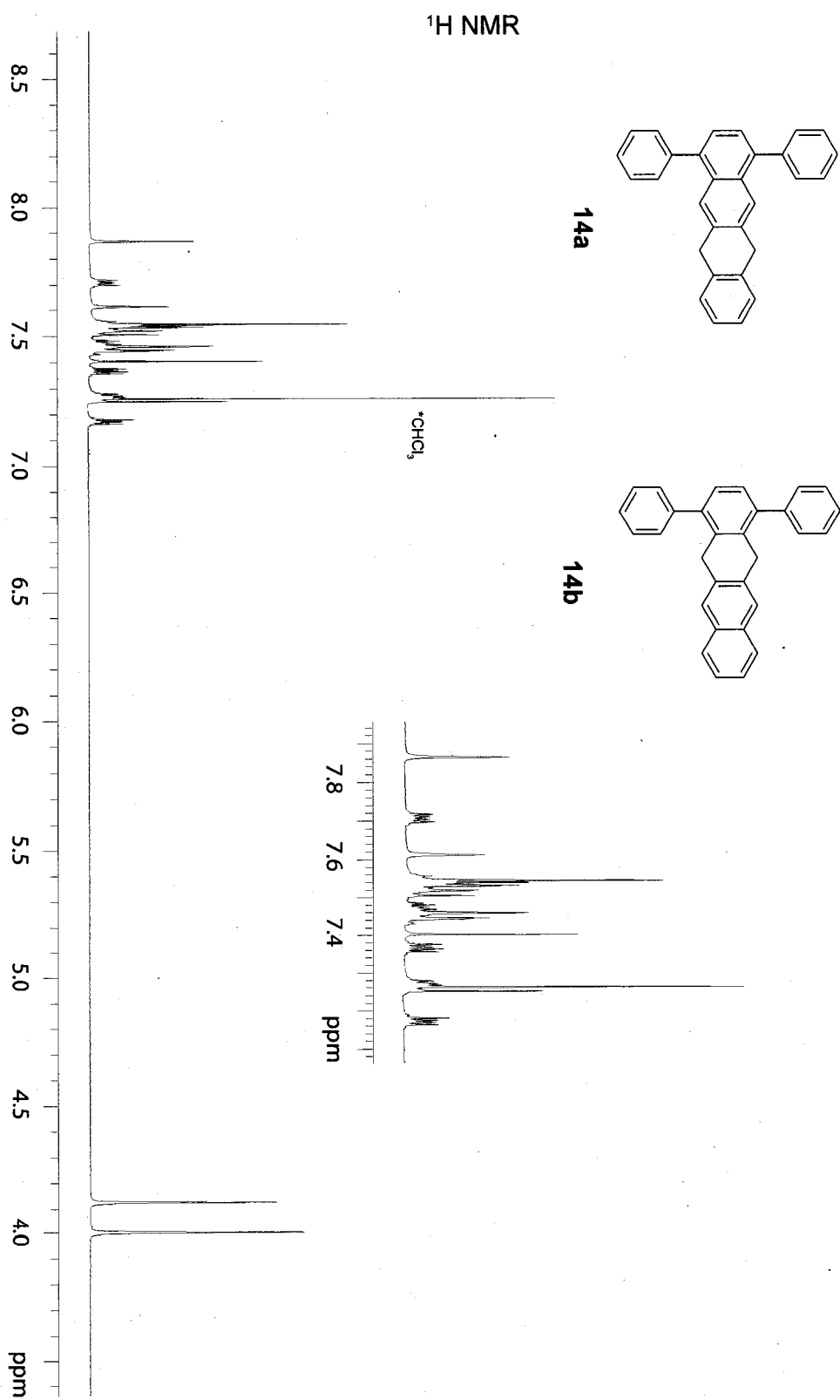


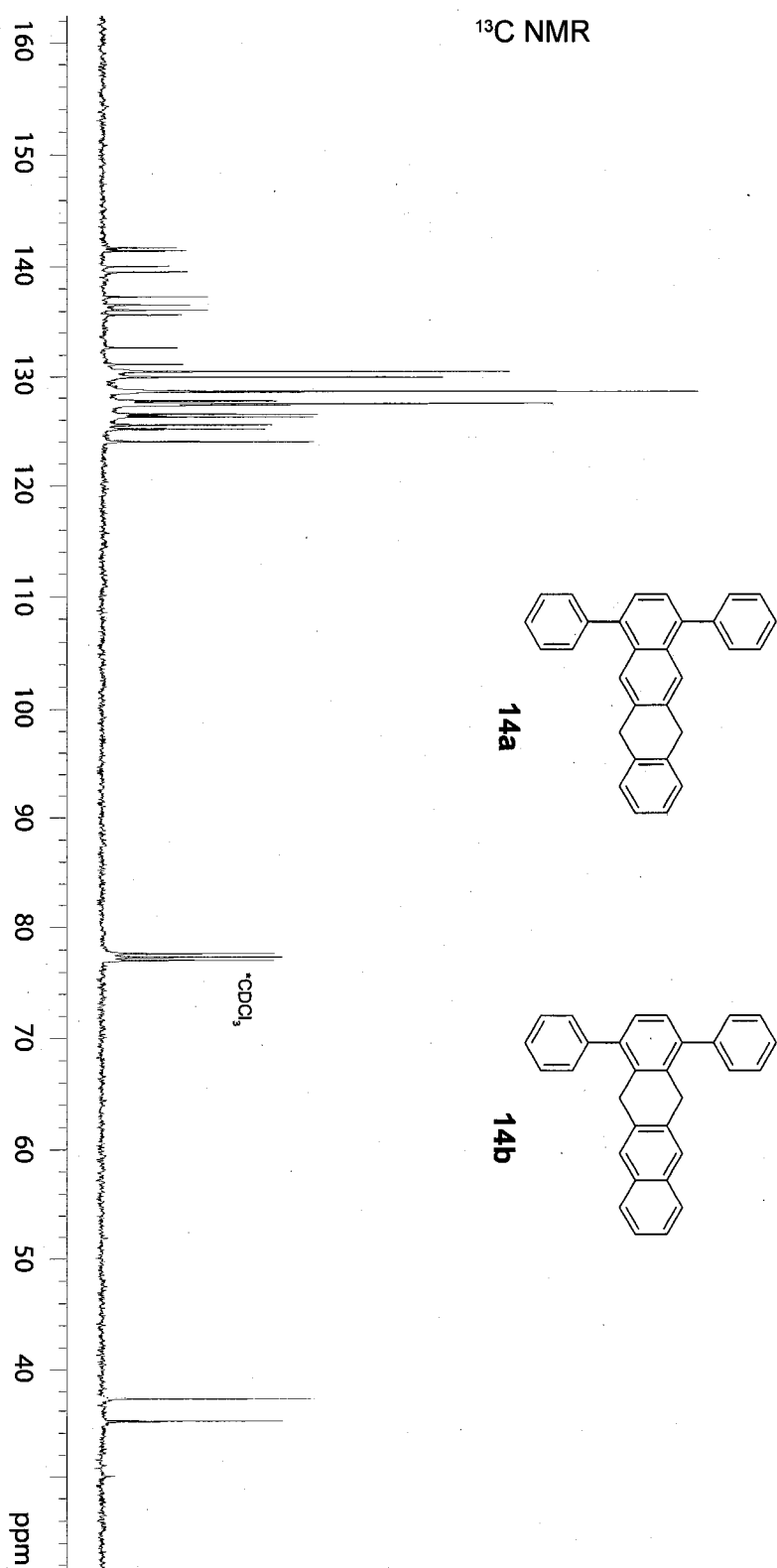


<sup>1</sup>H NMR

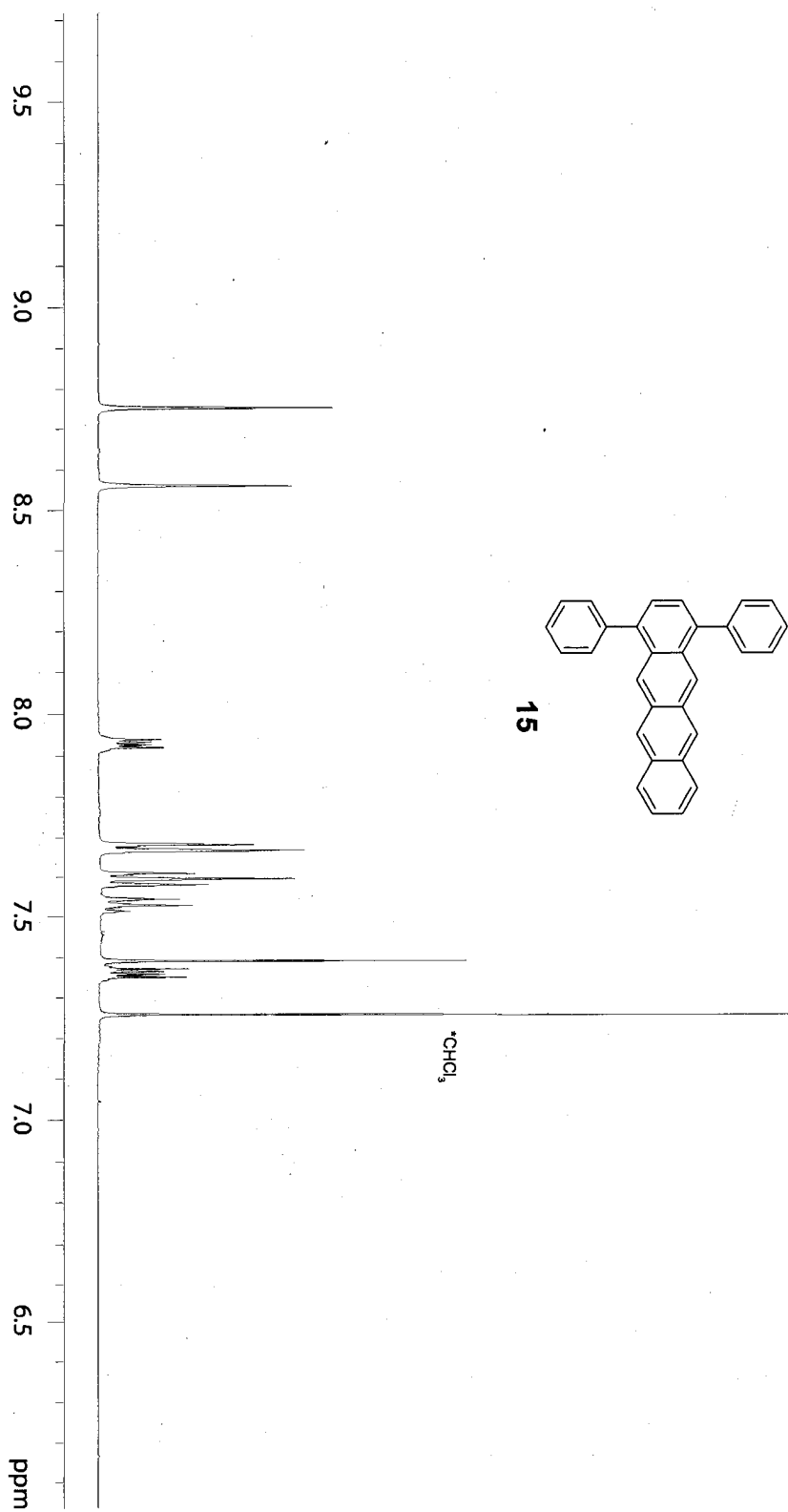




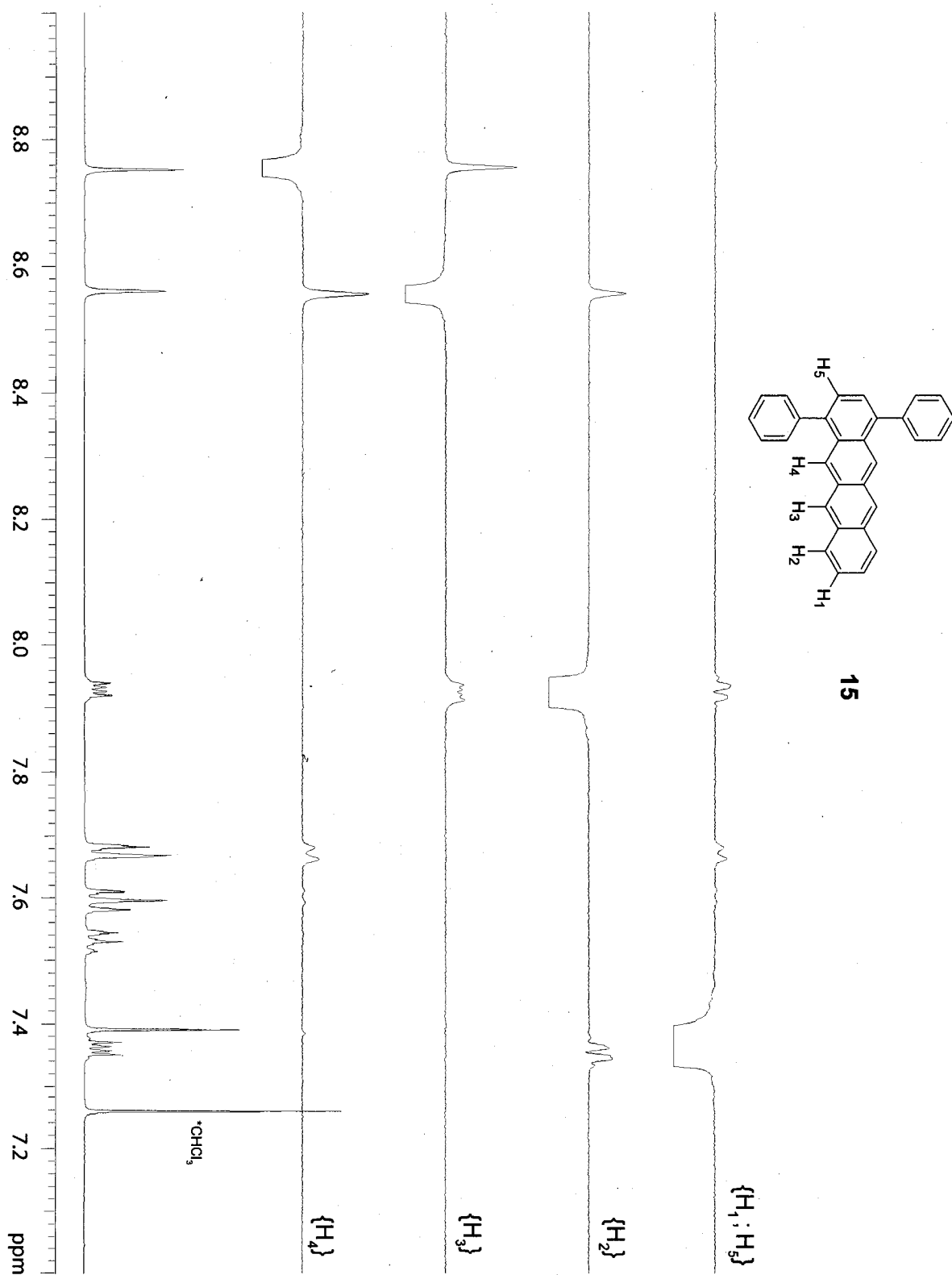




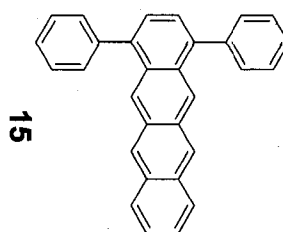
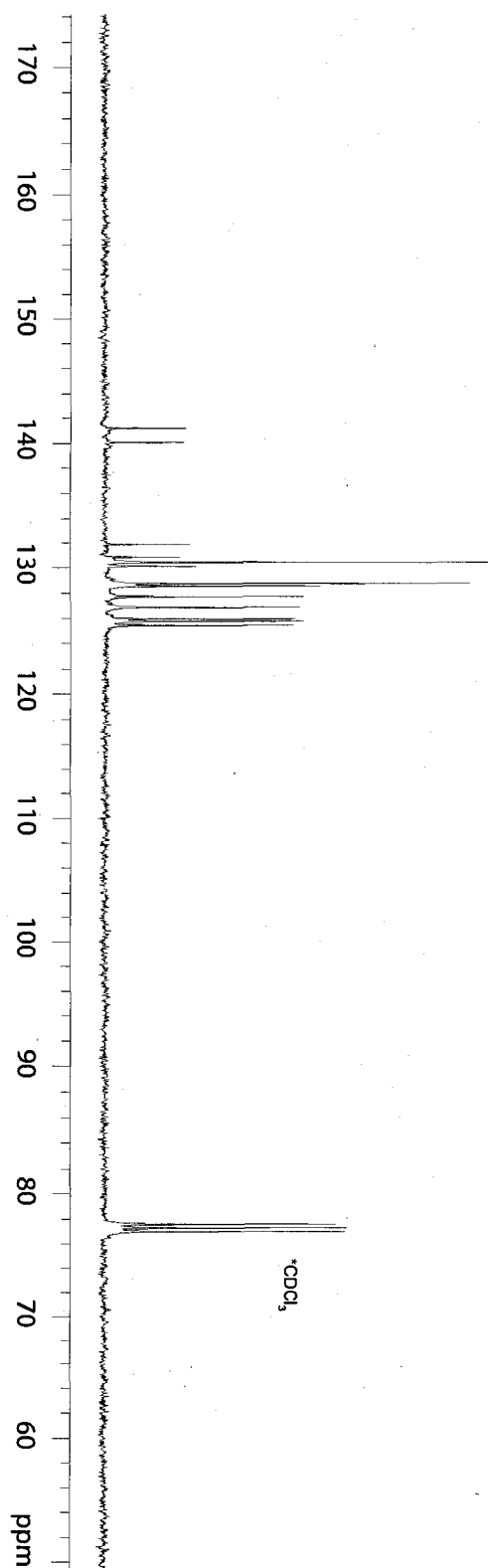
<sup>1</sup>H NMR



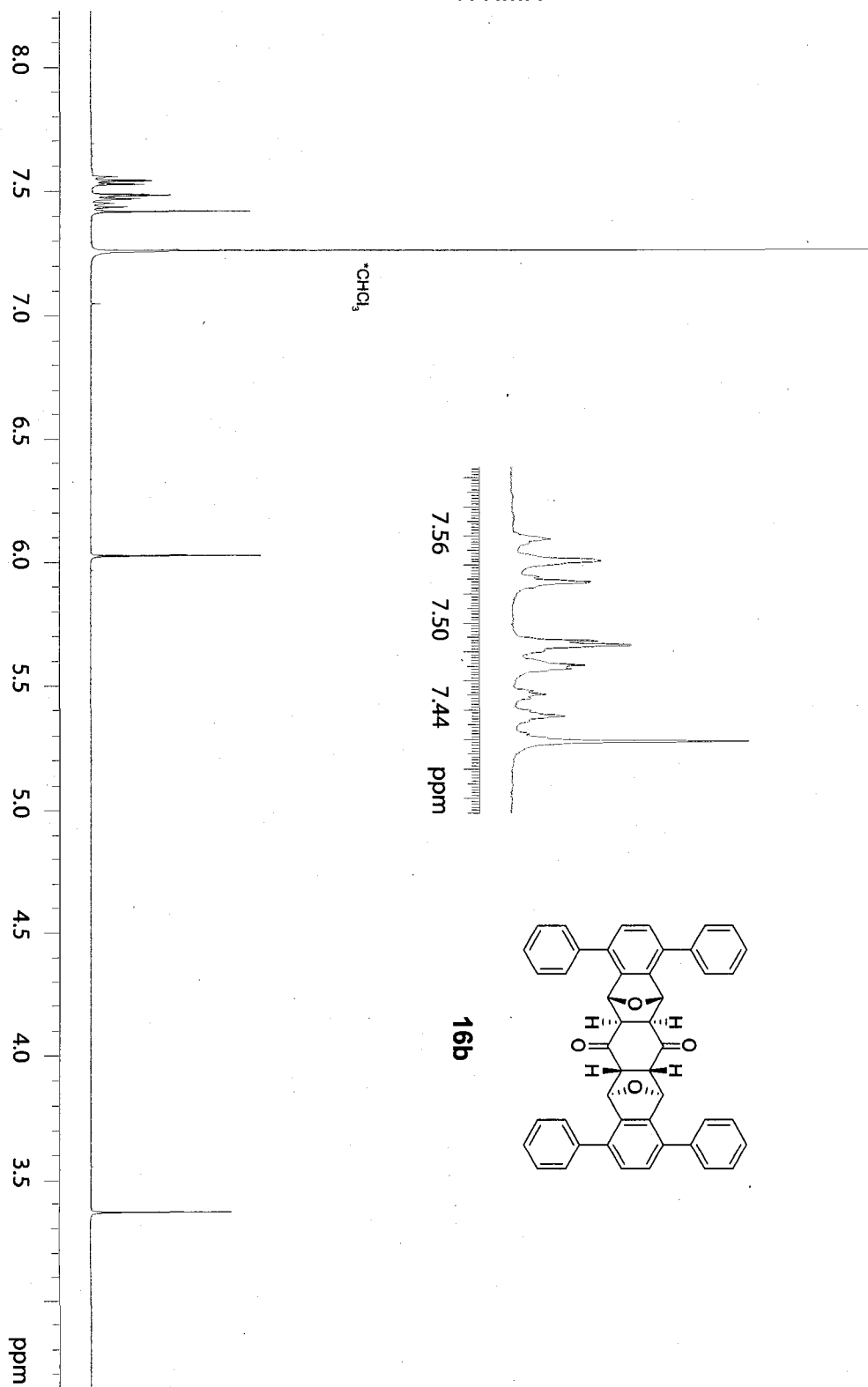
<sup>1</sup>H NMR and NOESY1D



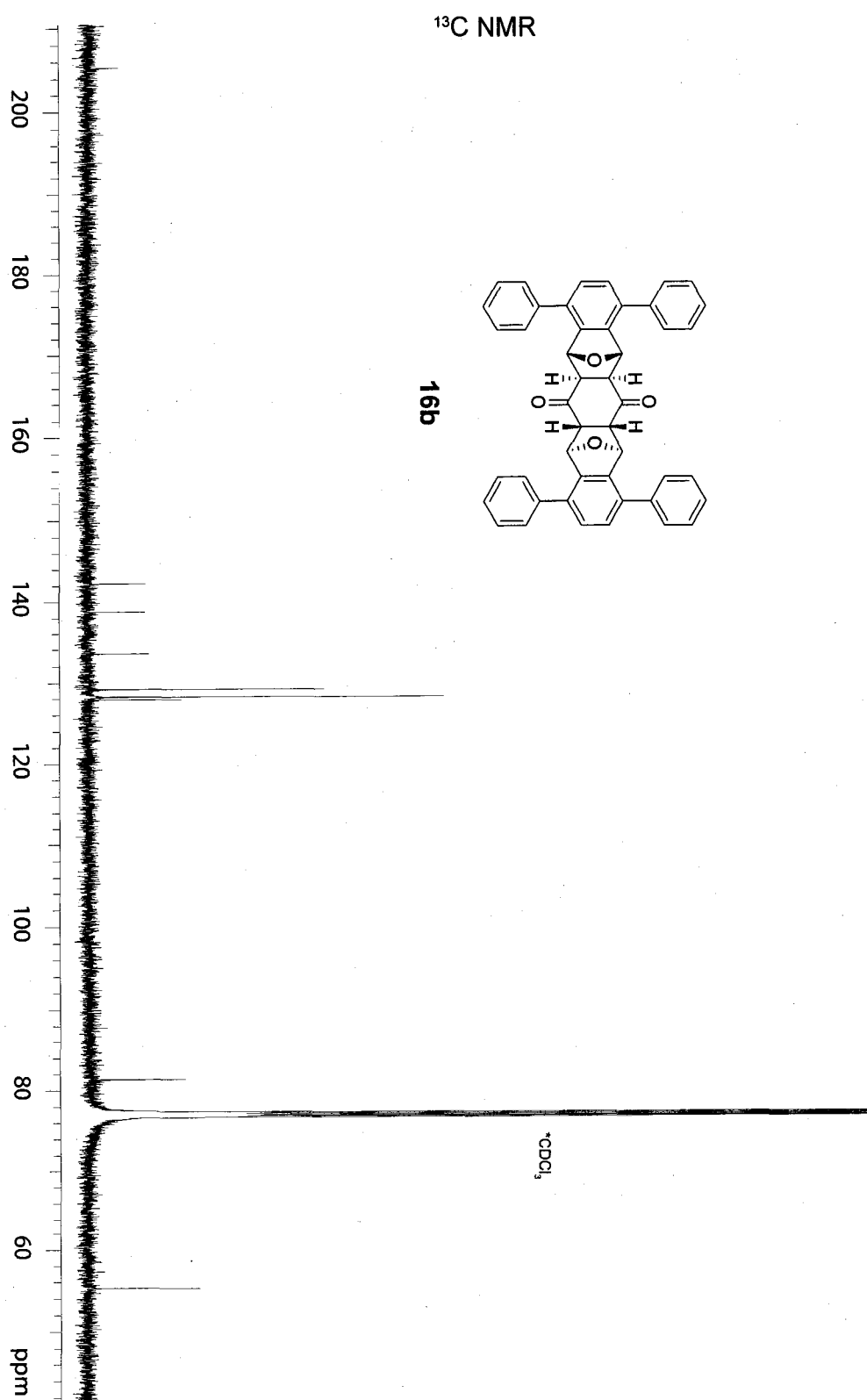
<sup>13</sup>C NMR

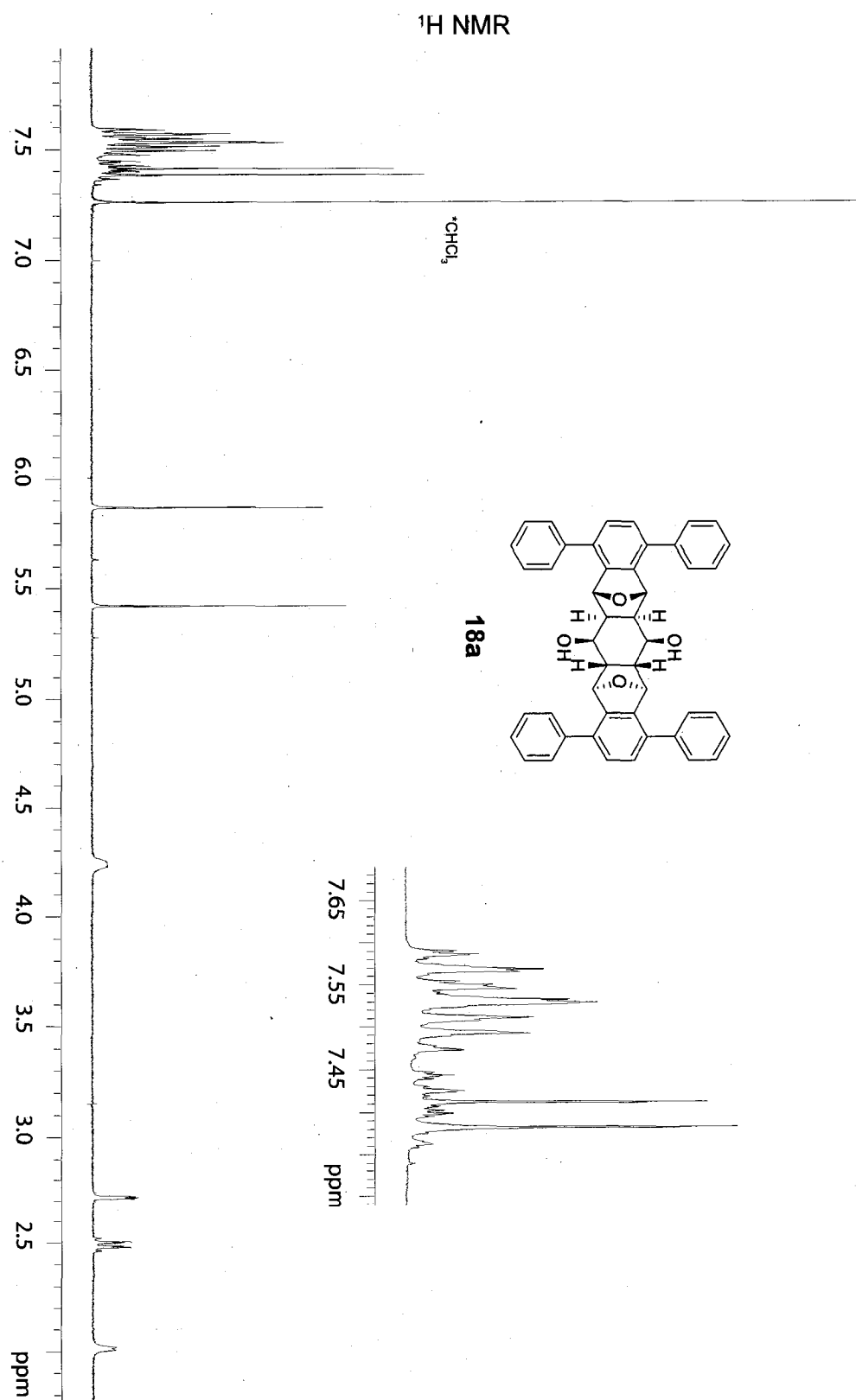


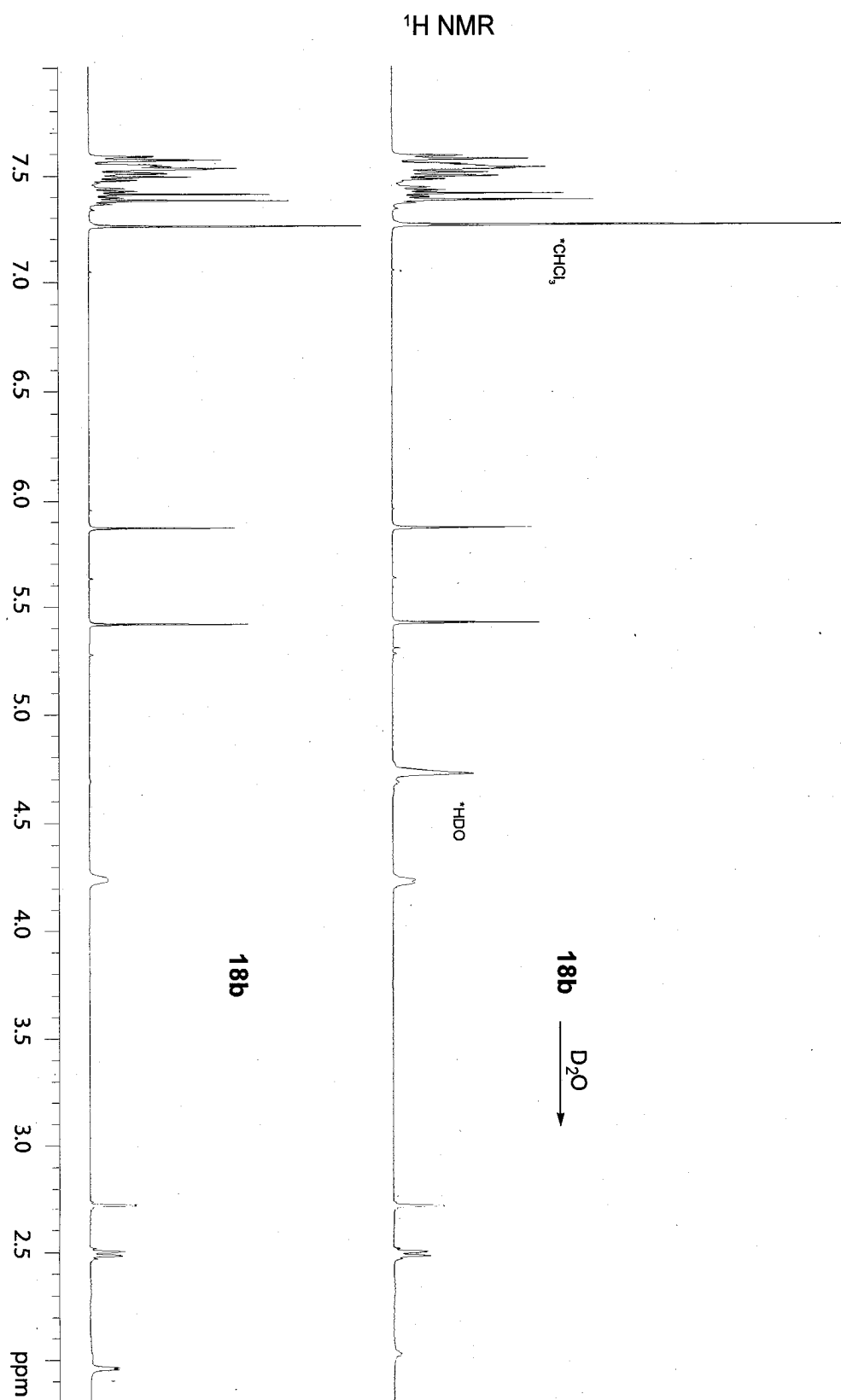
<sup>1</sup>H NMR



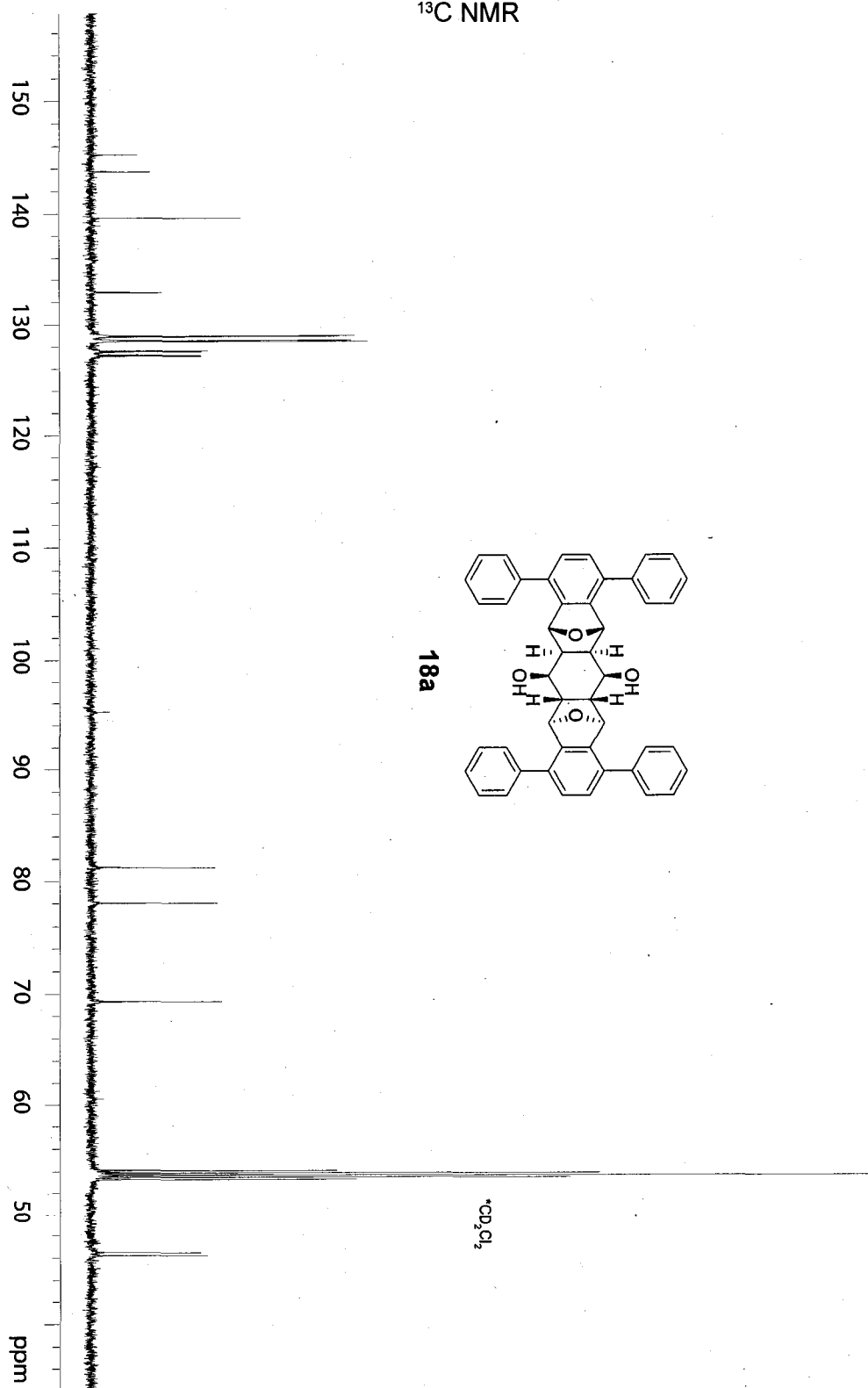




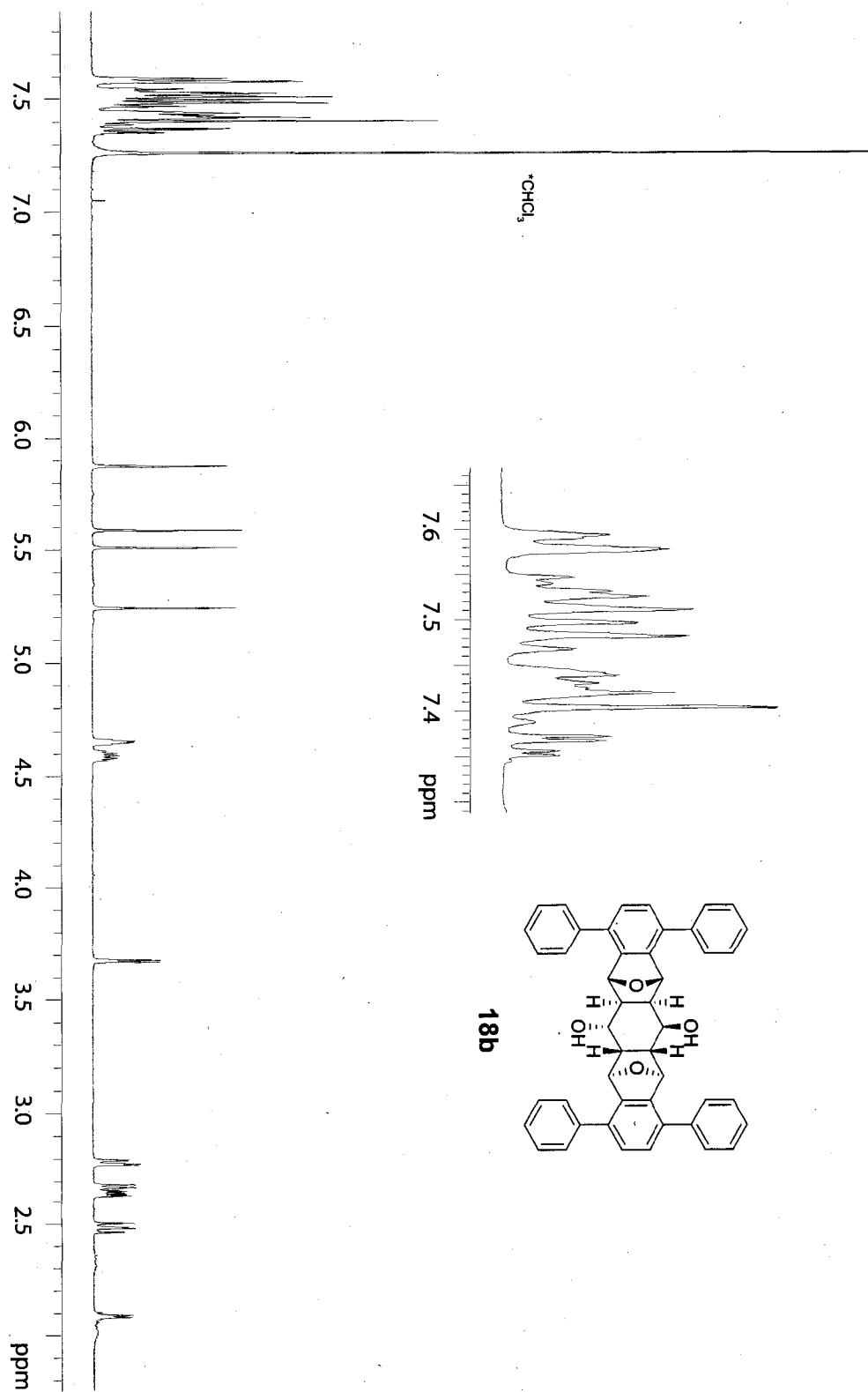


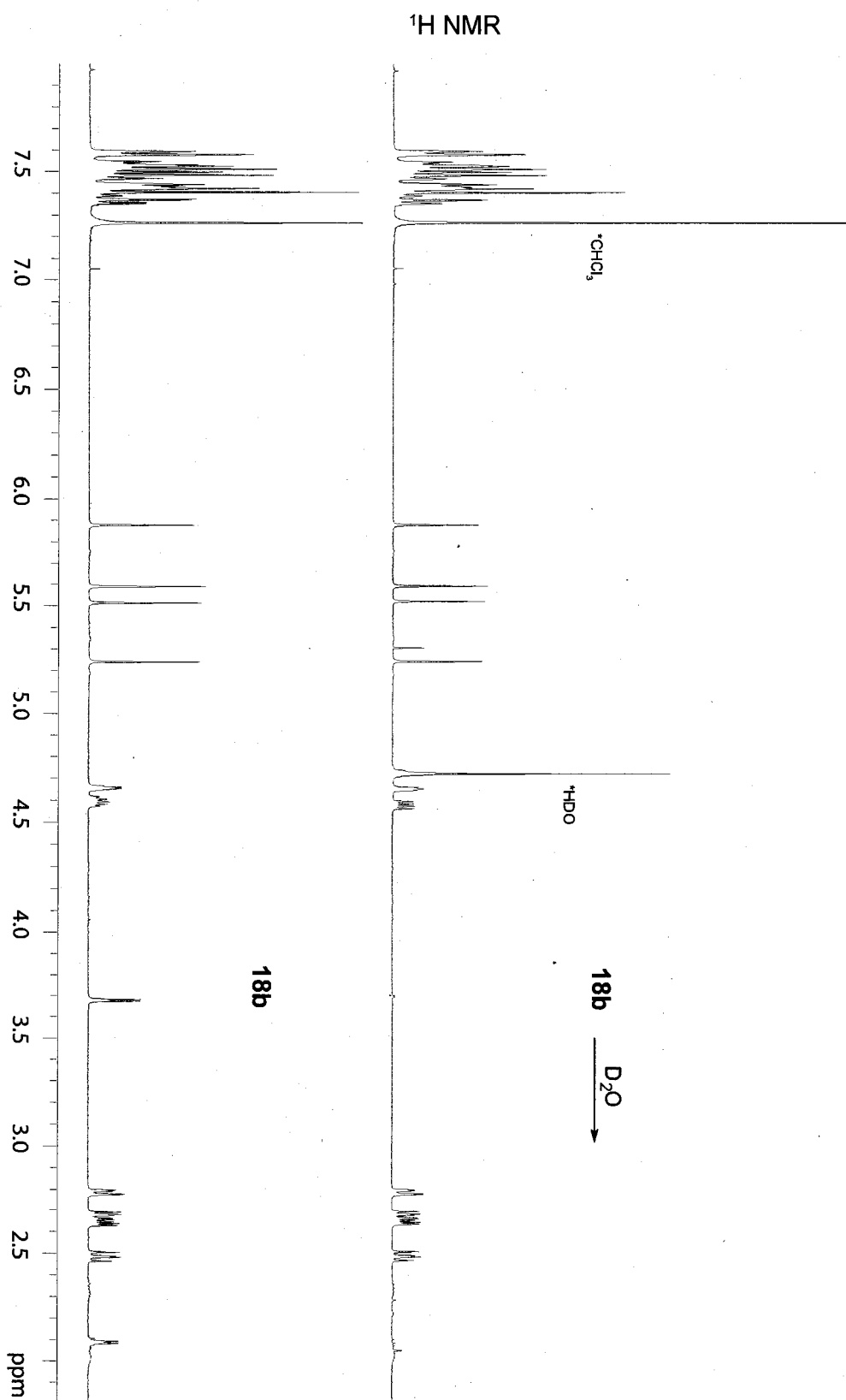


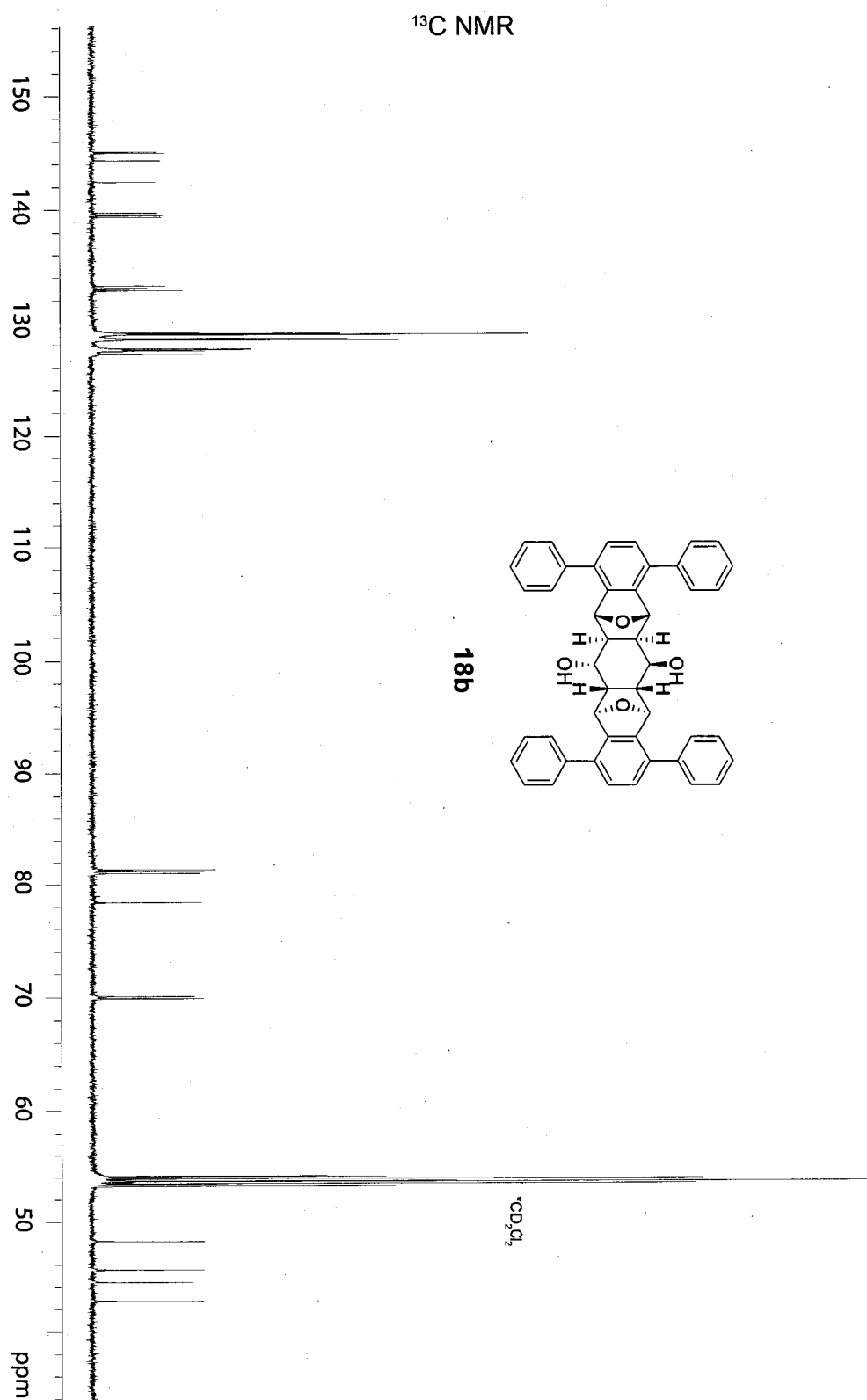
$^{13}\text{C}$  NMR

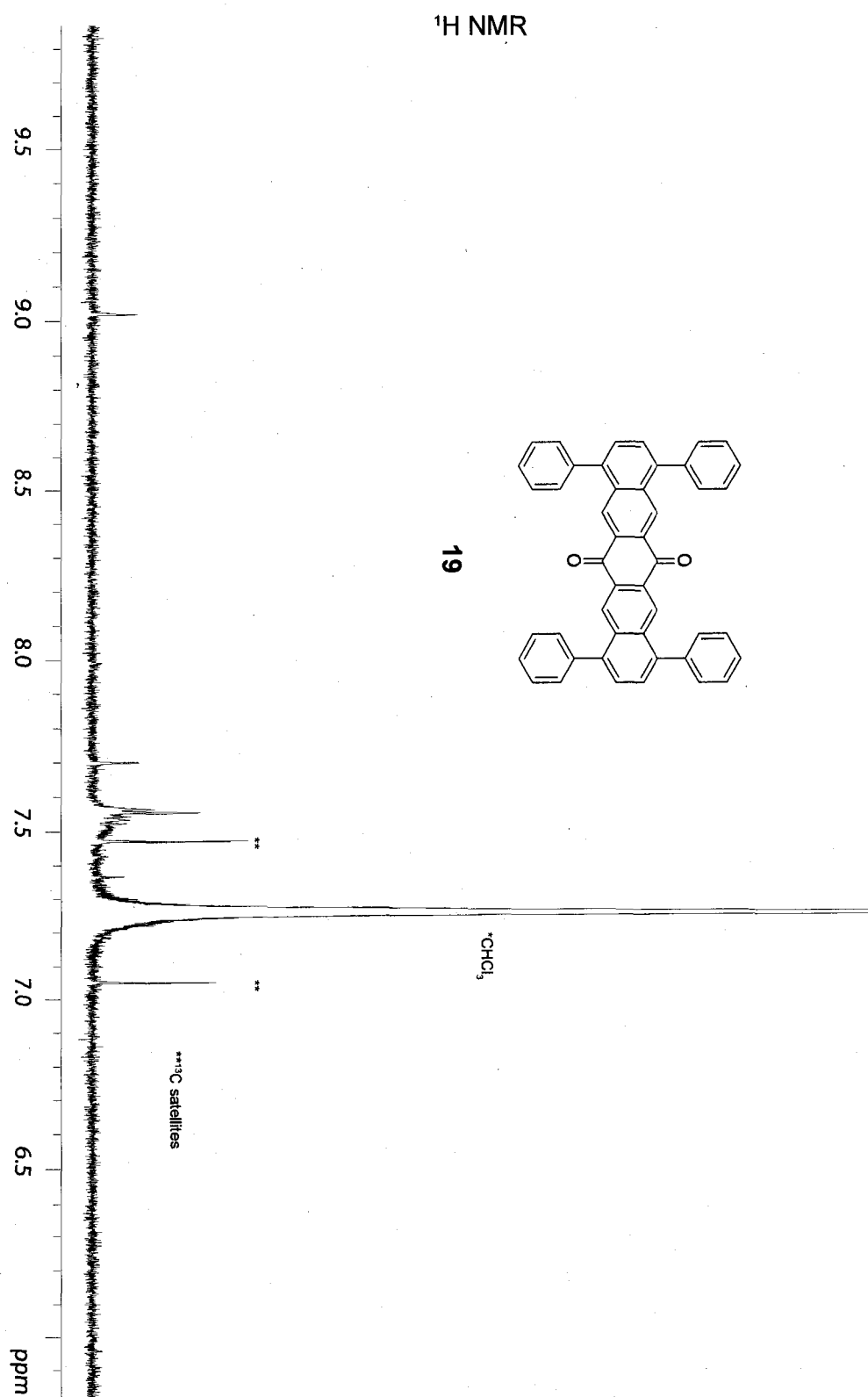


<sup>1</sup>H NMR

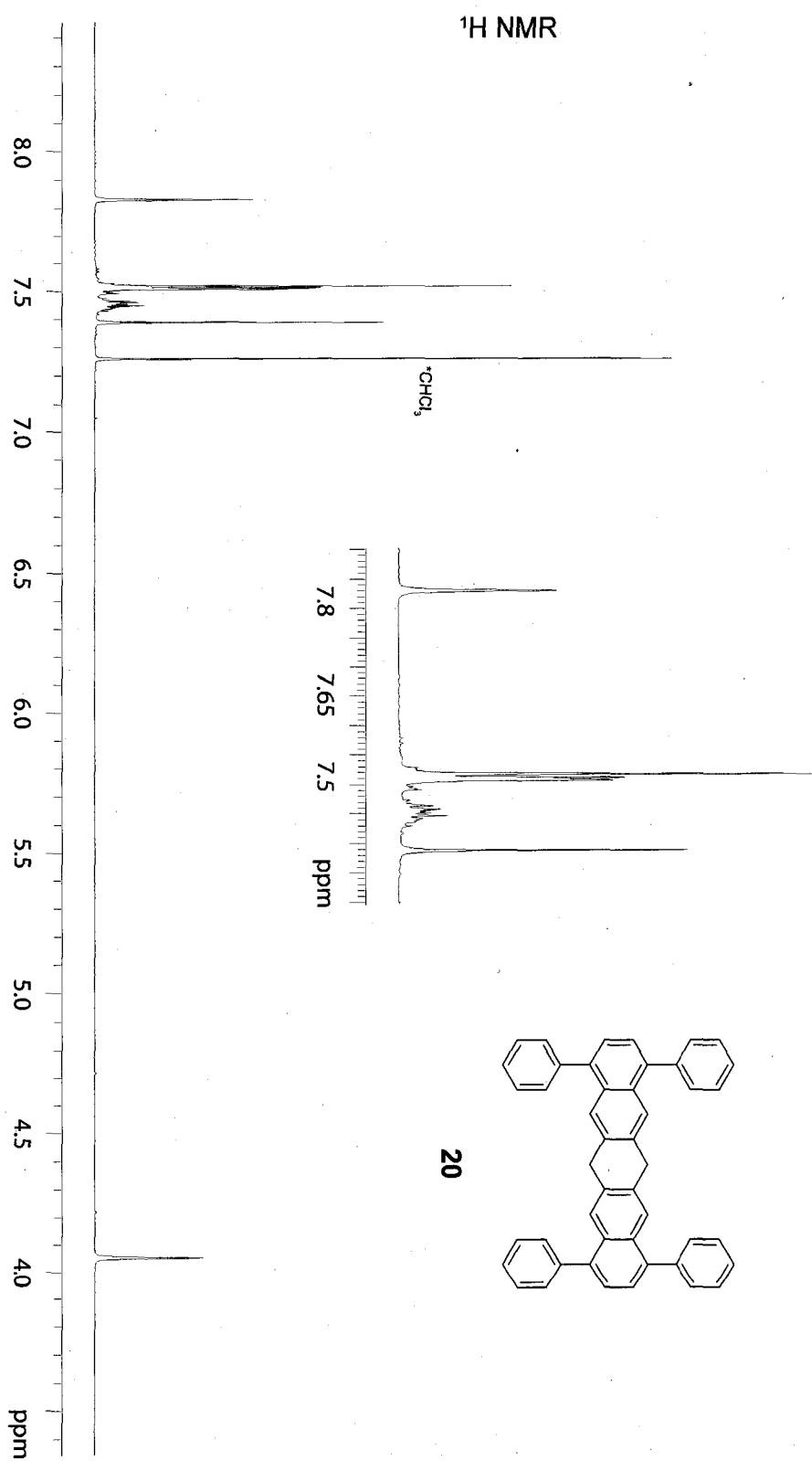


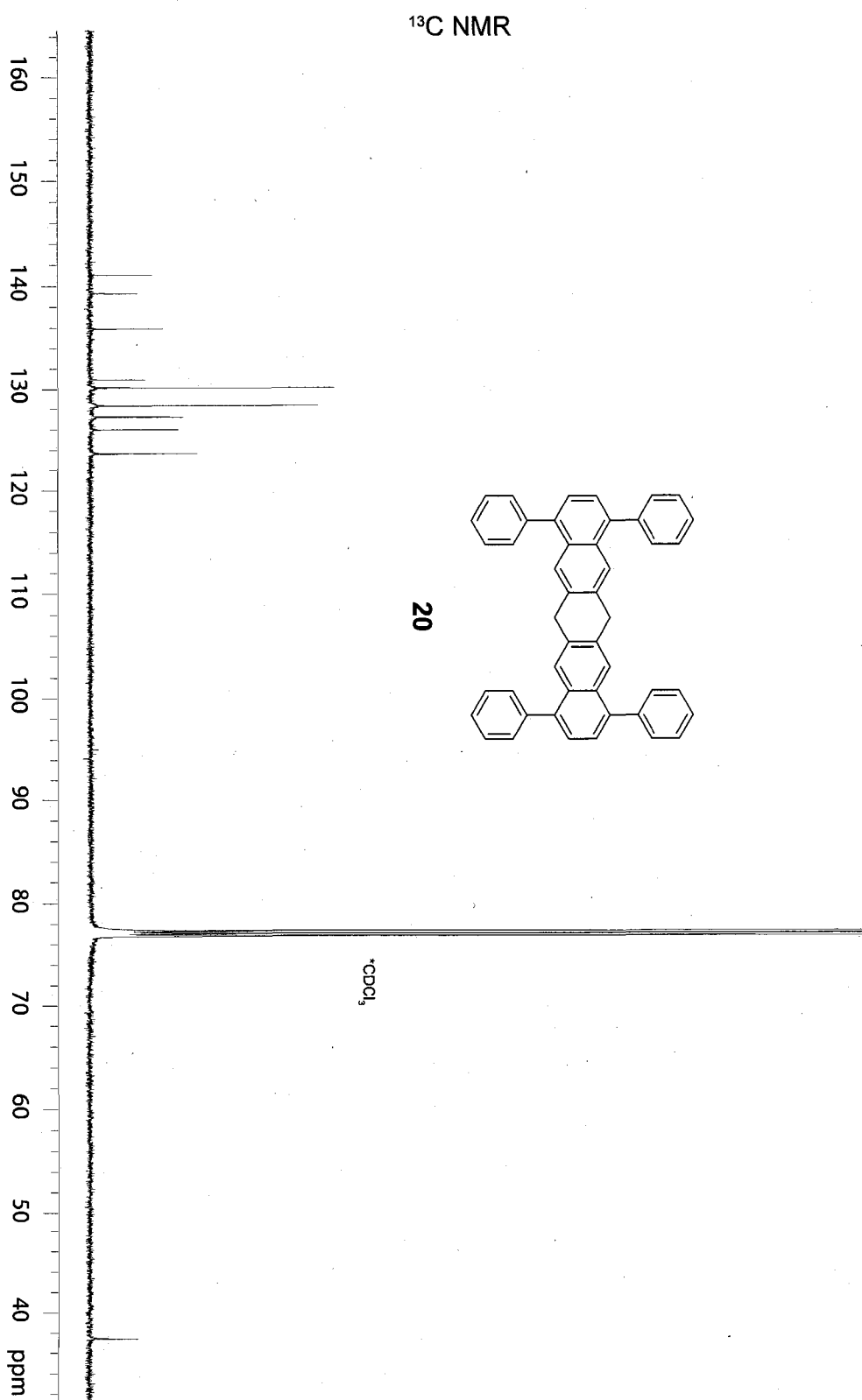




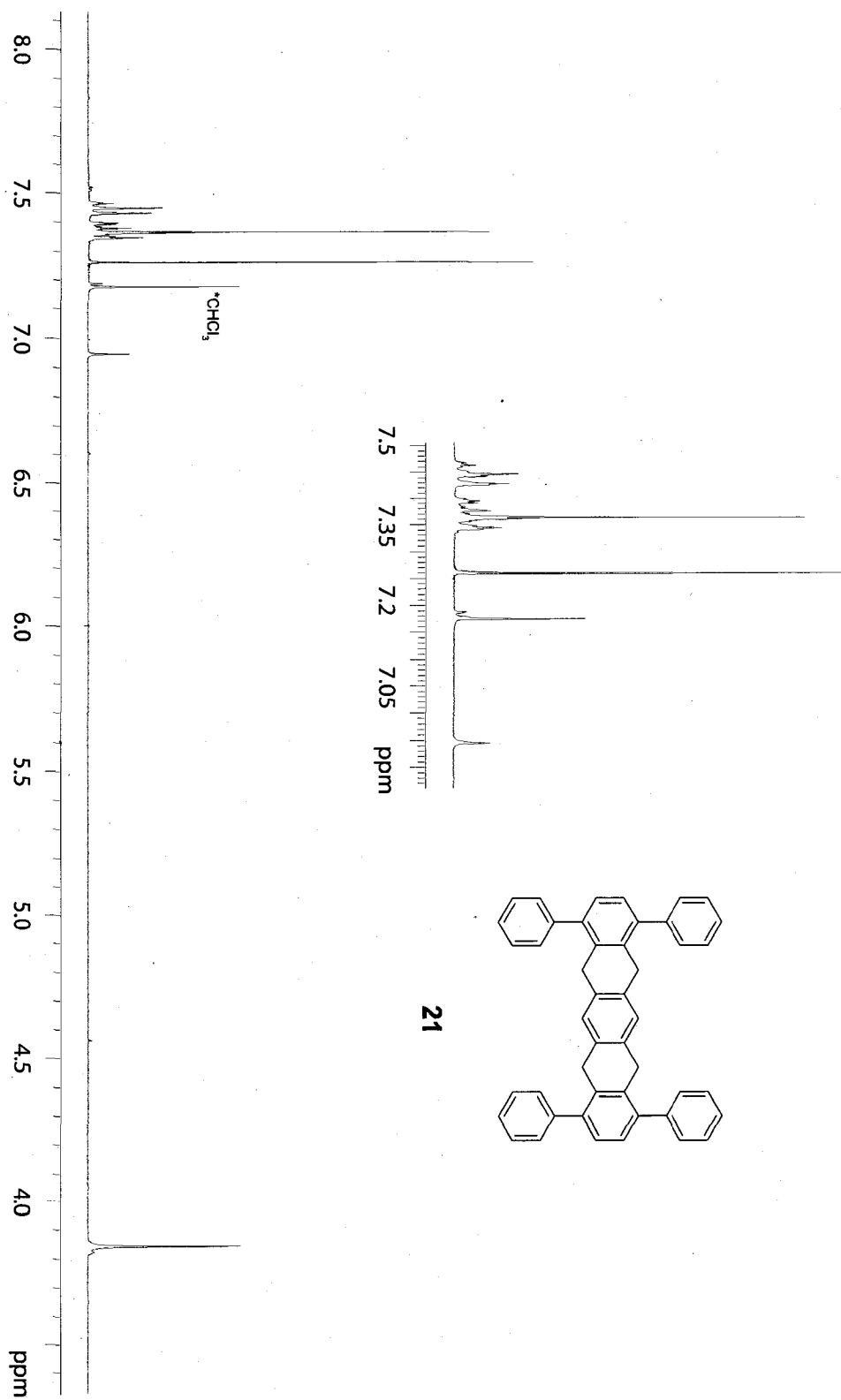




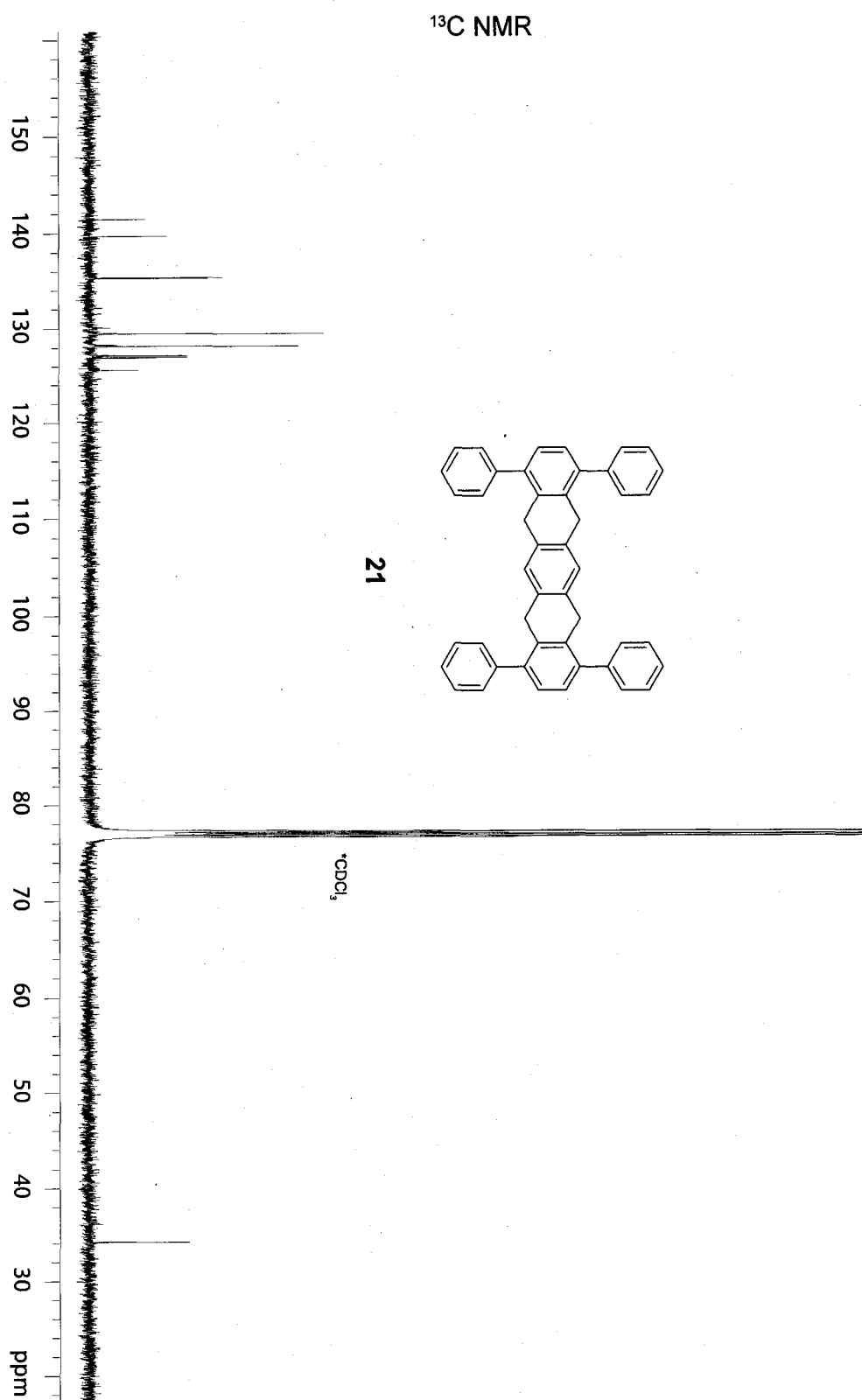


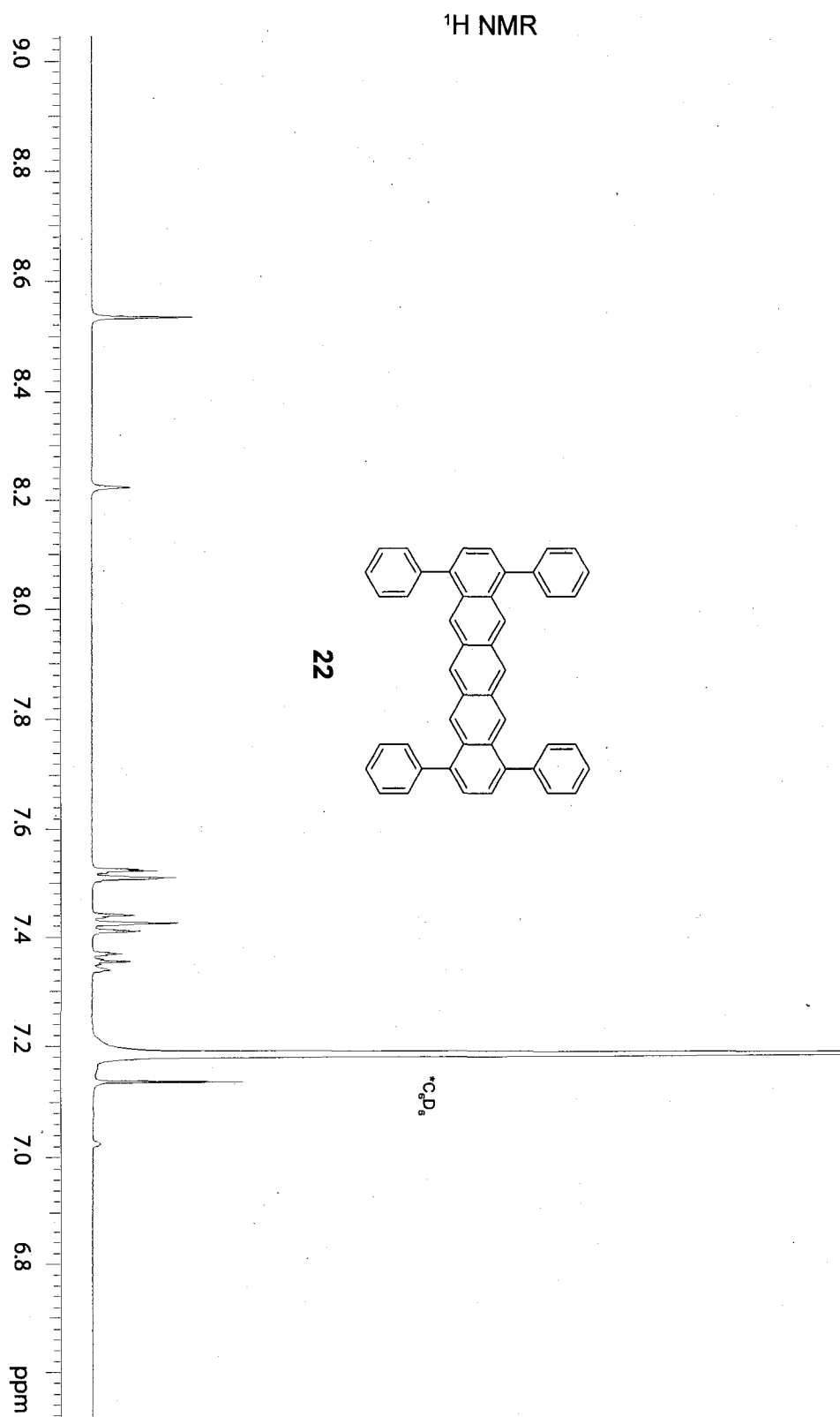


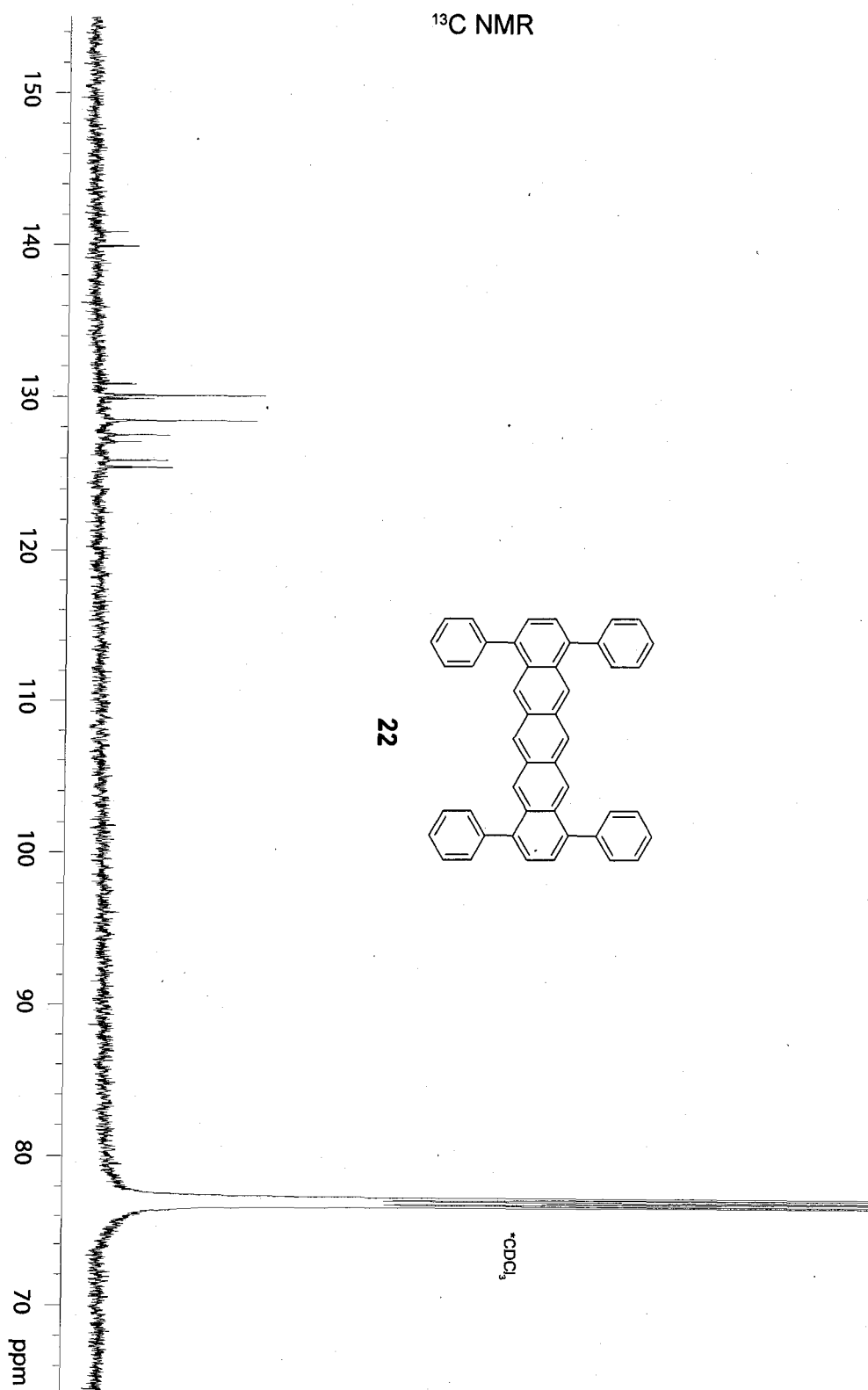
<sup>1</sup>H NMR



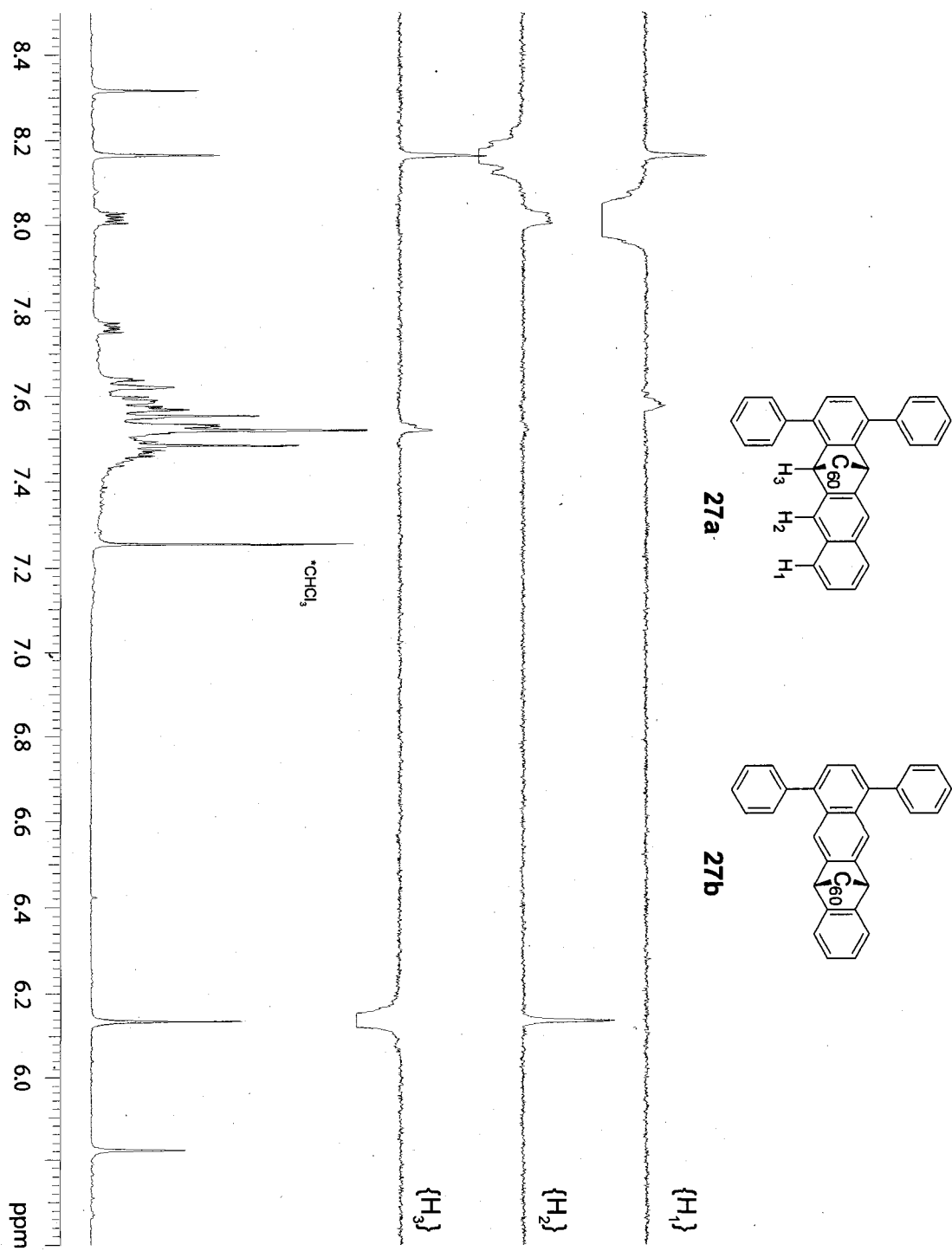
21



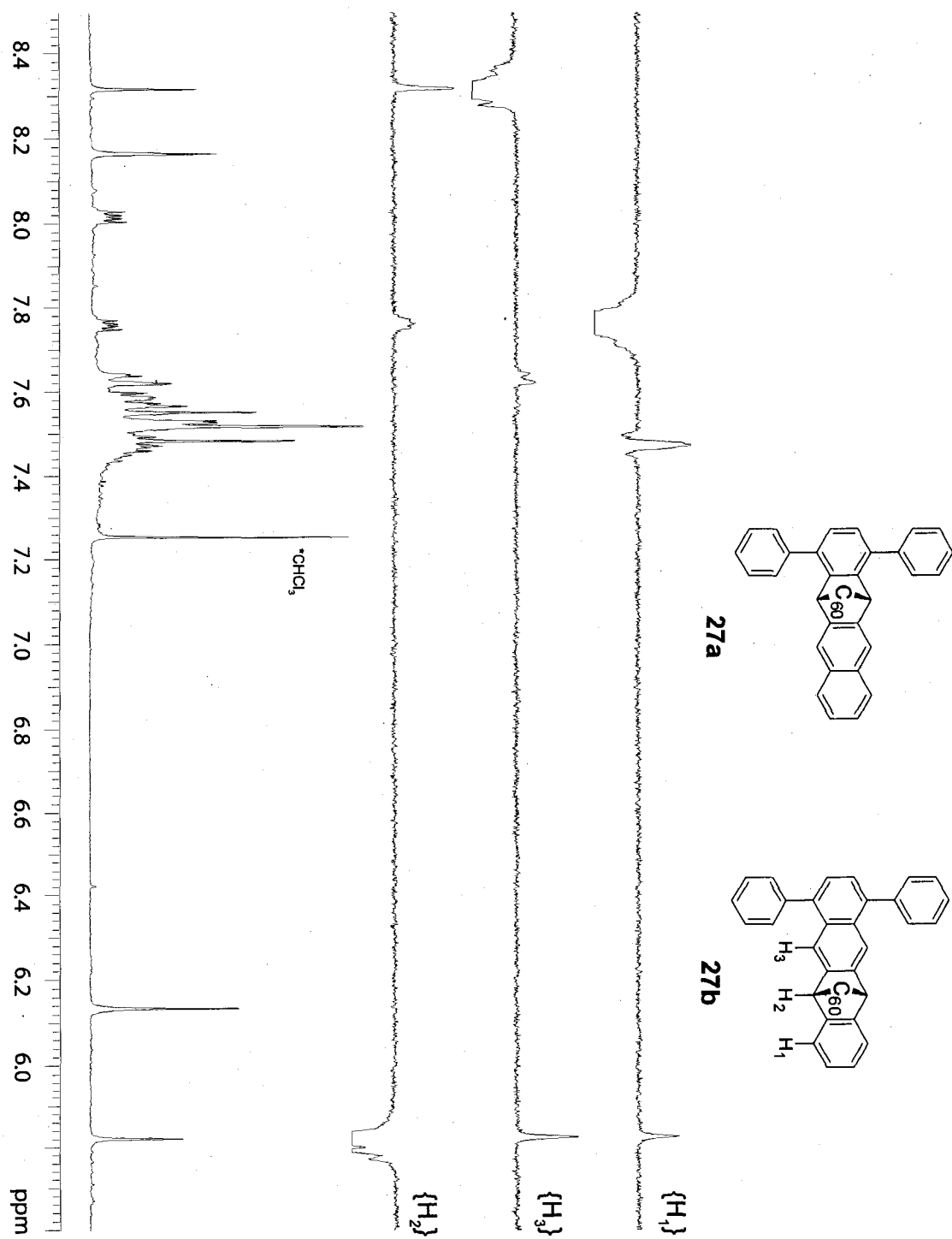




<sup>1</sup>H NMR and NOESY1D

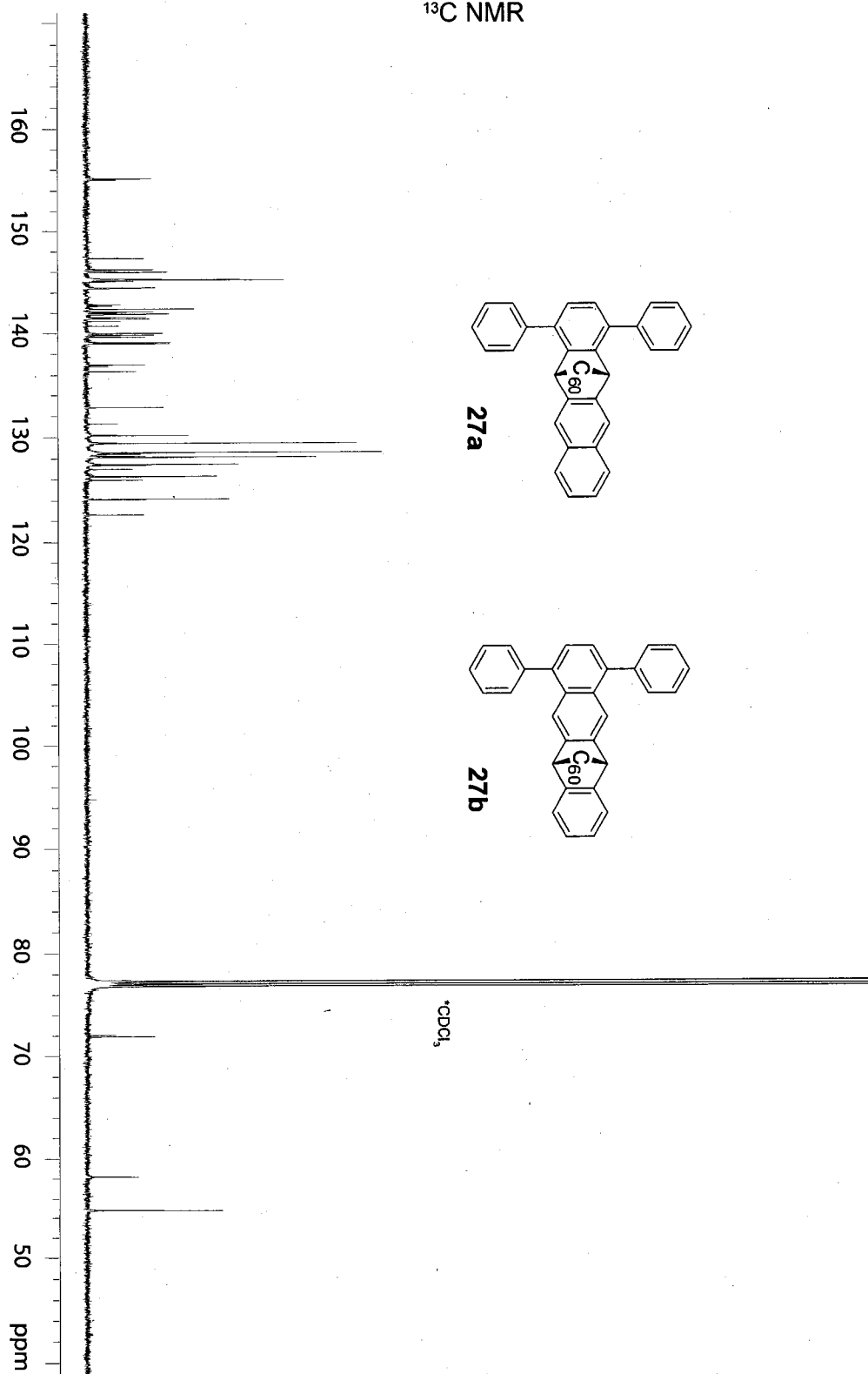


<sup>1</sup>H NMR and NOESY1D

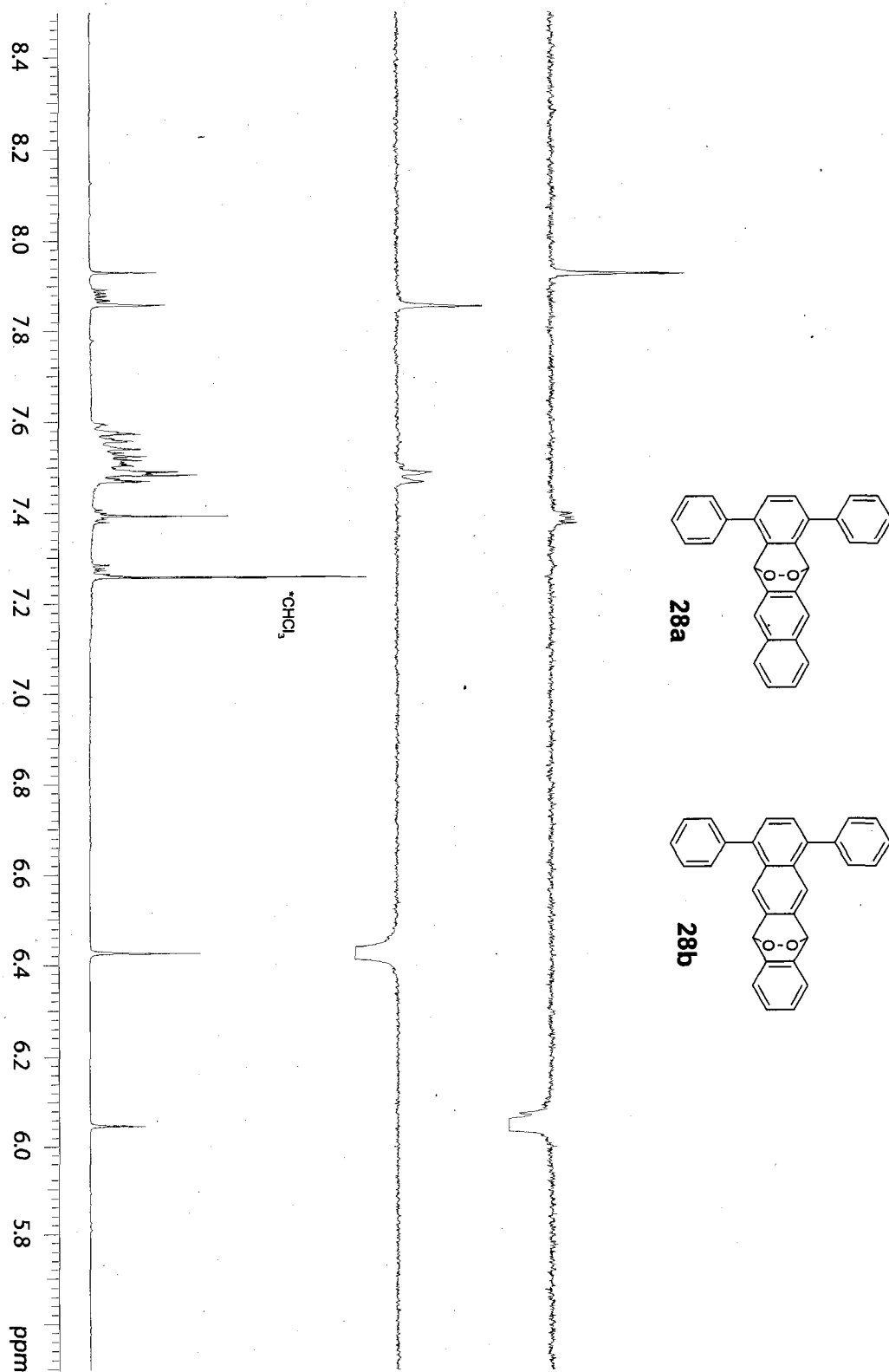




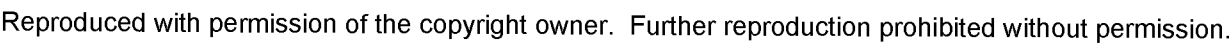
<sup>13</sup>C NMR



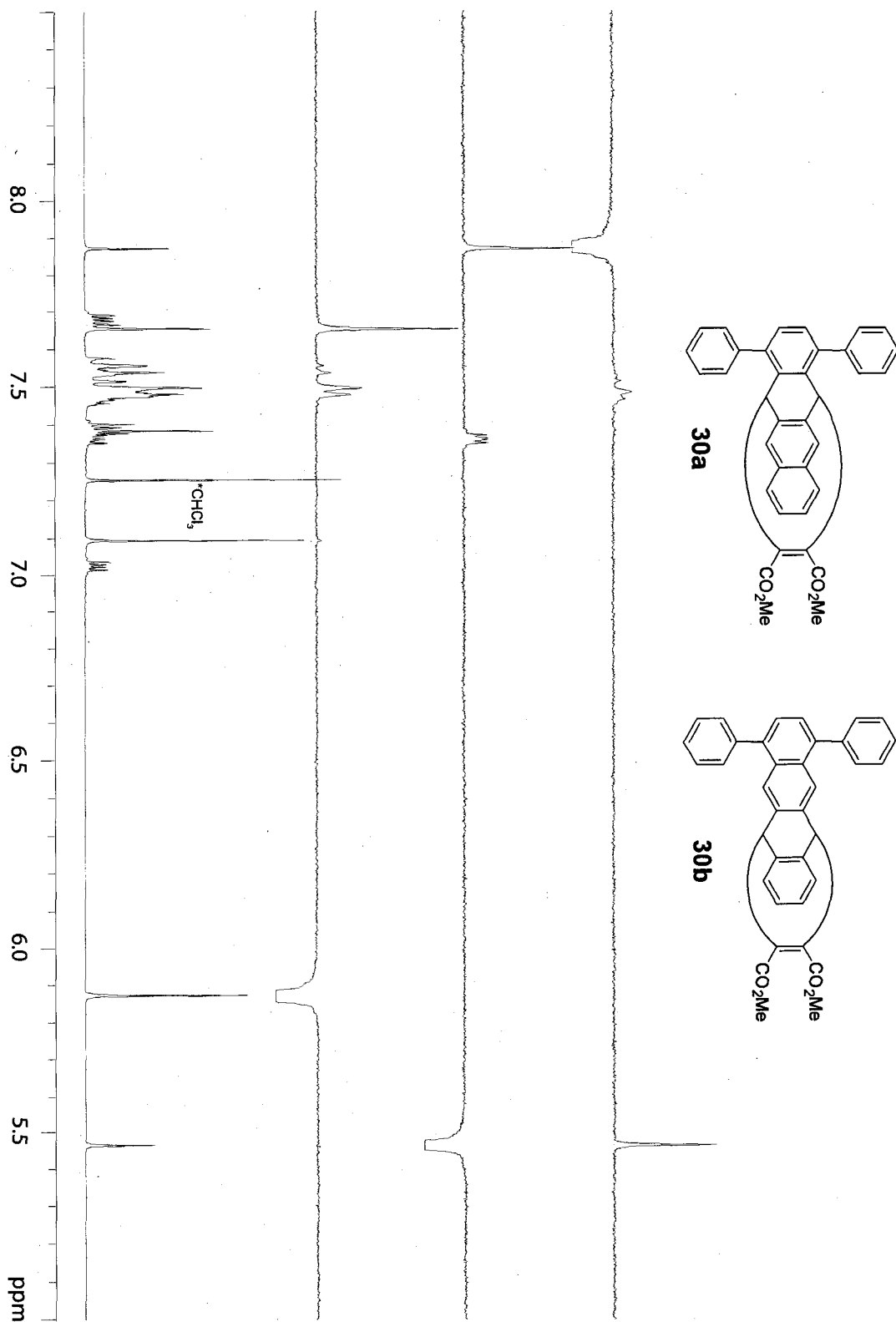
<sup>1</sup>H NMR and NOESY1D



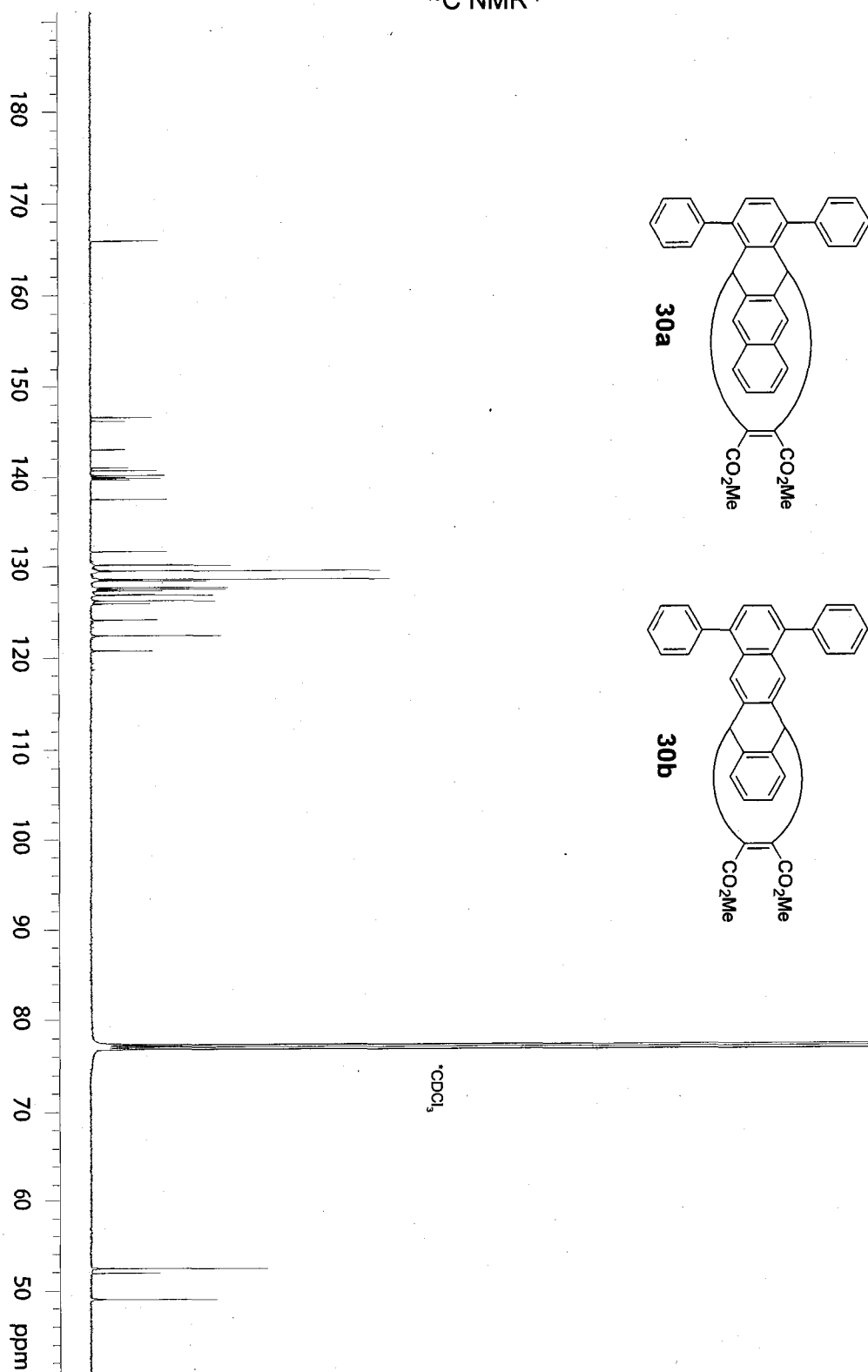
## 191

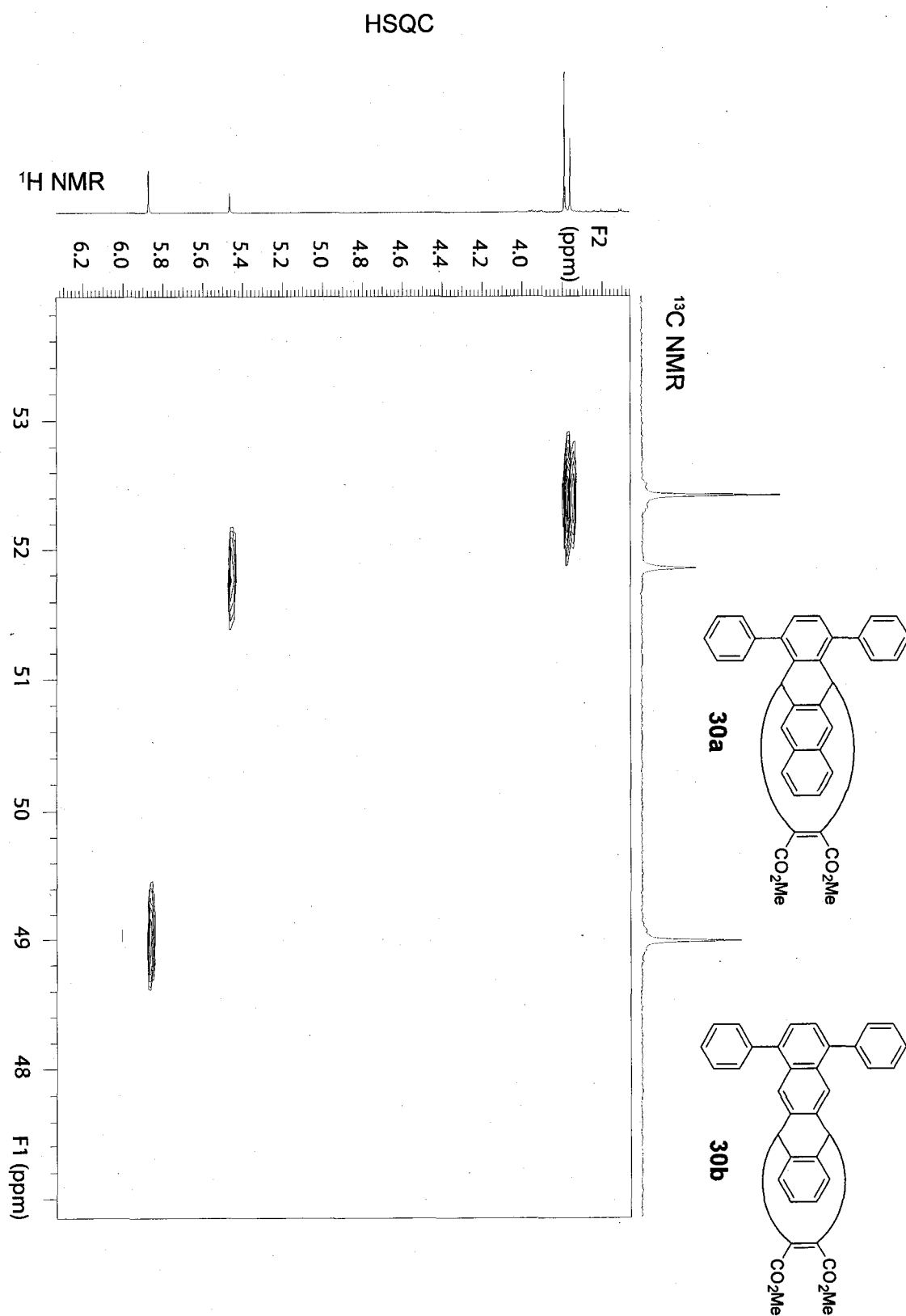


<sup>1</sup>H NMR and NOESY1D

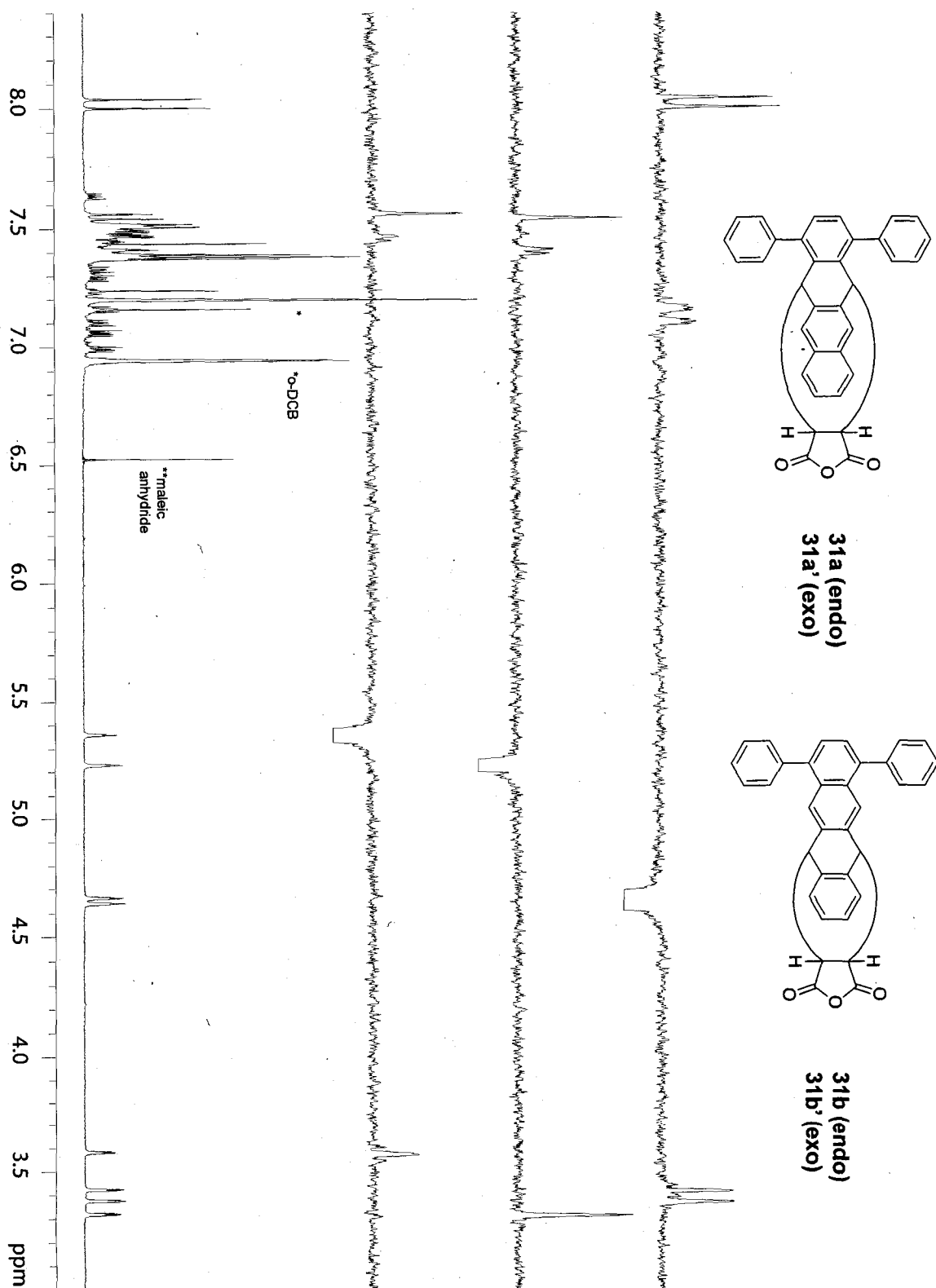


<sup>13</sup>C NMR





<sup>1</sup>H NMR and NOESY1D



The figure displays the chemical structures and  $^1\text{H}$  NMR spectra of four compounds: 31a, 31a', 31b, and 31b'.

**Chemical Structures:**

- 31a** and **31a'** are diastereomers of a bicyclic compound. They feature a naphthalene core fused to a cyclobutane ring, which is further fused to a succinic anhydride ring. The cyclobutane ring has two phenyl groups attached. The stereochemistry of the protons  $\text{H}_I$  and  $\text{H}_{II}$  is indicated.
- 31b** and **31b'** are diastereomers of a similar bicyclic compound, but with a different stereochemistry for the protons  $\text{H}_I$  and  $\text{H}_{II}$ .

**$^1\text{H}$  NMR Spectra:**

The  $^1\text{H}$  NMR spectra are shown in two parts. The top part shows the full spectrum, and the bottom part shows a zoomed-in view of the region between 4.1 and 3.2 ppm.

**Top Spectrum:**

- X-axis:  $^1\text{H}$  NMR (ppm), ranging from 4.1 to 2.9.
- Peaks are labeled: **31a** (5,12 endo) at ~3.6 ppm, **31b** (6,11 endo) at ~3.4 ppm, **31a'** (5,12 exo) at ~3.3 ppm, and **31b'** (6,11 exo) at ~3.2 ppm.

**Bottom Spectrum:**

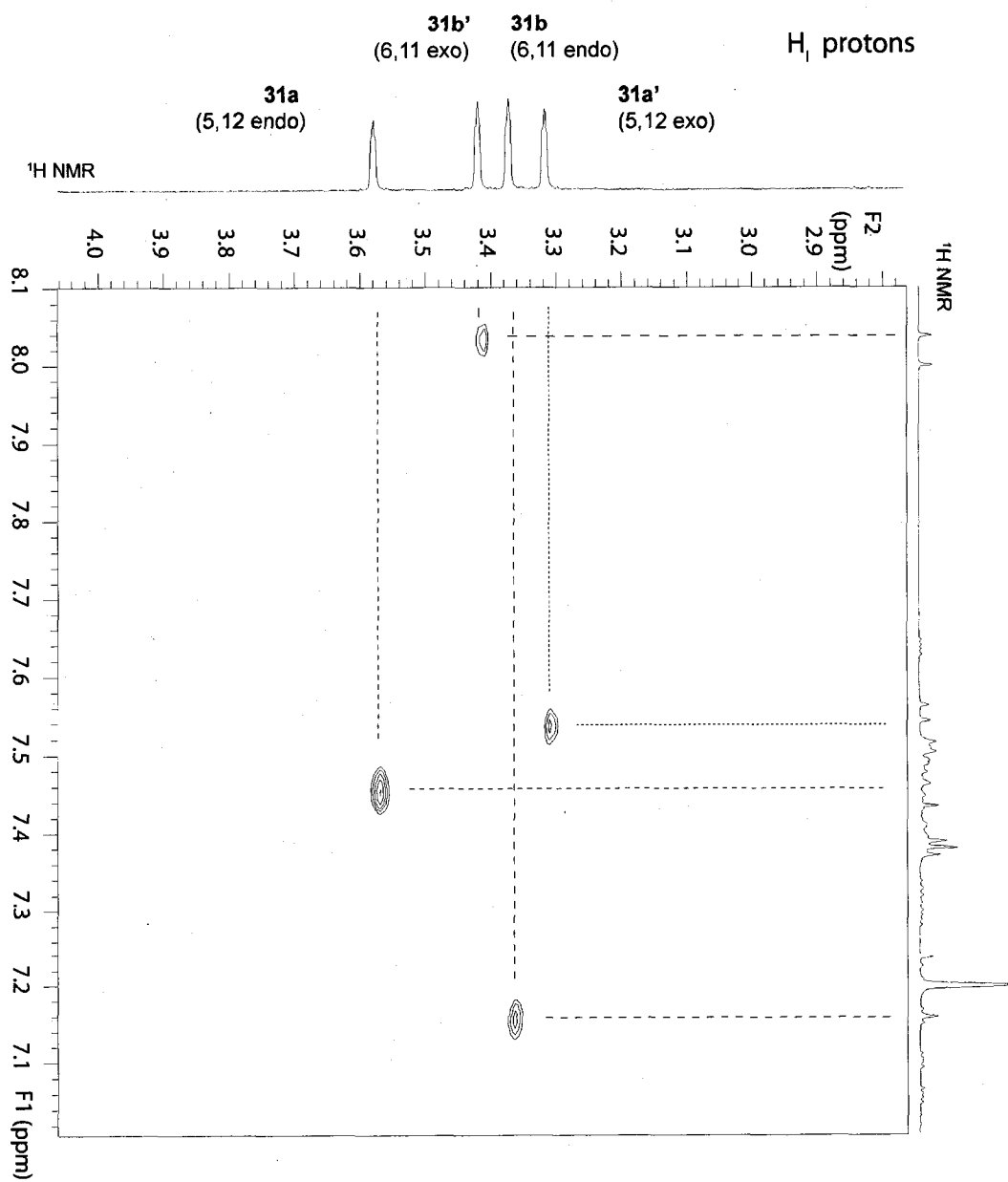
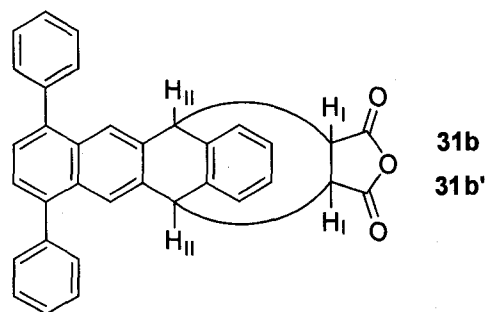
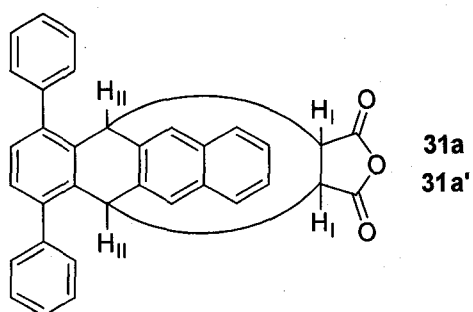
- X-axis:  $^1\text{H}$  NMR (ppm), ranging from 4.1 to 3.2.
- Peaks are labeled: **31a** (5,12 endo) at ~3.6 ppm, **31a'** (5,12 exo) at ~3.3 ppm, **31b'** (6,11 exo) at ~3.2 ppm, and **31b** (6,11 endo) at ~3.1 ppm.

**Integration:**

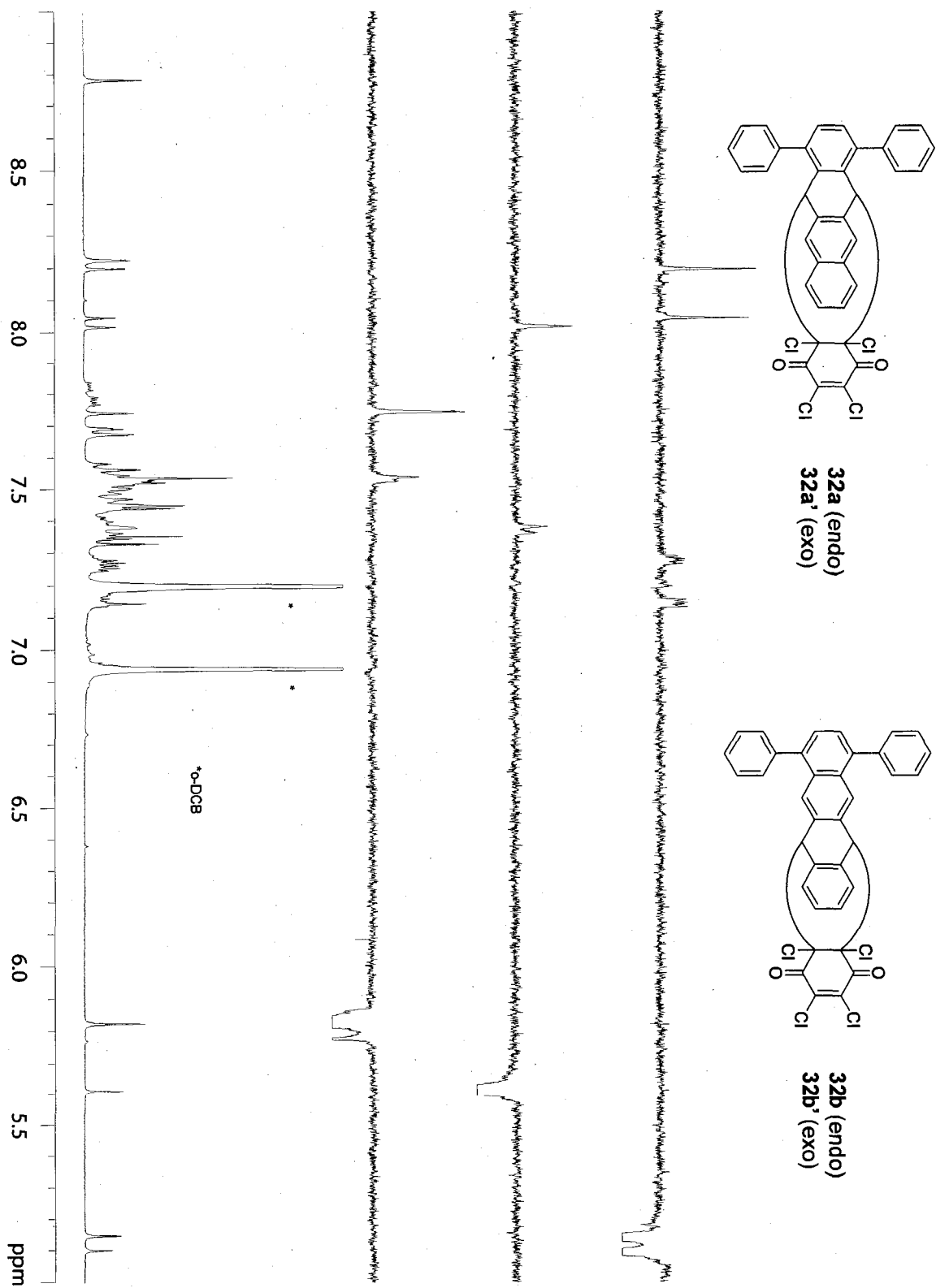
The integration values for the peaks are: **31a** (5,12 endo) = 1.00, **31a'** (5,12 exo) = 1.00, **31b'** (6,11 exo) = 1.00, and **31b** (6,11 endo) = 1.00.



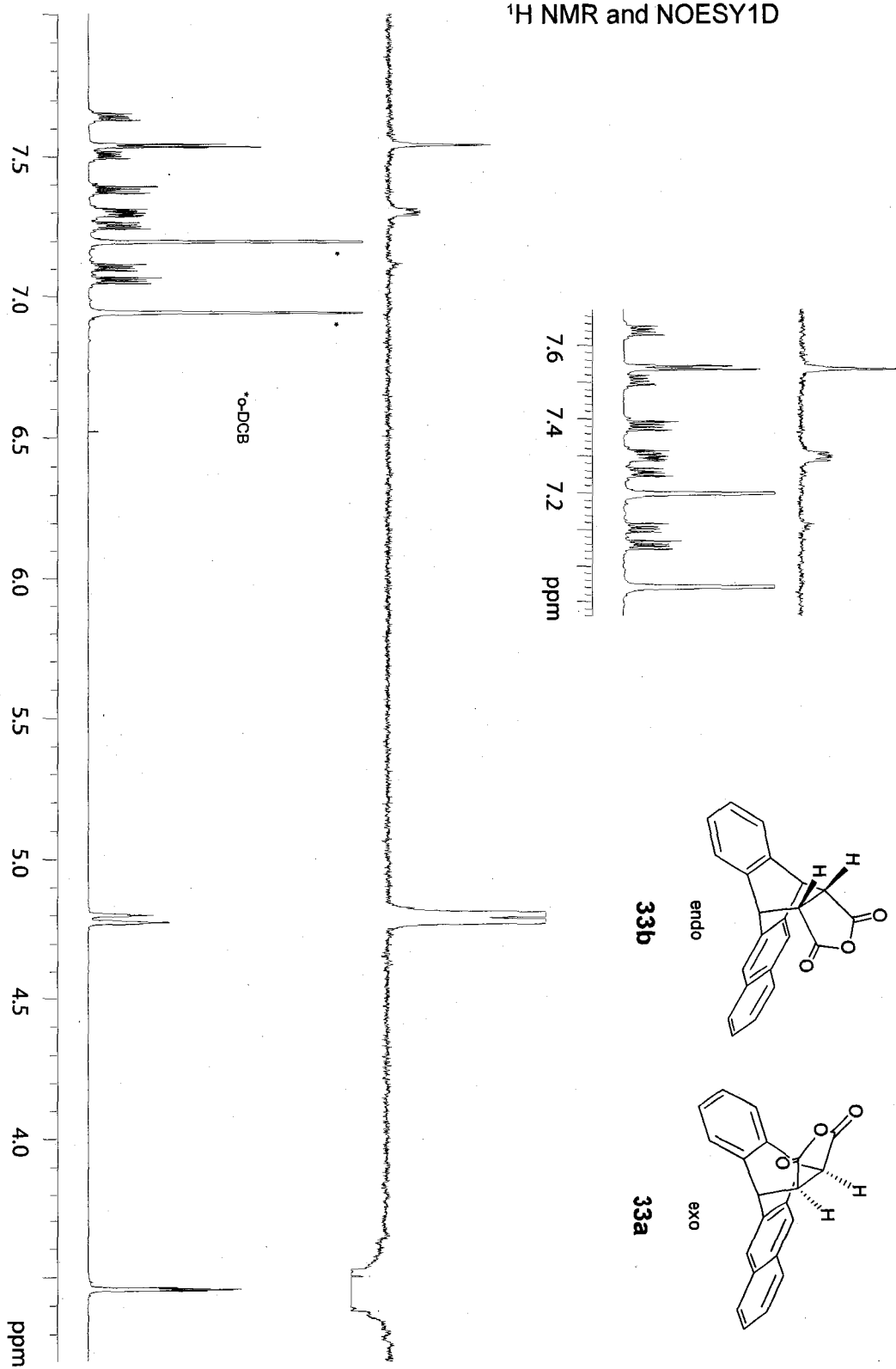
# NOESY2D



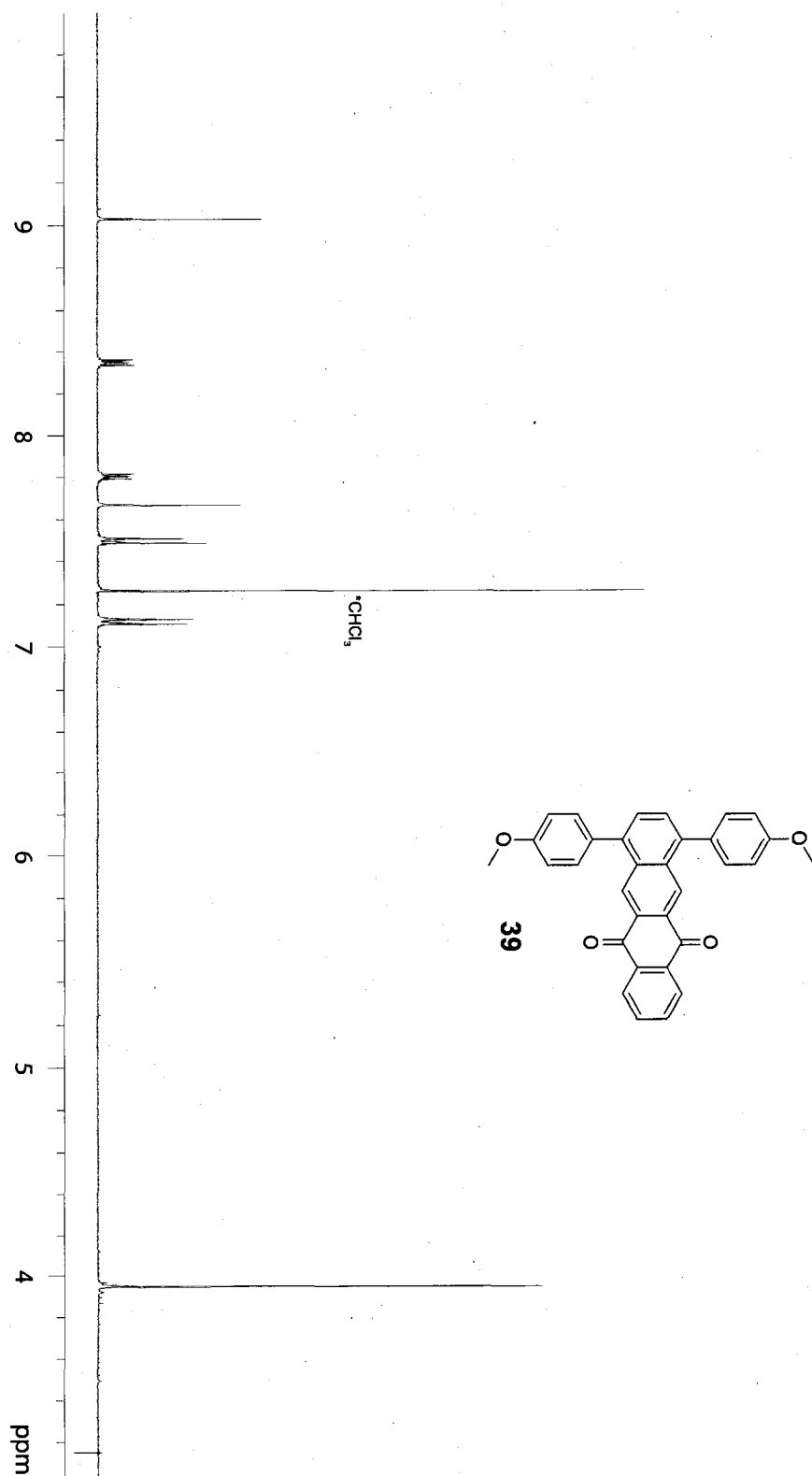
<sup>1</sup>H NMR and NOESY1D



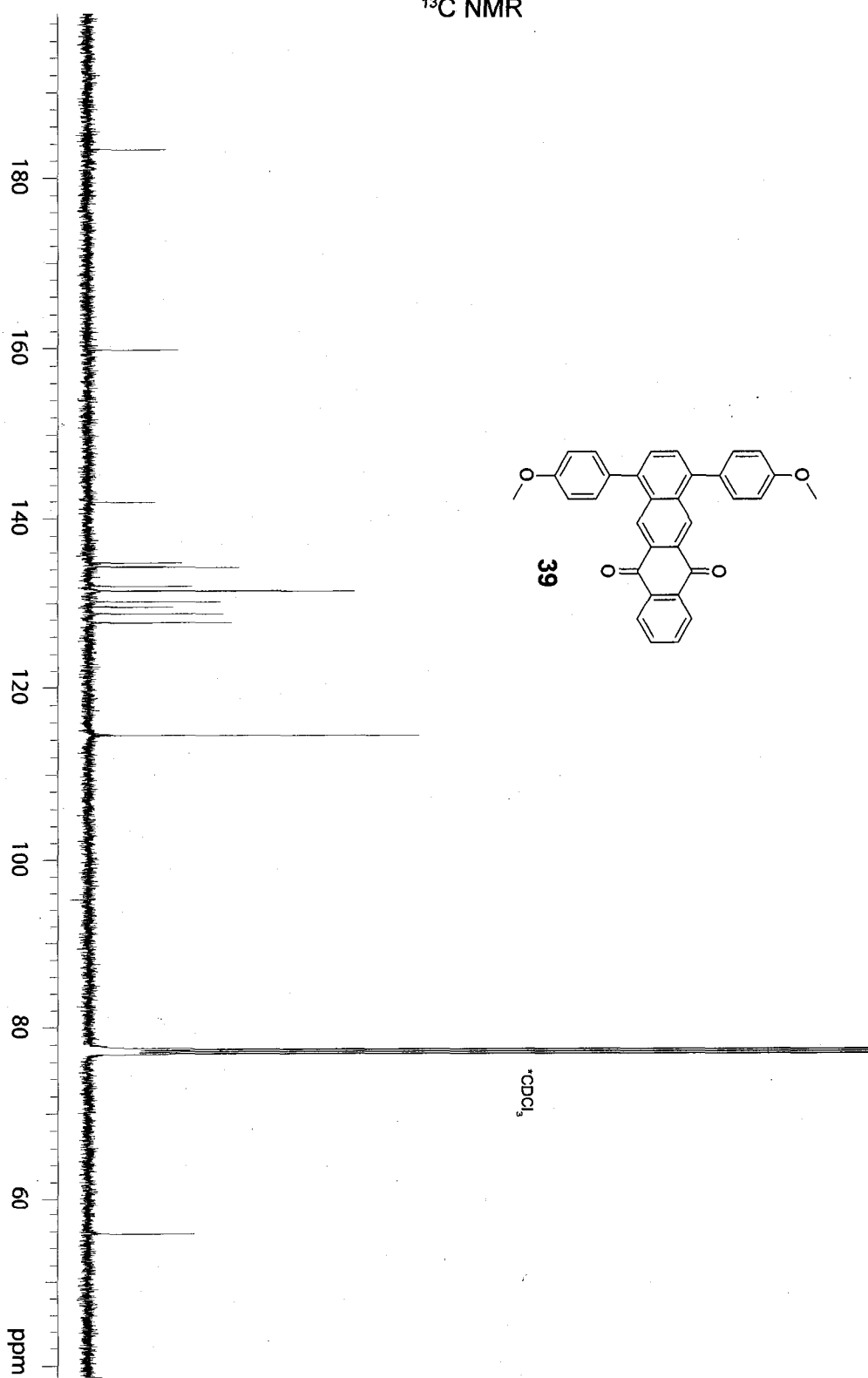
<sup>1</sup>H NMR and NOESY1D



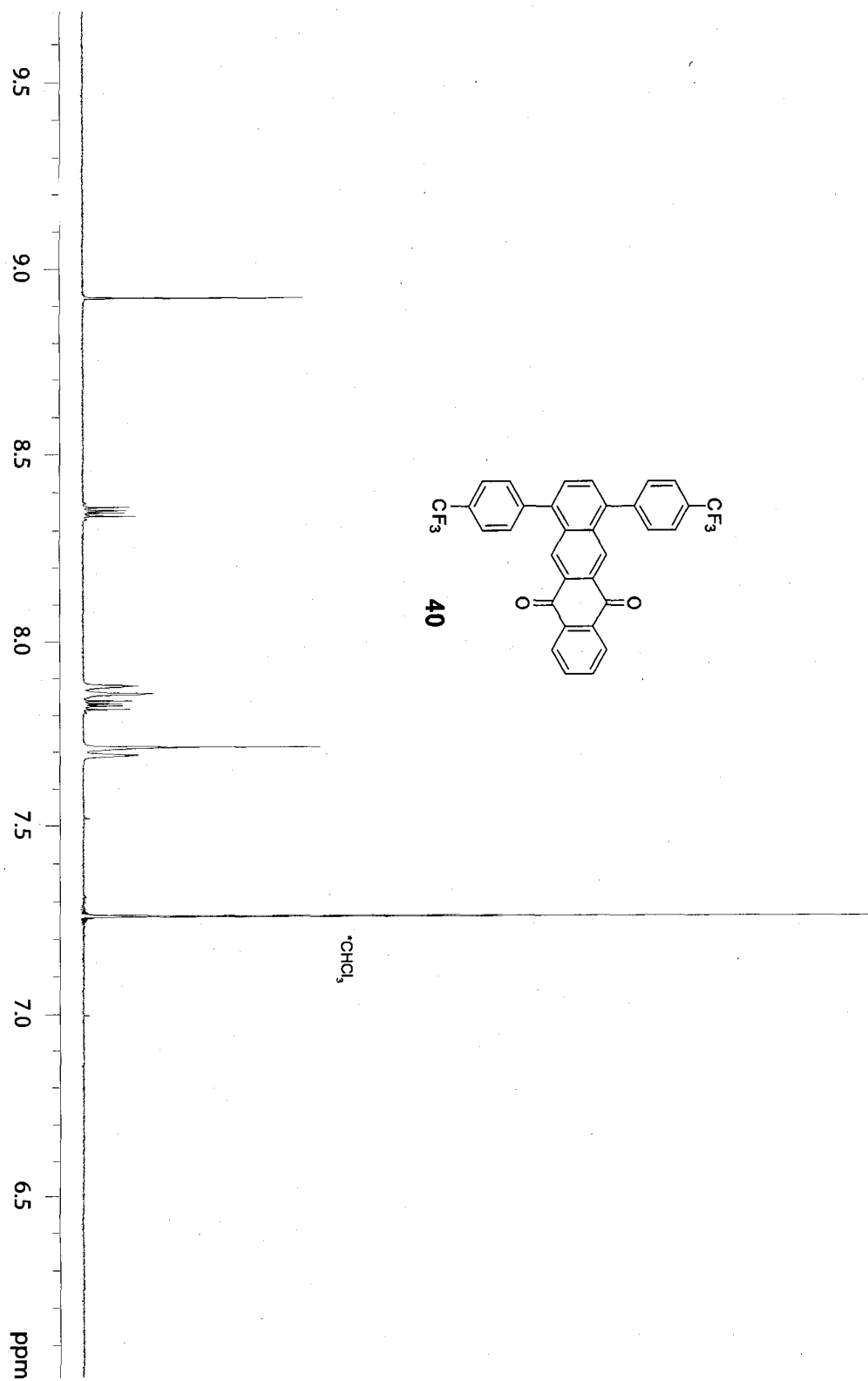
<sup>1</sup>H NMR



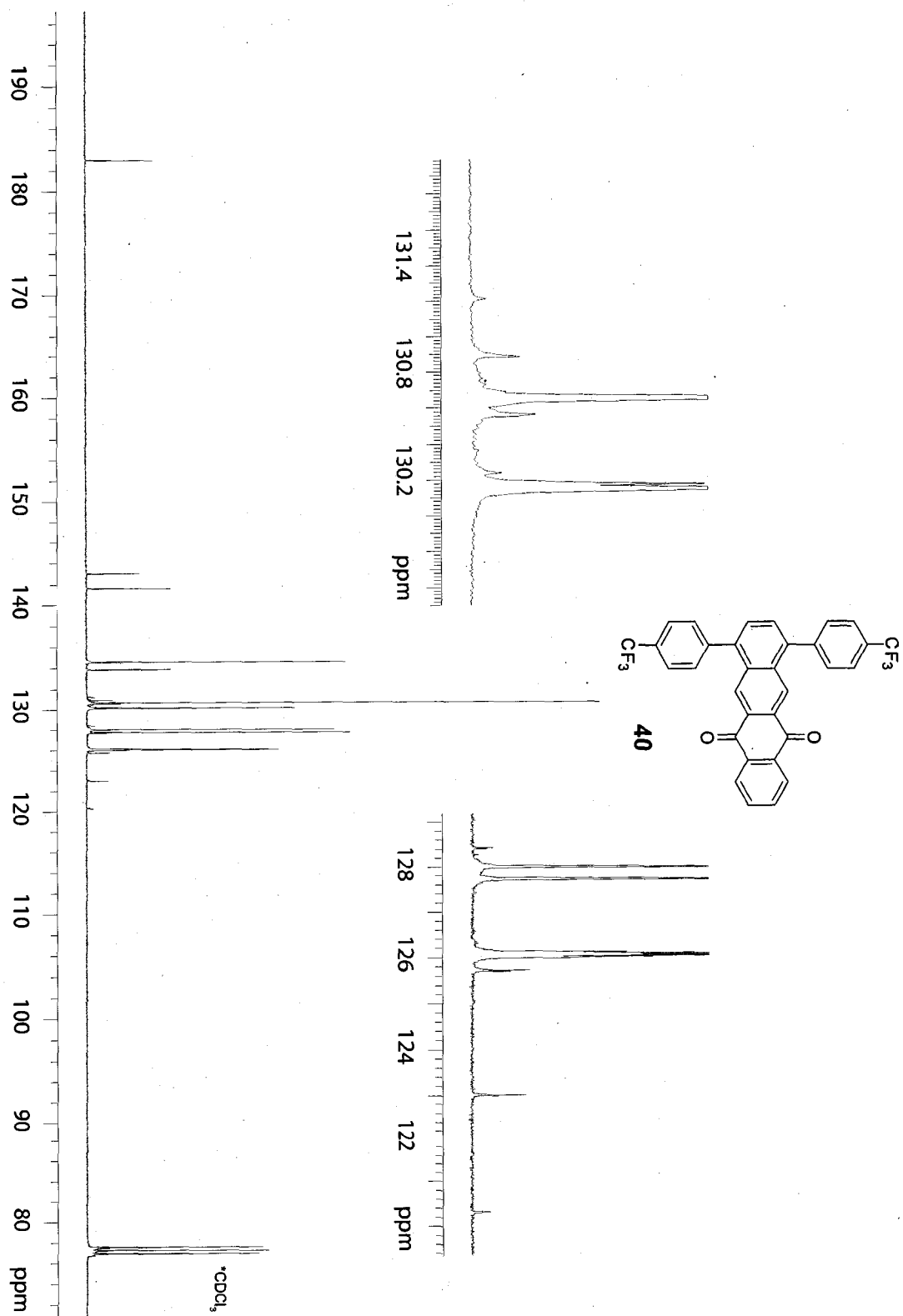
<sup>13</sup>C NMR



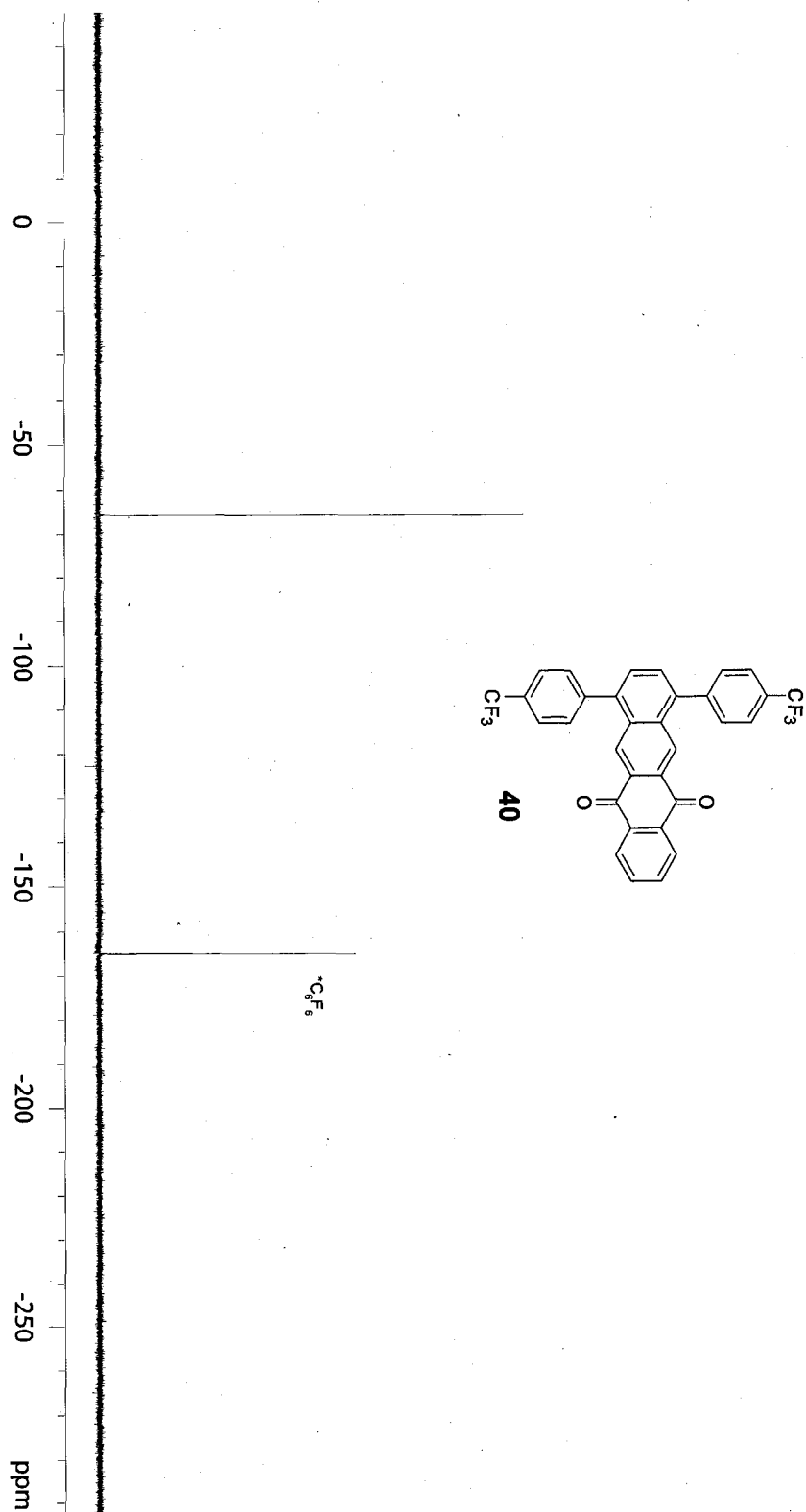
<sup>1</sup>H NMR



<sup>13</sup>C NMR

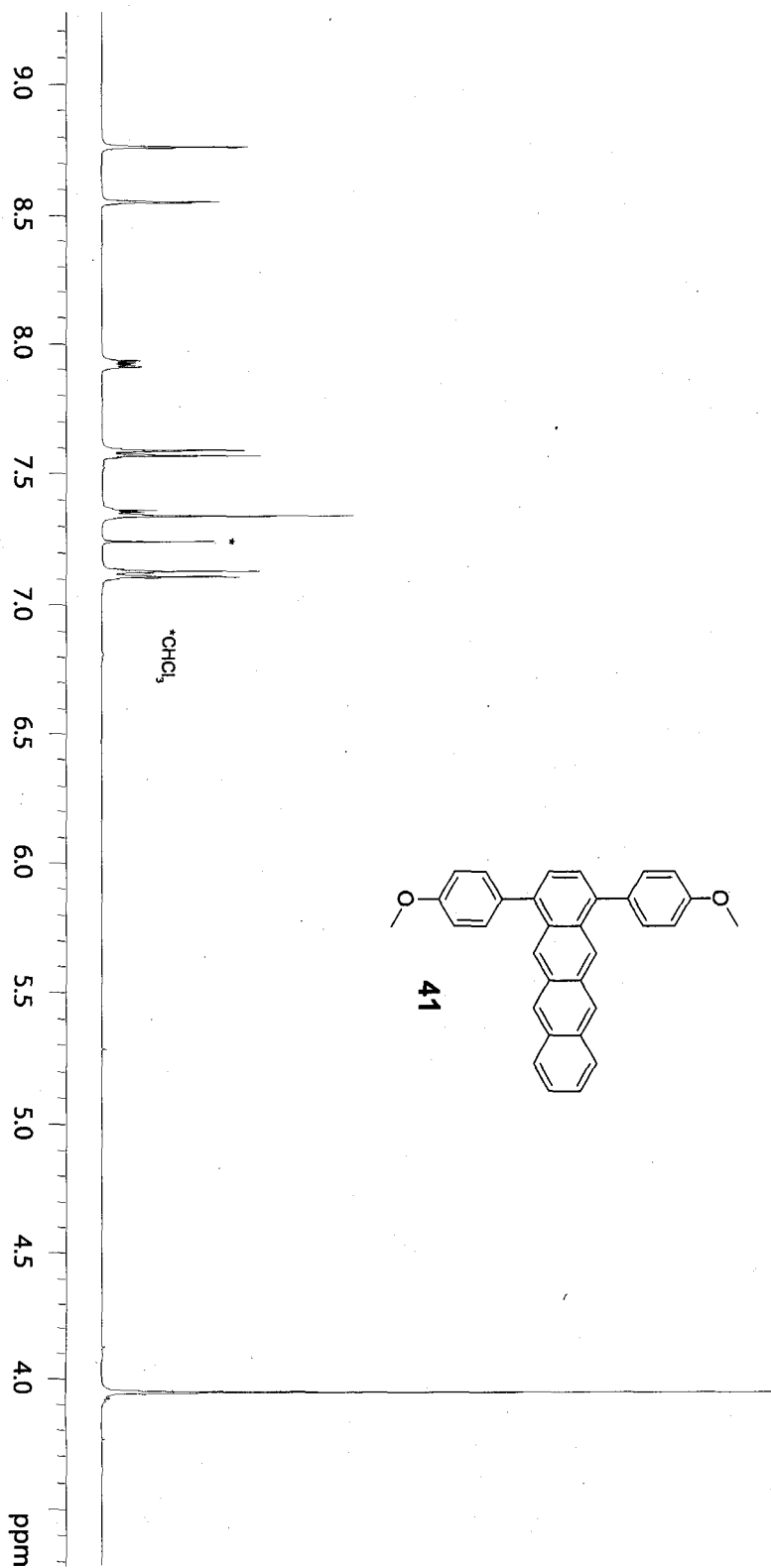


<sup>19</sup>F NMR

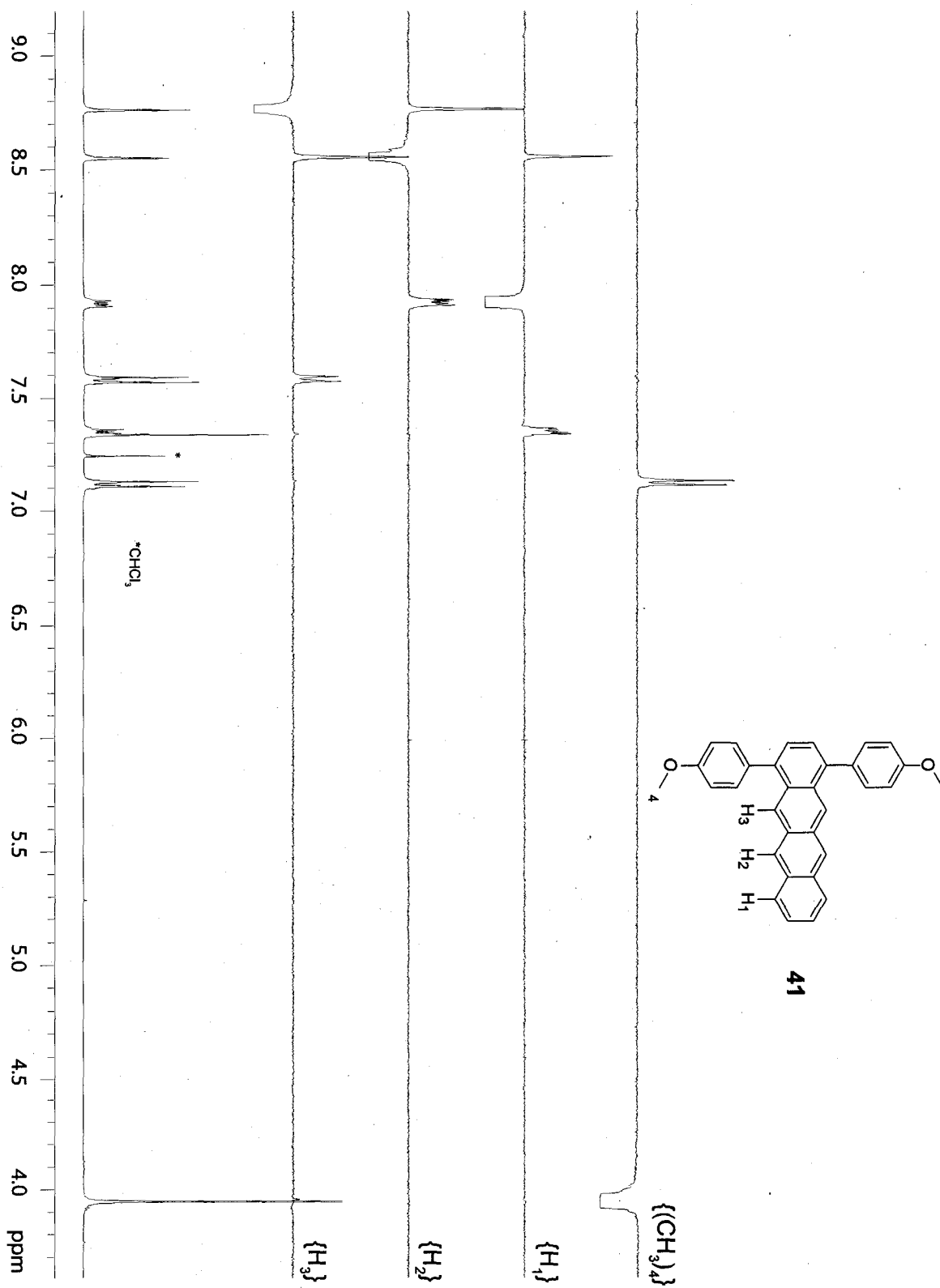




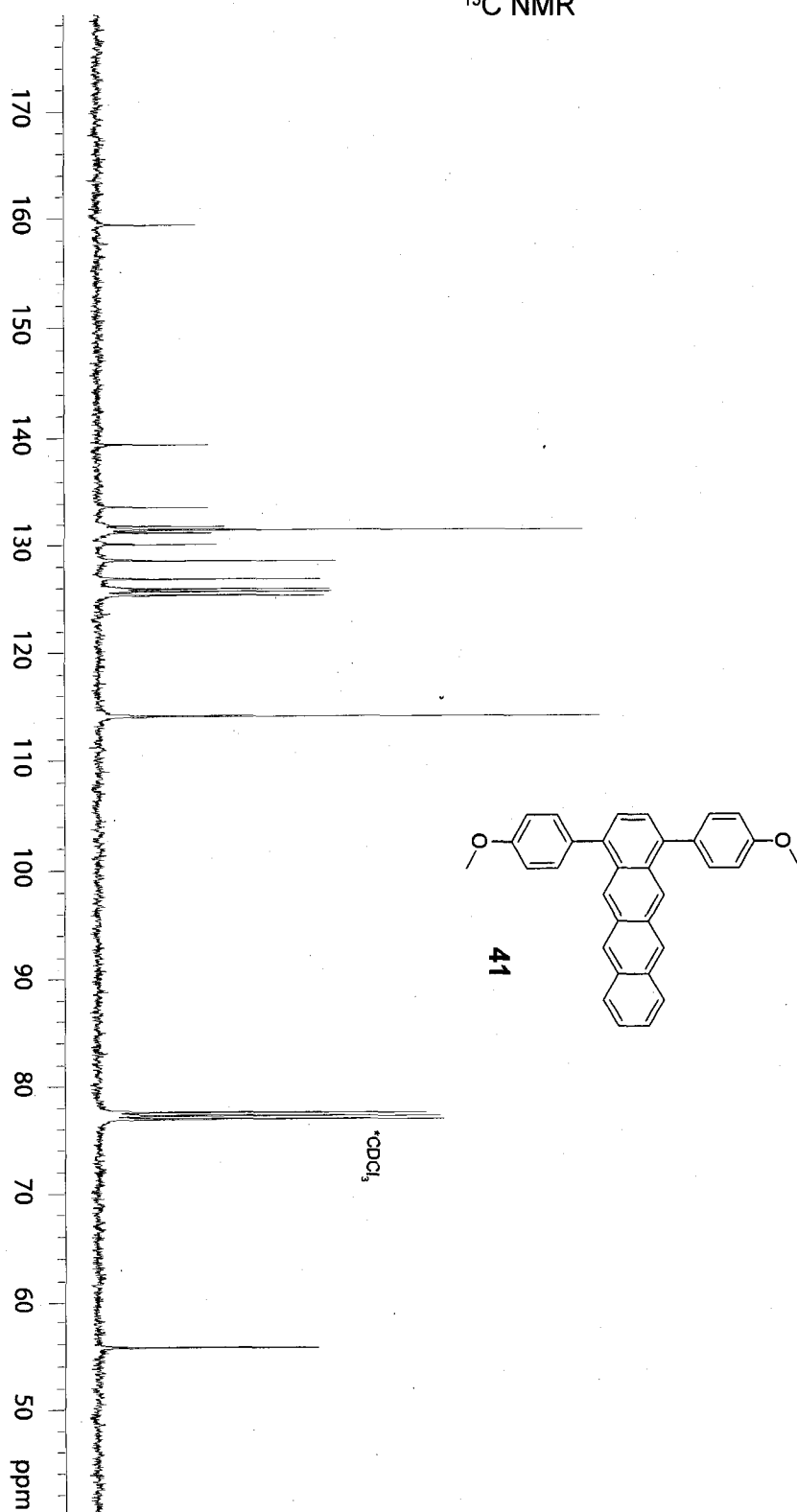
<sup>1</sup>H NMR



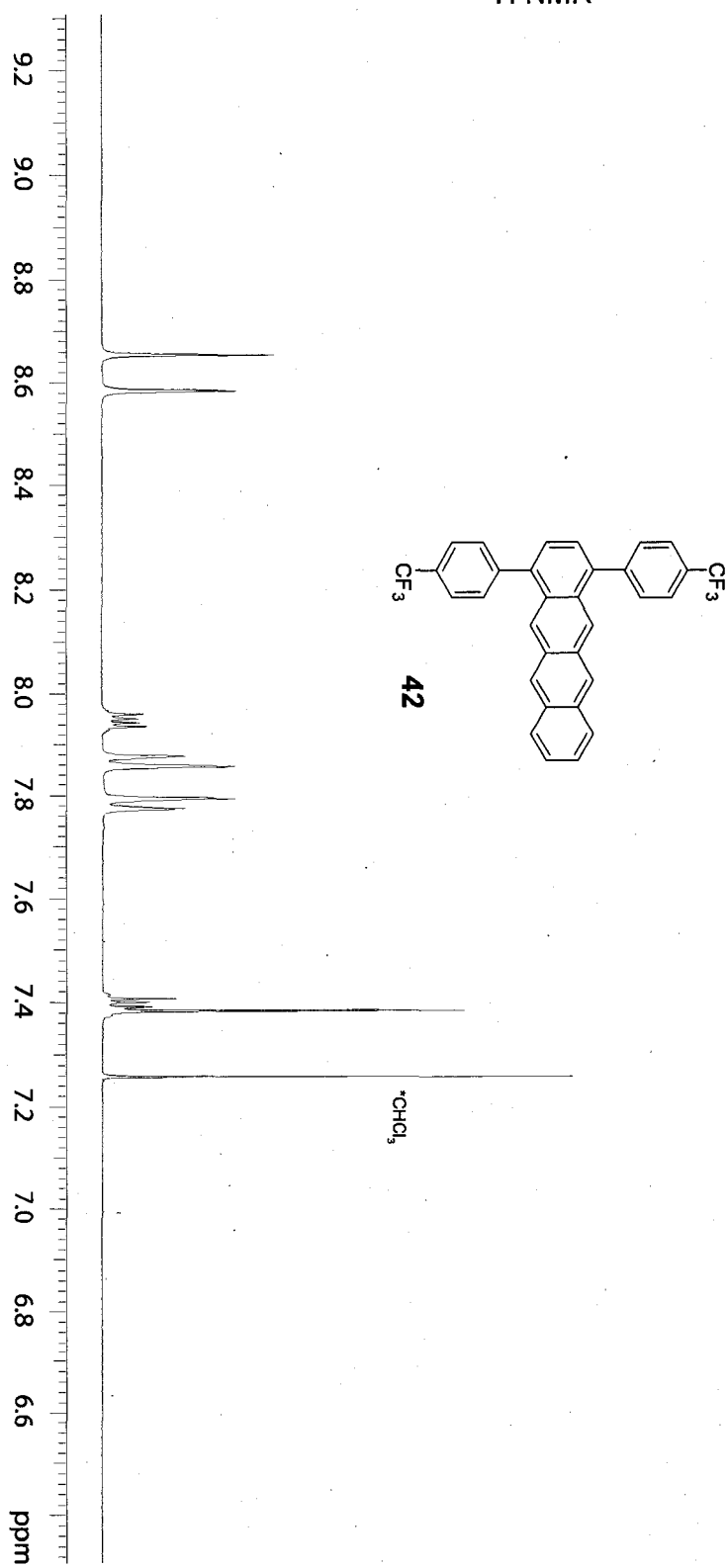
<sup>1</sup>H NMR and NOESY1D



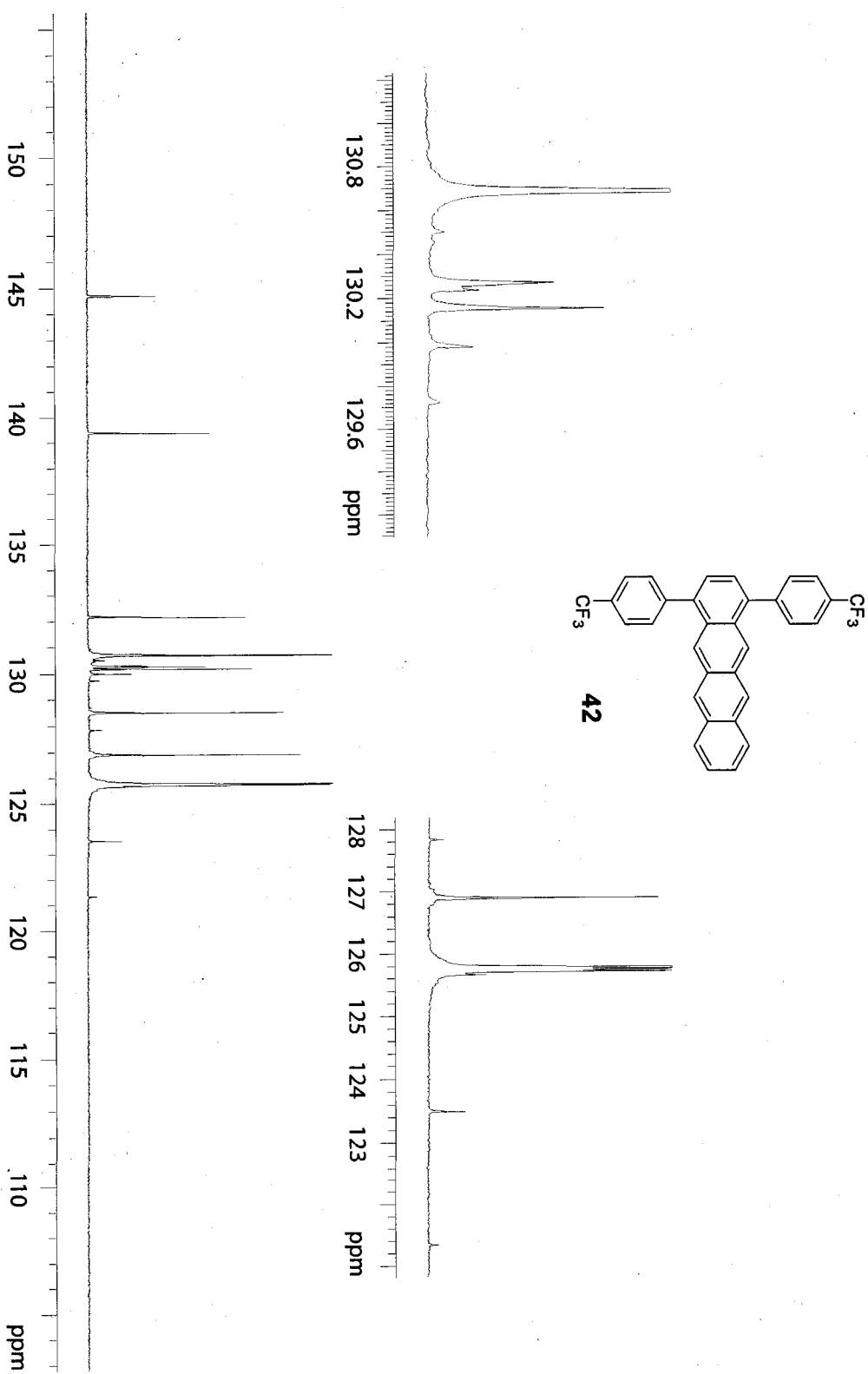
<sup>13</sup>C NMR



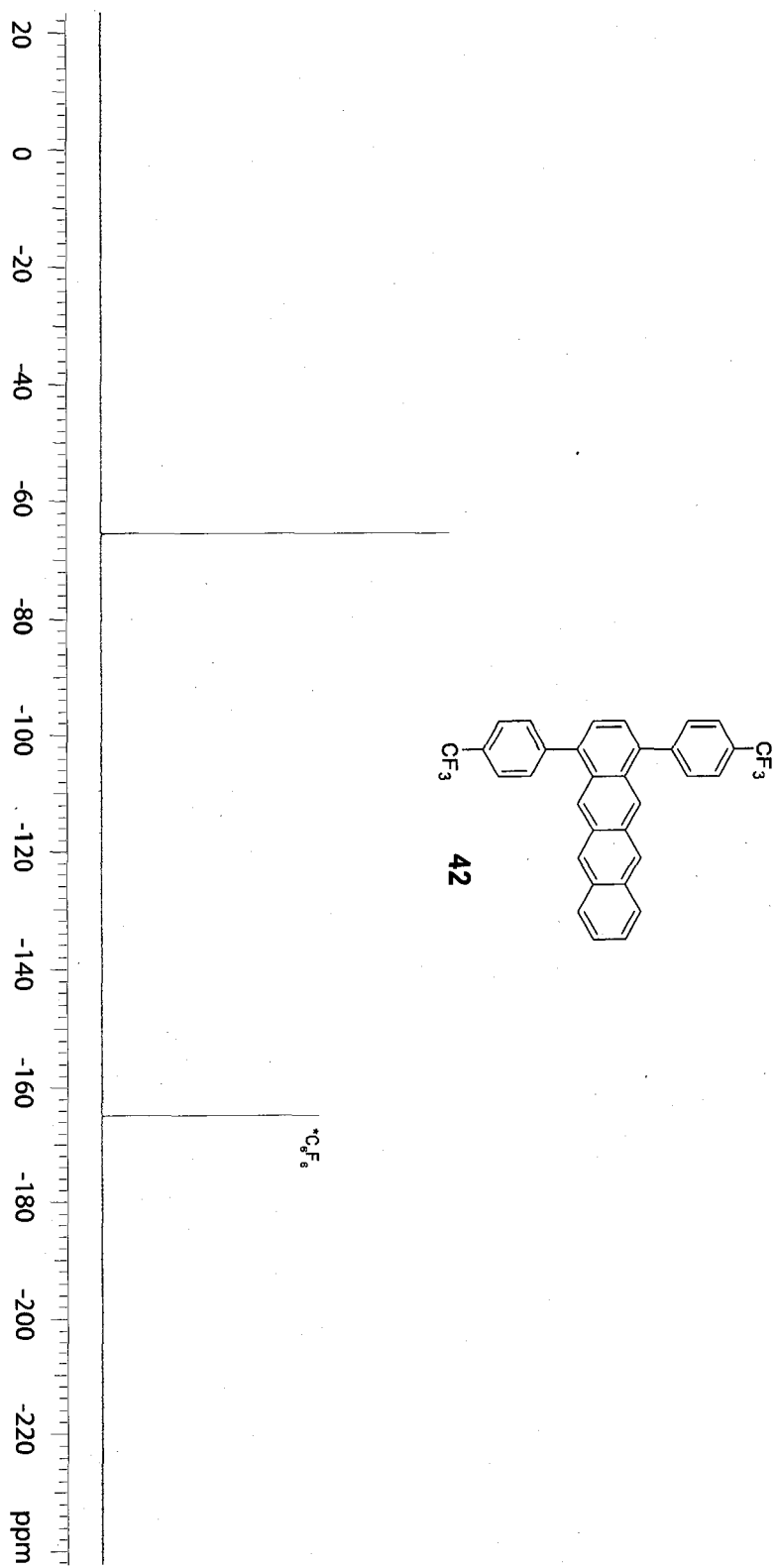
<sup>1</sup>H NMR

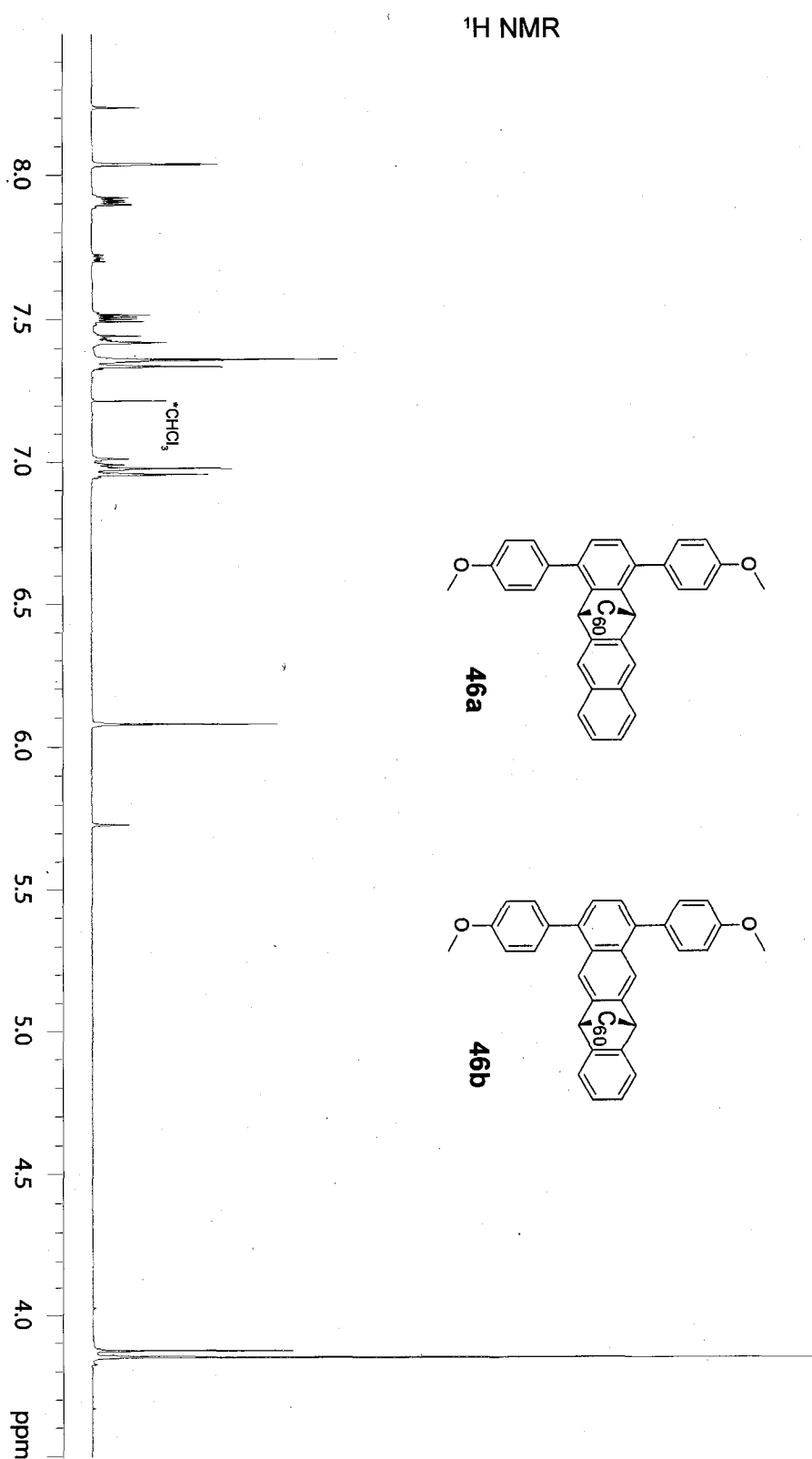


<sup>13</sup>C NMR

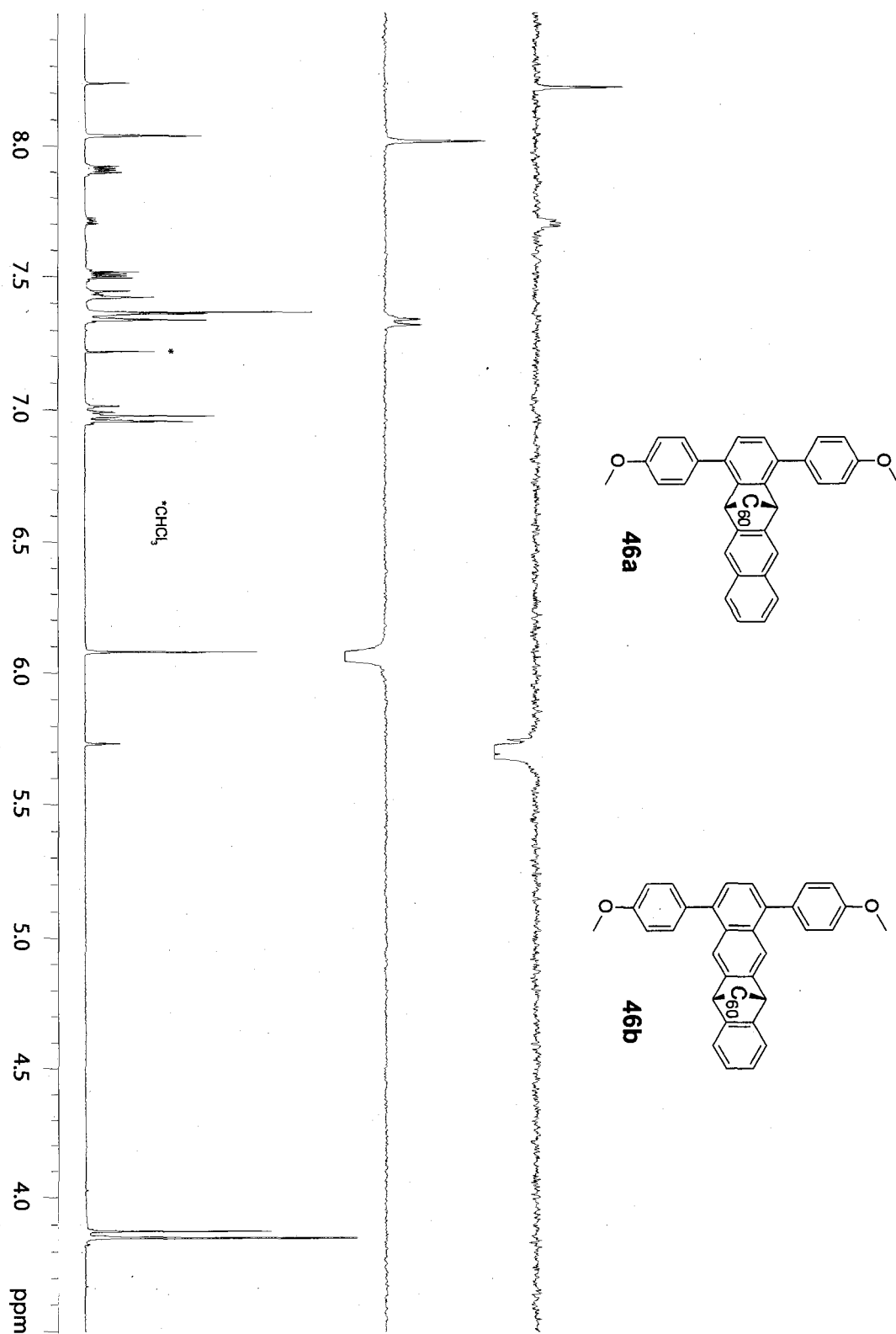


<sup>19</sup>F NMR



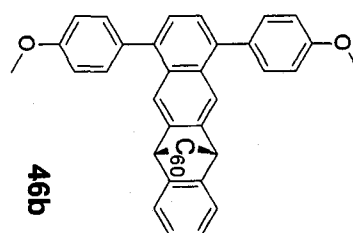
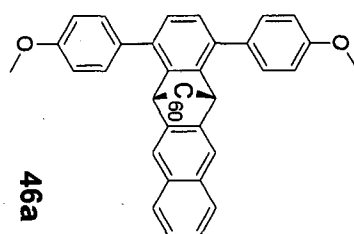
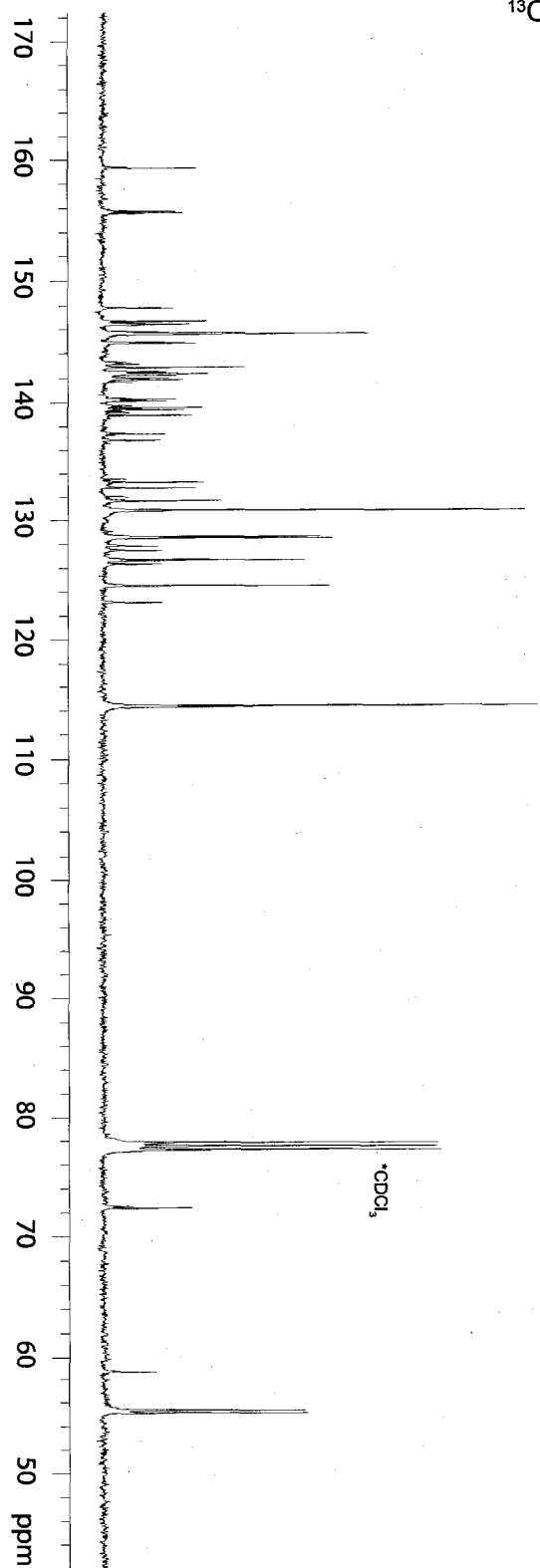


<sup>1</sup>H NMR and NOESY1D

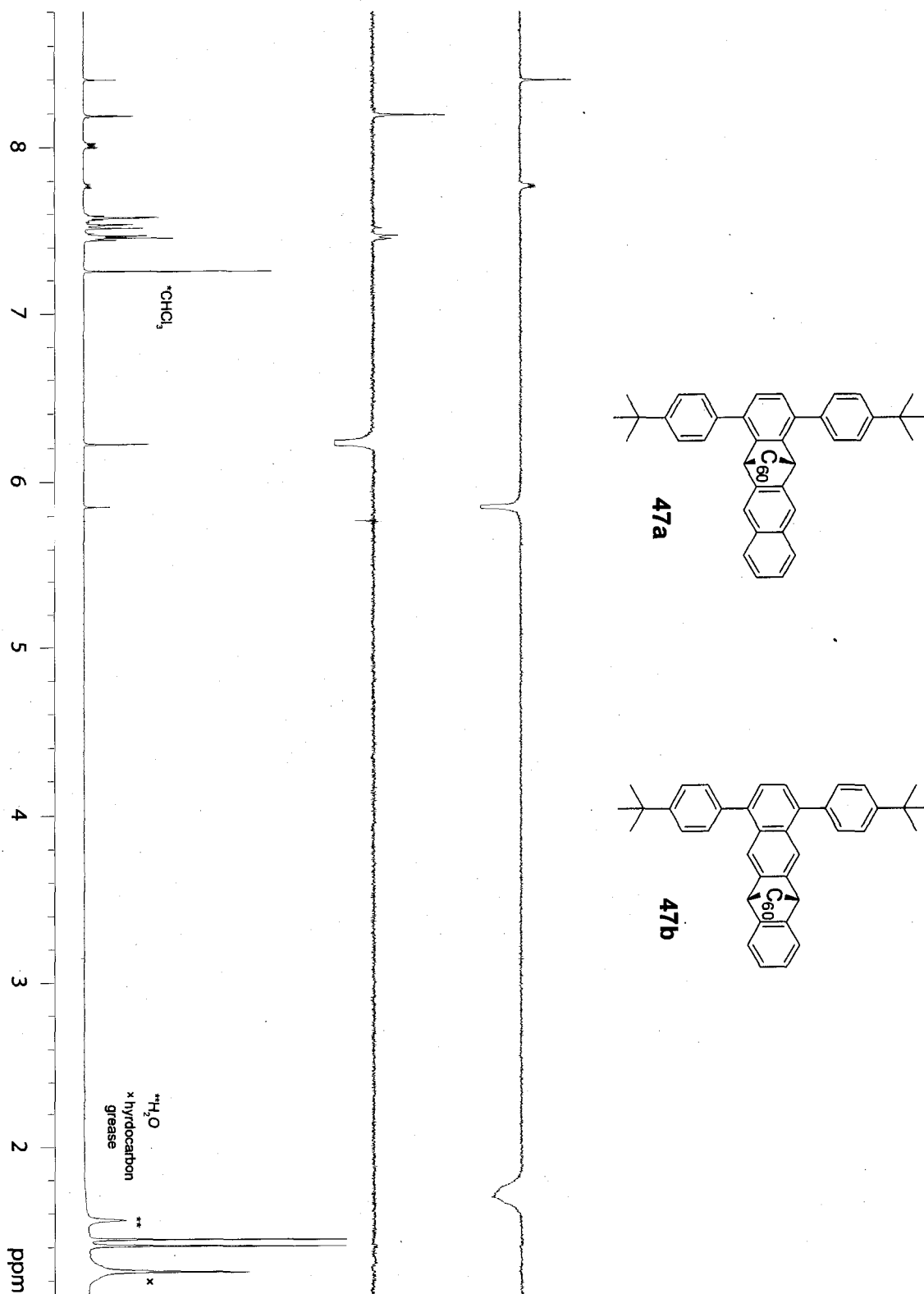




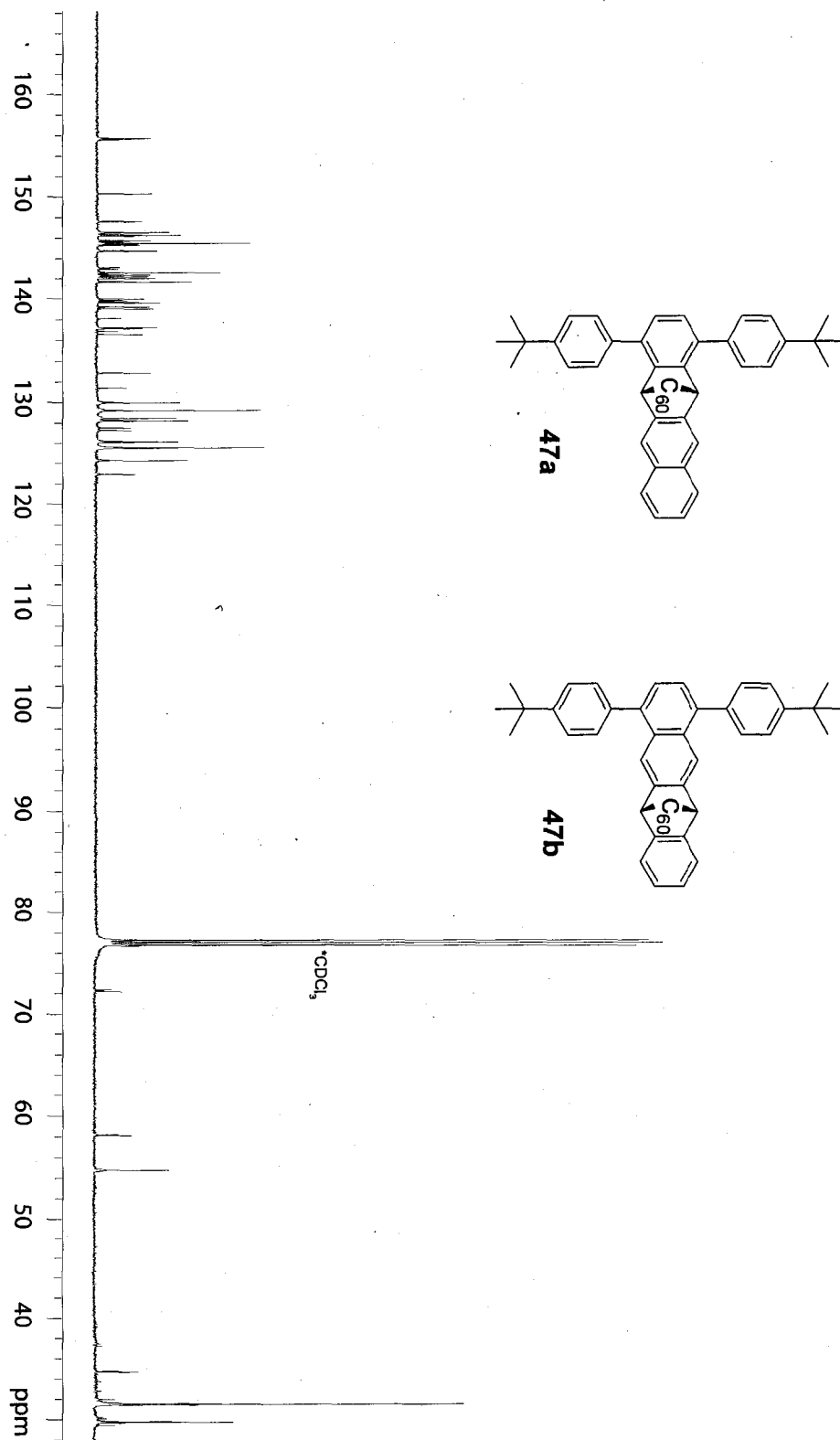
<sup>13</sup>C NMR



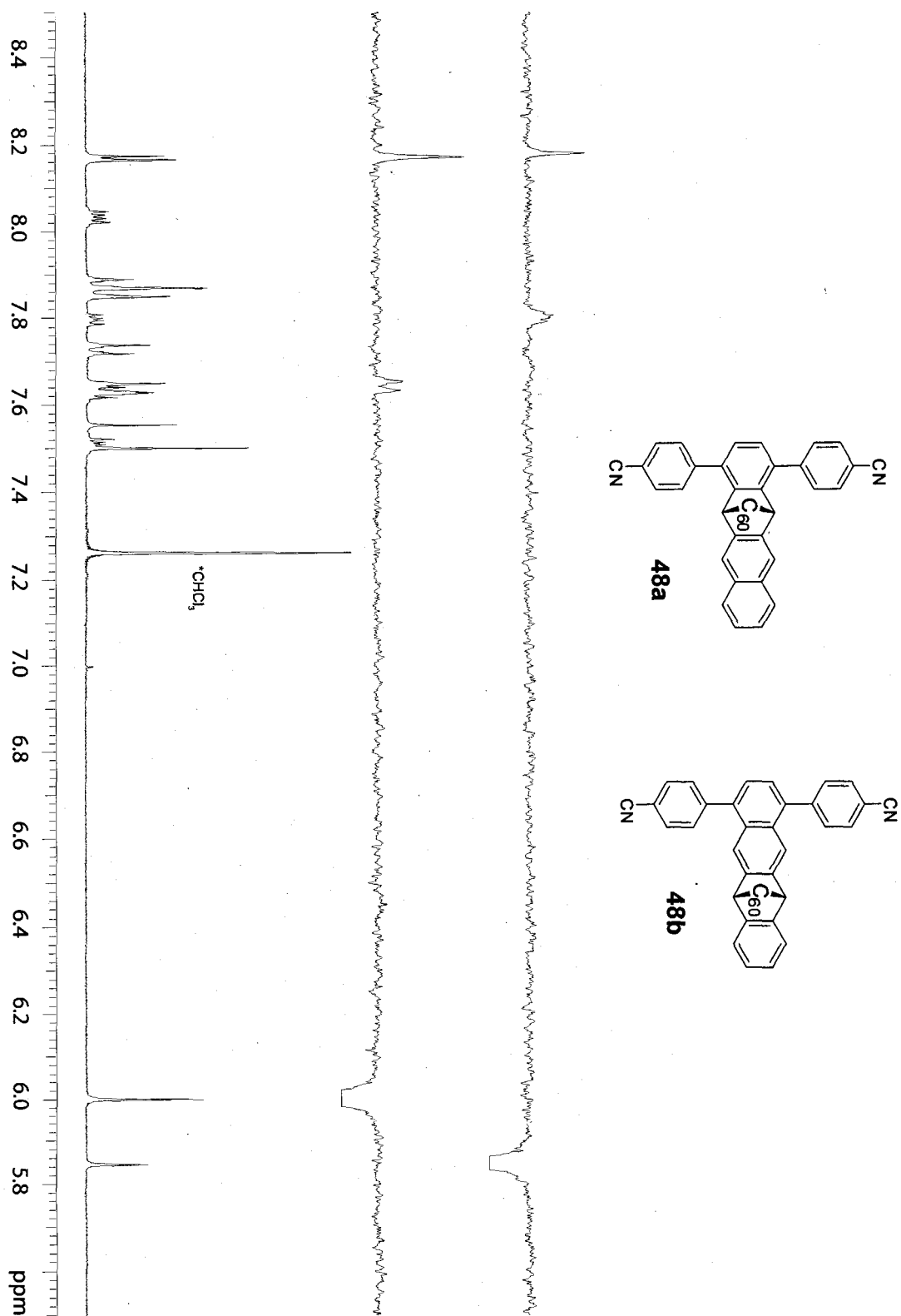
<sup>1</sup>H NMR and NOESY1D



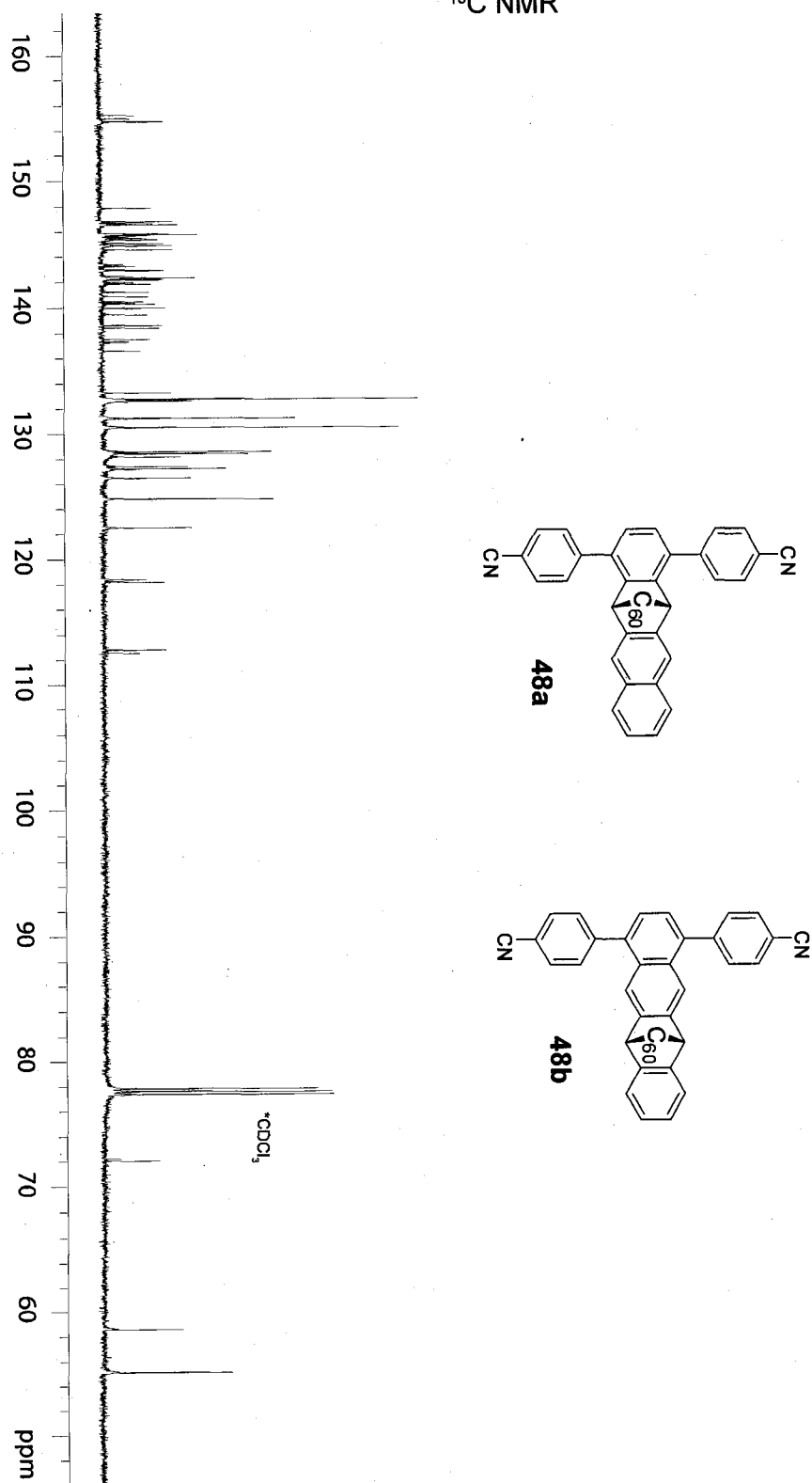
<sup>13</sup>C NMR



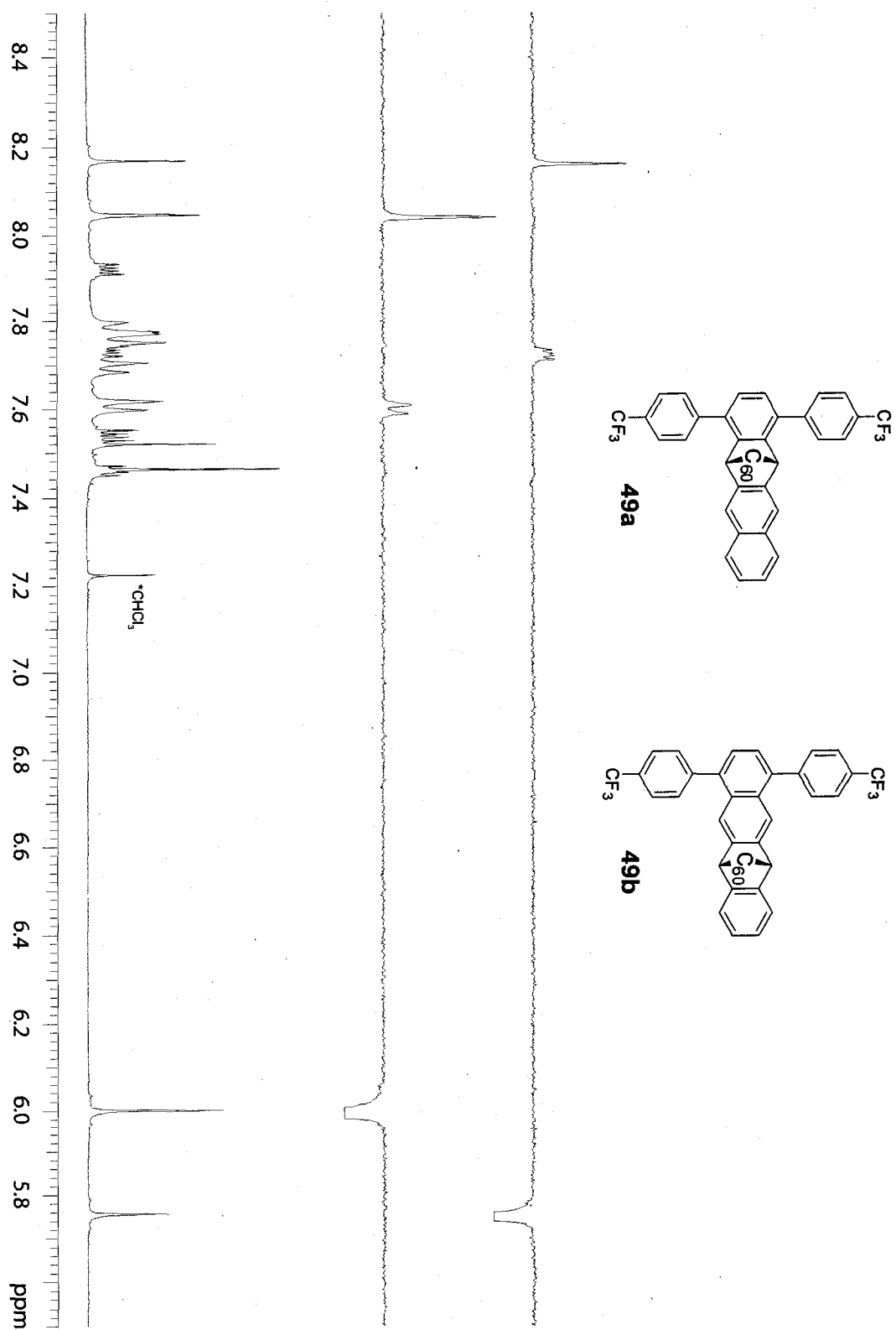
<sup>1</sup>H NMR and NOESY1D



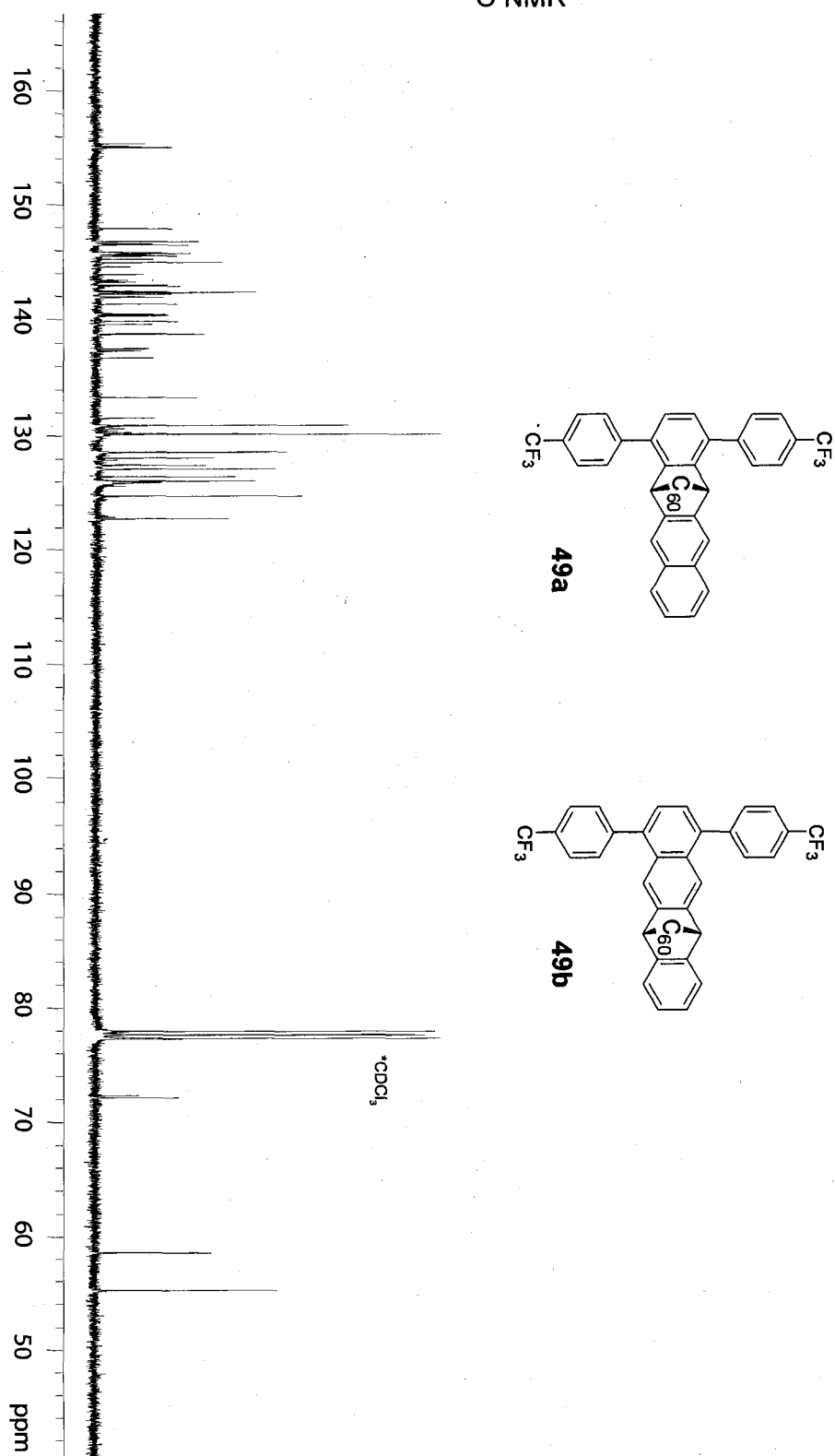
<sup>13</sup>C NMR



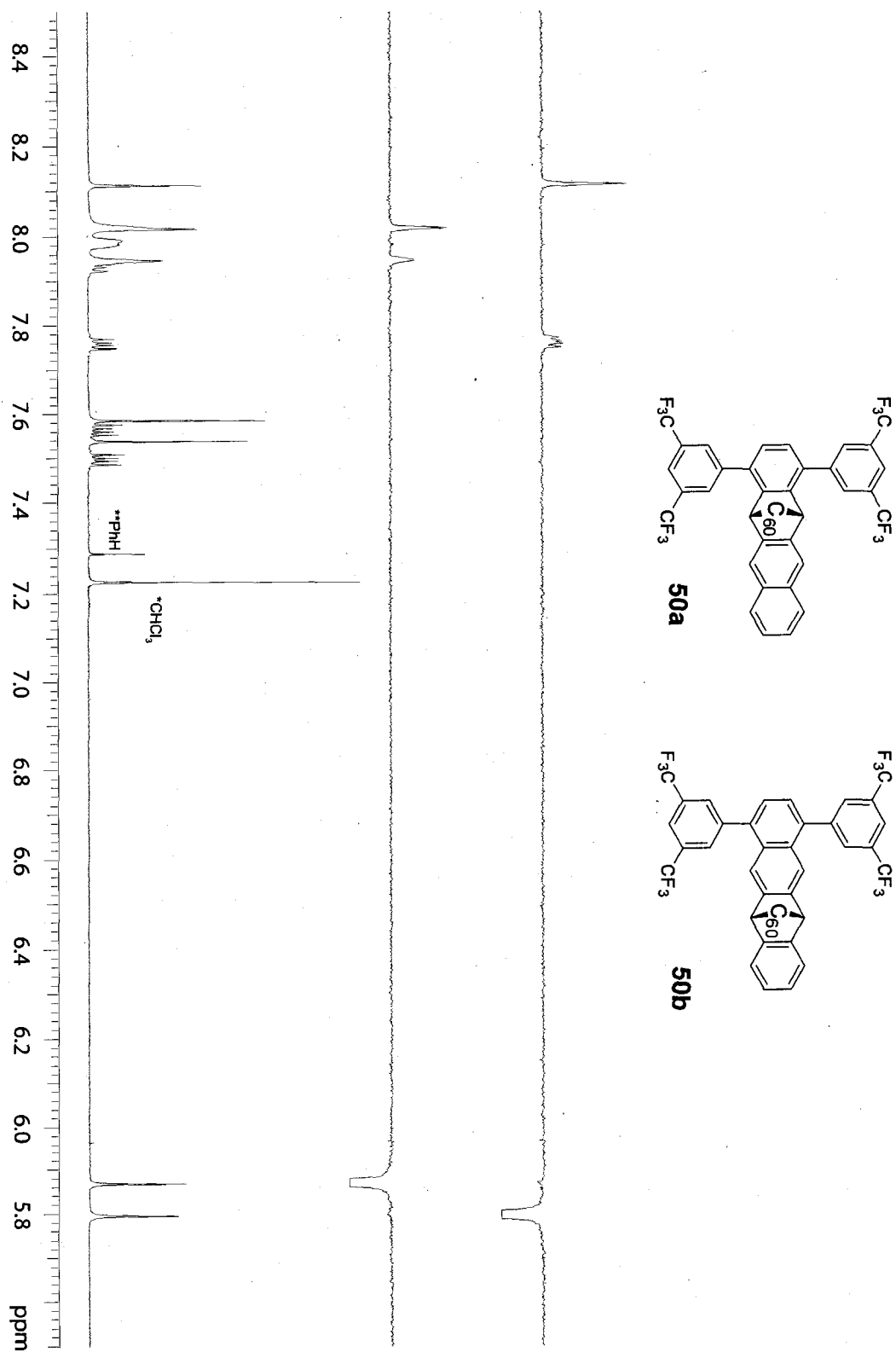
<sup>1</sup>H NMR and NOESY1D



<sup>13</sup>C NMR

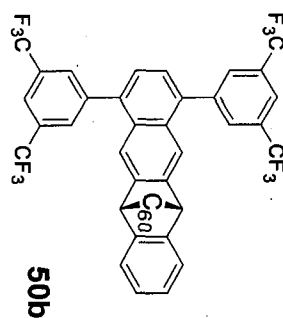
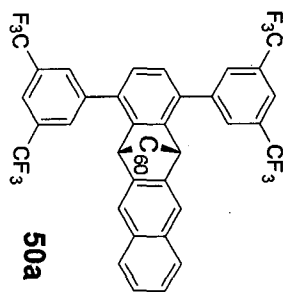
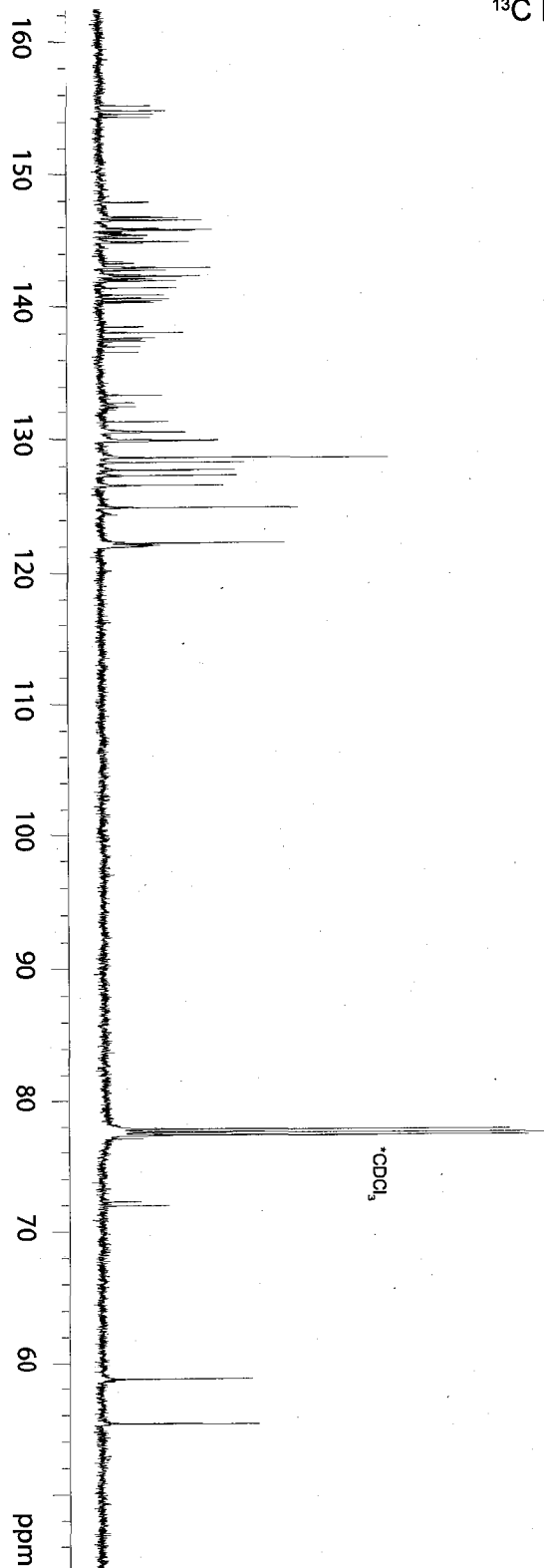


<sup>1</sup>H NMR and NOESY1D

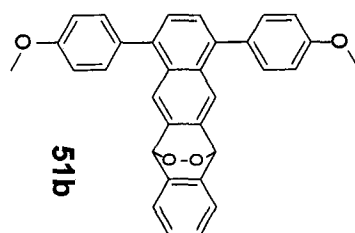
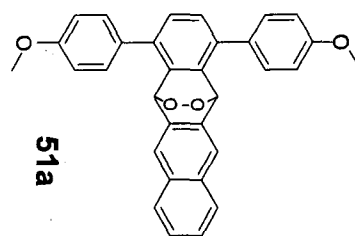
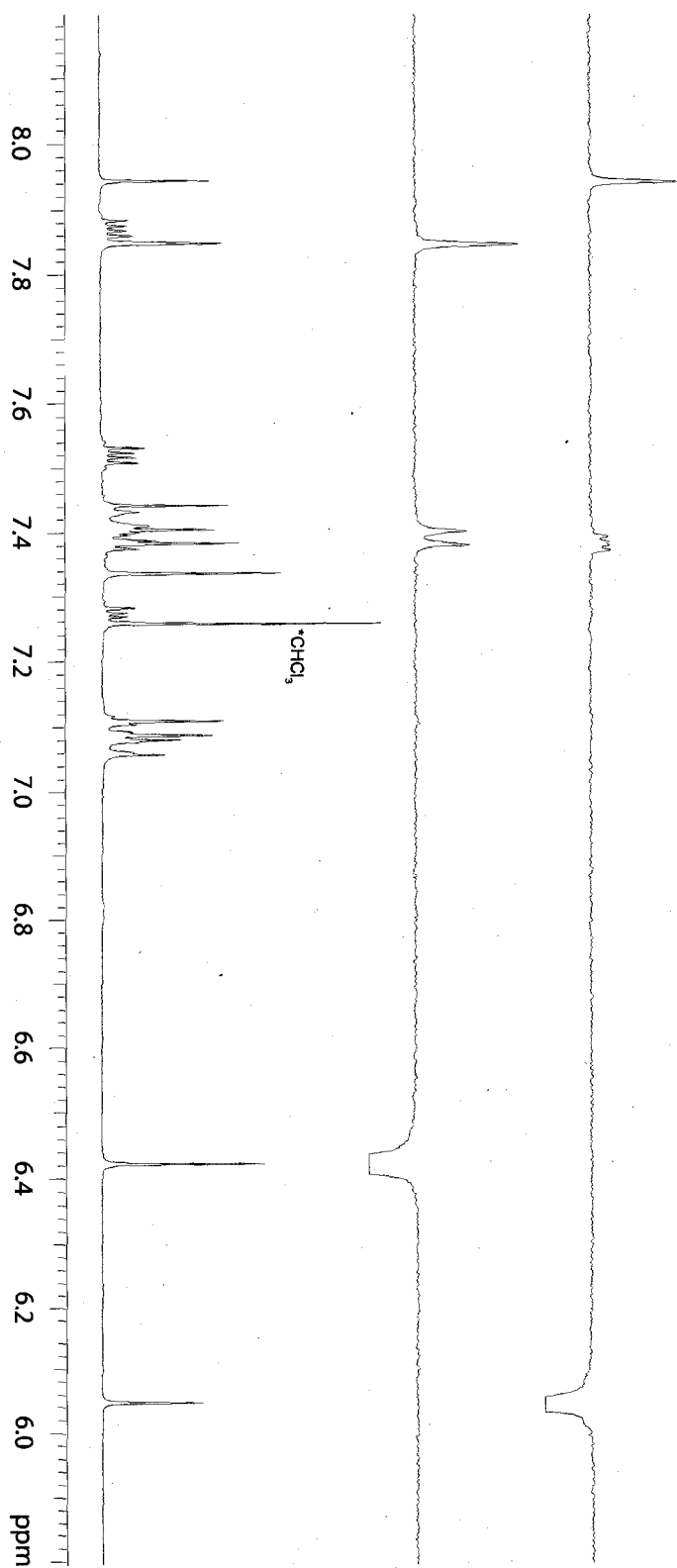




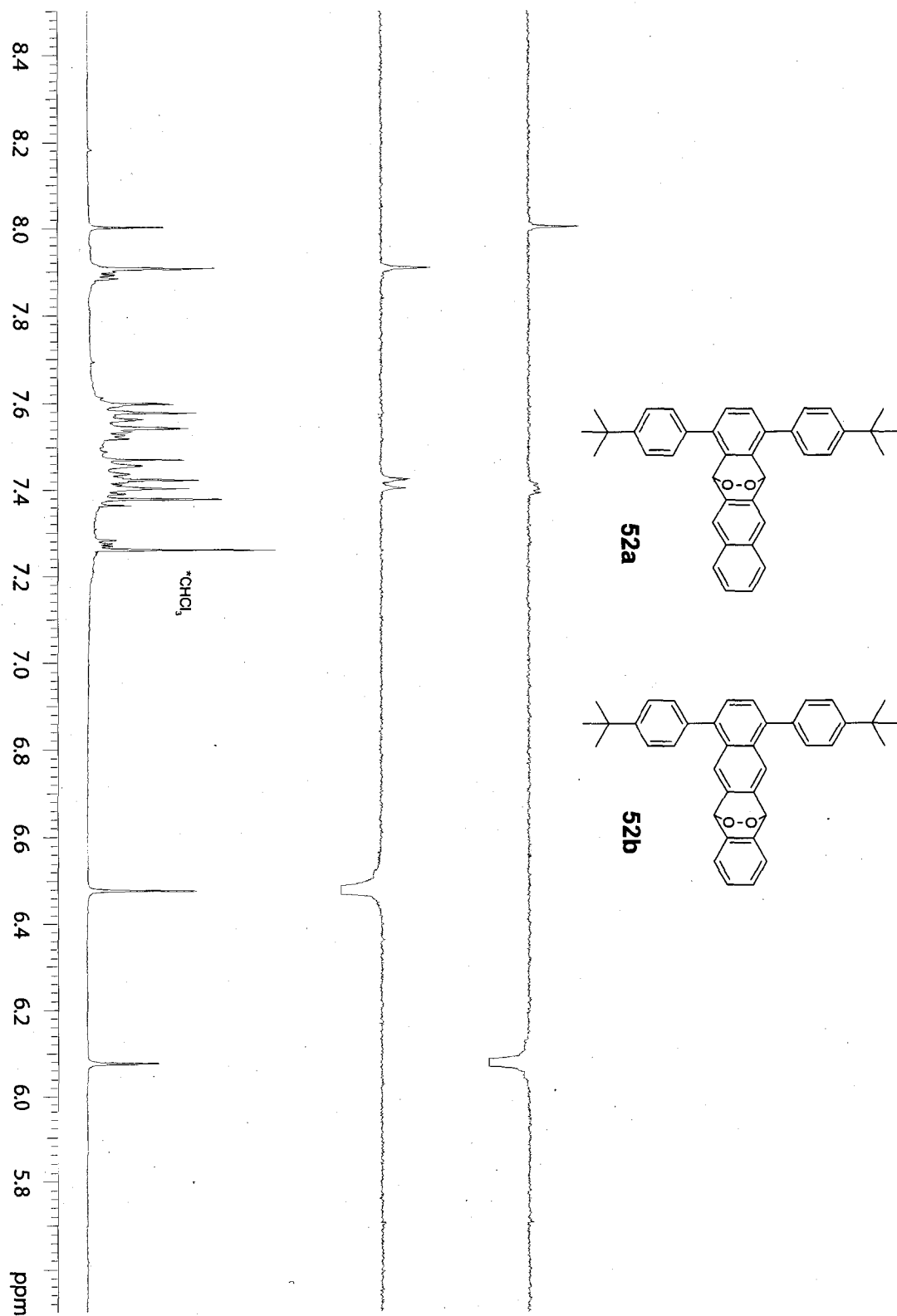
<sup>13</sup>C NMR



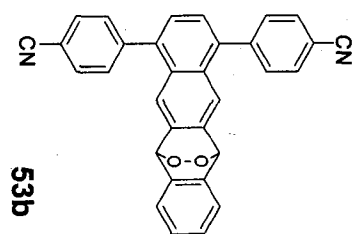
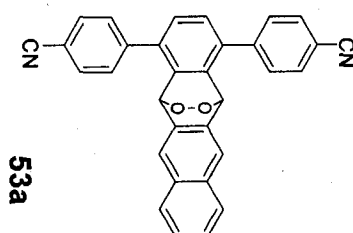
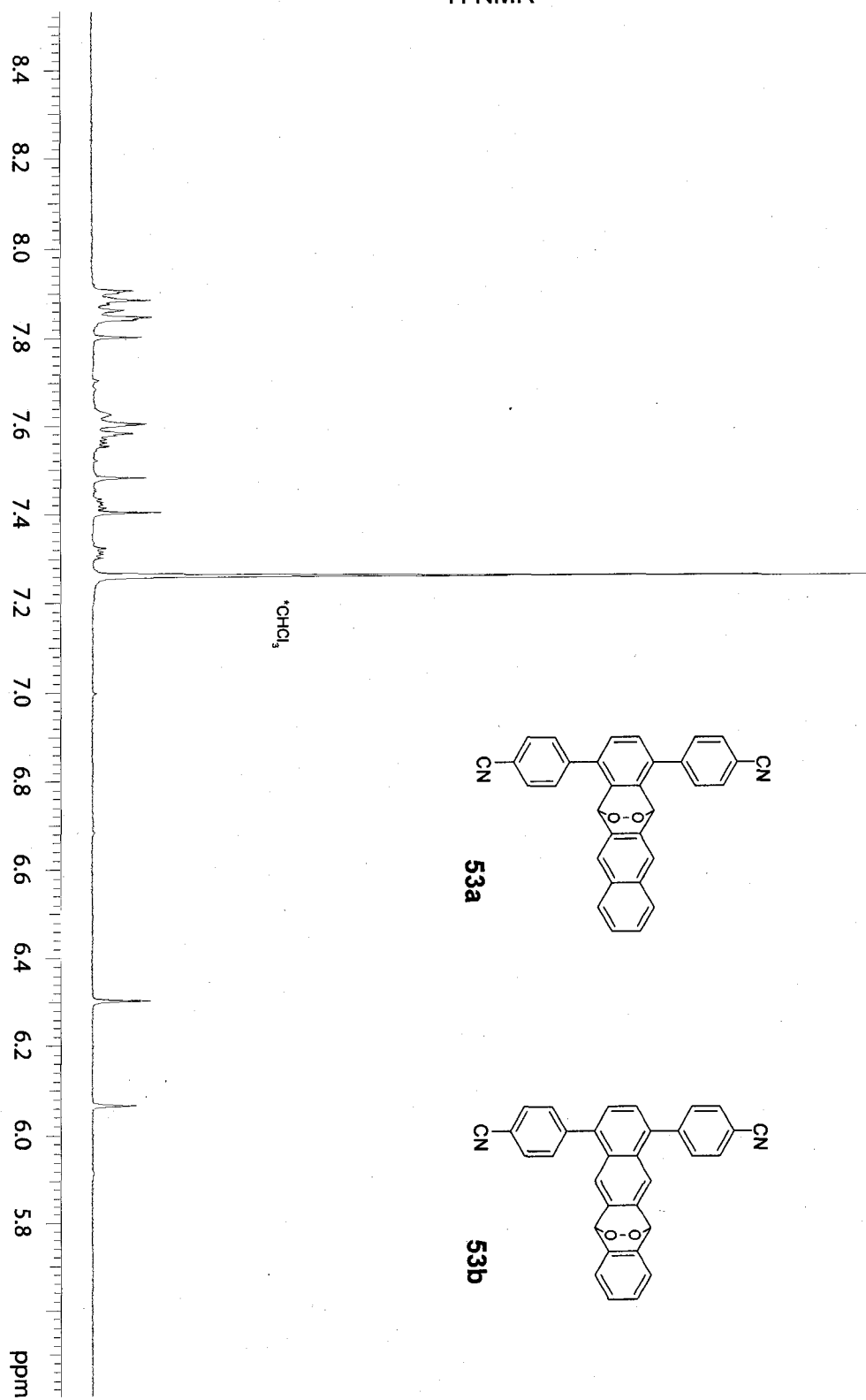
<sup>1</sup>H NMR and NOESY1D



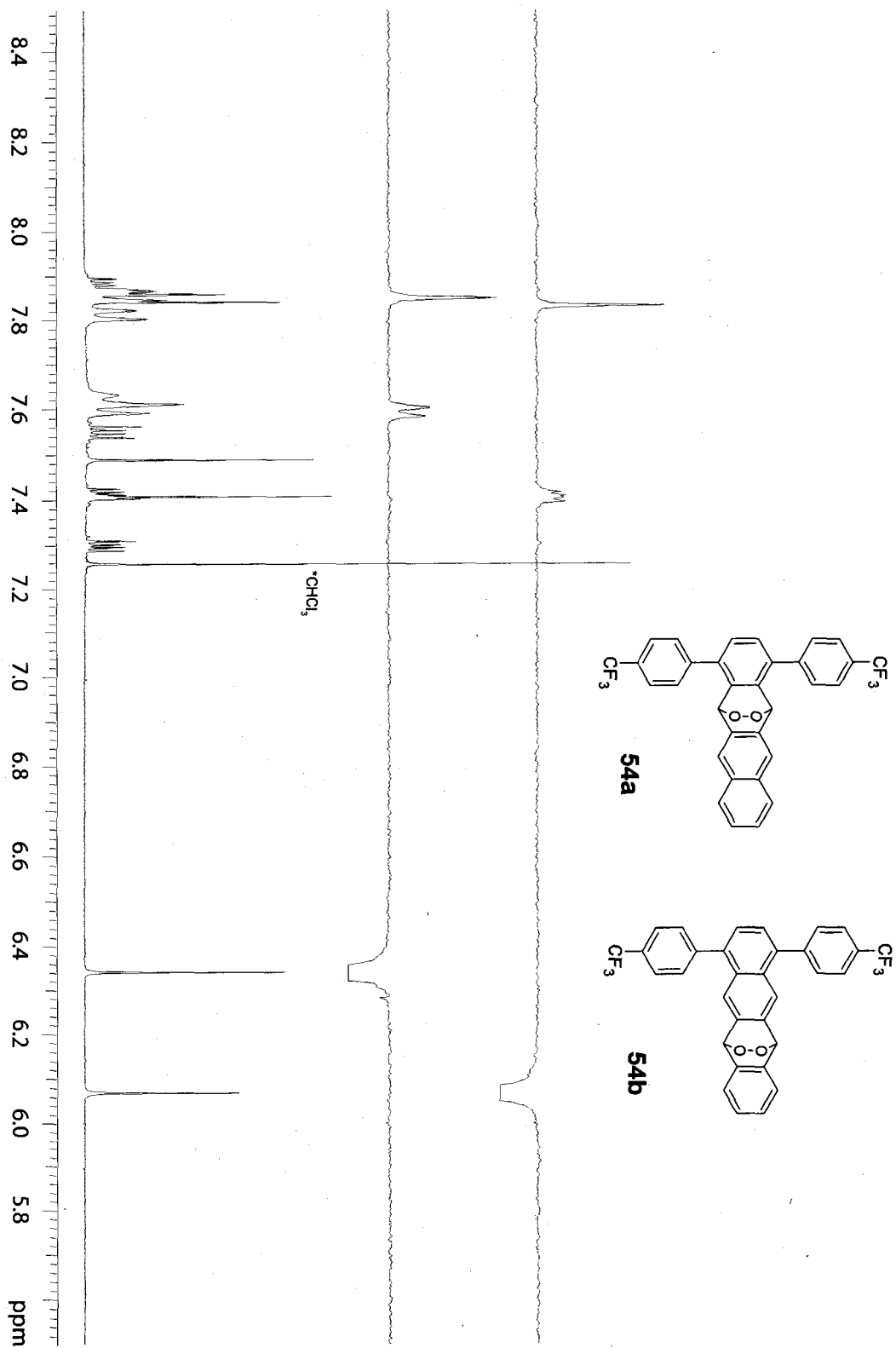
<sup>1</sup>H NMR and NOESY1D



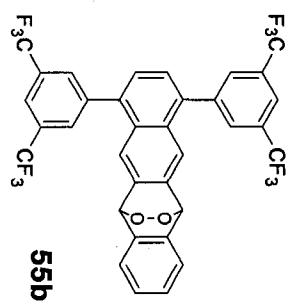
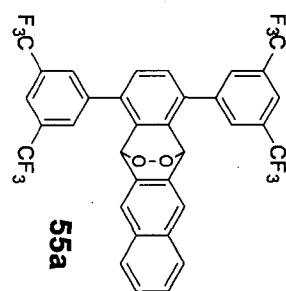
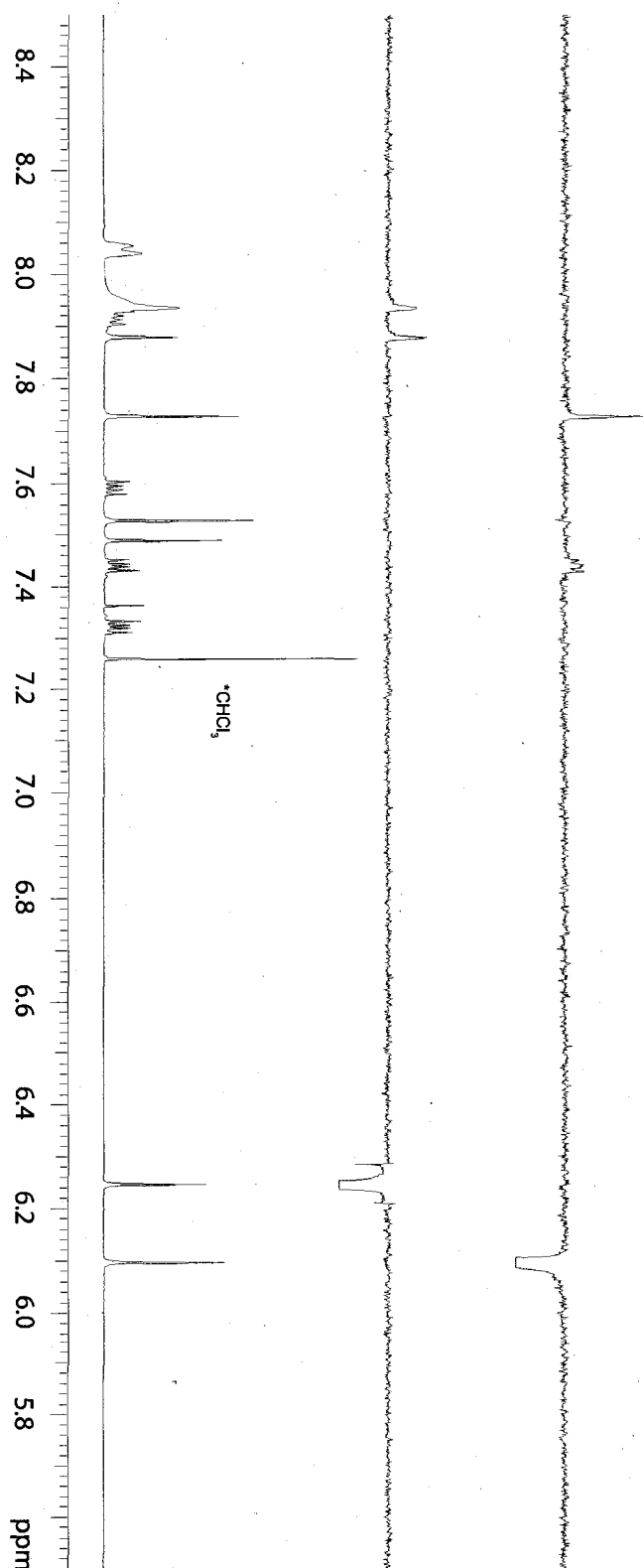
<sup>1</sup>H NMR

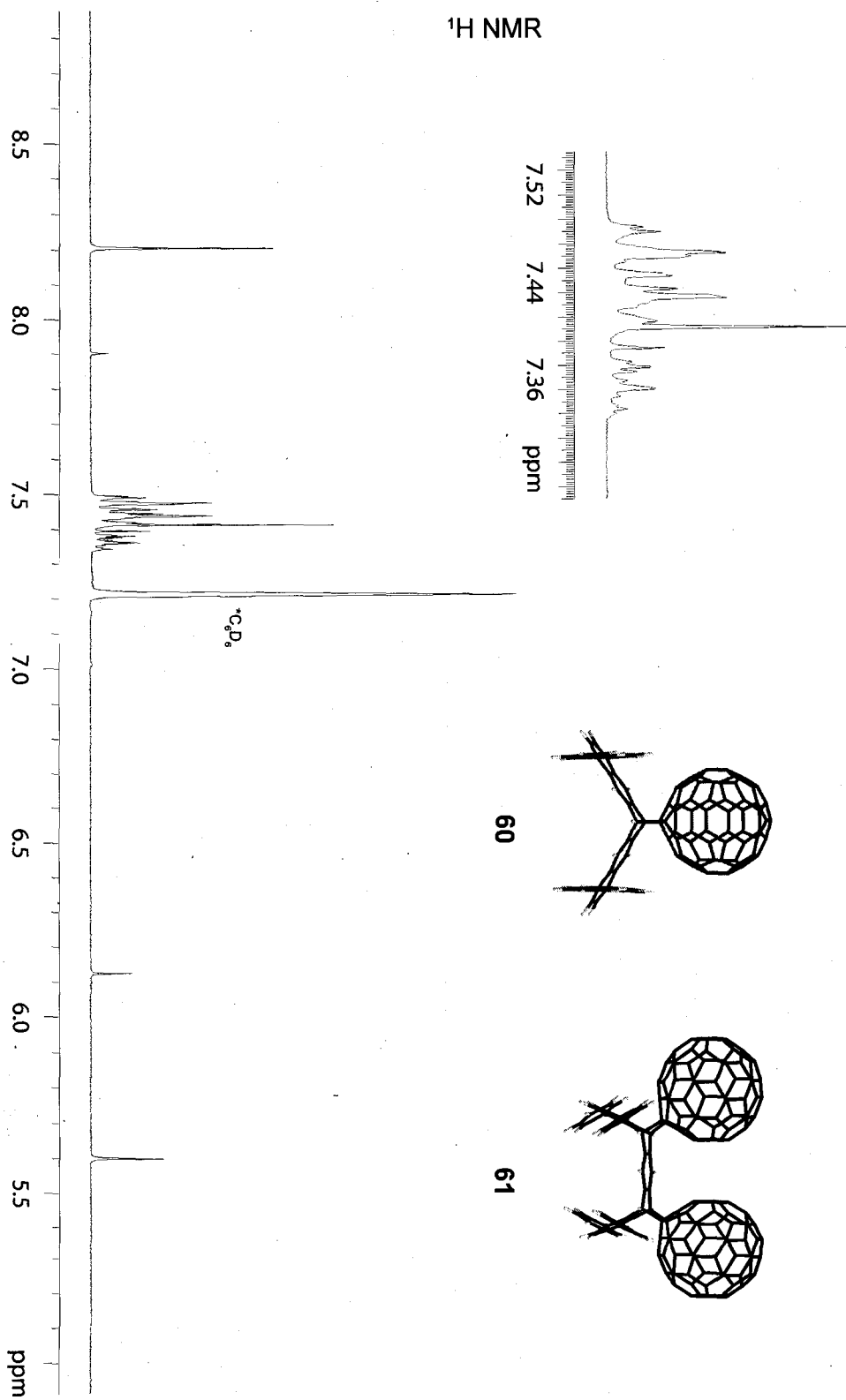


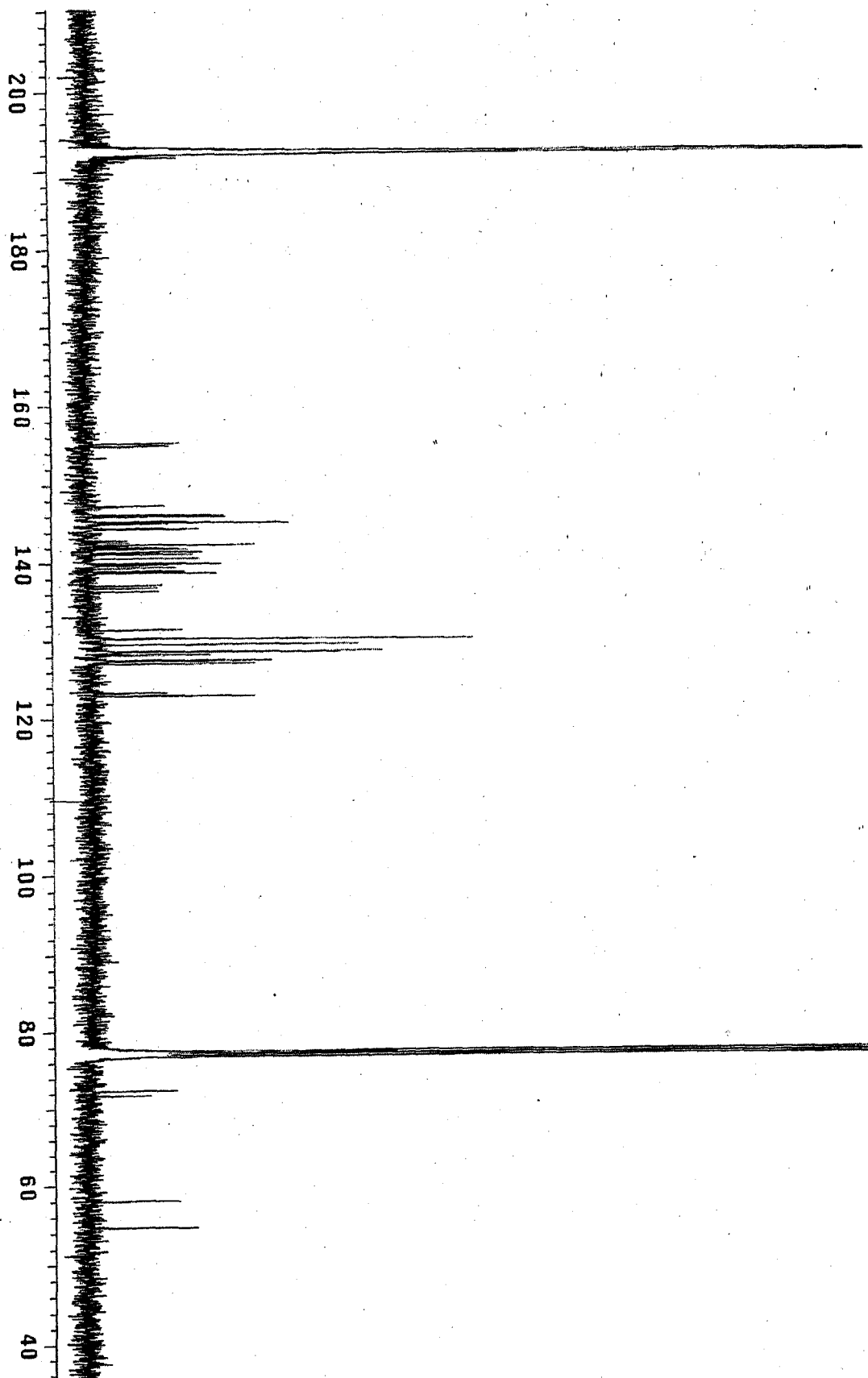
<sup>1</sup>H NMR and NOESY1D



<sup>1</sup>H NMR and NOESY1D

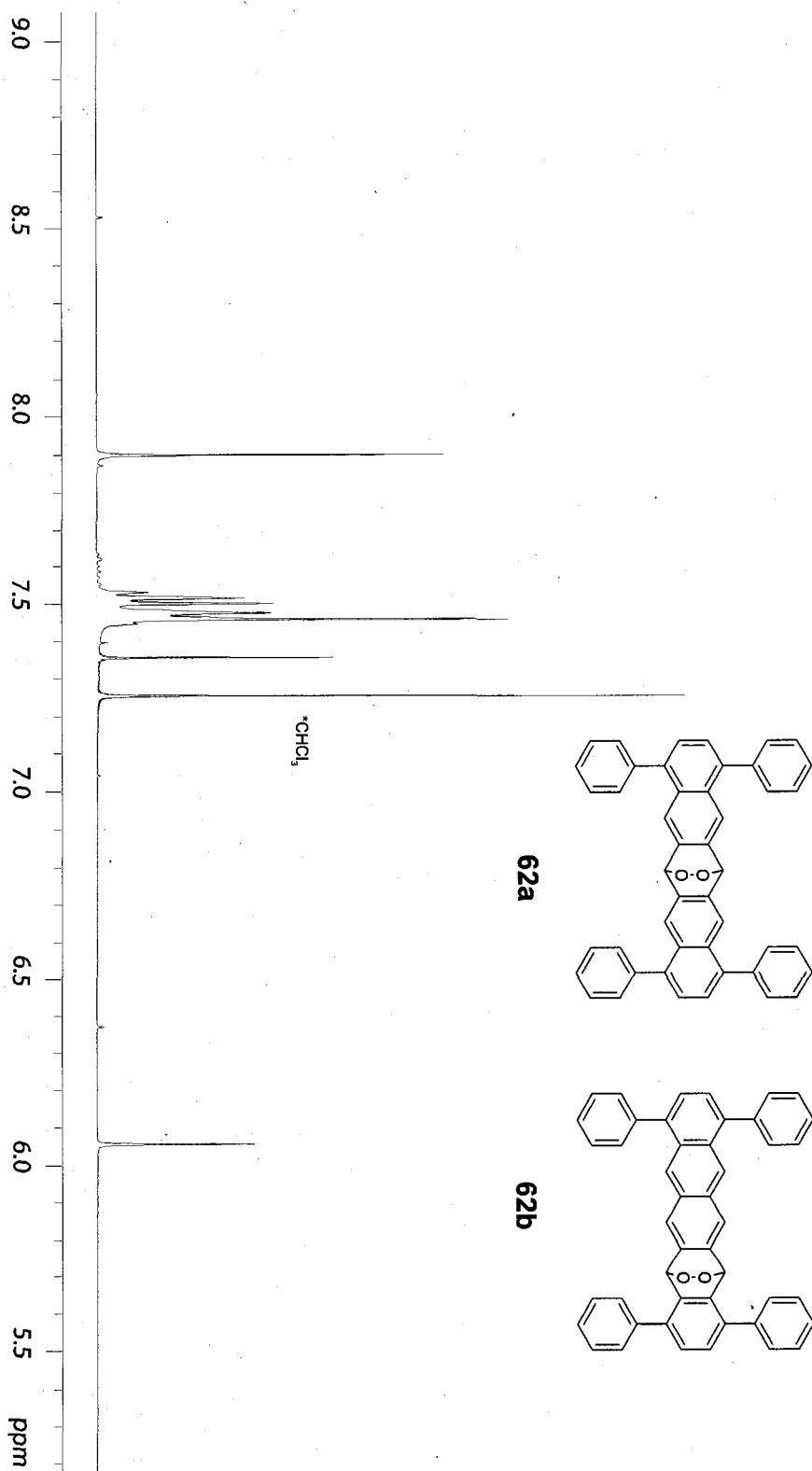




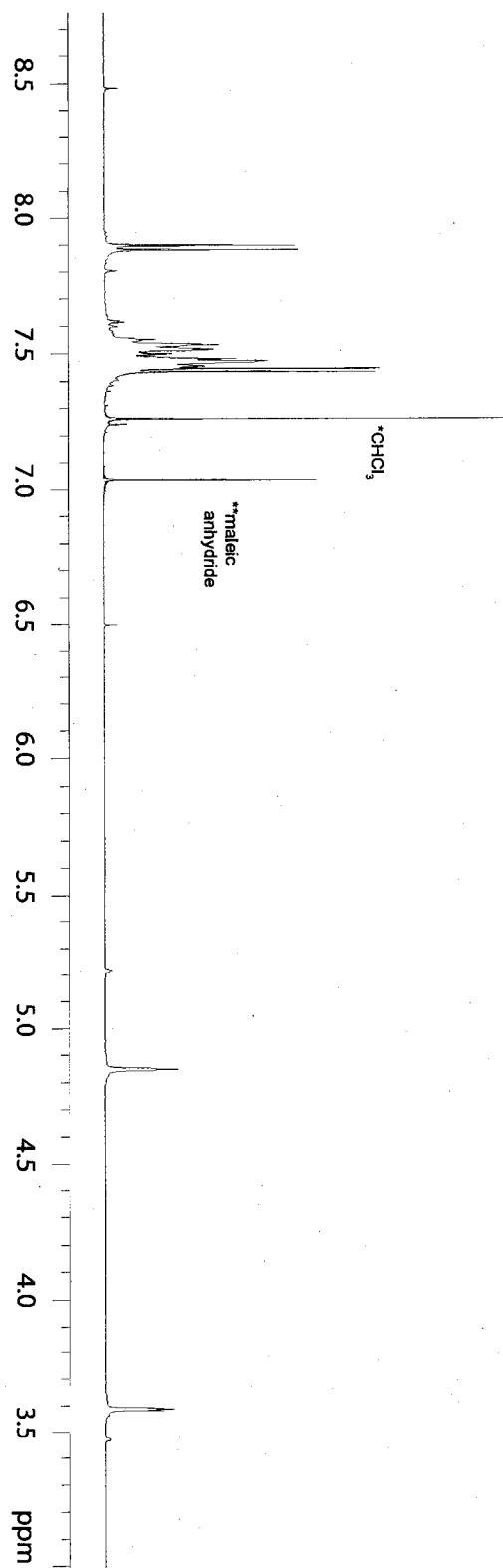




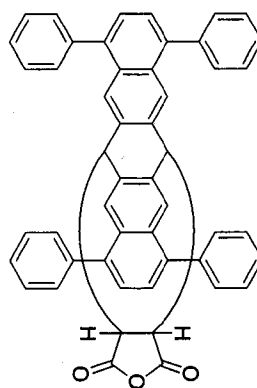
<sup>1</sup>H NMR



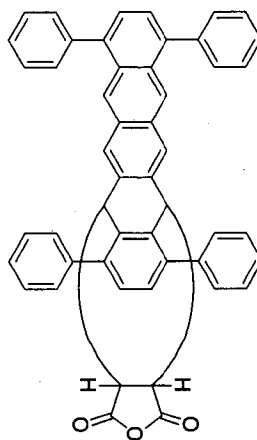
$^1\text{H}$  NMR



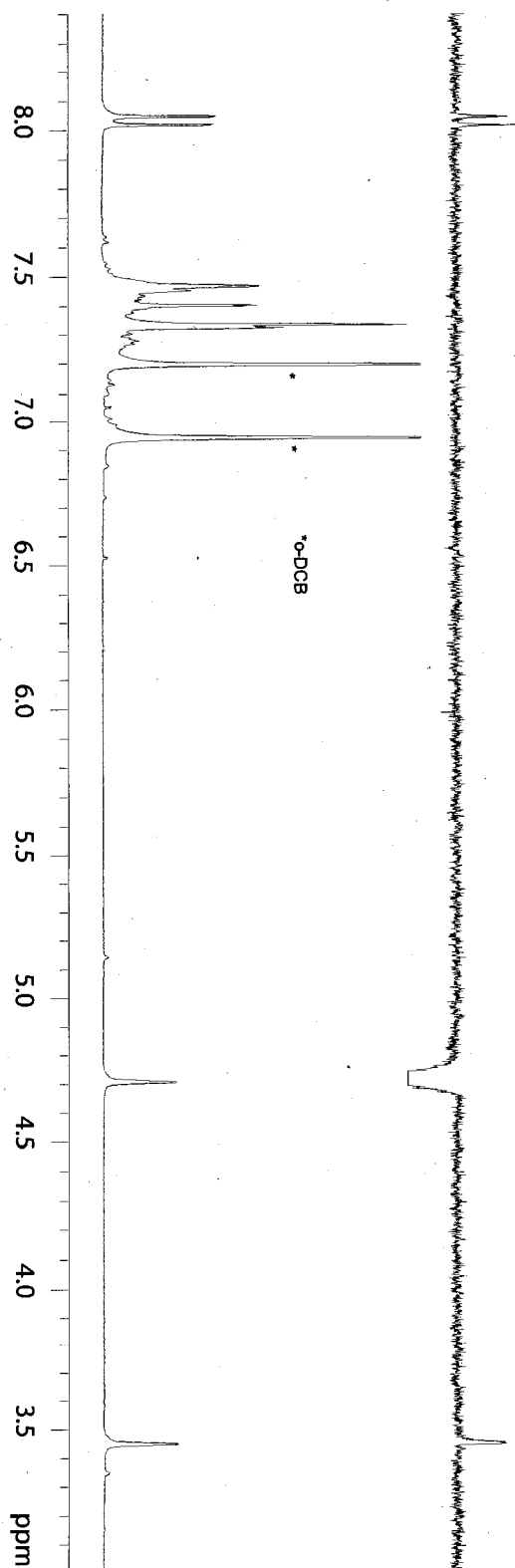
63a



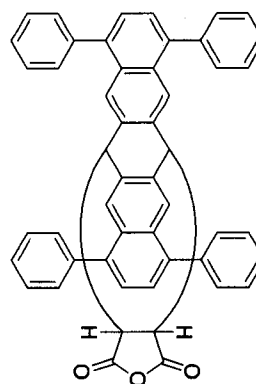
63b



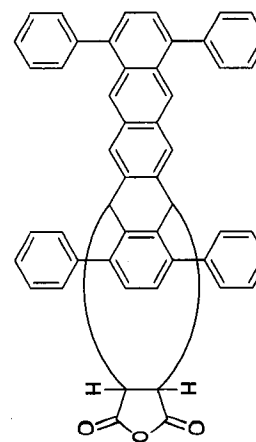
<sup>1</sup>H NMR and NOESY1D



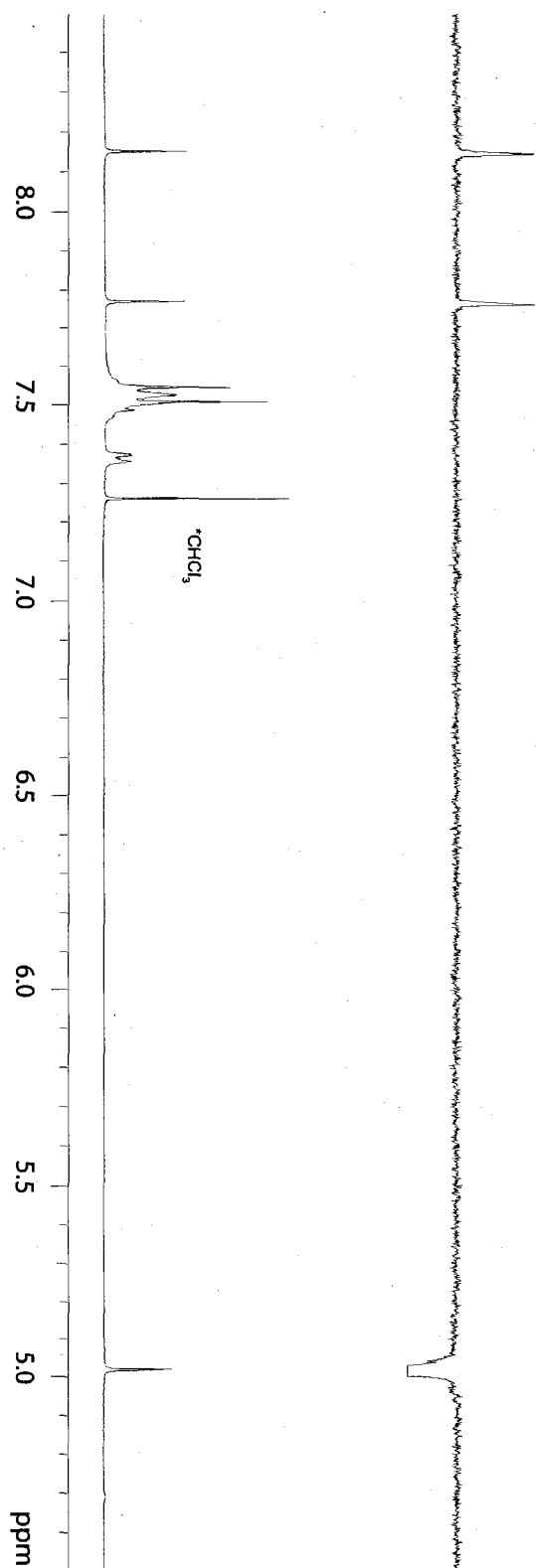
**63a**



**63b**



<sup>1</sup>H NMR and NOESY1D



**64a**

